# Transdifferentiation of
# Human Mesenchymal Stem Cells

Dissertation zur Erlangung des naturwissenschaftlichen
Doktorgrades der Julius-Maximilians-Universität Würzburg

vorgelegt von

**Tatjana Schilling**

aus

San Miguel de Tucuman, Argentinien

Würzburg, 2007

Eingereicht am: ........................................................................................................................

Mitglieder der Promotionskommission:

Vorsitzender: .............................................................................. Prof. Dr. Martin J. Müller

Gutachter: ..................................................................................... PD Dr. Norbert Schütze

Gutachter: ................................................................................ Prof. Dr. Georg Krohne

Tag des Promotionskolloquiums: ........................................................................................

Doktorurkunde ausgehändigt am: .......................................................................................

# Table of contents

# 1   Summary

## 1.1   Summary

With ageing, the loss of bone mass correlates with the expansion of adipose tissue in human bone marrow thus facilitating bone-related diseases like osteopenia and osteoporosis. The molecular mechanisms underlying these events are still largely unknown. Reduced osteogenesis and concurrently enhanced adipogenesis might not only occur due to the impairment of conventional osteogenic differentiation originating from mesenchymal stem cells (MSCs). Additionally, transdifferentiation of (pre-)osteoblasts into adipocytes could contribute to the fatty conversion. Therefore, the aim of the present study was to prove the existence of transdifferentiation between the adipogenic and osteogenic lineage and to elucidate molecular mechanisms underlying this phenomenon.

At first, a cell culture system of primary human MSCs was established that allowed for differentiation into the adipogenic and osteogenic lineage and proved that the MSC-derived adipocytes and pre-osteoblasts were capable of transdifferentiation (reprogramming) from one into the other lineage. Thereby, lineage-specific markers were completely reversed after reprogramming of pre-osteoblasts into adipocytes. The osteogenic transdifferentiation of adipocytes was slightly less efficient since osteogenic markers were present but the adipogenic ones partly persisted. Hence, plasticity also reached into the differentiation pathways of both lineages and the better performance of adipogenic reprogramming further supported the assumption of its occurrence *in vivo*.

The subsequent examination of gene expression changes by microarray analyses that compared transdifferentiated cells with conventionally differentiated ones revealed high numbers of reproducibly regulated genes shortly after initiation of adipogenic and osteogenic reprogramming. Thereof, many genes were correlated with metabolism, transcription, and signal transduction as FGF, IGF, and Wnt signalling, but only few of the established adipogenesis- and none of the osteogenesis-associated marker genes were detected within 24 h after initiation of transdifferentiation.

To find possible key control factors of transdifferentiation amongst the huge amount of regulated genes, a novel bioinformatic scoring scheme was developed that ranked genes due to their potential relevance for reprogramming. Besides the reproducibility and level of their regulation, also the possible reciprocity between the adipogenic and osteogenic transdifferentiation pathway was taken into account. Fibroblast growth factor 1 (FGF1) that ranked as one of the leading candidates to govern reprogramming was proven to inhibit adipogenic differentiation as well as adipogenic transdifferentiation in our cell culture system.

Further examination of the FGF signalling pathway and other highly ranked genes could help to better understand the age-related fatty degeneration at the molecular level and therefore provide target molecules for therapeutic modulation of the plasticity of both lineages in order to inhibit adipogenic degeneration and to enhance osteogenesis.

## 1.2 Zusammenfassung

Der Verlust an Knochenmasse im Alter ist mit der Ausbreitung von Fettgewebe im menschlichen Knochenmark assoziiert und fördert daher auch knochenspezifische Erkrankungen wie Osteopenie und Osteoporose. Die diesen Ereignissen zu Grunde liegenden Mechanismen sind immer noch weitgehend unbekannt. Die abnehmende Osteogenese und die gleichzeitig zunehmende Adipogenese treten wahrscheinlich nicht nur wegen der Beeinträchtigung der konventionellen osteogenen Differenzierung von mesenchymalen Stammzellen (MSZ) auf. Zusätzlich könnte auch die Transdifferenzierung (Reprogrammierung) von Osteoblasten(vorläufern) zu Adipozyten zur fettigen Umwandlung beitragen. Das Ziel der vorliegenden Studie war es daher, die Existenz der Transdifferenzierung zwischen dem adipogenen und osteogenen Differenzierungsweg nachzuweisen und die molekularen Mechanismen aufzuklären, die diesem Phänomen zu Grunde liegen.

Zunächst wurde ein Zellkultursystem primärer mesenchymaler Stammzellen etabliert, in dem eine Differenzierung zu Adipozyten und Osteoblasten durchgeführt werden konnte, und nachgewiesen, dass aus MSZ erhaltene Adipozyten und Osteoblastenvorläufer von einer zur anderen Zelllinie transdifferenziert (reprogrammiert) werden können. Dabei wurden die zelllinienspezifischen Marker nach der Reprogrammierung von Osteoblastenvorläufern zu Adipozyten vollständig umgekehrt. Die osteogene Transdifferenzierung von Adipozyten war etwas weniger effizient, da die osteogenen Marker zwar vorhanden waren, aber auch die adipogenen Marker weiterhin auftraten. Die Plastizität erstreckte sich also auch auf die Differenzierungswege der beiden Zellpopulationen, wobei das bessere Ergebnis bezüglich der adipogenen Reprogrammierung die Annahme ihres Auftretens *in vivo* weiter unterstützte. Die nachfolgende Untersuchung von Genexpressionsänderungen mittels Mikroarray-Analysen, die transdifferenzierte mit konventionell differenzierten Zellen verglichen, führte kurz nach Initiation der adipogenen und osteogenen Transdifferenzierung zum Auffinden zahlreicher, reproduzierbar regulierter Gene. Viele dieser Gene standen mit Metabolismus, Transkription und Signaltransduktion wie dem FGF-, IGF- und Wnt-Signalweg in Zusammenhang, es wurden allerdings nur einige Adipogenese- und keinerlei Osteogenese-assoziierte Markergene innerhalb 24 h nach Initiation der Transdifferenzierung detektiert. Um unter der großen Zahl an regulierten Genen mögliche Schlüsselkontrollfaktoren der

Transdifferenzierung zu finden, wurde ein neuartiges, bioinformatisches Punktesystem entwickelt, das Gene entsprechend ihrer potenziellen Relevanz für die Reprogrammierung auflistete. Dabei wurde neben der Reproduzierbarkeit und dem Ausmaß ihrer Regulation auch eine mögliche Reziprozität der Regulation zwischen dem adipogenen und osteogenen Transdifferenzierungsweg berücksichtigt. Es konnte nachgewiesen werden, dass der Fibroblastenwachstumsfaktor 1 (FGF1), der als einer der Hauptkandidaten für die Steuerung der Reprogrammierung eingeordnet worden war, in unserem Zellkultursystem sowohl die adipogene Differenzierung als auch die adipogene Transdifferenzierung hemmt.

Die weitere Untersuchung des FGF-Signalwegs und anderer, hoch gelisteter Gene könnte zum besseren Verständnis der altersbezogenen fettigen Degeneration auf molekularer Ebene beitragen und daher Zielmoleküle liefern, die eine therapeutische Beeinflussung der Plastizität zwischen beiden Zelllinien zur Verhinderung der fettigen Degeneration und zur Förderung der Osteogenese erlauben.

# 2   Introduction

## 2.1   Osteoporosis and the fatty degeneration of the bone marrow

With ageing, degenerative processes of the musculoskeletal system give rise to several painful diseases like osteoarthritis, tendinosis, and osteoporosis. While osteoarthritis and tendinosis affect the joints, osteoporosis is characterised by the general loss of bone mass [Rössler and Rüther, 2000]. During ongoing osteoporosis, bone density declines at first in the spine, ribcage, pelvis, and hip, thus facilitating the risk of fractures in these skeletal areas [Adler, 1983a; Brügger, 1980]. Thereby, age-related lower calcium absorption in the stomach and intestine, tissue hypoxia as well as changes of the endocrine metabolism, especially estrogen deficiency in postmenopausal women, account for these changes. At the histological level, these alterations disrupt the setup of the osteoid that is comprised of osteoblasts and not yet mineralised extracellular matrix and participates in bone remodelling [Bartl, 2001; Henriksen et al., 2007].

During progressing osteoporosis, the bone volume declines in favour of spreading marrow volume [Adler, 1983a; Justesen et al., 2001]. Since adipose tissue simultaneously augments in the bone marrow, it has been assumed that an inverse relationship between decreasing osteogenesis and increasing adipogenesis exists [Beresford et al., 1992; Burkhardt et al., 1987; Gimble et al., 2006; Koo et al., 1998; Meunier et al., 1971; Pei and Tontonoz, 2004]. Thereby, osteoporosis has even been discussed as the obesity of bone [Rosen and Bouxsein, 2006]. Moreover, osteopenia was detected in a mouse model with accelerated adipogenesis which further supports the detrimental effect of the imbalance between osteogenesis and adipogenesis on bone mass [Klein et al., 2004].

## 2.2   Adipose and bone tissue

### 2.2.1   Adipose tissue

Adipose tissue is composed of adipocytes that produce connective tissue matrix also containing nerve tissue, stromavascular cells, and immune cells [Frayn et al., 2003].
Thereby, brown and white adipocytes both accumulate lipids but carry out opposing functions. Brown adipose tissue stores less lipids and is involved in thermogenesis as an energy-dissipating organ while white adipose tissue strongly accumulates lipids serving as main energy storage of the organism [Krug and Ehrhart-Bornstein, 2005; Trayhurn et al., 2006]. Additionally, white adipose tissue secretes hormones and signalling factors that affect various physiological and pathophysiological processes [Cousin et al., 1993; Wajchenberg, 2000]. The metabolism of adipose tissues and the release of adipocyte-secreted proteins (adipokines) influence energy homeostasis, insulin sensitivity, and vascular homeostasis of

the organism [de Meis et al., 2006; Guerre-Millo, 2004; Trayhurn et al., 2006]. Adipokines like leptin and adiponectin (also called ADIPOQ) mediate beneficial effects on insulin sensitivity, energy balance, and vasculature (fig. 1) [Farooqi et al., 2002; Maeda et al., 2001; Yu et al., 2002]. In contrast, high amounts of other adipokines provoke detrimental effects. Tumour necrosis factor α (TNFα), interleukin 6 (IL6), and resistin generate insulin resistance while the effects of angiotensinogen (AGE) and plasminogen activator inhibitor 1 (PAI-1, also called SERPINE1) have been correlated with vascular complications of obesity, e.g. hypertension and fibrinolysis [Ailhaud et al., 2000; Mavri et al., 2001]. Moreover, acetylation-stimulating protein (ASP) stimulates triglyceride storage in adipocytes by enhancement of glucose transport and inhibition of lipolysis [Cianflone et al., 1999].
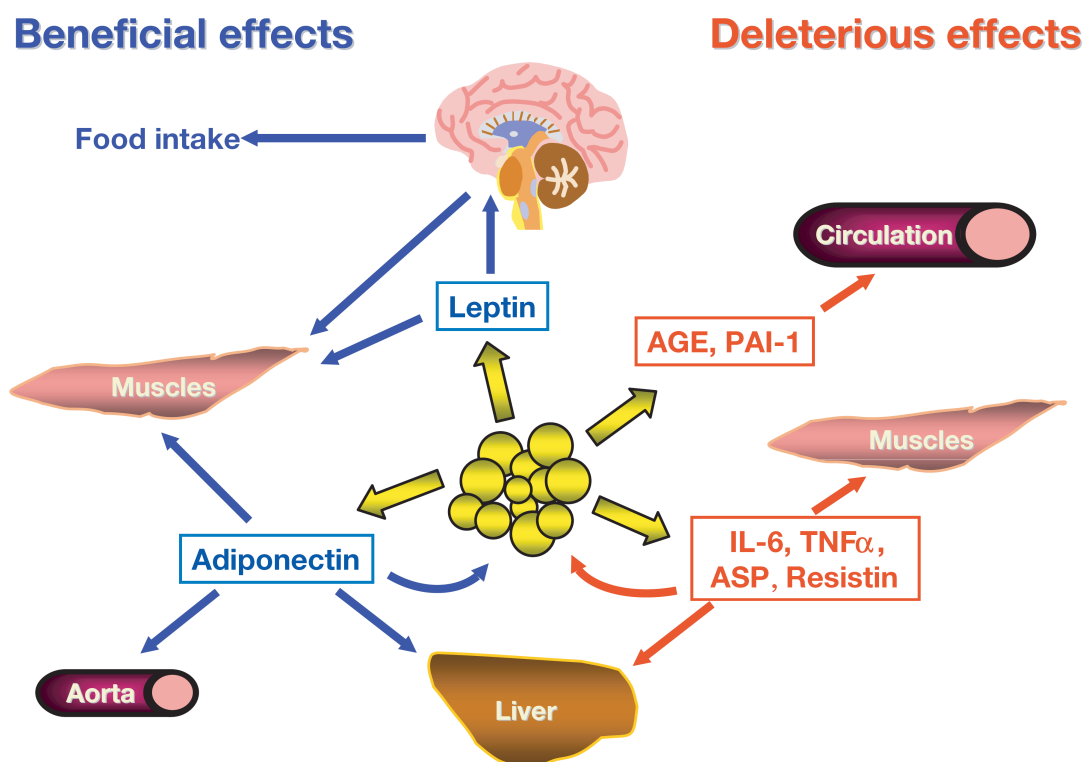


**Fig. 1     Influence of adipokines on energy homeostasis, insulin sensitivity, and vascular homeostasis**

Adipokines secreted by adipocytes of white adipose tissue (in the middle) influence several physiological processes. Excessive amounts of ASP, TNFα, IL6, and resistin disrupt insulin action in muscle and liver, whereas the raise of AGE and PAI-1 promotes hypertension and impaired fibrinolysis correlated with obesity. Moreover, leptin maintains the energy homeostasis and enhances insulin sensitivity as well as adiponectin. Figure by Guerre-Millo [2004].

## 2.2.2   Bone tissue

Bone functions to support the body thereby determining its shape and protecting the soft tissues [Adler, 1983b]. The shape of the skeleton and hence the structure of its bones is

adapted to the physical load exposure by bone resorption and bone accrual (see 2.2.3). Moreover, bone enables movement together with the skeletal muscles, tendons, ligaments, and joints.

Besides support of the body, the metabolic function of bone plays a very important role. Since calcium ion levels control organ and cellular activities, the storage and release of calcium and phosphate ions from bone is required to balance the serum levels of these ions [Martin, 1983; Rössler and Rüther, 2000] (fig. 2). Calcium and phosphate absorption via nutrition is controlled by 1,25-dihydroxyvitamin $D_3$ thus making calcium and phosphate available for mineralisation of bone [Bronner, 1994; Misof et al., 2003]. Further hormones including parathyroid hormone (PTH), epidermal growth factor, prostaglandins, and osteoclast activating factor, stimulate the release of minerals and organic compounds from bone. In contrast, hormonal inhibitors of bone resorption like calcitonin (CT) and glucocorticoids block calcium release from bone tissue. Disturbance of this storage and release mechanisms not only affects calcium metabolism but also causes changes regarding the toughness of bone.
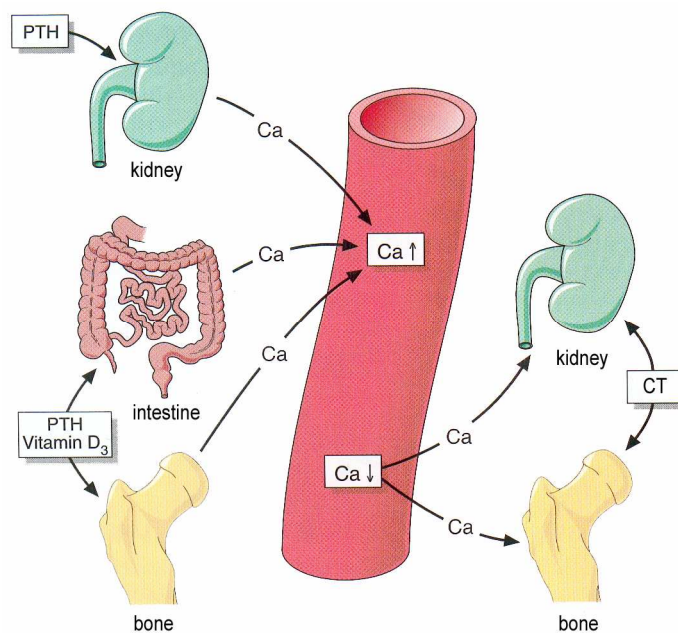


**Fig. 2      Regulation of calcium metabolism**

Parathyroid hormone (PTH) and 1,25-dihydroxyvitamin $D_3$ promote absorption of calcium (Ca) in the intestine and make Ca available from bone whereas PTH additionally represses calcium excretion via the kidney thus elevating Ca serum levels. Calcitonin (CT) increases calcium deposition in bone as well as Ca excretion in the kidney thereby diminishing Ca serum levels. Figure adapted from Rössler and Rüther [2000].

Bone tissue consists of 10% water, more than 70% inorganic, and approximately 20% organic matrix including bone cells like osteoblasts and osteocytes that are supplied with nutrients and oxygen by blood vessels [Adler, 1983b]. The osteoid comprises organic bone matrix and embedded osteoblasts that produce the matrix components before becoming

osteocytes. The organic matrix itself serves as a deposition site for minerals and is composed of 90% collagen type I and 10% other, non-collagenous proteins (e.g. glycoproteins like osteocalcin, osteonectin, integrin-binding sialoprotein, and osteopontin) and proteoglycans. The inorganic portion of bone matrix is composed of 90% calcium phosphate and 10% calcium carbonate. Thereby, calcium forms hydroxyapatite crystals incorporated into the organic matrix. The bone tissue encloses the bone marrow, which is located within the medullary cavity of long bones and the interstices of cancellous bone. Bone marrow contains hematopoietic as well as mesenchymal precursor cells whereas the former give rise to blood cells and the latter can generate several mesenchymal tissues (see 2.3.1).

### 2.2.3   Bone remodelling

Ossification of the skeleton is not completed until adolescence. Even afterwards bone is continuously remodelled in order to meet changing needs as well as to maintain bone quality and strength by replacement of aged bone matrix of lower density and reduced quality [Bartl, 2001; Caplan, 2005; Henriksen et al., 2007; Martin, 1983]. Bone remodelling thus comprises bone resorption as well as bone accrual and therefore provides calcium mobilisation and deposition within calcium homeostasis, replacement of old bone tissue, adaptation to altered loads, and repair of injured bone.

The circle of bone remodelling consists of distinct phases beginning with the activation of multinucleated osteoclasts (fig. 3). Osteoclasts are derived from monocytes of the hematopoietic lineage and function as bone resorbing cells [Bartl, 2001; Väänänen et al., 2000]. They attach to the bone surface with their ruffled border and secrete proteolytic enzymes that dissolve crystalline hydroxyapatite. The remaining organic matrix is absorbed by phagocytosis and is digested in the cytoplasma of the osteoclasts. Recruitment of osteoclasts to the site of bone resorption is controlled by several hormones (e.g. PTH, estrogen, and leptin) and growth factors. Subsequently, the reversal phase provides smoothing of the resorption lacuna and activation of osteoblasts. Osteoblasts derived from MSCs form the osteoid by synthesis of bone matrix that consists at first mainly of collagen type I (formation early phase) and serves as a scaffold for mineralisation lasting several weeks (formation late phase). About 10% of the osteoblasts are incorporated into the newly formed bone matrix and differentiate into osteocytes. These osteocytes reside in lacunae, which are connected by branched canaliculi and mediate metabolite transport inside the bone matrix. In the final quiescence phase, the surface of the bone is covered by lining cells, which are supposed to represent inactive osteoblasts and to protect bone. Additionally, lining cells as well as osteoblasts express membrane-bound and soluble molecules like receptor activator of NF-κB ligand (RANKL) and osteoprotegerin (also called tumour necrosis factor receptor superfamily member 11b, TNFRSF11B) that influence osteoclast differentiation [Hsu

et al., 1999; Lacey et al., 1998]. Thereby, RANKL interacts with osteoclast-specific RANK thus able to stimulate osteoclast differentiation. Contrarily, TNFRSF11B acts as a decoy receptor for RANKL thereby neutralising its osteoclastogenesis-stimulating effect. Further compounds like cyclosporin A and interferon γ as well as calcium ions have been reported to strongly diminish the resorption of bone matrix [Fuller et al., 2007].

Additionally, Wnt signalling has been shown to regulate osteogenesis *in vitro* and *in vivo* (see 2.3.3). Recent data also suggest that Wnt signalling not only affects osteogenesis but also influences osteoclasts either by impairment of osteoblasts to inhibit osteoclast differentiation or by direct transcriptional repression of RANKL in osteoclasts [Glass et al., 2005; Spencer et al., 2006].
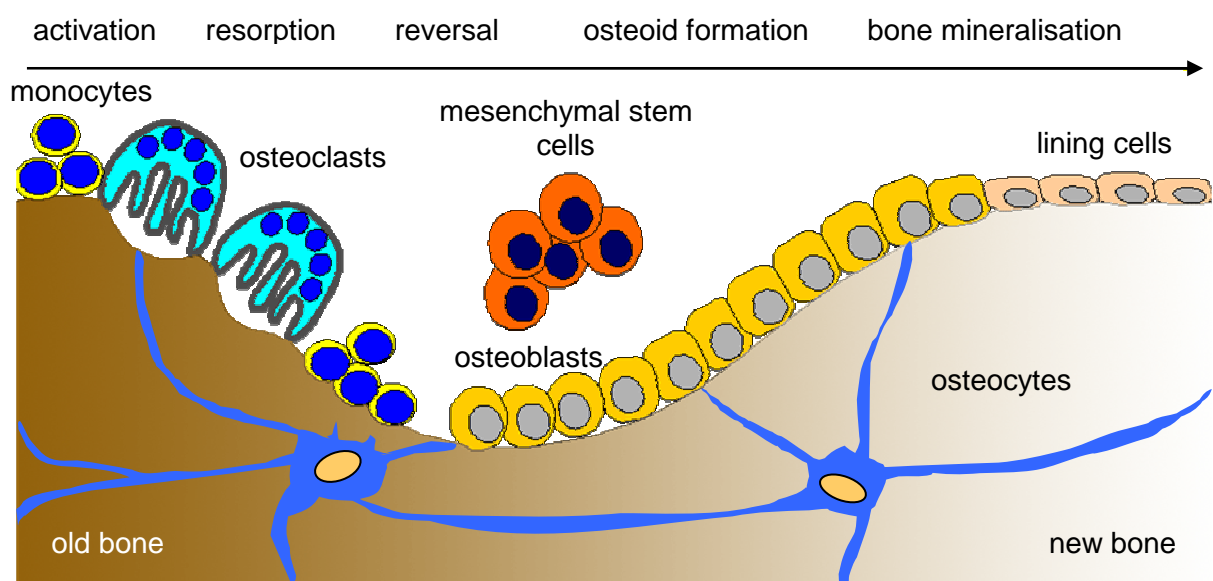


**Fig. 3    Bone remodelling**

After initial activation, bone resorption is conducted by osteoclasts whereas osteoid formation provides bone-forming osteoblasts. Osteoblasts produce extracellular matrix that becomes mineralised forming new bone.

## 2.3    Mesenchymal stem cells

### 2.3.1    Multilineage potential

Stem cells are undifferentiated cells that can renew themselves as well as differentiate into specialised cell types, thereby forming new organs during embryonic development and regenerating tissue during the entire life of the organism due to normal turnover or injury [Caplan, 1991; Duplomb et al., 2007]. While totipotent embryonic stem cells can give rise to all cell types of the organism, multipotent stem cells of the adult organism, e.g. mesenchymal stem cells (MSCs), are more restricted in their differentiation potential and therefore generate only a limited number of cell types.

MSCs have been isolated from the bone marrow and various other tissues, even from some that do not originate from the mesenchymal germ layer, and show fibroblast-like morphology

[da Silva Meirelles et al., 2006]. They have been shown to differentiate into cells of various mesenchymal tissues like bone, cartilage, muscle, and adipose tissue (fig. 4) [Barry and Murphy, 2004; Caplan, 1991; Friedenstein et al., 1974; Friedenstein et al., 1976; Muraglia et al., 2000; Nöth et al., 2002a; Pereira et al., 1995; Pittenger et al., 1999; Prockop, 1997; Verfaillie, 2002]. Their differentiation and tissue regeneration potential has already been used in therapeutic approaches like tissue engineering and gene therapy [Bianco et al., 2001; Caplan, 2005].
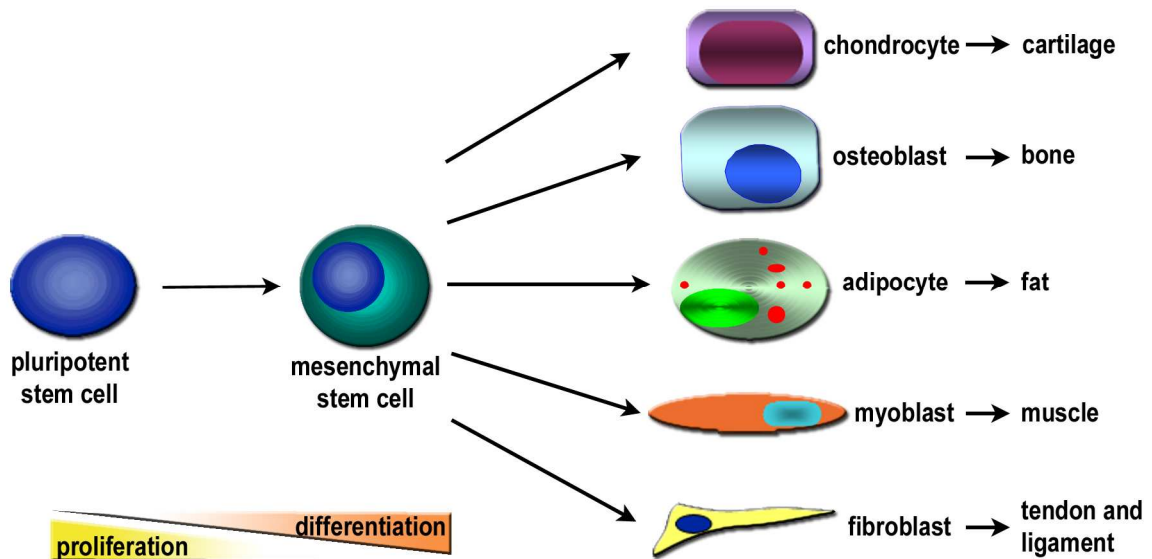


**Fig. 4       Multilineage potential of mesenchymal stem cells**

Multipotent MSCs originate from pluripotent stem cells during the embryonic development and persist in the adult organism. MSCs give rise to several mesenchymal tissues as depicted. In general, increasing differentiation status correlates with decreasing proliferation.

Differentiation of MSCs requires the action of specific regulatory genes and subsequent signalling. The establishment of empirical cell culture systems that provoke adipogenic and osteogenic differentiation *in vitro* has elucidated some of the mechanisms necessary for differentiation. The key factors and processes known to be involved in adipogenic and osteogenic differentiation, respectively, are summarised below.

## 2.3.2   Adipogenesis

*In vivo*, the formation of fat cells is stimulated by hormonal inducers. The subsequent transcriptional regulation of adipogenesis has been studied by several *in vitro* models employing human and murine MSCs or pre-adipocytes and in some knockout mice. For human MSCs, a differentiation cocktail containing dexamethasone, indomethacin, 3-isobutyl-1-methylxanthine, and insulin has commonly been used to obtain adipocytes [Nöth et al., 2002a; Nuttall et al., 1998; Pittenger et al., 1999].

The induction of adipogenesis *in vitro* is considered to involve one or two rounds of clonal expansion followed by the expression of adipogenesis-specific genes and attainment of the

adipogenic phenotype [MacDougald and Mandrup, 2002; Rosen et al., 2000]. Thereby, reports on the requirement for clonal expansion have been controversial [Patel and Lane, 2000; Qiu et al., 2001; Ross et al., 2002]. Activation of gene expression is achieved by the sequential action of C/CAAT enhancer binding proteins (C/EBPs) and peroxisome proliferator-activated receptor γ 2 (PPARγ2) (fig. 5). Transient induction of C/EBPβ and C/EBPδ provokes expression of C/EBPα and PPARγ2 [MacDougald and Lane, 1995; Tontonoz et al., 1994a]. Thereby, PPARγ2 heterodimerises with retinoid X receptor (RXR) to attain its transcriptional activity that induces transcription of C/EBPα [Rosen et al., 2000; Wu et al., 1999]. PPARγ2 and C/EBPα activate or enhance expression of other adipocyte-specific genes like lipoprotein lipase (LPL) acetyl CoA carboxylase, solute carrier family 2 (facilitated glucose transporter) member 4 (SLC2A4; formerly glucose transporter type 4 GLUT4), and fatty acid binding protein 4 (FABP4; formerly adipocyte P2, aP2) [Spiegelman et al., 1993].

Additionally, PPARγ2 activity can be increased by sterol regulatory element-binding protein 1 (SREBP1) independently from C/EBPβ and C/EBPδ [Kim et al., 1998; Spiegelman et al., 1993]. Maximal PPARγ2 activity *in vitro* was observed after binding of coactivators, e.g. p160 proteins and CBP/p300, to PPARγ2 [Gelman et al., 1999; Yao et al., 1996]. Loss-of-function studies in chimeric mice and over-expression studies in non-adipogenic fibroblasts suggest that PPARγ2 is necessary as well as sufficient for induction of adipogenesis [Rosen et al., 1999; Tontonoz et al., 1994c], however, requirement of C/EBPα for insulin sensitivity in adipocytes has been detected [Wu et al., 1999]. Moreover, *in vivo* studies also showed an inhibitory function of PPARγ on osteogenesis [Akune et al., 2004].
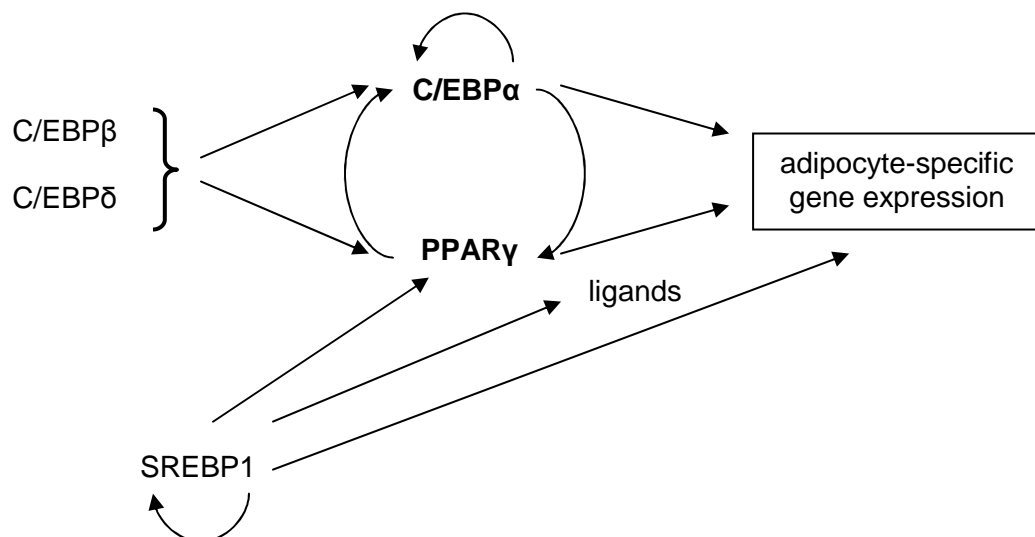


**Fig. 5    Transcription factors involved in induction of adipogenic differentiation**

Transient expression of C/EBPβ and C/EBPδ results in expression of PPARγ and C/EBPα, which are the key transcription, factors during adipogenesis. SREBP1 augments the expression of PPARγ and its ligands and also enhances the transcription of adipocyte-specific genes, which foster the adipogenic differentiation. Further transcription factors can promote or inhibit adipogenesis. Figure adapted from MacDougald and Mandrup [2002].

Further factors like insulin-like growth factor 1 (IGF1), macrophage colony-stimulating factor (MCSF), fatty acids, prostaglandins, and glucocorticoids have been shown to stimulate adipogenesis whereas Wnt signalling, TGFβ as well as several inflammatory cytokines and growth factors have been reported to inhibit adipogenic differentiation (reviewed in MacDougald and Mandrup [2002]).

Besides endocrine signals also paracrine and/or autocrine factors are considered to regulate progression of adipogenesis (fig. 6).

At the mRNA level, terminally differentiated adipocytes are characterised by sustained expression of PPARγ2, LPL, and FABP4 [Ailhaud et al., 1991; Barak et al., 1999; Fried et al., 1993; Gaskins et al., 1989; Tontonoz et al., 1994b]. The fibroblast-like morphology of pre-adipocytes changes into a more rounded shape during ongoing differentiation possibly due to changes in the synthesis of cytoskeletal and extracellular matrix-associated proteins [MacDougald and Lane, 1995]. Moreover, accumulation of lipid vesicles in the cytoplasm, which contain mainly triglycerides and cholesterol esters, augments during adipogenic differentiation.
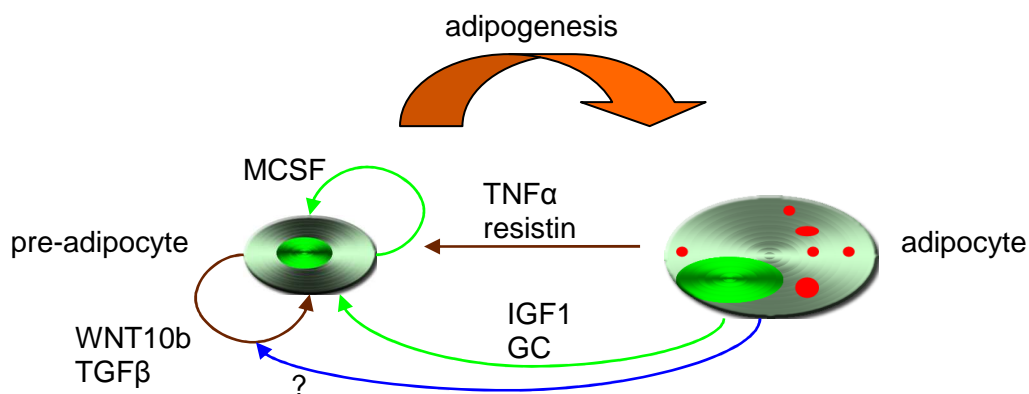


**Fig. 6      Influence of paracrine and autocrine signalling on the progression of adipogenesis**

Pre-adipocytes as well as adipocytes secrete factors that enhance or inhibit adipogenesis. When differentiated adipocytes exceed a critical size, they are considered to stimulate division and differentiation of pre-adipocytes either by direct stimulation (green arrows) or by inhibition of signalling pathways (blue arrow) that would otherwise inhibit adipogenesis (brown arrows). In pre-adipocytes, even autocrine signalling takes place that regulates adipogenic differentiation positively (green arrow) or negatively (brown arrow). Figure adapted from MacDougald and Mandrup [2002]. TNFα = tumour necrosis factor α.

### 2.3.3   Osteogenesis

The mechanisms of osteogenesis, which is crucial for bone formation, have been studied in several mouse models, osteoblast progenitor cell lines, and MSCs. *In vitro* assays use osteogenic supplements to induce differentiation. Thereby, ascorbic acid is required for accumulation of collagen type I alpha 1 (COL1A1) in the extracellular matrix of differentiating osteoblasts as well as for expression of bone gamma-carboxyglutamate (gla) protein (osteocalcin; OC) and alkaline phosphatase, liver/bone/kidney (ALP) while β-

glycerophosphate serves as exogenous phosphate source for matrix mineralisation [Franceschi and Iyer, 1992; Jaiswal et al., 1997].

At the transcriptional level, osteogenesis is induced by runt-related transcription factor 2 (RUNX2; formerly core-binding factor, runt domain, alpha subunit 1, CBFA1) and Sp7 transcription factor (SP7; formerly osterix) [Ducy et al., 2000; Ducy et al., 1997; Nakashima and de Crombrugghe, 2003; Nakashima et al., 2002].

RUNX2 requires heterodimerisation with core-binding factor β (CBFB) [Kundu et al., 2002; Miller et al., 2002] to attain its transcriptional activity. Moreover, post-transcriptional regulation of RUNX2 can be conducted via phosphorylation or protein-protein interactions. For example, RUNX2 activity is augmented by mitogen-activated protein kinase (MAPK) signalling where fibroblast growth factor 2 (FGF2) has been shown to increase phosphorylation of extracellular signal-regulated kinases 1 and 2 which in turn phosphorylate RUNX2 [Jaiswal et al., 2000; Xiao et al., 2002]. In contrast, phosphorylation of two distinct conserved serine residues of RUNX2 has been reported to inhibit its heterodimerisation with CBFB and therefore to decrease osteogenesis [Wee et al., 2002].

Proteins that interact with RUNX2 and enhance its activity include hairy and enhancer of split 1 as well as SMAD1, 4, and 5 [Ito and Miyazono, 2003; McLarren et al., 2000; Zhang et al., 2000]. Other proteins like SMAD3 inhibit RUNX2 [Alliston et al., 2001; Kang et al., 2005]. Thereby, SMAD proteins are activated by transforming growth factor, beta 1 (TGFβ1), a multifunctional regulator of osteogenesis whose positive or negative effect depends on binding to different, specific receptors.

SP7 as a zinc finger-containing transcription factor is specifically expressed in osteoblasts *in vivo* [Nakashima et al., 2002]. After initiation of osteogenesis by RUNX2, SP7 is required for differentiation of pre-osteoblasts into mature osteoblasts. Furthermore, SP7 has been reported to inhibit expression of SRY (sex determining region Y)-box 9 (SOX9) which acts as a transcription factor enhancing chondrogenesis. Further transcription factors enhancing osteogenic differentiation include distal-less homeobox 5 (DLX5) that is induced by BMP signalling [Erceg et al., 2003; Miyama et al., 1999; Tadic et al., 2001] as well as a transcriptional splice variant of FBJ murine osteosarcoma viral oncogene homolog B (ΔFOSB) [Sabatakos et al., 2000].

Moreover, several hormones and signalling pathways are involved in the regulation of osteogenesis [Ebert et al., 2007]. Thereby, BMP and FGF signalling play important roles. BMP2 has been reported to enhance osteoblast commitment and can also directly influence stabilisation of RUNX2 by acetylation which in turn inhibits degradation of the transcription factor by the ubiquitination pathway [Gori et al., 1999; Jeon et al., 2006]. Together with the corresponding FGF receptors (FGFRs), several of the hitherto 22 known FGFs influence embryonic bone development as well as the osteogenic differentiation potential of adult

MSCs [Battula et al., 2007; Marie et al., 2005; Ornitz, 2005]. Special importance has been attributed to FGF2 that has been reported to modulate expression of osteogenesis-specific genes depending on the duration of its activation [Ling et al., 2006; Xiao et al., 2002]. Furthermore, FGF2 has been shown to enhance BMP2 expression resulting in enhanced RUNX2 expression and therefore accelerated osteogenesis [Choi et al., 2005]. However, FGF2 has also been reported to inhibit osteogenesis in mouse adipose tissue-derived stromal cells [Quarto and Longaker, 2006]. Since there is evidence that differential FGF receptor activation is required to propagate the sequential transit from early to late osteoblast differentiation [Jacob et al., 2006], different sets of FGF receptors might mediate the controversial effects described above.

Altogether, the onset of osteogenic differentiation can be monitored *in vitro* by increasing mRNA levels of RUNX2 and CBFB followed by increasing amounts of SP7. Pre-osteoblasts show enhanced expression of COL1A1 and ALP whereas functional osteoblasts are characterised by high expression of further osteoblast-specific genes like integrin-binding sialoprotein (bone sialoprotein; IBSP) and OC (fig. 7) [Nakashima and de Crombrugghe, 2003]. Moreover, the COL1A1-rich extracellular matrix of mature osteoblasts becomes mineralised mainly by calcium and phosphate which form hydroxyapatite crystals [Currey, 1999; Hunter et al., 1996]. Thereby, induction of hydroxyapatite nucleation has been reported after addition of IBSP while other osteoblast-specific proteins like osteonectin inhibited mineralisation. Moreover, TGFβ signalling has recently been shown to regulate the mineral concentration of bone matrix via SMAD3, an inhibitor of RUNX2 as already mentioned [Balooch et al., 2005].
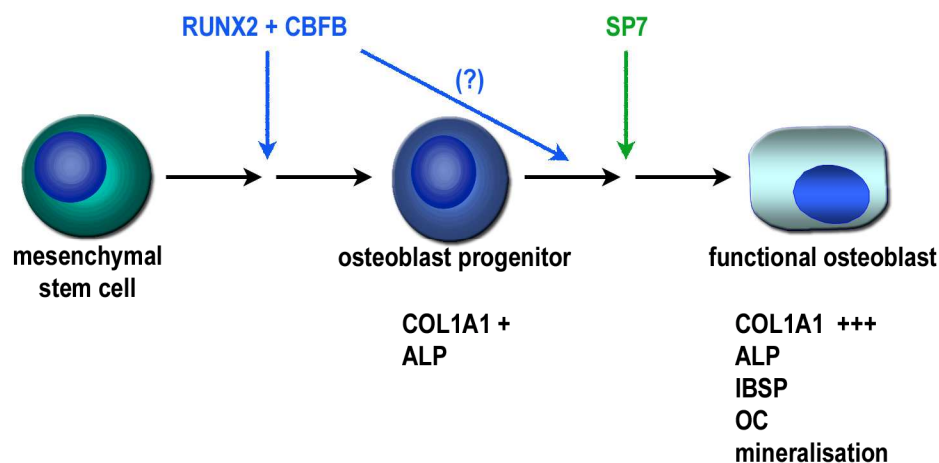


**Fig. 7      Markers of osteogenic differentiation**

Osteogenic differentiation is induced in multipotent MSCs by the action of the transcription factors RUNX2 and CBFB. The resulting pre-osteoblasts already express low levels of COL1A1 (indicated by +). They require the transcriptional activity of SP7 to differentiate into mature, functional osteoblasts. Mature osteoblasts express osteoblast-specific genes, high amounts of COL1A1 (indicated by +++), and produce mineralised extracellular matrix. Figure adapted from Nakashima and de Crombrugghe [2003].

### 2.3.4   Inverse relationship between adipogenic and osteogenic differentiation

Since osteoblasts and adipocytes share a common progenitor, the MSC, a close relationship between both differentiation pathways exists. Based on the observation that bone loss is accompanied by increasing adipose tissue in the bone marrow cavity [Beresford et al., 1992; Justesen et al., 2001; Koo et al., 1998], several factors have been reported to affect both differentiation pathways contrariwise.

Several of the lineage-specific proteins like PPARγ2 and ΔFOSB do not only enhance one differentiation pathway but concomitantly inhibit the other one [Akune et al., 2004; Moerman et al., 2004; Sabatakos et al., 2000]. The crucial role of PPARγ2 was also emphasised by the observation that rosiglitazone, a thiazolidinedione ligand of PPARγ2 that is employed as anti-diabetic drug for the treatment of diabetes type 2, enhanced adipogenesis and simultaneously inhibited osteogenesis *in vitro* and resulted in loss of bone mass and volume in rosiglitazone-treated mice [Ali et al., 2005; Lecka-Czernik et al., 2002; Rzonca et al., 2004]. A recent study examining short-term therapy with rosiglitazone in postmenopausal women also attributes detrimental skeletal effects to this drug [Grey et al., 2007]. Furthermore, activation or overexpression of 12/15-lipoxygenase that enzymatically generates endogenous ligands for PPARγ2 has been reported to enhance adipogenesis and to decrease osteogenesis *in vitro* as well as *in vivo* [Khan and Abu-Amer, 2003; Klein et al., 2004; Lecka-Czernik et al., 2002]: Thereby, the generation of a mouse strain that overexpresses 12/15-lipoxygenase provided an osteopenic phenotype whereas pharmacological inhibition of 12/15-lipoxygenase in two further mouse models of osteoporosis could improve bone mass and strength. Thus, these *in vivo* studies clearly link excess adipogenesis to phenotypes of low bone mass.

Various other signalling pathways can also determine the osteogenic and adipogenic lineage, respectively. Accordingly, members of the BMP family and further factors induced by BMP signalling inhibited adipogenesis while osteogenesis was accelerated [Gimble et al., 1995; Ichida et al., 2004; Jaiswal et al., 2000].

Another important signalling pathway promoting either the osteogenic or the adipogenic lineage is Wnt signalling that comprises 19 secreted, cysteine-rich gycosylated proteins [Logan and Nusse, 2004; Miller et al., 1999]. These glycoproteins are involved in various processes, e.g. in embryonic formation of the body plan as well as in cell growth and differentiation. Frizzled (FZD) receptors mediate their functions and induce canonical or non-canonical Wnt signalling, the mechanisms of which have not been completely elucidated yet. The activation of the FZD receptor complex in canonical Wnt signalling prevents degradation of intracellular β-catenin thereby increasing intracellular protein levels. Subsequent translocation of stabilised β-catenin into the nucleus allows for heterodimerisation with transcription factors (Lef/Tcfs) that is necessary for activation of target gene transcription.

Thereby, several Wnt proteins and Wnt co-receptors can either activate or inhibit FZD receptors. While several Dickkopf proteins have agonistic and/or antagonistic effects on Wnt signalling, secreted frizzled receptor proteins (sFRPs) represent another class of inhibitors and low-density lipoprotein receptor-related protein 5 (LRP5) enhances non-canonical Wnt signalling [Glass and Karsenty, 2007]. Whereas canonical Wnt signalling generally activates osteogenic differentiation, e.g. by direct stimulation of RUNX2 gene expression [Gaur et al., 2005], non-canonical Wnt signalling can either stimulate or diminish osteogenesis (fig. 8). In contrast to osteogenesis-accelerating LRP5- and WNT10b-correlated signalling, WNT5b disrupts this signal transduction [Bennett et al., 2002; Gustafson and Smith, 2006; Kanazawa et al., 2005; Rawadi et al., 2003]. Thereby, WNT10b and WNT5b exhibit opposing effects on adipogenesis, i.e. their activity inhibits and promotes the adipogenic lineage, respectively.
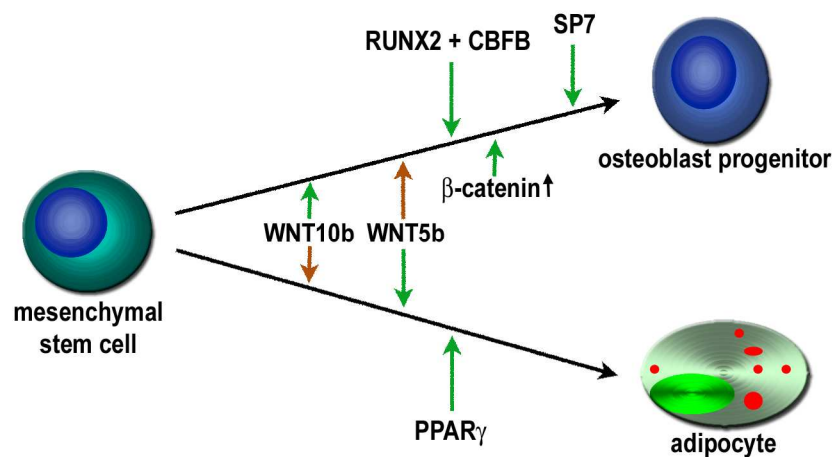


**Fig. 8      Reciprocal Wnt signalling affecting osteogenic and adipogenic differentiation**
Differentiation of MSCs is governed by the Wnt signalling pathway acting prior to expression of differentiation-inducing genes. Two members of Wnt signalling, i.e. WNT10b and WNT5b, have been reported to inhibit one lineage (brown arrow) while promoting the other (green arrow).

## 2.4   Transdifferentiation

Metaplasia or plasticity describes the conversion of one cell or tissue type into another. Thereby, this rather general term includes the conversion between undifferentiated stem cells as well as the switch between distinct differentiated cell or tissue types [Tosh and Slack, 2002]. In this work, usage of the terms 'transdifferentiation' or 'reprogramming' was restricted to describe the conversion of one "committed" or differentiated cell type into another, thereby not defining whether cells are directly switching from one phenoptype to another or if dedifferentiation followed by redifferentiation is required (fig. 9). Transdifferentiation moreover challenges the conventional, hierarchical view of the differentiation process where cells developing along a distinct lineage become determined, i.e. irreversibly committed to the pathway they commenced, and progress along the lineage-specific differentiation finally forming mature phenotypes [Caplan, 1991].
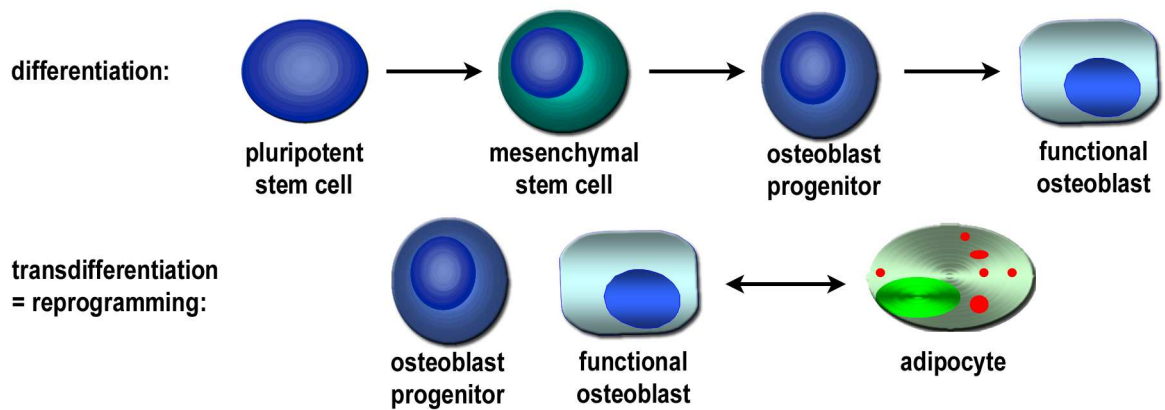
**Fig. 9      Models of differentiation and transdifferentiation**

During differentiation, pluripotent stem cells give rise to more restricted stem cells (e.g. MSCs) that differentiate into their terminal state (e.g. functional osteoblasts) via several cell divisions and intermediate phenotypes (e.g. osteoblast progenitors). Thus, progenitor cells have been considered to represent "committed" phenotypes having passed a "point of no return". In contrast, during transdifferentiation (reprogramming) one "committed" phenotype (e.g. (pre-)osteoblast) switches into another (e.g. adipocyte).

Nevertheless, the switch from one differentiated phenotype into another has been reported for conversion of pancreas into liver and vice versa, of myoblasts into adipocytes, and between osteoblast, adipocytes, and chondrocytes [Hu et al., 1995; Nuttall et al., 1998; Park et al., 1999; Ross et al., 2000; Song and Tuan, 2004]. However, some publications question the occurrence of transdifferentiation and rather attribute the phenotype change to cell fusion or heterogeneity of the cell population [Orkin and Zon, 2002; Terada et al., 2002; Verfaillie, 2002; Ying et al., 2002]. Indeed regarding *in vivo* experiments, fusion of bone marrow-derived stem cells with already differentiated cells of the target tissue has been reported for conversion into liver cells or into muscle cells, which are inherently capable of forming bi- and multinucleated phenotypes, respectively [Alvarez-Dolado et al., 2003; Rodic et al., 2004; Terada et al., 2002]. However, this issue is controversially discussed and does not meet our definition of a true transdifferentiation of already "committed" or differentiated cell types but rather shows plasticity of multipotential stem cells [Sato et al., 2005]. Additionally, due to the absence of differentiated cell types of another lineage *in vitro*, fusion can be excluded as a possible mechanism of metaplasia in these experiments. Regarding the criticism of possible heterogeneity, Song and Tuan [2004] even showed transdifferentiation of osteocalcin-expressing osteoblasts into adipocytes and chondrocytes, thus proving reprogramming at the single cell level and excluding heterogeneity as a reason *in vitro*.

## 2.5   Objective of this study

The age-related expansion of adipose tissue in the bone marrow and the concomitant loss of bone mass that is associated with diseases like osteoporosis have emphasised the requirement to further examine the correlation between the adipogenic and osteogenic differentiation pathway. Thereby, not only an impaired balance of conventional differentiation into adipocytes and osteoblasts starting from MSCs but also switching from one "committed" or differentiated phenotype into the other might contribute to the fatty degeneration.

Due to the paucity of work published hitherto regarding transdifferentiation between the adipogenic and osteogenic lineage, the present work aimed to establish a cell culture system based on human bone marrow-derived mesenchymal stem cells that would be capable of reprogramming between both lineages. Transdifferentiation of MSC-derived pre-osteoblasts and adipocytes into the respective other lineage, i.e. into adipocytes and osteoblasts, should help to elucidate the complex genetic reprogramming that was presumably required for the change of cell phenotype and function. Thus, microarray analyses were planned to examine global gene expression patterns arising shortly after initiation of adipogenic and osteogenic reprogramming. For the evaluation of regulated genes resulting from these analyses, a novel bioinformatic scoring scheme should be developed that would enable to filter out those gene products that are most likely to influence the onset of reprogramming. Finally, several of the highly ranked candidates should be addressed within functional analyses to determine their effect in differentiation and transdifferentiation events.

In summary, this study intended to

- establish a MSC-based cell culture system for adipogenic and osteogenic transdifferentiation
- examine global gene expression patterns early after initiation of transdifferentiation
- develop a novel bioinformatic scoring scheme providing the ranking of regulated genes according to their potential relevance for the onset of reprogramming
- examine the functional effect of highly-ranked gene products on differentiation and transdifferentiation.

The overall aim of this project was to identify presumable key factors of cell lineage switching, since the understanding of the underlying mechanisms of adipogenic and osteogenic reprogramming could help to develop novel therapeutic agents in the future that would not only prevent excess adipocyte formation but also stimulate osteogenesis in the bone marrow thus delaying the onset and alleviating the symptoms of age-related bone diseases.

# 3   Materials and methods

## 3.1   Materials

### 3.1.1   Consumables

| | |
|---|---|
| 96-well test plates | TPP, purchased from Biochrom AG, Berlin, Germany |
| Autoradiography films | Fuji, purchased from A. Hartenstein GmbH, Würzburg, Germany |
| AutoSeq G-50 columns | Amersham, purchased from GE Healthcare Europe GmbH, Munich, Germany |
| Blotting paper | Schleicher & Schuell, purchased from A. Hartenstein GmbH, Würzburg, Germany |
| Cell culture flasks (175 cm$^2$) | Greiner Bio-One GmbH, Frickenhausen, Germany |
| Cell culture flasks (25 cm$^2$, 75 cm$^2$, 150 cm$^2$) | TPP, purchased from Biochrom AG, Berlin, Germany |
| Cell strainers | BD Falcon, purchased from A. Hartenstein GmbH, Würzburg, Germany |
| Centrifugation tubes (15 ml, 50 ml) | TPP, purchased from Biochrom AG, Berlin, Germany |
| GeneChip HG-U 133A | Affymetrix UK Ltd., High Wycombe, UK |
| GeneChip HG-U 133 Plus 2.0 | Affymetrix UK Ltd., High Wycombe, UK |
| Lab-Tek Chamber Slides, Permanox (2-, 4-, and 8-well) | Nunc, purchased from A. Hartenstein GmbH, Würzburg, Germany |
| NucleoSEQ columns | Macherey-Nagel GmbH & Co. KG, Düren, Germany |
| Pasteur pipettes | A. Hartenstein GmbH, Würzburg, Germany |
| Pipette tips | Brandt, purchased from Laug & Scheller GmbH, Kürnach, Germany |
| Plastic pipettes, serological | Sarstedt AG & Co., Nümbrecht, Germany |
| Protran nitrocellulose transfer membrane | Whatman Schleicher & Schuell, purchased from A. Hartenstein GmbH, Würzburg, Germany |
| Reaction tubes (1.5 ml) | Sarstedt AG & Co., Nümbrecht, Germany |
| Sample tubes and caps for sequencing | Applied Biosystems Applera Deutschland GmbH, Darmstadt, Germany |
| Short plates | Bio-Rad Laboratories GmbH, Munich, Germany |
| Spacer plates with integrate spacers | Bio-Rad Laboratories GmbH, Munich, Germany |
| Sterile filter (0.2 µm) | Carl Roth GmbH & Co. KG, Karlsruhe, Germany |
| UVettes | Eppendorf AG, Hamburg, Germany |

### 3.1.2   Chemicals and reagents

| | |
|---|---|
| 2-Mercaptoethanol | AppliChem, purchased from A. Hartenstein GmbH, Würzburg, Germany |
| 2-Propanol | Carl Roth GmbH & Co. KG, Karlsruhe, Germany |

| | |
|---|---|
| 3-[(3-Cholamidopropyl)-dimethylammonio]-propane-sulfonate (CHAPS) | AppliChem, purchased from A. Hartenstein GmbH, Würzburg, Germany |
| 3-isobutyl-1-methylxanthine (IBMX) | AppliChem, purchased from A. Hartenstein GmbH, Würzburg, Germany |
| Acetic acid | Merck KGaA, Darmstadt, Germany |
| Acetone | AppliChem, purchased from A. Hartenstein GmbH, Würzburg, Germany |
| Agarose multi-purpose | Bioline GmbH, Luckenwalde, Germany |
| Albumin fraction V (pH 7.0) | AppliChem, purchased from A. Hartenstein GmbH, Würzburg, Germany |
| Albumin from bovine serum, cell culture tested (BSA) | Sigma-Aldrich Chemie GmbH, Schnelldorf, Germany |
| Alizarin red S | Chroma-Gesellschaft Schmidt & Co., Stuttgart, Germany |
| Ammonia solution (25%) | Merck KGaA, Darmstadt, Germany |
| Ammonium persulfate (APS) | Carl Roth GmbH & Co. KG, Karlsruhe, Germany |
| Boric acid | Merck KGaA, Darmstadt, Germany |
| Bromophenol blue sodium salt | Sigma-Aldrich Chemie GmbH, Schnelldorf, Germany |
| Chloral hydrate | Mallinckrodt Baker B. V., Deventer, Netherlands |
| Citric acid anhydrous | AppliChem, purchased from A. Hartenstein GmbH, Würzburg, Germany |
| Complete Protease Inhibitor Cocktail | Roche Diagnostics GmbH, Mannheim, Germany |
| Dexamethasone | Sigma-Aldrich Chemie GmbH, Schnelldorf, Germany |
| Dimethylsulfoxide (DMSO) | AppliChem, purchased from A. Hartenstein GmbH, Würzburg, Germany |
| Dithiothreitol (DTT) | AppliChem, purchased from A. Hartenstein GmbH, Würzburg, Germany |
| Dulbecco's phosphate buffered saline (PBS) powder | Biochrom AG, Berlin, Germany |
| Ethanol | AppliChem, purchased from A. Hartenstein GmbH, Würzburg, Germany |
| Ethanol, denatured | Carl Roth GmbH & Co. KG, Karlsruhe, Germany |
| Glacial acetic acid | Merck KGaA, Darmstadt, Germany |
| Glycerol 2-phosphate disodium salt hydrate | Sigma-Aldrich Chemie GmbH, Schnelldorf, Germany |
| Glycerol gelatine | Sigma-Aldrich Chemie GmbH, Schnelldorf, Germany |
| Glycerol | Merck KGaA, Darmstadt, Germany |
| Glycine | AppliChem, purchased from A. Hartenstein GmbH, Würzburg, Germany |
| Hematoxylin | Merck KGaA, Darmstadt, Germany |
| Heparin sodium salt | Sigma-Aldrich Chemie GmbH, Schnelldorf, Germany |
| Horse serum | PAA Laboratories GmbH, Pasching, Austria |
| Hydrochloric acid | Merck KGaA, Darmstadt, Germany |
| Indomethacin | Sigma-Aldrich Chemie GmbH, Schnelldorf, Germany |
| Insulin from bovine pancreas | Sigma-Aldrich Chemie GmbH, Schnelldorf, Germany |

| | |
|---|---|
| LE agarose | Biozym Scientific GmbH, Hessisch-Oldendorf, Germany |
| L-Ascorbic acid 2-phosphate sesquimagnesium salt | Sigma-Aldrich Chemie GmbH, Schnelldorf, Germany; |
| Methanol | AppliChem, purchased from A. Hartenstein GmbH, Würzburg, Germany |
| N,N,N',N'-tetramethylethylenediamine (TEMED) | Merck KGaA, Darmstadt, Germany |
| Oilred O | Merck KGaA, Darmstadt, Germany |
| peqGOLD 100 bp DNA Ladder Plus | PEQLAB Biotechnologie GmbH, Erlangen, Germany |
| Pharmalyte (pH 3 - 10) | Amersham, purchased from GE Healthcare Europe GmbH, Munich, Germany |
| Ponceau S solution | Sigma-Aldrich Chemie GmbH, Schnelldorf, Germany |
| Potassium aluminium sulfate | Merck KGaA, Darmstadt, Germany |
| Rainbow marker RPN 800 | Amersham, purchased from GE Healthcare Europe GmbH, Munich, Germany |
| Roti-Quant 5x concentrate | Carl Roth GmbH & Co. KG, Karlsruhe, Germany |
| Rotiphorese gel 40 (29:1) acrylamide/bisacrylamide mix | Carl Roth GmbH & Co. KG, Karlsruhe, Germany |
| Skim milk powder | AppliChem, purchased from A. Hartenstein GmbH, Würzburg, German |
| Sodium acetate | Carl Roth GmbH & Co. KG, Karlsruhe, Germany |
| Sodium chloride | AppliChem, purchased from A. Hartenstein GmbH, Würzburg, German |
| Sodium dodecyl sulfate (SDS) | Merck KGaA, Darmstadt, Germany |
| Sodium hydroxide pellets | Merck KGaA, Darmstadt, Germany |
| Sodium hydroxide solution (1 N) | AppliChem, purchased from A. Hartenstein GmbH, Würzburg, German |
| Sodium iodate | Merck KGaA, Darmstadt, Germany |
| Template Suppression Reagent | Applied Biosystems Applera Deutschland GmbH, Darmstadt, Germany |
| Thioglycolic acid | Sigma-Aldrich Chemie GmbH, Schnelldorf, Germany |
| Thiourea | Carl Roth GmbH & Co. KG, Karlsruhe, Germany |
| Triton X-100 | Carl Roth GmbH & Co. KG, Karlsruhe, Germany |
| Urea | Carl Roth GmbH & Co. KG, Karlsruhe, Germany |
| WST-1 cell proliferation agent | Roche Diagnostics GmbH, Mannheim, Germany |
| Xylene cyanol FF | Sigma-Aldrich Chemie GmbH, Schnelldorf, Germany |

## 3.1.3  Primers

### Tab. 1    Sequences of primers used for semi-quantitative RT-PCR expression analyses

| Primer sequences | | $T_A$ | Length of PCR product | Sequence ID |
|---|---|---|---|---|
| **adipose most abundant gene transcript 1 (APM1)** [a] | | | | |
| forward: 5'-GCTGGGAGCTGTTCTACTGC-3' | reverse: 5'-CGATGTCTCCCTTAGGACCA-3' | 59°C | 233 bp | NM_004797 |
| **alkaline phosphatase, liver/bone/kidney (ALP)** [a] | | | | |
| forward: 5'-TGGAGCTTCAGAAGCTCAACACCA-3' | reverse: 5'-ATCTCGTTGTCTGAGTACCAGTCC-3' | 51°C | 454 bp | NM_000478 |
| **apolipoprotein L domain containing 1 (APOLD1)** [f] | | | | |
| forward: 5'-CCAGGGGTACTCGGAAGG-3' | reverse: 5'-AGCAGCAGTCCCTGGAAG-3' | 55°C | 136 bp | NM_030817 |
| **Boc homolog (mouse) (BOC)** [a] | | | | |
| forward: 5'-CGTTGGCTTCAGACCTTTGT-3' | reverse: 5'-TTCATCCTTGGAGGTTCCAC-3' | 55°C | 222 bp | NM_033254 |
| **bone gamma-carboxyglutamate (gla) protein (osteocalcin) (OC)** [a] | | | | |
| forward: 5'-ATGAGAGCCCTCACACTCCTC-3' | reverse: 5'-GCCGTAGAAGCGCCGATAGGC-3' | 60°C | 294 bp | NM_199173 |
| **cDNA clone IMAGE:5263177 (AW274846)** [a] | | | | |
| forward: 5'-ATCAAAGCGACCCAAATGAC -3' | reverse: 5'-GCTTGGCGAAACCTCATTAC -3' | 53°C | 193 bp | AW274846 |
| **cDNA FLJ10145 fis, clone HEMBA1003322 (FLJ10145)** [a] | | | | |
| forward: 5'-CTGATGAGCTACGCAAACCA -3' | reverse: 5'-CCAAGAATAAACGGGCAAGA -3' | 56°C | 240bp | AK001007 |
| **centrosomal protein 55kDa (CEP55)** [a] | | | | |
| forward: 5'-AAGAAGGGCAGATGTGCAAC -3' | reverse: 5'-CATGCCTGCATCTGTTGTTC -3' | 55°C | 219 bp | NM_018131 |
| **chromosome 1 open reading frame 110 (C1orf110)** [a] | | | | |
| forward: 5'-AGTTCCAGCCCAGCTAGTGA -3' | reverse: 5'-AAGGCACCCTGTTTTCACAC -3' | 55°C | 308 bp | BC040018 |
| **chromosome 6 open reading frame 85 (C6orf85)** [a] | | | | |
| forward: 5'-ATTTTGCCTGGCTGGAATC -3' | reverse: 5'-TAGAGCAGCATGAGCAGGAA -3' | 53°C | 204 bp | NM_021945 |
| **chromosome 7 open reading frame 10 (C7orf10)** [a] | | | | |
| forward: 5'-GGAGCAGGAAATAACCAGCA-3' | reverse: 5'-GGACTCCACTGCCTTCAAAA-3' | 55°C | 193 bp | NM_024728 |
| **coiled-coil domain containing 69 (CCDC69)** [a] | | | | |
| forward: 5'-AGCAGGAGCTGGAGAGCTTA-3' | reverse: 5'-TTCTGACAGCTGCCTTGACA-3' | 55°C | 203 bp | NM_015621 |
| **cysteine-rich, angiogenic inducer, 61 (CYR61)** [a] | | | | |
| forward: 5'-CAACCCTTTACAAGGCCAGA-3' | reverse: 5'-TGGTCTTGCTGCATTTCTTG-3' | 55°C | 206 bp | NM_001554 |
| **D site of albumin promoter (albumin D-box) binding protein (DBP)** [g] | | | | |
| forward: 5'-CACTGGAGTGTGCTGGTGAC-3' | reverse: 5'-CTTGCGCTCCTTTTCCTTC-3' | 59°C | 244 bp | NM_001352 |
| **dual specificity phosphatase 6 (DUSP6)** [a] | | | | |
| forward: 5'-ACAGTGGTGCTCTACGACGA-3' | reverse: 5'-CAGTGACTGAGCGGCTAATG-3' | 55°C | 190 bp/ 627 bp | NM_001946, NM_022652 |
| **dual-specificity tyrosine-(Y)-phosphorylation regulated kinase 2 (DYRK2)** [b] | | | | |
| forward: 5'-GCCATGTAACCAGGAAACC-3' | reverse: 5'-TGCCGTCTATGAATGCTGTC-3' | 55°C | 255 bp | NM_003583, NM_006482 |
| **eukaryotic translation elongation factor 1 alpha 1 (EF1α)** [a] | | | | |
| forward: 5'-AGGTGATTATCCTGAACCATCC-3' | reverse: 5'-AAAGGTGGATAGTCTGAGAAGC-3' | 54°C | 235 bp | NM_001402 |
| **fatty acid binding protein 4, adipocyte (FABP4)** [a] | | | | |
| forward: 5'-AACCTTAGATGGGGGTGTCC-3' | reverse: 5'-ATGCGAACTTCAGTCCAGGT-3' | 57°C | 179 bp | NM_001442 |
| **fibroblast growth factor 1 (FGF1)** [a] | | | | |
| forward: 5'-CACAGTGGATGGGACAAGG-3' | reverse: 5'-CTTGAGGCCAACAAACCAAT-3' | 54°C | 250 bp | NM_000800 NM_033136 NM_033137 |
| **G0/G1 switch 2 (G0S2)** [a] | | | | |
| forward: 5'-CGTGCCACTAAGGTCATTCC-3' | reverse: 5'-TGCACACAGTCTCCATCAGG-3' | 57°C | 186 bp | NM_015714 |
| **hypothetical gene supported by BC072410 (LOC440416)** [a] | | | | |
| forward: 5'-CGTGATTAGCCTTCTTCAGCA-3' | reverse: 5'-GGTAAGGATGTACAGGAAAAATCA-3' | 55°C | 193 bp | AA166965 |
| **hypothetical protein FLJ37034 (FLJ37034)** [a] | | | | |
| forward: 5'-TGGGGATGGAGATGTTTGAT-3' | reverse: 5'-GAGCAAGCTGGTCTGGAAAG-3' | 55°C | 172 bp | H16258 |
| **hypothetical protein MGC4655 (MGC4655)** [e] | | | | |
| forward: 5'-GTCCCCCTTCCTGCCAAC-3' | reverse: 5'-AGCCCCTTGCGTTGTTCT-3' | 55°C | 175 bp | NM_033309 |
| **insulin-like growth factor 1 (somatomedin C) (IGF1)** [a] | | | | |
| forward: 5'-TGGATGCTCTTCAGTTCGTG-3' | reverse: 5'-CTGACTTGGCAGGCTTGAG-3' | 51°C | 177 bp | NM_000618 |
| **insulin-like growth factor binding protein 5 (IGFBP5)** [a] | | | | |
| forward: 5'-GACCGCAGAAAGAAGCTGAC-3' | reverse: 5'-GAATCCTTTGCGGTCACAAT-3' | 55°C | 210 bp | NM_000599 |
| **interleukin 8 (IL8)** [a] | | | | |
| forward: 5'-AAGGAAAACTGGGTGCAGAG-3' | reverse: 5'-CCCTACAACAGACCCACACA-3' | 57°C | 163 bp | NM_000584 |
| **KIAA1199 (KIAA1199)** [f] | | | | |
| forward: 5'-ATAACACGTGACCGGCATT-3' | reverse: 5'-CTCCAGTCGGGAACATTGAT-3' | 55°C | 223 bp | NM_018689 |
| **kruppel-like factor 4 (gut) (KLF4)** [a] | | | | |
| forward: 5'-GCCACCCACACTTGTGATTA-3' | reverse: 5'-ATGTGTAAGGCGAGGTGGTC-3' | 57°C | 245 bp | NM_004235 |
| **kruppel-like factor 6 (KLF6)** [a] | | | | |
| forward: 5'-CTCATGGGAAGGGTGTGAGT-3' | reverse: 5'-CAGGATCCACCTCTCTGCTC-3' | 55°C | 179 bp | NM_001300 |

| Primer sequences | | $T_A$ | Length of PCR product | Sequence ID |
|---|---|---|---|---|
| **lipoprotein lipase (LPL)** [a] | | | | |
| forward: 5'-GAGATTTCTCTGTATGGCACC-3' | reverse: 5'-CTGCAAATGAGACACTTTCTC-3' | 51℃ | 275 bp | NM_000237 |
| **nuclear receptor subfamily 4, group A, member 2 (NR4A2)** [a] | | | | |
| forward: 5'-TTTCTGCCTTCTCCTGCATT-3' | reverse: 5'-TGTGTGCAAAGGGTACGAAG-3' | 55℃ | 205 bp | NM_006186, NM_173171, NM_173172, NM_173173 |
| **peroxisome proliferator-activated receptor, gamma 2 (PPARγ2)** [a] | | | | |
| forward: 5'-GCTGTTATGGGTGAAACTCTG-3' | reverse: 5'-ATAAGGTGGAGATGCAGGCTC-3' | 51℃ | 350 bp | NM_005037, NM_015869, NM_138711, NM_138712 |
| **protein kinase C-like 2 (PRKCL2)** [a] | | | | |
| forward: 5'-ATGATGTCTGTGCTGTTTTGAAG-3' | reverse: 5'-GCCAATCACGCCAATAAACT-3' | 55℃ | 150 bp | NM_006256 |
| **prostaglandin E receptor 4 (subtype EP4) (PTGER4)** [c] | | | | |
| forward: 5'-TCATCTTACTCATTGCCACCTC-3' | reverse: 5'-TCACAGAAGCAATTCGGATG-3' | 58℃ | 150 bp | NM_000958 |
| **regulator of G-protein signalling 2, 24kDa (RGS2)** [a] | | | | |
| forward: 5'-AGCTGTCCTCAAAAGCAAGG-3' | reverse: 5'-CCCTTTTCTGGGCAGTTGTA-3' | 55℃ | 150 bp | NM_002923 |
| **regulator of G-protein signalling 4 (RGS4)** [a] | | | | |
| forward: 5'-AGTCCCAAGGCCAAAAAGAT-3' | reverse: 5'-ACGGGTTGACCAAATCAAGA-3' | 55℃ | 220 bp | NM_005613 |
| **scavenger receptor class A, member 5 (putative) (SCARA5)** [a] | | | | |
| forward: 5'-GGGGTGGGGAGTAGGAATAA-3' | reverse: 5'-GTTTGAGATTCCCCCAAGGT-3' | 55℃ | 194 bp | NM_173833 |
| **secreted frizzled-related protein 2 (SFRP2)** [a] | | | | |
| forward: 5'-AAAGGTATGTGAAGCCTGCAA-3' | reverse: 5'-TTGCTCTTGGTCTCCAGGAT-3' | 54℃ | 150 bp | NM_003013 |
| **serine/threonine kinase 38 like (STK38L)** [a] | | | | |
| forward: 5'-GAAAGGCCAGCAGCAATC-3' | reverse: 5'-GGGATAGAGCCACGTTGAGT-3' | 55℃ | 191 bp | NM_015000 |
| **serpin peptidase inhibitor, clade E (nexin, plasminogen activator inhibitor type 1), member 1 (SERPINE1)** [a] | | | | |
| forward: 5'-CCGAGGAGATCATCATGGAC-3' reverse: 5'-GGAGTTTCTTCTTTCCCGATG-3' | | 57℃ | 158 bp | NM_000602 |
| **solute carrier family 2 (facilitated glucose transporter), member 3 (SLC2A3)** [a] | | | | |
| forward: 5'-TCGCATCATTGCACTCTAGC-3' reverse: 5'-AAATGGGACCCTGCCTTACT-3' | | 55℃ | 167 bp | NM_006931 |
| **transmembrane protein 64 (TMEM64)** [a] | | | | |
| forward: 5'-CATCTTCGGTTGGACTGCTT-3' | reverse: 5'-GAGCCACTGGTATTTGGTTGA-3' | 60℃ | 256 bp | NM_001008495 |
| **transmembrane protein 166 (TMEM166)** [a] | | | | |
| forward: 5'-CAGGACATGCCCCTTTTCTA-3' | reverse: 5'-TTTCTCCGATCTCCATCCAC-3' | 55℃ | 151 bp | NM_032181 |
| **transmembrane protein 173 (TMEM173)** [f] | | | | |
| forward: 5'-GAGCAGGCCAAACTCTTCTG-3' | reverse: 5'-TGATGAGGAGCTCAGGCTCT-3' | 55℃ | 241 bp | NM_198282 |
| **tumor necrosis factor receptor superfamily, member 11b (osteoprotegerin) (TNFRSF11B)** [a] | | | | |
| forward: 5'-TAAAACGGCAACACAGCTCA-3' | reverse: 5'-GCCTCAAGTGCCTGAGAAAC-3' | 55℃ | 568 bp | NM_002546 |
| **zinc finger CCCH-type containing 12D (ZC3H12D)** [d] | | | | |
| forward: 5'- GTTCATGCCGCCTGATGAC -3' | reverse: 5'- TCTCCGGGTGGTAGAACTTG -3' | 55℃ | 155 bp | AK090441 |
| **zinc finger protein 331 (ZNF331)** [a] | | | | |
| forward: 5'-GGCCTGTCTGAACTCTGCTC-3' | reverse: 5'-ACGGCCAAGGGATTTACTTC-3' | 55℃ | 184 bp | NM_018555 |

Forward and reverse sequences of primers, the annealing temperature ($T_A$) for each primer pair, the expected length of the PCR product, and the sequence ID (preferably the reference sequence ID, if available) of the NCBI data base are stated. Superscripts indicate the type of PCR reaction mix as follows: a = standard PCR mix, b = 2.25 mM $MgCl_2$, c = 3.75 mM $MgCl_2$, d = 2% DMSO, e = 4% DMSO, f = 6% DMSO, g = 3.75 mM $MgCl_2$ and 8% DMSO. Due to the existence of alternative splice variants of the dual specifity phosphatase 6 mRNA, two PCR products of different length can be generated.

### 3.1.4 Recombinant proteins

| | |
|---|---|
| rhCYR61 | purified at the Orthopedic Clinic, Orthopedic Centre for Musculoskeletal Research, Molecular Orthopedics and Cell Biology by Susanne Jatzke and Rita Wagemanns |
| rhFGF acidic = rhFGF1 | R&D Systems, Wiesbaden-Nordenstadt, Germany |

| rhIGF-I = rhIGF1 | R&D Systems, Wiesbaden-Nordenstadt, Germany |
| rhOPG/TNFRSF11B = rhTNFRSF11B | R&D Systems, Wiesbaden-Nordenstadt, Germany |
| rmSFRP2 | R&D Systems, Wiesbaden-Nordenstadt, Germany |

Stock solutions of lyophilized proteins purchased from R&D Systems were prepared in 0.1% BSA in PBS at concentrations of 50 µg/ml rhFGF1, 100 µg/ml rhIGF1, 50 µg/ml TNFRSF11B, and 100 µg/ml rmSFRP2. Appropriate aliquots were stored at -20°C for up to 6 months. Thawed stock solutions were stored at 4°C for up to 4 weeks. For several experiments, rhFGF1 stock solution was further diluted to 10 µg/ml after thawing and stored at 4°C for up to 4 weeks.

RhCYR61 was extracted with 3 M Tris-glycine, pH 7 from the supernatants of virus-transfected SF-21 insect cells as described [Schütze et al., 2005a] and stored at 4°C. Protein concentration was measured directly before application by micro-Bradford analysis (see chapter 3.2.4.3).

### 3.1.5  Antibodies

| Anti-actin IgG fraction of antiserum | Sigma-Aldrich Chemie GmbH, Schnelldorf, Germany |
| Anti-FGF acidic antibody | R&D Systems, Wiesbaden-Nordenstadt, Germany |
| Anti-goat IgG-HRP antibody | R&D Systems, Wiesbaden-Nordenstadt, Germany |
| Anti-rabbit IgG peroxidase conjugate | Sigma-Aldrich Chemie GmbH, Schnelldorf, Germany |

### 3.1.6  Enzymes

| Amersham *Taq* DNA polymerase | GE Healthcare Europe GmbH, Munich, Germany |
| BIOTAQ DNA polymerase | Bioline GmbH, Luckenwalde, Germany |
| MangoTaq DNA polymerase | Bioline GmbH, Luckenwalde, Germany |
| BioScript RT | Bioline GmbH, Luckenwalde, Germany |
| SuperScript II RT | Invitrogen GmbH, Karlsruhe, Germany |
| 25% Trypsin (10x concentrate) | PAA Laboratories GmbH, Pasching, Austria |

### 3.1.7  Buffers and other solutions

**_Solutions for molecular biology_**

**_0.5 M EDTA, pH 8.0_**
   19 g       EDTA tetrasodium salt hydrate
   ad 100 ml distilled water
   pH adjusted to 8.0 and autoclaved

**_10% SDS_**
   10 g       sodium dodecyl sulfate
   ad 100 ml distilled water

**_3 M Sodium acetate (pH 4.3)_**
   24.6 g    sodium acetate
   ad 100 ml distilled water
   pH adjusted to 4.3

*10x TBE*
  108 g    Tris base
  55 g      boric acid
  9.05 g    EDTA tetrasodium salt hydrate
  ad 1 l distilled water
  pH adjusted to 8.3 and autoclaved

*50 mM Tris base*
  3.03 g    Tris base
  ad 500 ml distilled water
  pH adjusted to 7.2 - 7.5 and autoclaved
  for 10 mM Tris base diluted 1:5 with distilled water

*10x Loading dye*
  5 mg      bromophenol blue sodium salt
  5 mg      xylene cyanol FF
  4 ml       distilled water
  2 ml       0.5 M EDTA, pH 8.0
  3 ml       glycerol
  1 ml       10% SDS
  The filtered solution is stored at 4°C.


## Solutions for cell culture

*1x PBS*
  9.55 g    PBS Dulbecco w/o $Ca^{2+}$, $Mg^{2+}$
  ad 1 l distilled water
  pH adjusted to 7.4 and autoclaved

*1x PBS/EDTA*
  9.55 g    PBS Dulbecco w/o $Ca^{2+}$, $Mg^{2+}$
  0.2 g      EDTA tetrasodium salt hydrate
  ad 1 l distilled water
  pH adjusted to 7.4 and autoclaved

*2.5% Trypsin*
  5 ml      25% trypsin (sterile)
  ad 50 ml 1x PBS


## Solutions for protein preparation

*Lysis buffer*
  42.04 g  urea
  15.22 g  thiourea
  4 g       CHAPS
  0.77 g    DTT
  0.12 g    Tris base
  2 ml       Pharmalyte (pH 3 - 10)
  ad 100 ml distilled water and stored at 4°C.

*25x Complete protease inhibitor cocktail*
  1 tablet Complete protease inhibitor cocktail was dissolved in 2 ml distilled water and stored in aliquots at -20°C.
  Complete protease inhibitor cocktail was added to lysis buffer immediately before use to obtain a final concentration of 1x.

## *Solutions for staining*

### *4% Paraformaldehyde solution*
4 g paraformaldehyde was dissolved in about 75 ml 1x PBS at 55 - 60°C under stirring for 5 min. 100 - 150 µl sodium hydroxide was added until the solution became clear. After cooling down to room temperature, the pH was adjusted to 7.4 and the solution was filled up to 100 ml with 1x PBS.

### *0.5% Oilred O stock solution*
0.5 g      Oilred O
ad 100 ml 99% 2-propanol
0.3% Oilred O working solution was prepared by mixing 6 parts stock solution with 4 parts distilled water, incubated over night and filtrated before use.

### *Hemalaun solution*
1 g        Hematoxylin
dissolved in 1 l distilled water
plus
0.2 g      sodium iodate
50 g       potassium aluminium sulfate
50 g       chloral hydrate
1 g        citrate

## *Solutions for SDS-PAGE*

### *0.5% Bromophenol blue*
50 mg     bromophenol blue sodium salt
ad 10 ml distilled water

### *10% APS*
1 g        ammonium persulfate
ad 10 ml distilled water
storage in aliquots at -20°C

### *Upper buffer*
*4x stock solution:*

6.8 g      Tris base
28.55 g   glycine
2 g        SDS
ad 500 ml distilled water

*working solution:*

100 ml   4x stock solution
84 µl      thioglycolic acid
ad 400 ml distilled water

### *Lower buffer*
*10x stock solution:*

15.1 g    Tris base
71.4 g    glycine
ad 500 ml distilled water

*working solution:*

100 ml   stock solution
ad 1 l distilled water

*Separating gel buffer = 3 M Tris base, pH 8.8*
  363.42 g Tris base
  ad 1 l distilled water
  pH adjusted to 8.8

*Stacking gel buffer = 0.5 M Tris base, pH 6.8*
  60.57 g   Tris base
  ad 1 l distilled water
  pH adjusted to 6.8

*Sample buffer*

  *20x stock solution:*

  1.2 ml     0.5 M Tris base, pH 6.8
  1 ml        glycerol
  2 ml        10% SDS
  0.5 ml     0.5% bromophenol blue
  ad 9.5 ml distilled water
  stored at 4°C

  *working solution:*

  950 µl     stock solution
  50 µl       2-mercaptoethanol


### **Solutions for Western blotting**

*0.25 M EDTA, pH 8*
  9.5 g        EDTA tetrasodium salt hydrate
  ad 100 ml distilled water
  pH adjusted to 8

*5 M sodium chloride*
  58.44 g   sodium chloride
  ad 1 l distilled water

*1 M Tris-HCl, pH 7.5*
  121.14 g Tris-base
  ad 1 l distilled water
  pH adjusted to 7.5 by addition of hydrochloric acid

*10% Triton X-100*
  10 ml      Triton X-100
  ad 100 ml distilled water

*0.1% Tween 20*
  999 ml    1x PBS
  1 ml        Tween 20

*Transfer buffer*

  *10x stock solution:*

  30 g        Tris base
  144 g      glycine
  ad 1 l distilled water
  pH adjusted to 10 by addition of sodium hydroxide pellets

  *working solution:*

  100 ml    stock solution
  200 ml    methanol
  ad 1 l distilled water

*Washing buffer I*
    10 ml     1 M Tris-HCl, pH 7.5
    30 ml     5 M sodium chloride
    8 ml      0.25 M EDTA, pH 8
    10 ml     10% Triton X-100
    ad 1000 ml distilled water

*Washing buffer II*
    10 ml     1 M Tris-HCl, pH 7.5
    200 ml   5 M sodium chloride
    8 ml      0.25 M EDTA, pH 8
    10 ml     10% Triton X-100
    ad 1000 ml distilled water

The following solutions were always prepared freshly before use (amounts for 2 mini gels):

*Blocking solution*
    1.25 g   BSA
    1.25 g   skim milk powder
    1 ml     horse serum
    ad 50 ml 0.1% Tween 20

*Primary antibody solution*
    0.25 g   BSA
    0.25 g   skim milk powder
    0.25 ml  horse serum
    ad 25 ml 0.1% Tween 20
    plus appropriate dilution of the respective primary antibodies

*Secondary antibody solution*
    0.4 g    BSA
    0.4 g    skim milk powder
    0.4 ml   horse serum
    ad 40 ml 0.1% Tween 20
    plus appropriate dilution of the respective secondary antibodies

*Washing solution I*
    2 g      BSA
    2 g      skim milk powder
    2 ml     horse serum
    ad 200 ml washing buffer I

*Washing solution II*
    2 g      BSA
    2 g      skim milk powder
    2 ml     horse serum
    ad 200 ml washing buffer II

### 3.1.8  Cell culture media and additives

| | |
|---|---|
| DMEM/Ham's F-12 with L-Glutamine | PAA Laboratories GmbH, Pasching, Austria |
| DMEM high glucose (4.5 g/l) with L-Glutamine | PAA Laboratories GmbH, Pasching, Austria |
| FBS | GIBCO purchased from Invitrogen GmbH, Karlsruhe, Germany and PAA Laboratories GmbH, Pasching, Austria |

Penicillin/streptomycin 100x                          PAA Laboratories GmbH, Pasching, Austria


### *stock solutions*

*50 mg/ml L-Ascorbic acid 2-phosphate sesquimagnesium salt*
  in distilled water, sterile filtered, stored in aliquots at -20°C

*1 mM Dexamethasone*
  in ethanol, stored in aliquots at -80°C

*1 M Glycerol 2-phosphate disodium salt hydrate*
  in distilled water, sterile filtered, stored in aliquots at -20°C

*100 mM Indomethacin*
  in DMSO, stored in aliquots at -20°C

*1 mg/ml Insulin from bovine pancreas*
  in 0.05% acetic acid, sterile filtered, stored in aliquots at -20°C

*500 mM 3-Isobutyl-1-methylxanthine (IBMX)*
  in DMSO, stored in aliquots at -20°C

## 3.1.9   Kits

| | |
|---|---|
| Alkaline Phosphatase, Leukocyte Kit 86-C | Sigma-Aldrich Chemie GmbH, Schnelldorf, Germany |
| Big Dye Terminator v1.1 Cycle Sequencing | Applied Biosystems Applera Deutschland GmbH, Darmstadt, Germany |
| NucleoSpin RNA/Protein | Macherey-Nagel GmbH & Co. KG, Düren, Germany |
| Plus One 2D-Quant | Amersham, purchased from GE Healthcare Europe GmbH, Munich, Germany |
| RNeasy Mini | QIAGEN GmbH, Hilden, Germany |

## 3.1.10  Equipment

| | |
|---|---|
| Accu-jet pipettor | Brand, purchased from A. Hartenstein GmbH, Würzburg, Germany |
| Affymetrix Scanner 2500 and 3000 | Affymetrix UK Ltd., High Wycombe, UK |
| Autoclave H+P varioclave steam steriliser | THERMO ELECTRON GmbH, Oberschleißheim, Germany |
| Balances: Scaltec-SPO51 and Kern 77 | purchased from A. Hartenstein GmbH, Würzburg, Germany |
| BioPhotometer | Eppendorf AG, Hamburg, Germany |
| Centrifuge Heraeus Biofuge pico | THERMO ELECTRON GmbH, Oberschleißheim, Germany |
| Centrifuge Heraeus Labofuge 400 | THERMO ELECTRON GmbH, Oberschleißheim, Germany |
| $CO_2$ incubator Heraeus B5060 | THERMO ELECTRON GmbH, Oberschleißheim, Germany |
| Digital cameras: | |
|    Roper Scientific camera | Chromaphor Analysen-Technik GmbH, Duisburg, Germany |
|    AxioCam MRc | Carl Zeiss Jena GmbH, Jena, Germany |

| | |
|---|---|
| Electrophoresis power supplies | Bio-Rad Laboratories GmbH, Munich, Germany |
| | Consort, Turnhout, Belgium |
| Freezer Bosch Economic (-20°C) | Bosch GmbH, Gerlinge n-Schillerhöhe, Germany |
| Freezer IlShin (-80°C) | Nunc GmbH & Co. KG, Wiesbade n, Germany |
| Glassware | Schott, purchased from A. Hartenstein GmbH, Würzburg, Germany |
| Heating block | Boekel Scientific, purchased from A. Hartenstein GmbH, Würzburg, Germany |
| Horizontal shaker | A. Hartenstein GmbH, Würzburg, Germany |
| Hot air steriliser | Heraeus, purchased from THERMO ELECTRON GmbH, Oberschleißheim, Germany |
| Horizontal mini gel electrophoresis system EasyCast Model B2 | VWR International GmbH, Darmstadt, Germany |
| Laboratory dishwasher | Miele & Cie. KG, Gütersloh, Germany |
| Laminar airflow cabinet HERA safe | THERMO ELECTRON GmbH, Oberschleißheim, Germany |
| Magnetic stirrer and heater | A. Hartenstein GmbH, Würzburg, Germany |
| Micro-pipettes | ABIMED Analysentechnik GmbH, Langenfeld, Germany |
| Microscopes: Axiovert 25, Axioskop, and Axioskop 2 MOT | Carl Zeiss Jena GmbH, Jena, Germany |
| pH-meter inolab pH level 1 | WTW, purchased from A. Hartenstein GmbH, Würzburg, Germany |
| Photometer SLT Spectra Classic | Tecan Deutschland GmbH, Crailsheim, Germany |
| Refrigerator Fresh Center | Bosch GmbH, Gerlingen-Schillerhöhe, Germany |
| Sequencer ABI PRISM 310 Genetic Analyser | Applied Biosystems Applera Deutschland GmbH, Darmstadt, Germany |
| Sonificator Sonopuls | Bendelin electronic GmbH & Co. KG, Berlin, Germany |
| Thermal cycler PTC-200 | MJ Research, purchased from Biozym Scientific GmbH, Hessisch Oldendorf, Germany |
| Thermal printer | Seico, purchased from -ltf- Labortechnik GmbH & Co. KG, Wasserburg, Germany |
| Vacuum pump system | Vacuubrand, purchased from A. Hartenstein GmbH, Würzburg, Germany |
| Vertical gel electrophoresis system Mini-TransBlot electrophoretic transfer cell | Bio-Rad Laboratories GmbH, Munich, Germany |
| Vortexer Vortex-Genie 2 | Scientific Industries, purchased from A. Hartenstein GmbH, Würzburg, Germany |
| Water bath WB7 | Memmert, purchased from A. Hartenstein GmbH, Würzburg, Germany |
| Western blot device PerfectBlue semi-dry electroblotter | PEQLAB Biotechnologie GmbH, Erlangen, Germany |
| X-ray film cassette | Amersham, purchased from GE Healthcare Europe GmbH, Munich, Germany |

### 3.1.11 Software and online sources

| | |
|---|---|
| ABI PRISM 310 collection software | Applied Biosystems Applera Deutschland GmbH, Darmstadt, Germany |
| AxioVision 4.4.1.0 | Carl Zeiss Vision GmbH, Aalen, Germany |
| Bio-Capt 12.5 and Bio-1D 11.9 | -ltf- Labortechnik GmbH & Co. KG, Wasserburg, Germany |
| Data Mining Tool 3.0 and 3.1 | Affymetrix UK Ltd., High Wycombe, UK |
| Endnote 9.0.1 | Thomson, purchased from University of Würzburg, Germany |
| GeneChip Operating Software 1.2 | Affymetrix UK Ltd., High Wycombe, UK |
| Image-Pro Plus 4.1 | Media Cybernetics, purchased from Chromaphor Analysen-Technik GmbH, Duisburg, Germany |
| Magellan 3.00 | Tecan Deutschland GmbH, Crailsheim, Germany |
| Microarray Suite 5.0 | Affymetrix UK Ltd., High Wycombe, UK |
| Office Excel 2002 | Microsoft Deutschland GmbH, Unterschleißheim, Germany |
| Office Word 2002 | Microsoft Deutschland GmbH, Unterschleißheim, Germany |
| Photoshop Elements 4.0 | Adobe, purchased from University of Würzburg, Germany |
| Sequencing analysis software | Applied Biosystems Applera Deutschland GmbH, Darmstadt, Germany |

| | |
|---|---|
| e! Ensembl Human | http://www.ensembl.org/Homo_sapiens |
| GeneCards | http://www.genecards.org |
| GOstat analysis | http://gostat.wehi.edu.au |
| Invitrogen iPath | http://escience.invitrogen.com/ipath |
| NCBI Blast | http://www.ncbi.nlm.nih.gov/BLAST |
| NCBI Pubmed | http://www.ncbi.nlm.nih.gov/entrez/query.fcgi?DB=pubmed |
| NetAffx analysis Center | http://www.affymetrix.com/analysis/index.affx |
| Primer3 | http://frodo.wi.mit.edu/cgi-bin/primer3/primer3_www.cgi |

## 3.2 Methods

### 3.2.1 Isolation of human mesenchymal stem cells

Isolation of human MSCs was performed under the approval of the Local Ethics Committee of the University of Würzburg as well as with the informed consent of each patient, in the case of one underaged patient (10 years old) with the informed consent of the parents. Donors were aged 10 - 76 years, in average 57 ± 14 years (mean ± standard deviation, n = 51). The femoral heads of patients were removed during total hip joint replacement surgery due to dysplasia-related or age-related attrition of the joint. Thereby, it was assured that none of the patients received any pharmaceuticals affecting bone metabolism.
MSCs were obtained from trabecular bone following a modified isolation protocol described previously [Nöth et al., 2002b; Schütze et al., 2005a] and originally published by Haynesworth et al. [1992]. Shortly, the cancellous bone was collected and washed once with propagation medium (see next section) by centrifugation at 1200 rpm for 5 min and discarding of the supernatant to remove any fatty components. Subsequent washing of the remaining pellet by vortexing 5 times with 10 ml propagation medium released stromal cells. Thereby, after each vortexing step, the propagation medium enriched with stromal cells was filtered through a cell strainer to hold back bone fragments and collected in a fresh tube. After final centrifugation at 1200 rpm for 5 min, the cell pellet was resuspended in a known volume of propagation medium. Cell number and vitality were determined by mixing 50 µl cell

suspension with 50 µl Trypan blue and counting in a Neubauer counting chamber according to Lindl [2002] using the following equations:

$$cell\ number / ml = \frac{sum\ of\ living\ cells}{number\ of\ counted\ quadrants} \cdot 10^4 \cdot 2$$

$$vitality = percentage\ of\ living\ cells = \frac{sum\ of\ living\ cells}{sum\ of\ living\ cells + sum\ of\ dead\ cells}$$

The stromal cells were seeded at a density of more than $10^6$ cells/cm$^2$ into 150 cm$^2$ or 175 cm$^2$ cell culture flasks and incubated at 37°C in a humidified atmosphere with 5% $CO_2$ and 95% air. About 3 days after isolation, the supernatant containing non-adherent blood cells was removed, the MSCs selected by plastic adherence were washed with PBS and further incubated in fresh propagation medium.

### 3.2.2   Cell culture of human mesenchymal stem cells

#### 3.2.2.1   *Culture and propagation*

MSCs were cultured as described previously [Nöth et al., 2002b; Schütze et al., 2005a] in propagation medium consisting of DMEM/Ham's F-12 with L-Glutamine, 10% heat-inactivated FBS, 1x penicillin/streptomycin (final concentrations: 1 U/ml and 100 µg/ml, respectively), and 50 µg/ml L-ascorbic acid 2-phosphate. Cultures of MSCs at passage 0 usually reached confluence after 2 weeks. During this time, propagation medium was replaced every 3 - 4 days. Subsequently, cells were detached by exposure to PBS/EDTA for 10 min, addition of the same volume of 0.25% trypsin and further incubation for 2 min, both at 37°C. Addition of propagation medium inactivated the trypsin. The cells were pelleted by centrifugation (1200 rpm for 5 min), resuspended in fresh propagation medium, and the cell number and vitality were assessed.
For further propagation, cells were split at a ratio of 1:3 into new cell culture flasks. For experimental settings, MSCs of passages 0 to 3 were employed. Plating densities for these assays depended on the further applications of the cells (see next sections).

#### 3.2.2.2   *Differentiation*

Differentiation of confluent MSC monolayers was started in passage 1 or 2 by incubation in the respective differentiation medium. Adipogenic differentiation medium consisted of DMEM high Glucose with L-Glutamine, 10% heat-inactivated FBS, and 1x penicillin/streptomycin additionally containing 1 µM dexamethasone, 100 µM indomethacin, 500 µM IBMX, and 1 µg/ml insulin [Pittenger et al., 1999]. For osteogenic differentiation medium, normal propagation medium was supplemented with 10 mM glycerol 2-phosphate and 100 nM dexamethasone [Jaiswal et al., 1997]. MSCs were differentiated up to 3 weeks in adipogenic medium and for up to 4 weeks in osteogenic medium. Differentiation media were replaced every 2 - 3 days.
In the course of this doctorate, the usage of DMEM high glucose instead of DMEM/Ham's F-12 as basis for the osteogenic differentiation medium was found to accelerate the efficiency of osteogenic differentiation. DMEM high glucose with L-Glutamine plus 10% heat-inactivated FBS, and 1x penicillin/streptomycin, 50 µg/ml L-ascorbic acid 2-phosphate, 10 mM glycerol 2-phosphate, and 100 nM dexamethasone was therefore applied in all experiments regarding functional testing of recombinant proteins and protein analyses.
Control samples of post-confluent MSCs were cultured in control medium consisting of DMEM high Glucose with L-Glutamine, 10% heat-inactivated FBS, and 1x penicillin/streptomycin but without differentiation factors, since cells frequently detached when propagation medium was used for post-confluent incubation.

### 3.2.2.3  Transdifferentiation

Transdifferentiation experiments were started in passage 0 to 2 as soon as MSCs had reached confluence. Incubation of MSCs in osteogenic differentiation medium for 5, 10, and 14 to 15 d gave rise to pre-osteoblasts that were subjected to transdifferentiation (reprogramming) into adipocytes by subsequent incubation in adipogenic medium for 14 d. Fully differentiated adipocytes, obtained after 14 d in adipogenic medium, were transdifferentiated (reprogrammed) into osteoblasts by incubation in osteogenic medium for another 28 d. In parallel with the change of medium for initiation of transdifferentiation, control samples undergoing normal differentiation obtained fresh differentiation medium of the same kind as before. Differentiation media for all samples were replaced in parallel every 2 - 3 days.

### 3.2.2.4  Proliferation assay

The cell proliferation reagent WST-1 enables the spectrophotometric quantification of cell proliferation. As a tetrazolium salt, WST-1 (4-[3-(4-Iodophenyl)-2-(4-nitrophenyl)-2H-5-tetrazolio]-1,3-benzene disulfonate) is cleaved by mitochondrial dehydrogenases into formazan, which is accompanied by a change of colour from slightly red to dark red. Since cell proliferation augments the activity of mitochondrial dehydrogenases, the amount of formazan dye formed is directly proportional to the metabolic activity of proliferating cells and can be quantified by measurement of the absorbance at a wavelength of 450 nm.
To examine the potential proliferative effect of rhFGF1, MSCs were seeded in subconfluent and confluent settings with 4,000 and 13,000 cells per well of a 96-well test plate, respectively. Some wells were left empty to serve as control for the absorption of the media themselves. Approximately 24 h after seeding, MSCs were exposed to various media for another 48 h as stated in tab. 2. Thereby, the control medium consisted of DMEM high Glucose with L-Glutamine, 10% heat-inactivated FBS, and 1x penicillin/streptomycin, which served as the basis for both differentiation media.
WST-1 reagent was added to each well at a final dilution of 1:10. Absorbance was repeatedly measured 15 min to 2 h after addition of WST-1 reagent. Statistical analysis was performed with Microsoft Office Excel 2002. Mean ± SEM was calculated for each incubation condition. Mean extinction values were corrected by subtraction of the background absorbance mean value. Percentage of proliferation change was obtained by comparison of mean extinctions of specimens incubated with rhFGF1 and/or heparin to those incubated in sole control medium.

**Tab. 2    Incubation conditions for proliferation assay**

| no cells | control medium | | | | | |
|---|---|---|---|---|---|---|
| | adherent MSCs | | | | | |
| | | | plus 20 U/ml heparin | | | |
| | | | | plus rhFGF1 [ng/ml] | | |
| | | | | 6 | 12 | 25 | 50 |
| ≥ 5 wells | ≥ 20 wells | 6 wells | | 6 wells | 6 wells | 6 wells | 6 wells |
| | **controls** | | | **samples** | | | |
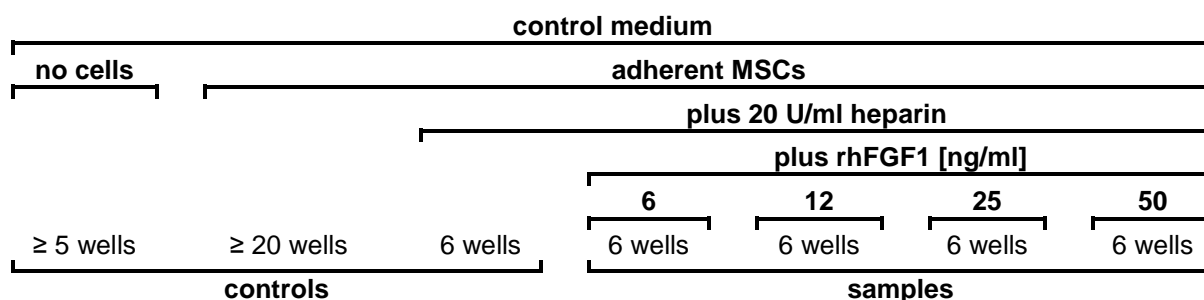
The proliferative effects of several incubation conditions were assessed. The number of wells per incubation condition is given for proliferation assays in a 96-well test plate. Background absorbance of the medium was determined in wells without cells.

### 3.2.2.5  Application of recombinant proteins in the cell culture

To assess the effects of recombinant proteins on differentiation and transdifferentiation, MSCs were plated onto Lab-Tek Chamber Slides with 4 wells at a density of 75,000 - 150,000 cells per well, respectively. When the monolayers had reached confluence one to

three days after plating, the experiments were started. The effects of several recombinant proteins on adipogenic and osteogenic differentiation as well as the effect of rhFGF1 on adipogenic transdifferentiation were tested. Concentrations of recombinant proteins were chosen according to literature describing their usage in cell culture experiments [Nakayama et al., 2006; Oshima et al., 2005; Schütze et al., 2005a; Simonet et al., 1997; Tang et al., 1996; Wesche et al., 2005]. Normal adipogenic and osteogenic differentiation, adipogenic transdifferentiation as well as post-confluent incubation in control medium (DMEM high Glucose with L-Glutamine, 10% heat-inactivated FBS, and 1x penicillin/streptomycin) were performed in parallel and served as controls.

For adipogenic differentiation, different batches of MSCs were subjected to incubation in adipogenic differentiation medium together with 50 ng/ml TNFRSF11B, 500 ng/ml rmSFRP2, 50 ng/ml rhFGF1 plus 2 U/ml heparin, 500 ng/ml rhCYR61, and 10 ng/ml rhIGF1, respectively. Thereby in all batches, one part of the cells received recombinant proteins in parallel with the adipogenic factors at confluence (at d 0), another part obtained pre-incubation of recombinant proteins at confluence in propagation medium, i.e. without adipogenic factors, 2 - 3 d before incubation with adipogenic medium further on containing the respective recombinant protein. Different concentrations of rhFGF1 (0, 6, 12, 25, and 50 ng/ml rhFGF1, each plus 20 U/ml heparin) were tested with further batches of MSCs during adipogenic differentiation with and without pre-incubation with rhFGF1 as described above. The effect of pre-incubation with rhFGF1 (0, 6, 12, 25, and 50 ng/ml rhFGF1, each plus 2 U/ml heparin) for 3 d prior to incubation in adipogenic medium without rhFGF1 was assessed. Adipogenic lineage development was assessed by Oilred O staining 0, 7, 14, and partly 21 d after addition of adipogenic factors. Another trial examined the adipogenic potential of rmSFRP2 (500 ng/ml) regarding spontaneous adipogenic differentiation in absence of other adipogenic factors. Here, Oilred O staining was performed 0, 7, 14, and 21 d after addition of rmSFRP2.

For osteogenic differentiation, MSCs were subjected to osteogenic differentiation medium in the presence of 50 ng/ml TNFRSF11B, 500 ng/ml rmSFRP2, 50 ng/ml rhFGF1 plus 2 U/ml heparin, 500 ng/ml rhCYR61, and 10 ng/ml rhIGF1, respectively. Recombinant proteins and osteogenic factors were added simultaneously. Osteogenic lineage development was monitored by ALP and Alizarin red S staining performed 0, 14 and 28 d after addition of osteogenic factors. Spontaneous osteogenic differentiation was assessed by application of potentially osteogenic TNFRSF11B (50 ng/ml) and rhFGF1 (50 ng/ml, plus 2 U/ml heparin), respectively, without further osteogenic factors. Additional controls contained 2 U/ml heparin only and 0.0005% BSA only. Here, cytochemical staining was performed 0, 14 and 28 d after addition of recombinant protein.

Moreover, the effect of rhFGF1 on adipogenic transdifferentiation was assessed. Thereby, adipogenic transdifferentiation was initiated as described in section 3.2.2.3 by incubation of pre-osteoblasts (derived from MSCs after 14 d in osteogenic differentiation medium) in adipogenic differentiation medium for another 14 d. RhFGF1 (0, 6, 12, 25 and 50 ng/ml rhFGF1 plus 2 U/ml heparin each) was added to the adipogenic medium from d 14 onwards and progress of transdifferentiation was examined compared to transdifferentiating cells not subjected to rhFGF1. Cytochemical staining of lipid vesicles was performed at the beginning of each experiment, at the time of initiation of transdifferentiation as well as 14 d afterwards. The size of areas containing lipid vesicles was semi-quantitatively measured for 6 randomly taken microphotographs of each incubation using Photoshop Elements 4.0. Thereby after 7 and 14 d of incubation, 3 and 4 independent experiments, respectively, were analysed. The significance of changes was determined by Mann-Whitney-U test.

### 3.2.3    Methods in molecular biology

#### 3.2.3.1    Isolation of cellular RNA

MSCs were seeded into cell culture flasks of appropriate sizes at a ratio of 1:3. Transdifferentiation experiments were started at confluence, whereas confluent monolayers at d 0 as well as normally differentiated cells served as controls. Total cellular RNA was isolated from the controls at d 0, after 14 d, 14 d + 3 h, 14 d + 24 h, and 28 d in osteogenic medium as well as after 14 d, 14 d + 3 h, and 14 d + 24 h in adipogenic medium. Transdifferentiated RNA samples were obtained 3 h and 24 h after initiation of reprogramming as well as 14 d after adipogenic and 28 d after osteogenic transdifferentiation initiation. In additional experiments, RNA was isolated from cells transdifferentiated after 5 d and 10 d of osteogenic pre-differentiation in parallel with the respective controls (5 d and 10 d in osteogenic medium).

To isolate total RNA, the RNeasy Mini kit was used according to the manufacturer's instructions. Briefly, cell pellets were homogenised in a guanidine isothiocyanate- and β-mercaptoethanol-containing lysis buffer that inactivates RNases. Equal volumes of 70% ethanol were added to generate appropriate binding conditions before the samples were loaded onto RNeasy mini columns for centrifugation. Thereby, the RNA was bound to the silica-gel-based membranes of the columns. Possibly remaining DNA was removed by on-column digestion with DNase I. Contaminants were washed out by appropriate buffers followed by elution of purified RNA in water. Samples were stored at -80°C.

To obtain highly pure RNA specimens for application in Affymetrix microarray analyses, cell monolayers were homogenised by TRIZOL reagent directly in the culture flasks according to the manufacturer's instructions. In short, phase separation was achieved by addition of chloroform and centrifugation at 4500 rpm. For RNA precipitation, the upper aqueous phase, containing the RNA, was incubated with isopropanol and RNA was pelleted by centrifugation at 4500 rpm. The RNA pellets were subsequently resuspended in lysis buffer and purified by RNeasy Mini kit as described above.

Concentration of RNA specimens was determined by 1:25 dilution of RNA suspension in 10 mM Tris (pH 7.2 - 7.5). Absorption was measured using UV light permeable cuvettes. RNA content was determined at 260 nm, whereas extinction of 1 $E_{260}$ corresponds to 40 µg/ml RNA. Since proteins absorb at 280 nm and contaminants like carbohydrates and peptides absorb at 230 nm, purity of RNA was estimated by the quotients $E_{260}/E_{280}$ and $E_{260}/E_{230}$. Thereby, for pure RNA $E_{260}/E_{280}$ should be 2.0 and $E_{260}/E_{230}$ should be larger than 2.0.

#### 3.2.3.2    Reverse transcriptase polymerase chain reaction (RT-PCR)

RT-PCR analysis allows for detection of gene expression of specific genes in cells and tissues. After reverse transcription of total RNA into cDNA by RT, gene specific primers anneal on different strands in the DNA sequence of the gene of interest. *Taq* DNA polymerase elongates the annealed primers yielding double stranded PCR products specific for this gene.

Identical amounts of total RNA (1 - 2 µg) were reverse transcribed into cDNA using the Promega M-MLV RT, RNase H(-) point mutant, the SuperScript II RT or the Bioline BioScript RT with the respective, provided buffer system. The procedure of cDNA synthesis was performed according to the manufacturers' instructions using random hexamers in a 30 µl volume. Briefly, denaturing of secondary structures of RNA and annealing of random hexamers was achieved by heating to 70°C and subseq uent chilling on ice. Reaction buffer, dNTPs, and RT were added and random hexamers were extended at 25°C prior to elongation of first strand cDNA species at 42°C. Th e reaction was stopped by incubation at 70°C and each specimen was diluted with HPLC water  to a final volume of 50 µl.

Afterwards, PCR reactions were performed in a PTC-200 Peltier thermal cycler using cDNA specimens and gene specific primers. Amersham *Taq* DNA polymerase, BIOTAQ™ DNA polymerase or MangoTaq™ DNA polymerase were used according to the manufacturers'

instruction with the respective, provided buffer system. In short, the standard assay comprised 1x PCR buffer containing 1.5 - 1.7 mM MgCl$_2$, 0.3 mM dNTPs, 5 pmol forward primer, 5 pmol reverse primer, and 1 µl of cDNA in a final volume of 30 µl. Modified assays were performed with higher amounts of MgCl$_2$ and/or by addition of DMSO as stated in section 3.1.3. The applied PCR reaction steps are listed below.

1) Initial denaturing step:   94℃          3 min
2) Denaturing step:           94℃          45 s
3) Annealing step:            51 - 60℃     45 s     (depending on the  primer pair)
4) Elongation step:           72℃          1 min
5) Final elongation step:     72℃          3 min
6) Cooling step:              12℃          forever

Steps 2) - 4) were repeated 22 - 48 times depending on the intensity of the band for each PCR product.

Several of the PCR primers used were already established in the laboratory, others were designed using the free online software Primer3 [Rozen and Skaletsky, 2000] (tab. 1). Whenever possible, intron-spanning primer pairs were chosen to exclude false positive detection of DNA contaminants in the RNA specimens. After optimisation of PCR reaction conditions regarding annealing temperature, cycle number as well as MgCl$_2$ and/or DMSO concentration, gene specificity of each primer pair was assessed by sequencing analysis of the respective PCR product (see section 3.2.3.4).

### 3.2.3.3  Agarose gel electrophoresis

For visualisation of PCR products and estimation of their length, specimens were applied onto agarose gels containing ethidium bromide and subjected to 1D gel electrophoresis. Ethidium bromide intercalates into double-stranded DNA or RNA and fluoresces when exposed to UV light.

1.5 - 2.0 % agarose gels were prepared by dissolving the agarose powder in 0.5x TBE buffer by boiling in a microwave. Ethidium bromide was added to the liquid agarose solution to a final concentration of 5% before the solution was filled into appropriate gel trays and combs were inserted that left behind pockets for loading of the probes. The gel polymerised during cooling to room temperature.

Equal volumes of PCR products were loaded onto the agarose-ethidium bromide gel. Thereby, PCR products obtained by use of MangoTaq™ DNA polymerase were directly loaded into the gel pockets, since the respective buffer system already contains loading dyes. The other PCR products were supplemented with 1x loading dye prior to application onto the gel. As marker for band sizes, a 100 bp DNA ladder containing DNA fragments of 100 - 3.000 bp was also loaded onto the gel. Separation of differently sized DNA markers and PCR products was achieved by application of direct current with a voltage of 0.9 V per cm$^2$ agarose gel. Thereby, negatively charged DNA fragments moved to the anode. PCR bands fluorescing due to the intercalation of ethidium bromide were visualized by exposure to UV light in a UV chamber connected to a digital camera. Photographs of the fluorescing bands were made with ltf Bio-Capt software. Densitometric evaluation of transcript amounts was performed using ltf Bio-1D software, whereas band intensities of different specimens were normalized onto those of EF1α serving as house keeping gene.

### 3.2.3.4  DNA sequencing

DNA sequencing allows for identification of the nucleotide order of a given DNA fragment. The chain termination method uses normal dNTPs as well as modified ddNTPs for PCR. This results in termination of DNA synthesis when a ddNTP is incorporated and therefore generates fragments of random length. Each of the different ddNTPs (ddATP, ddCTP, ddGTP, and ddTTP) is labelled with a distinct fluorescent dye that fluoresces at a different wavelength. Differently sized DNA fragments, each with a fluorescent dye at its end, are separated by electrophoresis. Fluorescence is measured at the different wavelengths and assigned to the type of ddNTP as well as the position in the DNA fragment.

In this work, specificity of PCR products was affirmed by dye terminator sequencing analyses using the Big Dye Terminator v1.1 Cycle Sequencing Kit and one of the primers by which the PCR product was generated. According to the manufacturer's instructions, a PCR mix was prepared containing 5 pmol forward or reverse primer and 1 - 2 µl PCR product in a final reaction volume of 20 µl. Sequencing PCR conditions are stated below.

1) Initial denaturing step:   94°C        4 min
2) Denaturing step:           94°C        30s
3) Annealing step:            1 min        50°C
4) Elongation step:           60°C        1 min
5) Final elongation step:     72°C        5 min
6) Cooling step:              12°C        forever

Steps 2) - 4) were repeated 24 times.

To purify the PCR products of the sequencing PCR from salts, excess nucleotides, and primers, they were loaded onto Autoseq G50 or NucleoSeq columns according to the manufacturer's instructions. After centrifugation, these columns retained the contaminants, whereas the eluates containing the sequencing PCR products were processed. For precipitation of DNA, eluates were supplemented with 3 M sodium acetate (pH 4.3) and ethanol to obtain a final concentration of 0.1 M sodium acetate in 80% ethanol. After incubation at room temperature for 15 min and centrifugation at 13.000 rpm for 20 min, the supernatant was discarded, whereas the pellet was washed with 70% ethanol and air dried. The dried pellet was resuspended in 15 µl Template Suppression Reagent and transferred into sample tubes for sequencing. After denaturation at 94°C for 4 min and subsequent chilling on ice, condensed water was spun down and the sample tubes were placed into the tray of the sequencer. Sequencing parameters were set with the ABI PRISM 310 collection software, sequencing analyses were performed by the Sequencing analysis 3.4 software. Obtained DNA sequences were compared to the online data base of NCBI by inserting into NCBI blast search.

### 3.2.3.5  cDNA microarray analysis

cDNA microarray analysis allows for large-scale expression profiling of total or messenger RNA specimens. Thereby, thousands of oligo-nucleotide probes are fixed onto a chip in certain locations and match parts of known or predicted mRNA molecules. Comparison of separate chips probed with RNA specimens obtained from differently treated cells enables estimation of gene expression differences of the distinct conditions.

Affymetrix GeneChip hybridisation, staining, and scanning of the chips as well as computation and pairwise comparison of the obtained signals were performed by PD Dr. L. Klein-Hitpass at the Institute of Cell Biology, University of Duisburg-Essen, Germany.

Total RNA specimens were used to generate double-stranded cDNA that was further employed in an *in vitro* transcription reaction that produced biotin-labelled, single-stranded cRNA. The cRNA was fragmented before hybridisation onto the GeneChips. The hybridisation cocktail containing fragmented cRNA, hybridisation controls, BSA, and herring sperm DNA was applied onto the GeneChips for 16 h. The hybridisation controls allowed for normalising between different GeneChips later on. The settings of the fluidics station, e.g. GeneChip type and sample descriptions, were controlled by the Microarray Suite 5.0 or the GeneChip Operating Software 1.2. The fluidics station conducted automated washing and staining after hybridisation. Subsequently, each GeneChip was scanned by GeneChip scanner 2500 or 3000. Thereby, the staining of hybridised cRNA by streptavidin phycoerythrin conjugate results in emission of light at 570 nm, that is proportional to the bound cRNA. The software assigned the light emission to the respective probe sets and computed their intensities. The generated data files containing the GeneChip images for each specimen were further analysed and compared pairwise by the Data Mining Tool 3.0 or 3.1.

Total RNA specimens were obtained from confluent MSCs, after 14 d + 3 h, and 14 d + 24 h of osteogenic and adipogenic differentiation as well as 3 h and 24 after initiation of adipogenic and osteogenic transdifferentiation as depicted in figures 1 and 2. Cell culturing

and RNA isolation were performed as described in sections 3.2.2.1, 3.2.2.2, and 3.2.3.1. RNA specimens of transdifferentiated samples were compared to (pre)differentiated controls, whereas sample and control specimens were taken at the same time points, i.e. 3 h and 24 h after initiation of transdifferentiation and after continuing with differentiation, respectively. For adipogenic transdifferentiation, one first microarray was conducted using the 4 of the smaller GeneChips HG-U 133A that can detect 14,500 genes. Two further microarray experiments for adipogenic transdifferentiation and two microarray experiments for osteogenic transdifferentiation employed altogether 16 of the more complete GeneChips HG-U 133 Plus 2.0 that can detect 38,500 genes.

Thus, comparison of the expression profiles of transdifferentiated cells to those of (pre)differentiated ones allowed for detection of differentially expressed probe sets. In doing so, only those probe sets were stated as differentially regulated that fulfilled the following criteria: increase or decrease call according to change p-values of ≤ 0.001 or ≥ 0.999 in at least one of the compared signals and signal $\log_2$ ratio ≤ -1.32 or ≥ 1.32 for GeneChips HG-U 133A or signal $\log_2$ ratio ≤ -1 or ≥ 1 for GeneChips HG-U 133 Plus 2.0, respectively. The logarithmic ratio corresponds to at least 2.5-fold changes in gene expression for the smaller GeneChips and at least 2-fold changes in gene expression for the larger GeneChips, whereas negative values indicate a decrease and positive values indicate an increase of gene expression in transdifferentiated samples compared to the respective (pre)differentiated control.

Gene ontology (GO) analyses regarding differentially regulated genes were performed using the online tools of the Affymetrix NetAffx analysis Center and the GOstat analysis software developed by Beissbarth and Speed [2004]. The latter analyses were performed by PD Dr. L. Klein-Hitpass applying the Benjamini and Hochberg correction [Benjamini and Hochberg, 1995]. Thereby, all probe sets of the respective applied GeneChip that exhibited at least one P detection call in the compared samples for each of the repeated experimental sets served as reference.

Further information regarding individual gene products was supplied by the Invitrogen iPath tool or from the GeneCards website.

### 3.2.4   Methods in protein analysis

#### 3.2.4.1   Preparation of intracellular protein

To examine gene expression profiles not only at the mRNA level, protein was extracted from MSCs at the day of confluence (d 0), after 14 d of adipogenic and osteogenic differentiation as well as 1, 2, and 3 d after initiation of adipogenic and osteogenic transdifferentiation, respectively. Therefore, cell monolayers were detached and pelleted at the indicated time points from cell culture flasks as described in chapter 3.2.2.1.

Cell pellets were lysed in at least 500 µl lysis buffer with Complete protease inhibitor cocktail and sonified. Centrifugation at 1200 rpm for 10 min was performed to clear the supernatant containing the protein, which was aliquoted and stored at -80℃.

For one batch of MSCs, intracellular protein was isolated in parallel with total RNA using the NucleoSpin RNA/Protein kit according to the manufacturer's instruction. In short, cell pellets were dissolved in lysis buffer, which inactivated RNases and proteases present in the samples. After filtration of each lysate, RNA and DNA were bound to the silica membrane of NucleoSpin RNA/Protein columns by centrifugation, whereas the protein was collected with the flow-throughs. Washing of the columns with membrane desalting buffer prepared the columns for subsequent DNA digestion by rDNase I. After 3 washing steps that inactivated the DNase and removed any contaminants, the RNA was eluated in RNase-free water and stored at -80℃ in aliquots. Protein-containing flo w-throughs were mixed with protein precipitator, incubated at room temperature and centrifuged. The supernatants were discarded, the pellets were washed with 50% ethanol, dried at room temperature, and dissolved in 100 µl protein loading buffer containing reducing agent at 96℃ to denature all proteins. After cooling down to room temperature, samples were cleared by centrifugation and supernatants were stored in aliquots at -20℃.

### 3.2.4.2   Protein precipitation in culture supernatants

Additional protein samples were prepared from culture supernatants of MSC monolayers at confluence (d 0), after 14 and 17 d of adipogenic and after 14, 17, and 28 d of osteogenic differentiation as well as 3 d after initiation of adipogenic and osteogenic transdifferentiation, respectively. To reduce contamination by serum proteins, 2 d prior to harvesting of the supernatants, the cell monolayers were incubated in propagation medium and differentiation medium, respectively, that contained only 0.5% heat-inactivated FCS instead of 10% (compare section 3.2.2).

Precipitation of proteins was achieved by vortexing of the supernatants with the 4-fold volume of pre-chilled acetone and incubation at -20°C for at least 1 h. After centrifugation at 4500 rpm and 4°C for 10 min, the supernatants were  discarded whereas the pellet was air dried for 5 min and resolved in at least 500 µl lysis buffer with Complete protease inhibitor cocktail. Aliquots of protein samples derived from cell culture supernatants were stored at -80°C.

### 3.2.4.3   Determination of protein concentration

Due to its adhesive nature rhCYR61 protein tends to precipitate during storage at 4°C. Therefore, concentrations of the protein preparations were determined prior to each application in (trans)differentiation assays using the Micro-Bradford method. Based on the method established by Bradford [1976], Roti-Quant 5x contains the dye Coomassie brilliant blue-G250, which can exist in 3 states absorbing at separate wave lengths. Binding to protein molecules transfers the dye from the cationic into the anionic state. Protein concentration is widely proportional to the change of absorption due to the switch to the anionic state, which is measured at 595 nm.

In particular, calibration standards of 25, 50, 75, 100, 150, and 250 µg/ml BSA in 100 mM glycine and 1x Roti-Quant working solution diluted in distilled water were prepared. Thereby, standards were diluted in the same solution as used for elution of protein during preparation. To obtain a calibration curve, 10 µl 100 mM glycine (as blank) and 10 µl of each calibration standard (25 - 250 µg/ml BSA) were vortexed and measured in duplicates. Protein samples were measured analogously after mixing of 10 µl protein samples in 500 µl volumes of Roti-Quant working solution. Measurement of absorption was conducted 5 to 30 min after preparation of the dye-protein mixes in ½ micro cuvettes at 595 nm in a photometer that also calculated absolute protein concentrations according to the obtained calibration curve.

Protein concentration of cell lysates and protein solutions obtained from cell culture supernatants could not be determined by the Bradford method, because the lysis buffer used to solve these proteins contained disturbing compounds, e.g. high amounts of CHAPS, urea, thiourea, and DTT that would also bind to or reduce the dye. Hence, the Plus One 2D-Quant kit was used according to the manufacturer's instruction. Briefly, protein of BSA calibration standards containing 10, 20, 30, 40, and 50 µg protein as well as of 5 - 10 µl of protein samples to be measured were prepared in duplicates and quantitatively precipitated under addition of the appropriate reagents by centrifugation. Protein pellets were resolved in a copper-containing solution shortly before addition of the colour reagent working solution, whereas copper ions could bind to the proteins. Copper solution plus colour reagent working solution served as blank. Since the colorimetric agent binds to unbound copper, changes of its absorption are inversely related to protein concentration. The mixes were transferred into ½ micro cuvettes and absorption was measured 15 - 60 min after addition of the colour reagent at 480 nm in a photometer that generated the calibration curve due to absorption of standards and calculated absolute amounts of protein for the initially applied protein solution volume.

### 3.2.4.4   SDS-polyacrylamide gel electrophoresis (SDS-PAGE)

SDS-polyacrylamide gel electrophoresis is applied to separate a mix of denatured proteins obtained from cell lysates or cell culture supernatants by their mass. Thereby, the sample buffer containing 2-mercaptoethanol as a reducing agent and SDS as a detergent linearise

the proteins. Moreover, the latter charges the proteins negatively by binding to disulfide linkages of the amino acids, whereas the amount of this negative charge is proportional to the protein mass. Hence, application of a direct current results in migration of proteins across the gel towards the anode with different velocities and therefore proteins are separated due to their mass.

The gel consists of two compartments differing in acrylamide concentration and pH. The small upper area is formed by the stacking gel with lower acrylamide concentration that allows for an even accumulation of protein samples loaded into the pockets located in this compartment. The lower area consists of the separating gel with higher acrylamide concentration where differently sized proteins are resolved during electrophoresis. The compositions of both gels are stated in tab. 3.

**Tab. 3    Composition of SDS-acrylamide gels**

|  | **5% stacking gel** | **12.5% separating gel** |
|---|---|---|
| distilled water | 2.4 ml | 4.8 ml |
| Rotiphorese gel 40 (29:1) acrylamide/bisacrylamide mix | 0.5 ml | 3.75 ml |
| stacking gel buffer | 1 ml | – |
| separating gel buffer | – | 1.25 ml |
| 10% SDS | 0.04 ml | 0.1 ml |
| TEMED | 0.004 ml | 0.004 ml |
| 10% APS | 0.04 ml | 0.1 ml |

Volumes are given for preparation of 2 mini gels. TEMED and APS were added not until immediately before use of the mixture since these compounds act as radical starters for gelling.

After cleaning with 70% denatured ethanol, one short glass plate and one spacer glass plate with integrated spacers were put together for each gel, clamped into special fasteners, and fitted onto a special rack for gel casting. Thus, the bottom and both lateral rims of the plates were sealed. First, the separating gel was cast between the plates filling about ⅔ of the space and covered with 2-propanol. After polymerisation of the separating gel, 2-propanol was removed and the stacking gel was poured on it. Combs were inserted for the later pockets and polymerisation was awaited. Together with the glass plates serving as gel trays, the mini gels were carefully removed from the fasteners and fitted into a mini electrophoresis cell designed to hold 2 mini gels, which was inserted into a mini buffer tank. Upper buffer was filled between the gel trays up to their upper rim and combs were removed. Lower buffer was filled into the mini buffer tank up to the bottom of the gel trays.

Equal quantities of protein samples were diluted with distilled water to a final volume of 10 µl. After mingling with 10 µl sample buffer, samples were incubated for 5 min at 80°C and subsequently for 5 min on ice. 20 µl sample per lane were loaded onto the gels, as size standard 10 µl rainbow marker were applied. The mini buffer tank was covered with its lid and direct current was applied at a voltage of 190 V for about 30 min. Progression of sample migration was controlled by location of bromophenol blue included in the sample buffer and by resolving of the coloured rainbow marker bands. Mini gels were then employed for western blotting.

### 3.2.4.5  Western blotting

Western blotting, also called immunoblotting, is a method to detect distinct proteins in a given sample and to compare the amounts of this protein between several samples. Previously, by SDS-PAGE separated proteins are transferred to a membrane, where they are accessible to detection by protein specific antibodies that link them to reporter enzymes that allow for their visualisation.

For the assembly of the western blot, blotting paper as well as nitrocellulose membrane were soaked with transfer buffer. Placed on the bottom plate electrode of the blotting chamber, 3 layers of blotting paper, the nitrocellulose membrane, the gel, and another 3 layers of blotting paper were assembled into a stack in this order. The upper plate electrode was placed on top and a direct current of 150 mA per membrane was applied for 2 - 3 h. Proteins were blotted onto the nitrocellulose membrane due to migrating according to their negative charge towards the anode (bottom electrode). Efficiency of blotting was controlled by incubating the nitrocellulose membrane for 10 min in Ponceau S solution that reversibly stains all protein bands on the membrane but is much less sensitive than detection by antibodies. After short washing in distilled water, red protein bands were visible. Subsequent agitation in blocking solution for 2 h not only washes out the Ponceau S but also inhibits non-specific binding of the antibodies to the membrane. Incubation with the primary antibody solution containing 1:100 anti-FGF1 and 1:5000 anti-actin was performed over night at 4°C. After washing the membrane 4x 15 min in washing solution I, it was further agitated for 1 h in the secondary antibody solution containing 1:2000 anti-rabbit IgG and 1:2000 anti-goat IgG, both labelled with horseradish peroxidase as reporter enzyme. 4x 15 min washing with washing solution II prepared the membrane for detection of bound antibodies by using the ECL Plus kit that contains the Lumigen PS-3 acridan substrate. This substrate is converted into acridinium ester intermediates by the horseradish peroxidase activity of the antibodies. The intermediate compound reacts with peroxide also contained in the kit resulting in the emission of light that can be detected on an autoradiography film.

According to the manufacturer's instructions, each membrane was exposed to the ECL Plus reagents for several min. After removing of the solution, the membranes were wrapped into cling film and placed in an X-ray film cassette. 2 autoradiography films were applied on each membrane in a dark room, one exposed for 2 min the other for up to 1 h. The first film was immediately developed to estimate the appropriate exposure time for the second one. Proteins detected by the primary antibodies emerged as dark bands, the size standard was copied by overlaying on the respective nitrocellulose membrane.

### 3.2.5  Cytochemical methods

For staining of cell monolayers, MSCs were seeded onto 2-well or 4-well Lab-Tek Chamber Slides at densities of 150,000 - 300,000 (2-well) and 75,000 - 150,000 cells (4-well) per well resulting in confluence 1 - 2 d after seeding. Staining of monolayers for osteogenic and adipogenic markers was performed at the day of confluence and during (trans)differentiation depending on the incubation condition (7, 14, 28, and 42 d after starting of the experiment).

### 3.2.5.1  Alizarin red S staining

Alizarin red S staining of $Ca_2HPO_4$ deposition typically for mineralised extracellular matrix of (pre-)osteoblasts was performed as described previously [Laczka-Osyczka et al., 1998]. Briefly, 1% Alizarin red S dye dissolved in 0.25% ammonia water served as staining solution. Cell monolayers were washed with 1x PBS, fixed for 10 min in ice cold methanol, washed with distilled water, and incubated for 2 min in the Alizarin red S staining solution. Excess dye was removed by repeated washing with distilled water prior to embedding with glycerol gelatine. Stained areas appeared dark red to red brown.

### 3.2.5.2 Alkaline phosphatase (ALP) staining

Staining of cytoplasmic ALP was performed as indicator for osteogenic development by using Alkaline Phosphatase, Leukocyte Kit 86-C according to the manufacturer's instruction but without counterstaining of cell nuclei. Briefly, culture medium was pipetted off thoroughly and cell monolayers were fixed for 30 s by citrate-acetone-formaldehyde solution. After washing with distilled water, staining for ALP activity was performed by incubation for 15 min in an alkaline diazonium salt solution containing sodium nitrite, naphtol, and Fast blue BB. The latter provided blue staining of cells containing active ALP. After washing with distilled water, cell monolayers were embedded in glycerol gelatine.

### 3.2.5.3 Oilred O staining

Oilred O staining was employed to stain intracellular lipid vesicles, which are generated during adipogenic development. As described previously by Pittenger et al. [1999], cell monolayers were washed with PBS, fixed in 4% paraformaldehyde solution for 10 min, and washed with distilled water. After 5 min incubation in 60% 2-propanol, cell monolayers were stained with filtered Oilred O working solution for 10 min. After washing with 60% 2-propanol and distilled water, cell nuclei were counterstained by incubation in hemalaun for 2 min and subsequent blueing by thorough rinsing in tap water. Intracellular lipid vesicles stained light orange to red.

# 4   Results

## 4.1   Adipogenic and osteogenic differentiation potential of human mesenchymal stem cells

Adipogenic and osteogenic differentiation of human MSCs was achieved by incubation of confluent monolayer cultures with differentiation-inducing supplements as described previously [Nöth et al., 2002a]. Adipogenic and osteogenic differentiation were monitored by determination of mRNA levels of adipogenic (PPARγ2 and LPL) and osteogenic markers (ALP and OC). Additionally, cytochemical staining analyses were performed that detected adipogenesis-specific accumulation of intracellular lipid vesicles (Oilred O staining) and osteogenesis-specific ALP activity as well as deposition of mineralised extracellular matrix (Alizarin red S staining) [Aubin, 1998; Pittenger et al., 1999; Rosen et al., 2000; Stein et al., 1996].

While undifferentiated, confluent monolayers did not express lineage specific markers, these markers were present during the respective differentiation assays (fig. 10). The osteogenic markers ALP and OC augmented during osteogenic incubation. ALP mRNA was detected from day 10 onwards with increasing levels, OC mRNA levels were highest after 10 d and 15 d of osteogenic differentiation. After 28 d of osteogenic differentiation, also weak expression of adipogenic markers was observed at the mRNA level. After 14 d of adipogenic differentiation, the lineage-specific markers PPARγ2 and LPL were expressed, whereas only very small amounts of ALP mRNA were detected.

Cytochemical staining further confirmed the osteogenic and adipogenic differentiation potential of the employed MSCs. In accordance to the mRNA levels of ALP, only few cells of the confluent, undifferentiated monolayer showed ALP activity, whereas ALP activity steadily extended during osteogenic differentiation homogeneously over the monolayer (fig. 11). Distinct calcium hydrogen phosphate deposition in the extracellular matrix stained by Alizarin red S was detected from day 14 onwards (fig. 12). During adipogenic differentiation, the amount and the size of lineage-specific intracellular lipid vesicles stained by Oilred O were increased (fig. 13).

Hence analysis of lineage-specific mRNA levels as well as cytochemical staining of lineage-specific markers, proved differentiation of MSCs into osteoblasts after 28 d of osteogenic incubation and into adipocytes after 14 d of adipogenic incubation as previously shown [Schütze et al., 2005b].
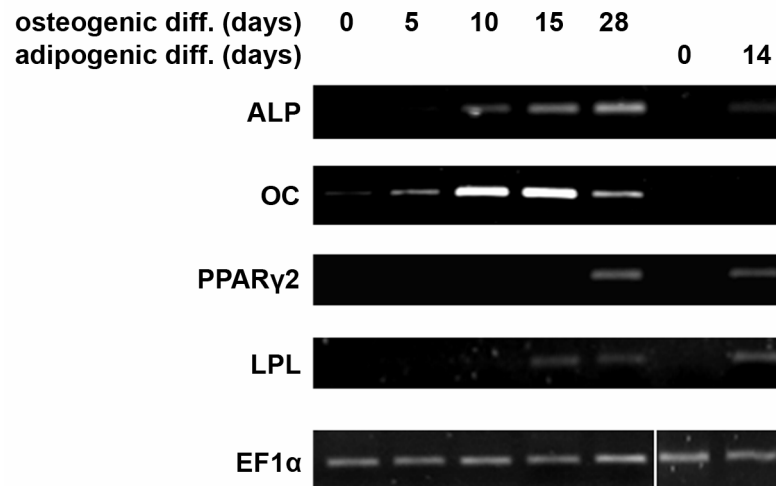
**Fig. 10   Gene expression during osteogenic and adipogenic differentiation**

MSCs were subjected to osteogenic and adipogenic incubation at day 0, when the undifferentiated monolayer had reached confluence. As stated, MSCs were incubated for up to 28 d in osteogenic differentiation medium and for 14 d in adipogenic medium, respectively. RNA was isolated at the given time points. RT-PCR analyses for osteogenic (ALP, OC) and adipogenic markers (PPARγ2 and LPL) were performed while mRNA levels of the house keeping gene EF1α served as internal controls. The figure depicts the representative expression patterns under the described conditions. diff. = differentiation.
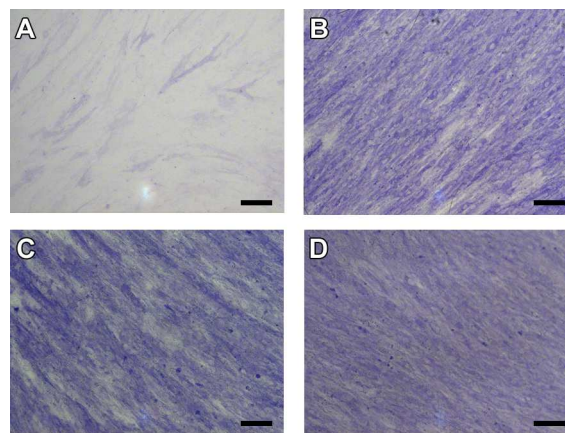


**Fig. 11   ALP staining during osteogenic differentiation**

Representative staining of ALP activity (in blue) is displayed for undifferentiated MSCs (A) and during the course of osteogenic differentiation, i.e. after 7 d (B), 14 d (C), and 28 d (D) of osteogenic incubation. Scale bar = 100 µm.
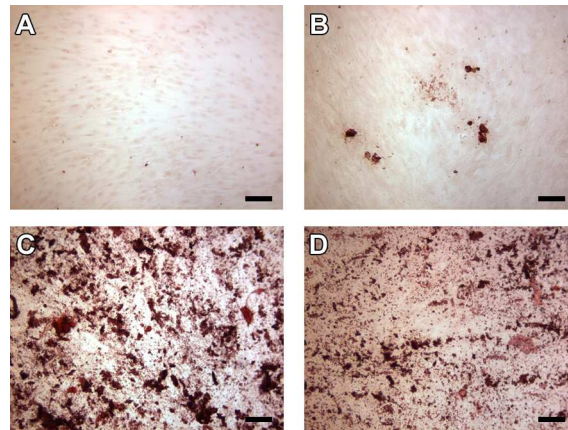
**Fig. 12    Alizarin red S staining during osteogenic differentiation**

Representative staining for mineralised extracellular matrix (in red) in undifferentiated MSCs (A) as well as in monolayers incubated for 7 d (B), 14 d (C), and 28 d (D) in osteogenic medium. Scale bar = 100 µm.
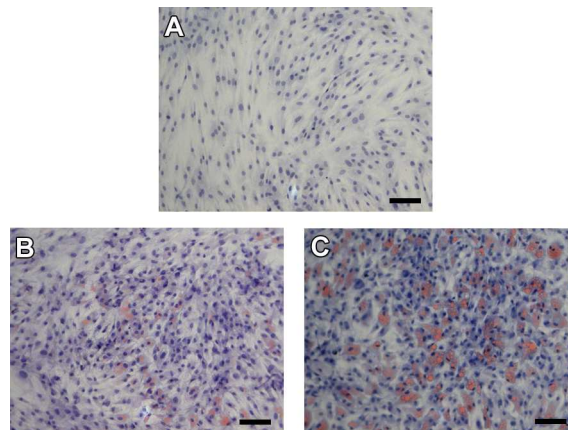


**Fig. 13    Oilred O staining during adipogenic differentiation**

Representative staining for intracellular lipid vesicles (in orange) in undifferentiated MSCs (A) as well as monolayers incubated for 7 d (B) and 14 d (C) in adipogenic medium is depicted. Cell nuclei were counterstained with hemalaun and appear blue. Scale bar = 100 µm.

## 4.2    Adipogenic and osteogenic transdifferentiation potential of human mesenchymal stem cells

The confirmation of the adipogenic and osteogenic differentiation potential of MSCs applied in our cell culture system served as prerequisite for the examination of the transdifferentiation potential of these MSCs. Thereby, transdifferentiation was initiated by switching to the respective other differentiation medium as depicted in fig. 14 and fig. 15. The same means as for differentiation were employed to monitor the transdifferentiation processes, i.e. analysis of mRNA levels of lineage-specific marker genes as well as lineage-specific cytochemical staining.
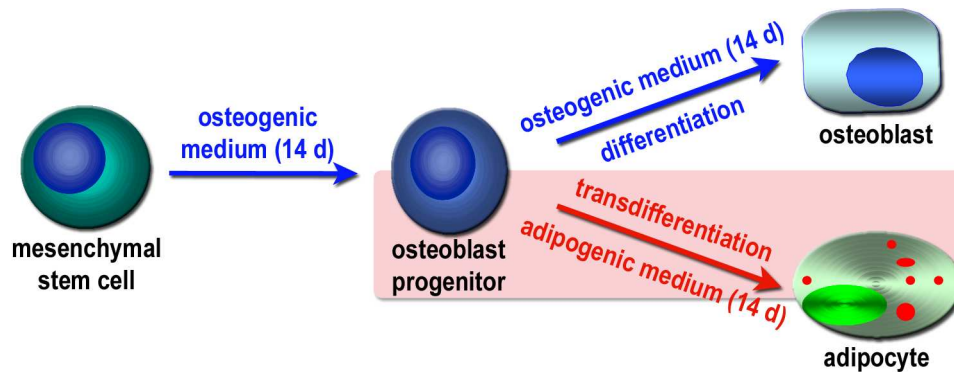
**Fig. 14    Model of adipogenic transdifferentiation**

MSCs were differentiated into osteoblast progenitors prior to adipogenic transdifferentiation (light red box). Control samples were further on incubated in fresh osteogenic medium, i.e. conventionally differentiated into osteoblasts.
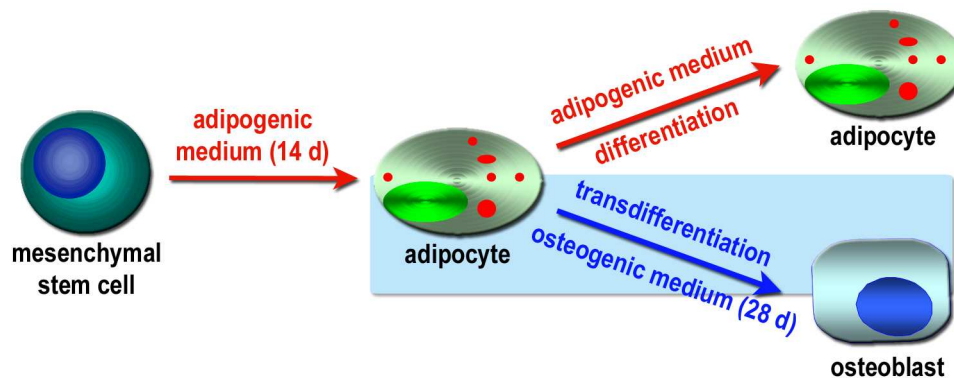


**Fig. 15    Model of osteogenic transdifferentiation**

MSCs were differentiated into adipocytes prior to osteogenic transdifferentiation (light blue box). Control samples were further on cultured in fresh adipogenic medium.

## 4.2.1    Adipogenic transdifferentiation

The adipogenic transdifferentiation potential of pre-osteoblasts obtained after up to 15 d of osteogenic incubation was assessed, since these pre-osteoblasts expressed osteogenic markers but no adipogenic ones unlike fully differentiated osteoblasts that additionally showed weak expression for adipogenesis-specific LPL and PPARγ2 mRNA (fig. 16). The duration of osteogenic pre-incubation of 5 d, 10 d, and 14 d/15 d was chosen arbitrarily to vary the pre-differentiation period examining its potential influence on the transdifferentiation capability. The pre-osteoblasts were subjected to reprogramming by incubation in adipogenic differentiation medium for another 14 d, i.e. for the same period of time that is necessary for conventional adipogenic differentiation starting from MSCs.

This assay resulted in strong expression of adipogenic marker mRNAs (LPL and PPARγ2) whereas osteogenic marker mRNA levels declined (ALP) or expression was even not detectable any more (OC) (fig. 16). Thereby, the duration of pre-incubation did not affect the transdifferentiation capability of the cells. Due to this observation, only monolayers subjected

to 14 d of osteogenic pre-differentiation were employed and incubated for another 14 d in adipogenic medium prior to the analysis of lipid vesicle formation by Oilred O staining. As for conventionally differentiated, MSC-derived adipocytes (fig. 17 A), the transdifferentiated cells (fig. 17 B) accumulated intracellular lipid vesicles that were homogeneously distributed over the monolayer. This shows that in our cell culture system, pre-osteoblasts were capable of adipogenic transdifferentiation resulting in an adipogenic phenotype.
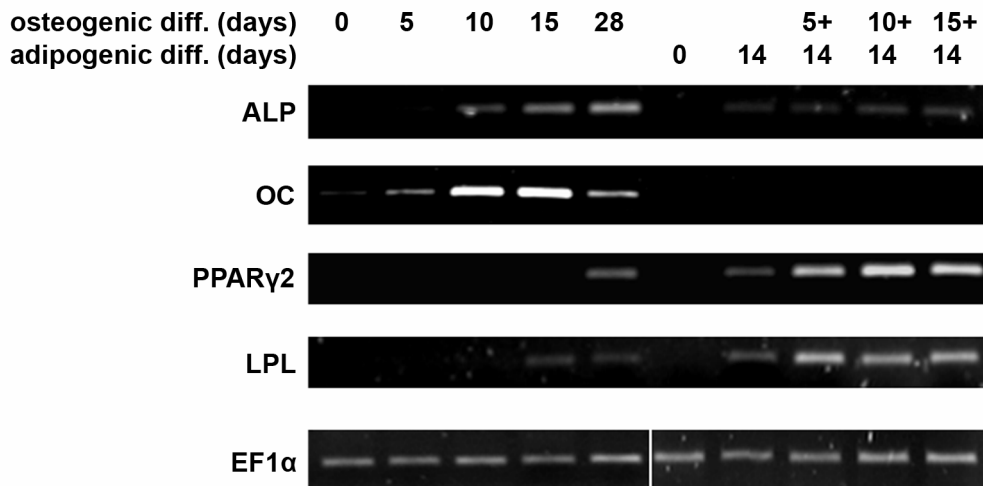


**Fig. 16    Gene expression after adipogenic transdifferentiation**

MSCs were subjected to osteogenic and adipogenic incubation at day 0, when the undifferentiated monolayer had reached confluence. As stated, MSCs were incubated for up to 28 d in osteogenic differentiation medium and for 14 d in adipogenic medium, respectively. After 5, 10, and 14 d/15 d of osteogenic pre-differentiation, further samples were transdifferentiated by application of adipogenic medium for another 14 d as stated. RNA was isolated at the given time points. RT-PCR analyses for osteogenic (ALP, OC) and adipogenic markers (PPARγ2 and LPL) were performed while mRNA levels of the house keeping gene EF1α served as internal controls. The figure representatively displays changes in marker gene expression under the stated incubation conditions. diff. = differentiation.
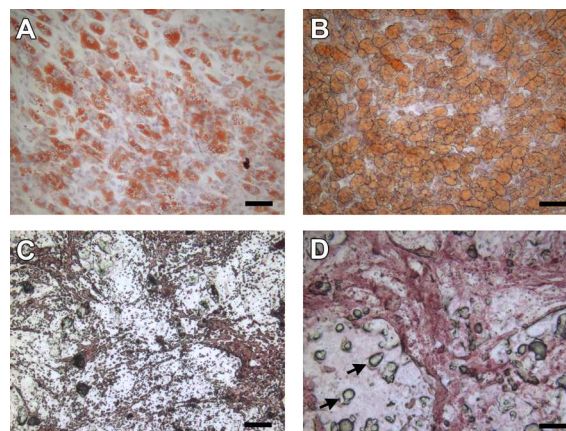


**Fig. 17    Oilred O and Alizarin red S staining of (trans)differentiated MSCs**

Fully differentiated adipocytes (A; 14 d in adipogenic medium) as well as transdifferentiated adipocytes (B; 14 d in osteogenic medium plus 14 d in adipogenic medium) were stained by Oilred O for intracellular lipid vesicles that appear orange whereas cell nuclei counterstained with hemalaun appear blue. Fully differentiated osteoblasts (C;

28 d in osteogenic medium) and transdifferentiated osteoblasts (D; 14 d in adipogenic medium plus 14 d in osteogenic medium) were stained for mineralised extracellular matrix by Alizarin red S appearing red. Arrows in D point at residual lipid vesicles. The figure represents the general phenotypes generated under the applied conditions. Scale bar = 100 μm.

### 4.2.2   Osteogenic transdifferentiation

To assess the osteogenic transdifferentiation potential, fully differentiated adipocytes obtained after 14 d of adipogenic incubation were subjected to reprogramming into osteoblasts by further incubation in osteogenic differentiation medium for another 28 d, i.e. for the same period of time that is necessary for conventional osteogenic differentiation starting from MSCs. Here, shorter durations of adipogenic incubation prior to initiation of transdifferentiation were not examined, since only fully differentiated adipocytes showed distinct accumulation of lipid vesicles (fig. 13).

In this assay, strong expression of osteogenic marker mRNAs (ALP and OC) was detected 28 d after initiation of transdifferentiation but also adipogenic marker mRNAs (LPL and PPARγ2) were still expressed (fig. 18). Transdifferentiated monolayers stained positive for mineralised extracellular matrix (fig. 17 D) like fully differentiated osteoblasts obtained from MSCs (fig. 17 C). This confirmed the osteogenic reprogramming, but in accordance to the results at the mRNA level, residual lipid vesicles were also detectable in the monolayers of transdifferentiated samples. This shows that at least in part our cell culture system allows for osteogenic transdifferentiation of fully differentiated adipocytes resulting in the development of an osteogenic phenotype.
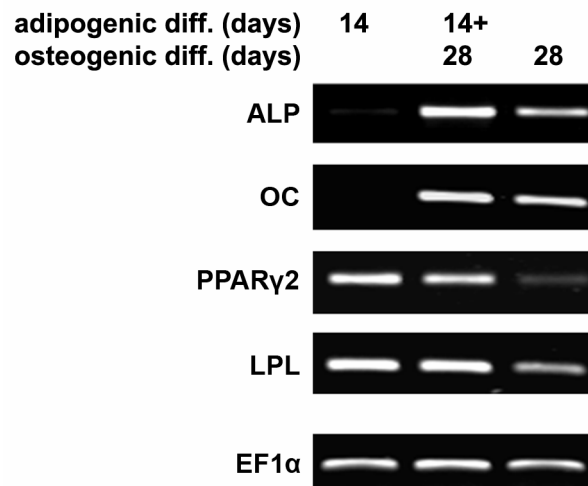


**Fig. 18   Gene expression after osteogenic transdifferentiation**

Prior to RNA isolation, MSCs were incubated in adipogenic medium for 14 d and in osteogenic medium for 28 d, respectively, as stated. Further samples of fully differentiated adipocytes (14 d in adipogenic medium) were transdifferentiated into osteoblasts by incubation in osteogenic differentiation medium for another 28 d before RNA was isolated. Representative results of RT-PCR analyses for osteogenic (ALP, OC) and adipogenic markers (PPARγ2 and LPL) are depicted while mRNA levels of the house keeping gene EF1α served as internal controls. diff. = differentiation.

## 4.3 Affymetrix microarray analyses of adipogenic and osteogenic transdifferentiation

RNA specimens isolated shortly after initiation of adipogenic and osteogenic transdifferentiation were employed for cDNA microarray analyses. Thereby, the time points of RNA isolation were chosen arbitrarily 3 h and 24 h after initiation of transdifferentiation to detect gene regulation in the early stage of reprogramming.

### 4.3.1 Regulation of gene products shortly after initiation of transdifferentiation

#### 4.3.1.1 Affymetrix GeneChip HG-U 133A

In a first attempt, RNA specimens isolated during adipogenic transdifferentiation (fig. 19) were compared to further on in osteogenic medium incubated osteoblast progenitors using the Affymetrix GeneChip HG-U 133A that was able to detect regulation of about 14,500 genes.
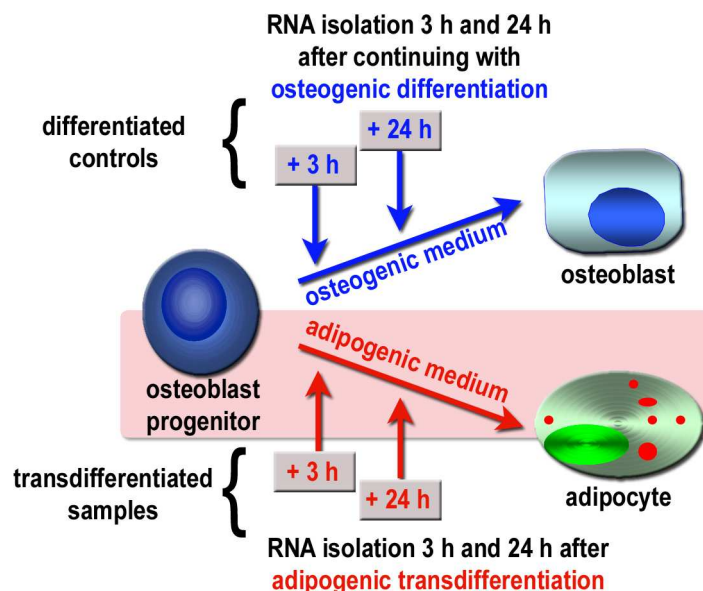


**Fig. 19   Time points for microarray analyses during adipogenic transdifferentiation**

Osteoblast progenitors were subjected to adipogenic transdifferentiation (samples; red box) as well as to osteogenic differentiation (controls). RNA specimens isolated 3 h and 24 h after initiation of the reprogramming from transdifferentiated samples as well as from normally differentiated controls were applied for microarray analyses. Thereby, transdifferentiated samples were compared to their respective differentiated control isolated at the same time point.

The comparison of transdifferentiating osteoblast progenitors with osteoblast progenitors that continued with normal differentiation yielded 258 at least 2.5-fold regulated probe sets corresponding to 202 gene products. Detailed distribution of regulated probe sets regarding the time points of RNA isolation are shown in fig. 20. In the appendix, tab. 12 and tab. 13 list regulated probe sets due to their degree of regulation (fold change) from highest up-regulation to highest down-regulation. Amongst the regulated genes, only three

adipogenesis-associated genes were detected to be up-regulated 24 h after initiation of transdifferentiation: LPL (3.1-fold and 3.6-fold in 2 different probe sets), C/EPBα (10.5-fold), and FABP4 (14.5-fold). None of the other established adipogenesis- or osteogenesis-related markers showed differential expression early during adipogenic transdifferentiation within the examined 24 h time frame.
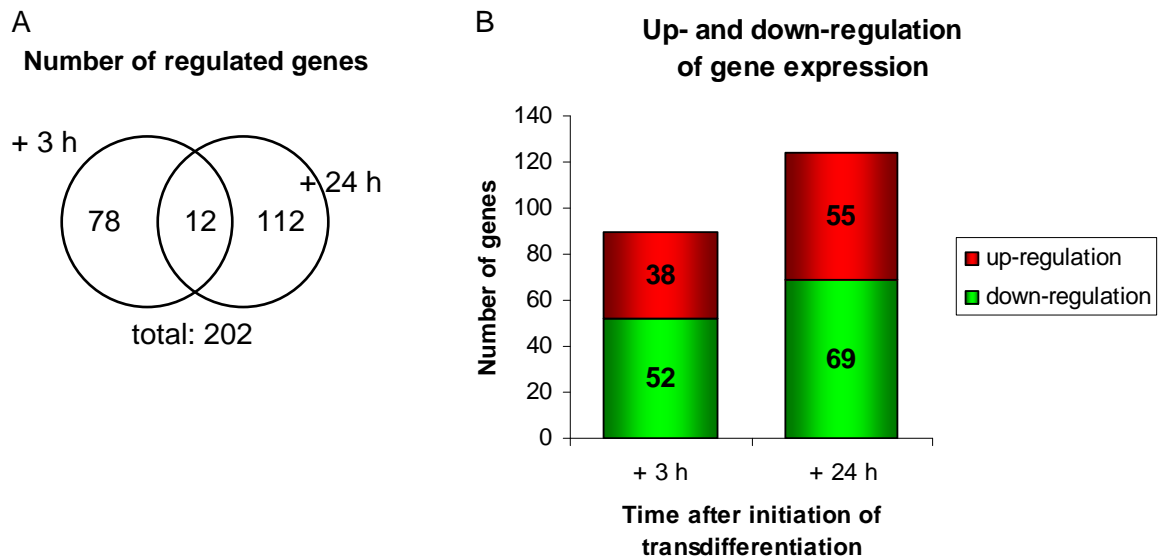


**Fig. 20   Numbers of regulated genes during adipogenic transdifferentiation – microarray analysis with GeneChips HG-U 133A**

The number of at least 2.5-fold regulated genes is stated for the microarray experiment employing the smaller Affymetrix GeneChips HG-U 133A for adipogenic transdifferentiation. The Venn diagram (A) shows the distribution of regulated genes according to the time points of RNA isolation, thereby the intersection displays the number of genes regulated at both time points examined. Discrimination between numbers of up- and down-regulated genes for both time points is depicted in B.

### 4.3.1.2   *Affymetrix GeneChip HG-U 133 Plus 2.0*

Since in the meantime the more complete Affymetrix GeneChip HG-U 133 Plus 2.0 was available, further microarray analyses were conducted by usage of these GeneChips that were able to detect gene regulation of 38,500 genes. Moreover, both transdifferentiation directions were assessed. Thereby, analyses for each transdifferentiation direction were performed in duplicates employing different MSC charges. Again, transdifferentiated RNA samples were compared to those obtained from normally differentiated cells (fig. 19 and fig. 21). Since the microarray analysis for each transdifferentiation direction was performed in duplicates, only those genes were taken into account that exhibited the same regulation pattern in the repeated microarray analyses using different charges of MSCs while the amount of regulation was at least 2-fold. For adipogenic transdifferentiation, the analyses resulted in 414 reproducibly regulated genes whereas 922 reproducibly regulated genes were detected for osteogenic transdifferentiation. Fig. 22 displays the distribution of regulated

genes according to the time points after initiation of transdifferentiation as well as the number of up- and down-regulated genes for each transdifferentiation pathway. In the appendix, all at least 2-fold regulated probe sets (tab. 14, tab. 15, tab. 16, and tab. 17) are listed.
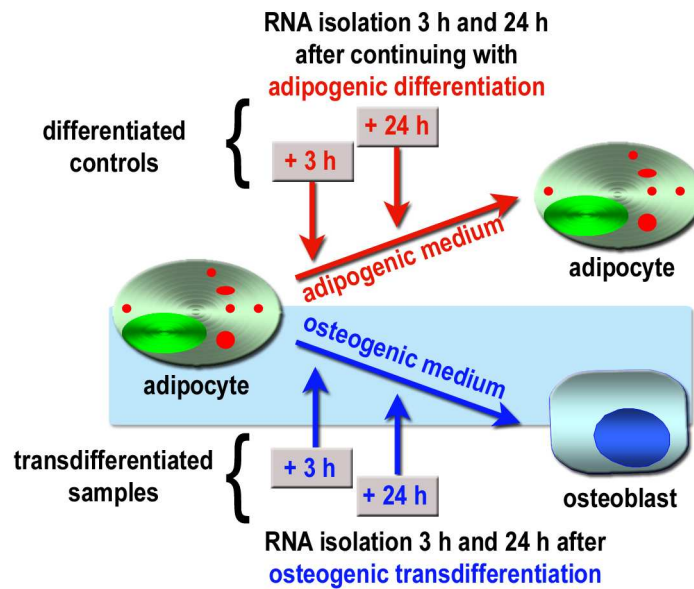


**Fig. 21    Time points for microarray analyses during osteogenic transdifferentiation**

Fully differentiated adipocytes were subjected to osteogenic transdifferentiation (samples; blue box) as well as to adipogenic differentiation (controls). RNA specimens isolated 3 h and 24 h after initiation of the reprogramming from transdifferentiated samples as well as from normally differentiated controls were applied for microarray analyses. Thereby, transdifferentiated samples were compared to their respective differentiated control isolated at the same time point.

**A**     **Numbers of reproducibly regulated genes during transdifferentiation**



**Osteoblasts into adipocytes**

+ 3 h     90     28     296     + 24 h

total: 414

**Adipocytes into osteoblasts**

+ 3 h     41     35     846     + 24 h

total: 922

**B**     **Gene regulation during transdifferentiation**
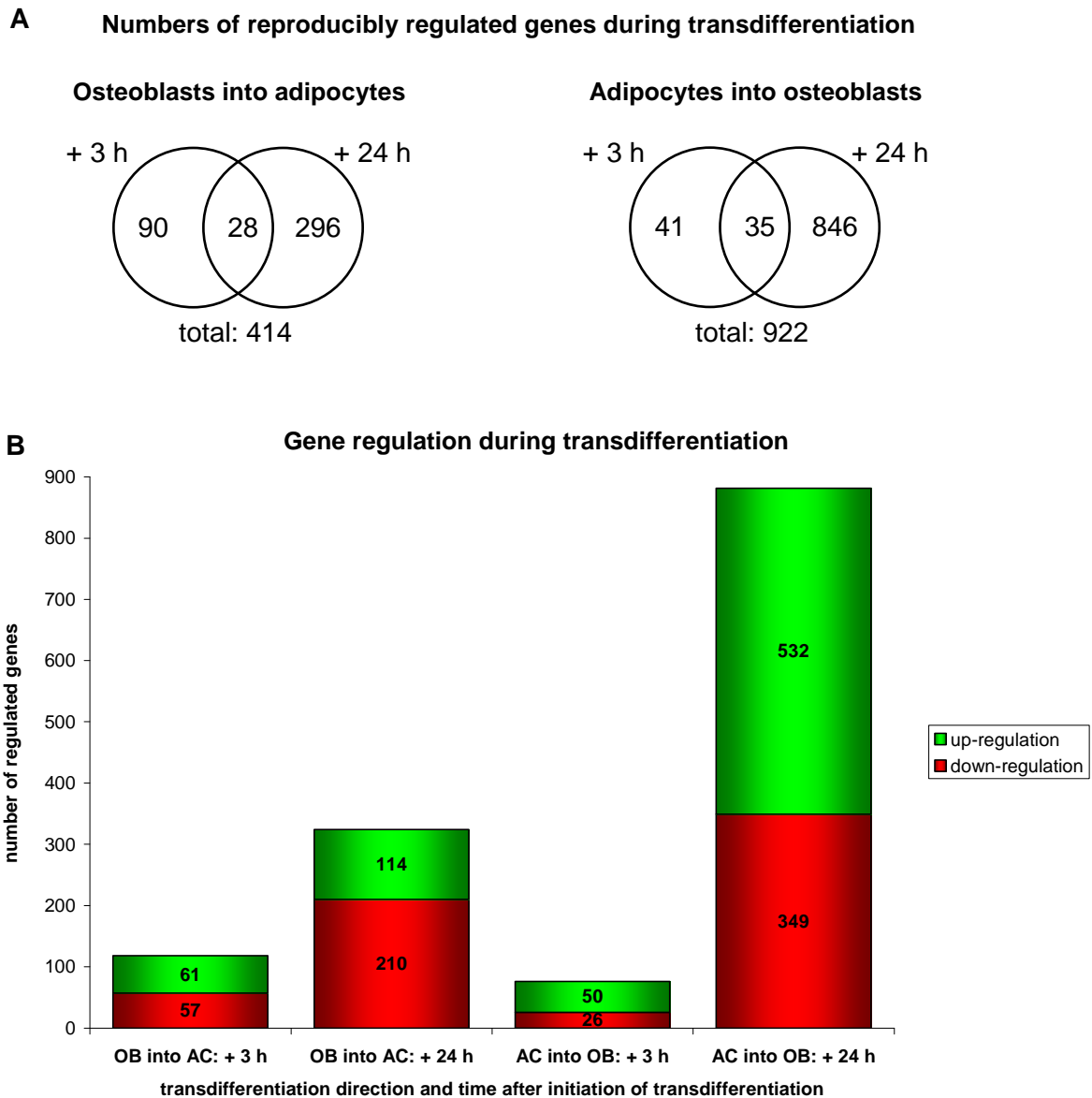


**Fig. 22   Numbers of reproducibly regulated genes during transdifferentiation – microarray analyses with GeneChips HG-U 133 Plus 2.0**

For adipogenic as well as for osteogenic transdifferentiation, the numbers of reproducibly and at least 2-fold regulated genes are stated for the microarray experiments employing the more complete Affymetrix GeneChips HG-U 133 Plus 2.0. The Venn diagrams (A) depict the distribution of regulated genes according to the time points of RNA isolation. Thereby the intersection displays the number of genes regulated at both time points examined. The graph in B shows the discrimination between numbers of up- and down-regulated genes for both time points and both transdifferentiation directions (OB into AC = adipogenic transdifferentiation and AC into OB = osteogenic transdifferentiation).

## 4.3.2    Re-evaluation of microarray data by semi-quantitative RT-PCR

The results of differential gene regulation obtained by Affymetrix array analyses employing the small as well as the larger GeneChips were re-evaluated by semi-quantitative RT-PCR after establishment of the respective PCR reactions.

For the first microarray analysis that employed the smaller Affymetrix GeneChips and only examined one charge of adipogenic transdifferentiation, a selection of 22 regulated genes was assessed by densitometric evaluation of RT-PCR bands on agarose gels. These genes were chosen due to their high fold changes obtained by microarray analysis and under consideration of their functional properties that could be potentially relevant during adipogenic transdifferentiation. Re-evaluation by RT-PCR that employed the same RNA samples as for the microarray resulted in accordance of regulation for 20 of 22 genes products (tab. 4 and tab. 5). 3 h after initiation of adipogenic transdifferentiation, 10 of 11 gene products that should be regulated according to the microarray analysis were confirmed (tab. 4). 24 h after initiation of adipogenic transdifferentiation, 11 of 12 genes were in accordance with the microarray data (tab. 5). One of the two genes whose regulation could not be confirmed by RT-PCR encoded for a gene without known function (APOLD1, formerly hypothetical protein DKFZp434F0318) the other one was a hypothetical gene (MGC4655). Taking RNA samples from two additional MSC charges subjected to adipogenic transdifferentiation and comparing their gene regulation with the microarray data resulted in accordance for 16 of the above 20 confirmed gene regulations in at least one of the two additional RNA samples, 9 of these genes even matched the microarray results for both additional transdifferentiation experiments (tab. 4 and tab. 5).

**Tab. 4  Accordance of microarray data and RT-PCR analyses 3 h after initiation of adipogenic transdifferentiation – GeneChips HG-U 133A**

| Gene name (gene symbol) | Identical RNA probes | | | Additional RNA probes | | |
| --- | --- | --- | --- | --- | --- | --- |
| | Fold change | | Accordance with microarray data | Fold change | | Number of accordances with microarray data |
| | Micro-array analysis | RT-PCR analysis | | 1st additional RT-PCR analysis | 2nd additional RT-PCR analysis | |
| apolipoprotein L domain containing 1 (APOLD1) | 4.5 | -5.5 | - | n. r. | n. r. | n. r. |
| cysteine-rich, angiogenic inducer, 61 (CYR61) | -5.2 -4.1 | -5.2 | ++ | 1.6 | -1.8 | 1 |
| dual specificity phosphatase 6 (DUSP6) | -4.0 -4.8 | -7.4 | ++ | -22.1 | -8.7 | 2 |
| Kruppel-like factor 4 (gut) (KLF4) | 2.8 | 2.8 | ++ | 1.5 | 1.7 | 2 |
| nuclear receptor subfamily 4, group A, member 2 (NR4A2) | 9.6 7.4 9.5 | 2.9 | ++ | 2.2 | 1.5 | 2 |
| prostaglandin E receptor 4 (subtype EP4) (PTGER4) | -4.0 | -4.2 | ++ | 1.1 | 1.1 | 0 |
| protein kinase C-like 2 (PRKCL2) | -2.6 | -1.5 | + | 21.5 | 1.3 | 0 |
| regulator of G-protein signalling 2, 24kDa (RGS2) | 6.1 | 1.2 | + | -1.2 | 1.4 | 1 |
| serine/threonine kinase 38 like (STK38L) | -3.8 -3.5 | -1.5 | + | 1.4 | -1.4 | 1 |
| solute carrier family 2 (facilitated glucose transporter), member 3 (SLC2A3) | 2.9 3.5 4.7 | 1.3 | + | 1.2 | 1.6 | 2 |
| zinc finger protein 331 (ZNF331) | 7.6 | 3.0 | ++ | 1.2 | -3.9 | 1 |

Microarray data and densitometric evaluation of fold changes of gene regulation 3 h after initiation of adipogenic transdifferentiation. Thereby, positive values indicate fold change of up-regulation whereas negative values state fold change of down-regulation of gene expression. In the column 'microarray analysis', multiple values per gene product represent fold changes of different probe sets detecting the same gene. Accordance between microarray analysis and RT-PCR analysis was assessed under the following criteria:

\+        same algebraic sign and -2.0 < fold change ≤ -1.2 or 1.2 ≤ fold change < 2.0 in RT-PCR

++        same algebraic sign and fold change of ≤ -2.0 or fold change ≥ 2.0 in RT-PCR

\-         meeting none of the above described criteria

n. r. = not re-evaluated.

**Tab. 5  Accordance of microarray data and RT-PCR analyses 24 h after initiation of adipogenic transdifferentiation – GeneChips HG-U 133A**

| Gene name (gene symbol) | Identical RNA probes | | | Additional RNA probes | | |
|---|---|---|---|---|---|---|
| | Fold change | | Accordance with microarray data | Fold change | | Number of accordances with microarray data |
| | Micro-array analysis | RT-PCR analysis | | 1st additional RT-PCR analysis | 2nd additional RT-PCR analysis | |
| adipose most abundant gene transcript 1 (APM1) | 5.7 | 4.0 | ++ | -4.7 | 1.3 | 1 |
| kruppel-like factor 6 (KLF6) | -3.1 -2.6 | -3.8 | ++ | -1.5 | -1.2 | 2 |
| D site of albumin promoter (albumin D-box) binding protein (DBP) | 8.3 | 4.9 | ++ | n. a. | n. a. | n. a. |
| dual-specificity tyrosine-(Y)-phosphorylation regulated kinase 2 (DYRK2) | -2.7 | -1.2 | + | 1.1 | -1.0 | 0 |
| fatty acid binding protein 4, adipocyte (FABP4) | 14.5 | 1.8 | + | 9.5 | 9.4 | 2 |
| hypothetical protein MGC4655 (MGC4655) | -2.8 | 3.7 | - | n. r. | n. r. | n. r. |
| insulin-like growth factor binding protein 5 (IGFBP5) | 3.5 3.5 | 6.5 | ++ | n. d./c. | 1.2 | 2 |
| interleukin 8 (IL8) | -3.1 -3.6 | n. d./s. | ++ | -2.1 | -1.1 | 1 |
| putative lymphocyte G0/G1 switch gene (G0S2) | 9.6 | 2.1 | ++ | 11.8 | 2.6 | 2 |
| regulator of G-protein signalling 4 (RGS4) | -7.7 -7.0 -4.1 | -3.4 | ++ | -4.0 | -2.0 | 2 |
| serine/threonine kinase 38 like (STK38L) | -3.3 -3.2 | -2.7 | ++ | -1.1 | -1.7 | 1 |
| tumour necrosis factor receptor superfamily, member 11b (osteoprotegerin) (TNFRSF11B) | -2.9 -29.4 | -7.2 | ++ | 8.3 | -2.4 | 1 |

Microarray data and densitometric evaluation of fold changes of gene regulation 24 h after initiation of adipogenic transdifferentiation. The fold changes of gene regulation and the accordance to microarray data are displayed as described for tab. 4. n. a. = not available, mRNA could not be detected in examined probes; n. d./s. = not determined, quantitation was not possible due to absence in transdifferentiated sample; n. d./c. = not determined, quantitation was not possible due to absence in control.

For the microarray analyses performed with the Affymetrix GeneChips HG-U 133 Plus 2.0, a selection of reproducibly regulated genes was re-evaluated by RT-PCR, too. Besides 11 genes with known functions, also 16 at the time point of examination accounted hypothetical gene products were examined. This additional assessment of hypothetical gene products was performed in the course of the medical doctorate of Ulrike Meyer. Even though some of these considered hypothetical gene products have been renamed in the meantime due to novel findings regarding their cellular localisation or structural motifs, their distinct functions are still unknown [GeneCards, 2006].

Both, established and hypothetical genes exhibited distinct regulation for at least one of the both transdifferentiation processes. Most of them showed a reciprocal regulation pattern between both transdifferentiation directions. Additionally, all chosen genes with known functions were listed amongst the top 50 of regulated genes ranked for their potential

relevance during transdifferentiation by bioinformatic analysis (see 4.3.5.2). The RT-PCR experiments were conducted using the same RNA samples as for the second microarray set of adipogenic and osteogenic transdifferentiation. Altogether, microarray data delivered 27 processes of gene regulation for 11 genes with known function and 37 processes of regulation for 16 genes with unknown function. Thereby, each time point of RNA isolation in each transdifferentiation direction was considered as single process. Gel bands for some of the examined genes are depicted in fig. 23. Densitometric analysis of gel bands resulted in confirmation of 23 of the 28 processes of gene regulation, i.e. accordance for 82%, for established genes (tab. 6). Accordance for genes with unknown function was detected in 22 of the 37 processes of gene regulation, i.e. in 59% (tab. 7).
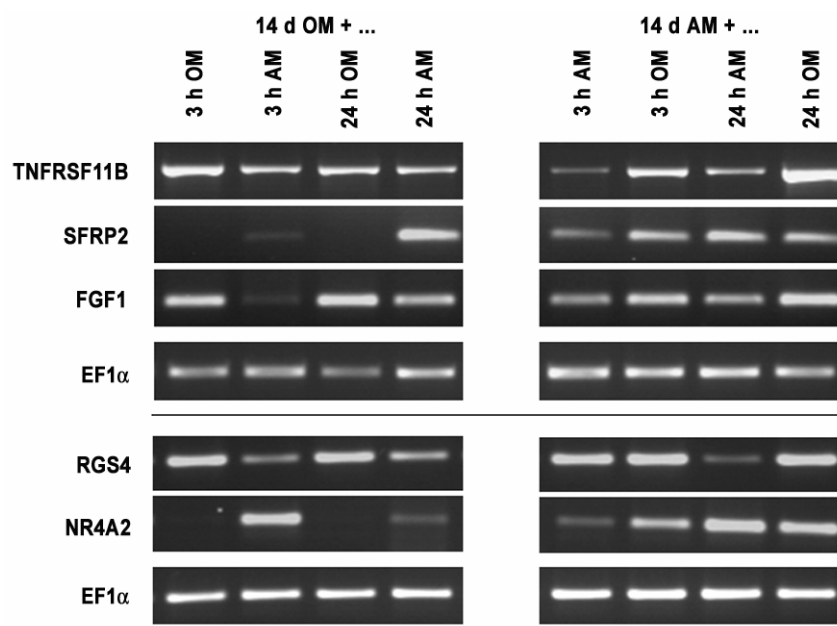


**Fig. 23    Examination of gene regulation during adipogenic and osteogenic transdifferentiation by semi-quantitative RT-PCR analyses**

Gene expression levels for some of the genes selected for re-evaluation (see also tab. 6) are visualised by gel electrophoresis of RT-PCR products. Eukaryotic translation elongation factor 1 alpha 1 (EF1α) served as house keeping gene and reported the quality of cDNA. Gene expression is shown for MSCs that were incubated in osteogenic differentiation medium (OM; left side) or adipogenic differentiation medium (AM; right side) for 14 d prior to initiation of transdifferentiation. The change to the respective other differentiation medium induced adipogenic (left side, 3 h AM and 24 h AM) and osteogenic transdifferentiation (right side, 3 h OM and 24 h OM), whereas control samples were further on cultivated in a fresh aliquot of the same differentiation medium as before. Isolation of RNA samples was performed at the stated time points, fully differentiated adipocytes (14 d + 3 h and 14 d + 24 h in AM) and committed osteoblasts (14 d + 3 h and 14 d + 24 h in OM) served as controls.

**Tab. 6   Accordance of microarray data and RT-PCR analyses for genes with known function –**
**GeneChips HG-U 133 Plus 2.0**

| Gene name | bioinformatic score | Fold change | | Process of gene regulation | Accordance |
|---|---|---|---|---|---|
| | | RT-PCR analysis | Microarray analysis | | |
| cysteine-rich, angiogenic inducer, 61 (CYR61) | 26.28 | -2.6 | -3.7<br>-3.8 | OB into AC:  3 h | ++ |
| | | -8.5 | -10.9<br>-24.3 | OB into AC:  24 h | ++ |
| | | 6.6 | 9.6<br>13.6 | AC into OB:  24 h | ++ |
| fatty acid binding protein 4, adipocyte (FABP4) | 19.80 | 15.5 | 20.4<br>62.2 | OB into AC:  24 h | ++ |
| fibroblast growth factor 1 (FGF1) | 27.98 | -2.4 | -7.3<br>-6.0<br>-9.6 | OB into AC:  24 h | + |
| | | 2.2 | 22.3<br>5.0<br>16.2 | AC into OB:  24 h | + |
| G0/G1switch 2 (G0S2) | 17.96 | 30.4 | 19.3 | OB into AC:  24 h | ++ |
| | | -1.3 | -3.0 | AC into OB:  24 h | + |
| insulin-like growth factor 1 (somatomedin C) (IGF1) | 21.08 | 4.4 | 17.4<br>5.1<br>7.2<br>8.3 | OB into AC:  24 h | ++ |
| | | -3.0 | -3.4<br>-2.6 | AC into OB:  24 h | ++ |
| kruppel-like factor 6 (KLF6) | 19.49 | -4.5 | -2.5<br>-2.1 | OB into AC:  3 h | ++ |
| | | -1.2 | -3.2<br>-3.1 | OB into AC:  24 h | + |
| | | -2.6 | 2.3<br>2.1 | AC into OB:  3 h | - |
| | | 1.9 | 2.8<br>2.5 | AC into OB:  24 h | + |
| nuclear receptor subfamily 4, group A, member 2 (NR4A2) | 28.38 | not detectable in control | 15.8<br>17.8<br>15.2 | OB into AC:  3 h | ++ |
| | | not detectable in control | 7.0<br>6.7<br>5.1 | OB into AC:  24 h | ++ |
| | | 2.5 | -3.5<br>-5.4 | AC into OB:  3 h | - |
| regulator of G-protein signalling 4 (RGS4) | 42.47 | -2.5 | -5.5<br>-9.4<br>-13.5 | OB into AC:  3 h | ++ |
| | | -1.7 | -3.2<br>-5.0<br>-8.6 | OB into AC:  24 h | + |
| | | 1.0 | 1.9<br>2.1<br>2.1 | AC into OB:  3 h | - |
| | | 4.8 | 16.0<br>25.6<br>39.9 | AC into OB:  24 h | ++ |
| secreted frizzled-related protein 2 (SFRP2) | 28.64 | not detectable in control | 18.3<br>10.8 | OB into AC:  24 h | ++ |
| | | -1.0 | -22.5<br>-4.5 | AC into OB:  24 h | - |
| serpin peptidase inhibitor, clade E (nexin, plasminogen activator inhibitor type 1), member 1 (SERPINE1) | 22.97 | -31.1 | -4.0<br>-4.8<br>-3.6 | OB into AC:  24 h | ++ |
| | | -2.3 | 1.2<br>3.2<br>1.0 | AC into OB:  3 h | - |
| | | 4.2 | 7.2<br>14.6<br>12.8 | AC into OB:  24 h | ++ |
| tumour necrosis factor receptor superfamily, member 11b (osteoprotegerin) (TNFRSF11B) | 32.28 | -2.2 | -8.9<br>-19.2 | OB into AC:  24 h | + |
| | | 3.4 | 21.6<br>29.4 | AC into OB:  24 h | ++ |

For genes with known function, the bioinformatic score (see 4.3.5.2) and fold changes of gene expression obtained by microarray data as well as densitometric evaluation are listed for adipogenic and osteogenic transdifferentiation, respectively. Thereby, positive values indicate fold change of up-regulation whereas negative values state fold change of down-regulation of gene expression. In the column 'microarray analysis', multiple values per gene product represent fold changes of different probe sets detecting the same gene. Accordance

between microarray analysis and RT-PCR analysis performed with identical RNA samples was assessed under the following criteria:

+       same algebraic sign and -2.5 < fold change ≤ -1.2 or 1.2 ≤ fold change < 2.5

++     same algebraic sign and fold change ≤ -2.5 or fold change ≥ 2.5

-       meeting none of the above described criteria

**Tab. 7   Accordance of microarray data and RT-PCR analyses for genes with unknown function – GeneChips HG-U 133 Plus 2.0**

| Gene name | bioinformatic score | Fold change | | Process of gene regulation | Accordance |
|---|---|---|---|---|---|
| | | RT-PCR analysis | Microarray analysis | | |
| cDNA clone IMAGE:5263177 (AW274846) | 8.39 | -1.3 | 10.1 | OB into AC:  24 h | + |
| | | -2.3 | -4.7 | AC into OB:  24 h | + |
| Boc homolog (mouse) (BOC) | 13.93 | -2.0 | 3.7 3.2 | OB into AC:  24 h | - |
| | | 1.4 | -3.2 -3.6 | AC into OB:  24 h | - |
| chromosome 1 open reading frame 110 (C1orf110) | n. a. | 5.0 | -14.9 | OB into AC:  3 h | - |
| | | -10.1 | -24.8 | OB into AC:  24 h | ++ |
| chromosome 6 open reading frame 85 (C6orf85) | n. a. | 4.9 | 6.7 | OB into AC:  24 h | ++ |
| | | 3.3 | -5.2 | AC into OB:  24 h | - |
| chromosome 7 open reading frame 10 (C7orf10) | 5.01 | -1.0 | -2.8 | OB into AC:  24 h | - |
| | | 2.5 | 2.8 | AC into OB:  24 h | ++ |
| coiled-coil domain containing 69 (CCDC69) | 15.59 | 1.4 | 3.5 3.4 | OB into AC:  24 h | + |
| | | -2.0 | -1.4 -1.5 | AC into OB:  3 h | + |
| | | 1.8 | -3.2 -2.7 | AC into OB:  24 h | - |
| centrosomal protein 55kDa (CEP55) | n. a. | 2.5 | 6.8 | AC into OB:  24 h | ++ |
| cDNA FLJ101145 fis, clone HEMBA1003322 (FLJ10145) | 14.63 | -1.4 | -2.9 -3.5 | OB into AC:  3 h | + |
| | | 1.2 | -3.9 -2.6 | OB into AC:  24 h | - |
| | | 1.1 | 3.7 | AC into OB:  24 h | - |
| hypothetical protein FLJ37034 (FLJ37034) | 17.20 | no expression detectable | -3.0 | OB into AC:  24 h | - |
| | | 1.8 | 3.7 | AC into OB:  3 h | + |
| | | -1.7 | 19.3 | AC into OB:  24 h | - |
| KIAA1199 (KIAA1199) | 15.23 | -1.1 | -1.4 -2.4 | OB into AC:  24 h | - |
| | | 1.6 | 3.9 3.8 | AC into OB:  24 h | + |
| hypothetical gene supported by BC072410 (LOC440416) | 16.71 | -1.1 | -4.0 | OB into AC:  24 h | - |
| | | not detectable in control | 6.5 | AC into OB:  24 h | ++ |
| scavenger receptor class A, member 5 (putative) (SCARA5) | n. a. | -2.4 | 2.1 | OB into AC:  3 h | - |
| | | 1.9 | 13.1 8.1 | OB into AC:  24 h | + |
| | | 1.8 | -3.6 -2.7 | AC into OB:  24 h | - |
| transmembrane protein 64 (TMEM64) | 12.16 | 1.8 | -2.2 -1.8 -1.7 | AC into OB:  24 h | - |
| transmembrane protein 166 (TMEM166) | 16.11 | -2.4 | -3.4 | OB into AC:  3 h | + |
| | | not detectable in sample | -3.7 | OB into AC:  24 h | ++ |
| | | not detectable in control | 19.4 | AC into OB:  24 h | ++ |
| transmembrane protein 173 (TMEM173) | 18.46 | -2.5 | -2.4 | OB into AC:  24 h | ++ |
| | | 5.0 | 5.5 | AC into OB:  24 h | ++ |
| zinc finger CCCH-type containing 12D (ZC3H12D) | 9.69 | -5.5 | -3.7 | OB into AC:  3 h | ++ |
| | | -1.5 | -3.0 | OB into AC:  24 h | + |
| | | 1.9 | 1.7 | AC into OB:  3 h | + |
| | | 2.5 | 3.1 | AC into OB:  24 h | ++ |

For hypothetical genes and genes with unknown function, the bioinformatic score (see 4.3.5.2) and fold changes of gene expression obtained by microarray data as well as densitometric evaluation are displayed for adipogenic

and osteogenic transdifferentiation, respectively. Depiction and criteria for evaluation of accordance are the same as stated in tab. 6.

Amongst the established marker mRNAs for adipogenic and osteogenic differentiation, only few of the known adipogenesis-associated genes like LPL, FABP4, and C/EBPα were detected by microarray analyses showing at least 2-fold up-regulation 24 h after initiation of adipogenic transdifferentiation. Densitometric analyses confirmed increased LPL mRNA levels and additionally revealed higher amounts of PPARγ2 for cells subjected to adipogenic transdifferentiation. No significant up-regulation was obtained for the osteogenic marker mRNAs shortly after osteogenic transdifferentiation by microarray data as well as by RT-PCR.

### 4.3.3  Gene ontology analyses

Regulated genes of the single microarray analysis of adipogenic transdifferentiation employing the smaller GeneChips were analysed for their affiliation regarding the main Gene Ontology (GO) categories *cellular component*, *molecular function*, and *biological process* distinguishing between the direction and the time points of regulation.

Using the Affymetrix NetAffx Analysis Center, in the GO class of *molecular function*, many regulated genes belonged to the sub classes of binding and catalytic activity equally for up- and down-regulation and for both time points of RNA isolation (fig. 24). Sub classes included binding, nucleic acid binding or nucleotide binding, and ion binding. For both time points examined, many down-regulated genes belonged to the class of signal transducer activity (fig. 24 C and D). Additionally 24 h after initiation of transdifferentiation, a higher number of regulated genes was affiliated to the category of transporter activity (fig. 24 B). For the GO class of *biological process*, the NetAffx Analysis Center revealed the sub classes of cellular process, physiological process, and regulation of biological process containing high numbers of regulated genes independent from the time point and direction of regulation (fig. 25). In the sub category of cellular process, many genes were further grouped into the sub class of cell communication. Regulated genes belonging to the sub class of physiological process were distributed into the inferior classes of cellular physiological process and metabolism. Furthermore, regulated genes associated with the class of development were found for both regulation directions. More detailed branching into GO classes and the numbers of probe sets contained in each class are stated in the respective GO graphs (fig. 24 and fig. 25).

GOstat analyses for reproducibly regulated genes of the microarray analyses employing the larger GeneChips were performed separately for the different RNA isolation time points. A selection of major over-represented GO classes is displayed separately for both time points and both transdifferentiation directions examined (tab. 8). Complete GOstat results are stated in the appendix (tab. 18, tab. 19, tab. 20, and tab. 21). Major over-represented GO

classes include for both transdifferentiation directions the categories of development, transcription, signal transduction, extracellular region, and cytoskeleton.
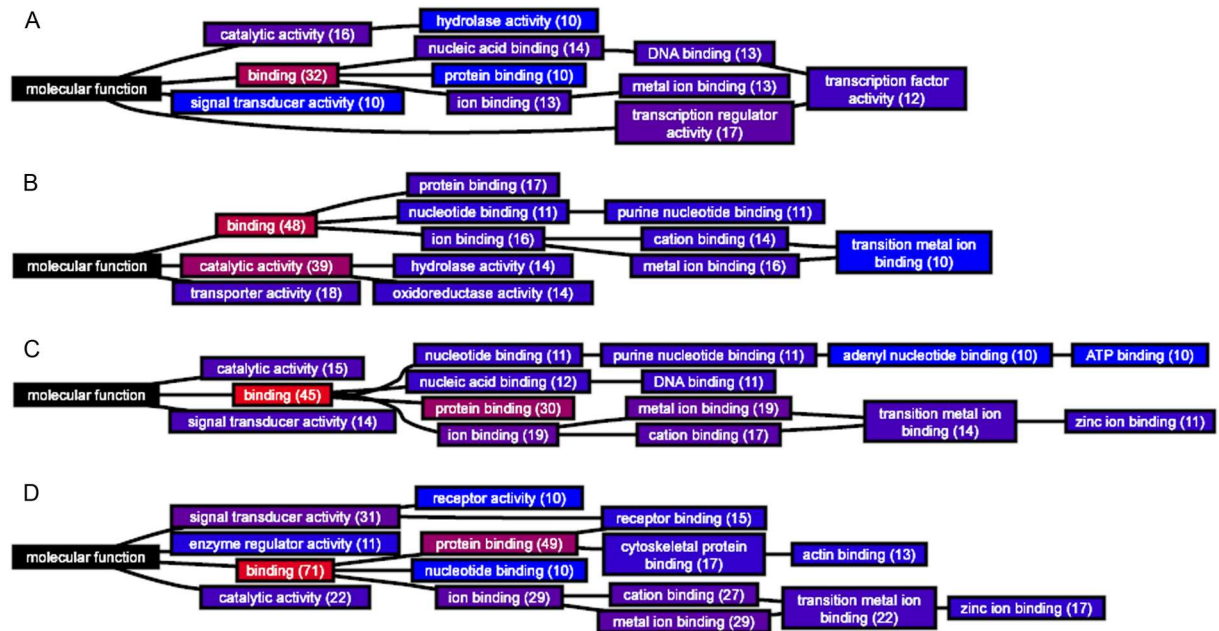


**Fig. 24    GO graphs of regulated genes associated with the GO classes of molecular function**

Regulated probe sets obtained by the first microarray analysis for adipogenic transdifferentiation were submitted into the Affymetrix NetAffx Analysis Center. The results of classification into different and hierarchical structured GO classes are shown separately for numbers of up-regulated genes 3 h (A) and 24 h (B) after initiation of adipogenic transdifferentiation as well as for numbers of down-regulated genes 3 h (C) and 24 h (D) after initiation of transdifferentiation. Thereby, only those GO classes are depicted that contained at least 10 members. Each rectangular node states the designation of the GO class and the corresponding number of included regulated probe sets in parentheses. Moreover, the colour of each node depends on the number of included probe sets ranging from blue boxes with low probe set number to red boxes with high probe set number. Branching into inferior GO categories is indicated by black curves originating from the superior class.
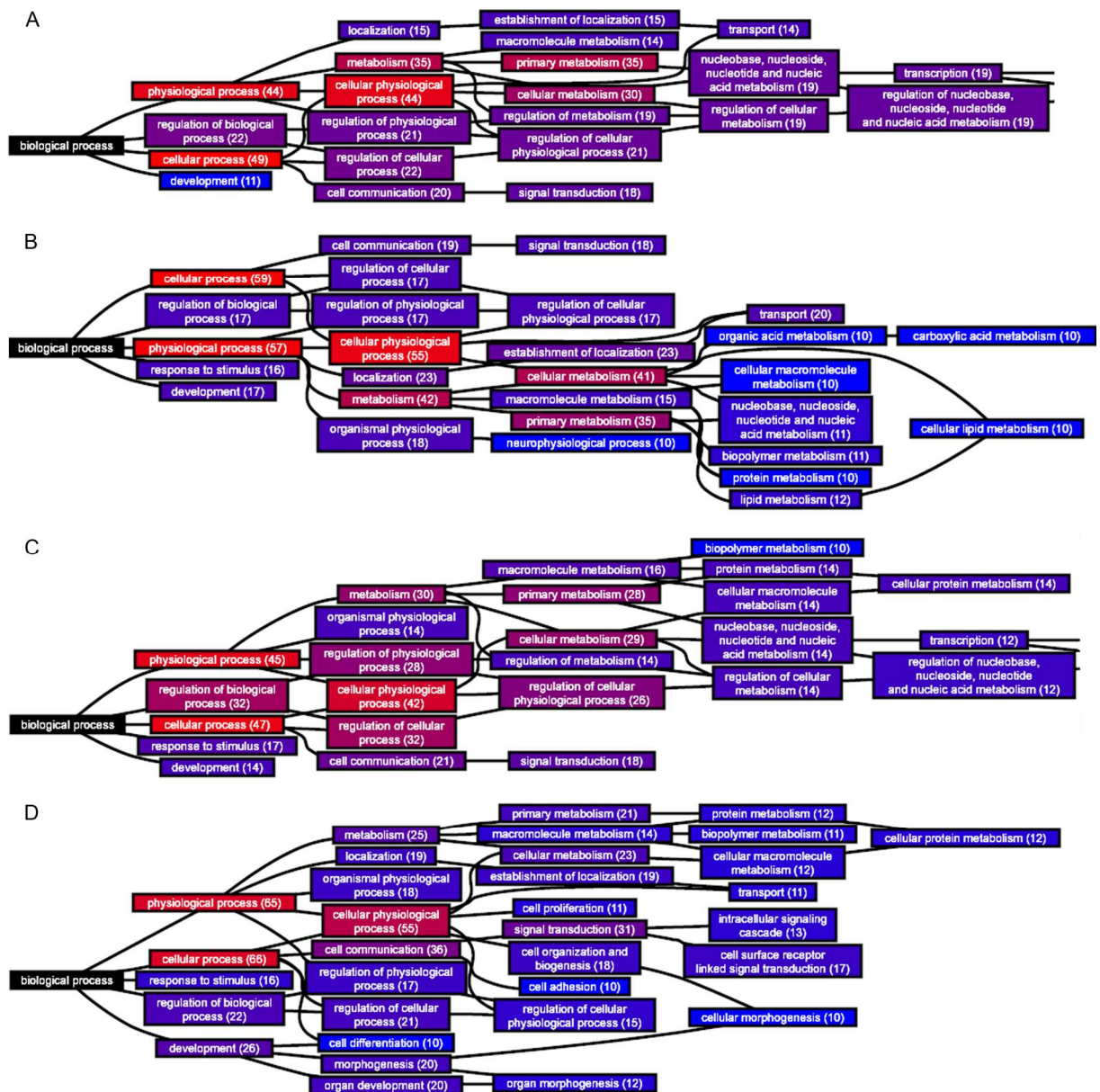
**Fig. 25    GO graphs of regulated genes associated with the GO classes of biological process**

The distribution of regulated probe sets into the GO classes of *biological process* was obtained and depicted analogously to the GO analysis regarding the class of *molecular function* described for fig. 24. Accordingly, the branching into different and hierarchical structured GO classes is shown separately for numbers of up-regulated genes 3 h (A) and 24 h (B) after initiation of adipogenic transdifferentiation and for numbers of down-regulated genes 3 h (C) and 24 h (D) after initiation of transdifferentiation.

**Tab. 8    Major over-represented GO classes for adipogenic transdifferentiation – GeneChips HG-U 133 Plus 2.0**

| GO term | Gene symbol | Regulated genes | Genes on array | GOstat p-value |
|---|---|---|---|---|
| **3 h after initiation of adipogenic transdifferentiation** *biological process* | | | | |
| development | **EPHA2** APOLD1 SLC2A14 SIX2 ENC1 EGR2 **KLF6** CXCL1 LIF DLX5 HMGA2 HLX1 KLF4 SEMA4C **CYR61** EGR3 BICD1 TGIF | 18 | 736 | 0.000858 |
| transcription | **NR4A2** SIX2 KLF7 CBX4 CREM ZNF281 **ID4** EGR2 **KLF6** ZNF331 HIVEP1 CHD1 DLX5 KLF4 HLX1 HMGA2 ZNF217 EGR3 TCF8 TGIF MSC | 21 | 1064 | 0.0025 |
| signal transduction | EPHB3 **EPHA2** CCL20 STK38L TNFRSF1B DUSP6 **RASD1 NR4A2** CREM GPR157 RGS2 **RAB20** GPRC5A PTGER4 CXCL1 LIF GNAL ITGAV CCL3 | 19 | 1117 | 0.0342 |
| *molecular function* | | | | |
| transcription regulator activity | **NR4A2** KLF7 SIX2 CBX4 CREM ZNF281 **ID4** EGR2 **KLF6** DLX5 HLX1 KLF4 EGR3 ZNF217 TCF8 TGIF MSC | 17 | 588 | 0.0000595 |
| signal transducer activity | RGS2 GPRC5A PTGER4 EPHB3 **EPHA2** CCL20 CXCL1 LIF TNFRSF1B GNAL SEMA4C **NR4A2** ITGAV CCL3 GPR157 | 15 | 773 | 0.0339 |
| **24 h after initiation of adipogenic transdifferentiation** *cellular component* | | | | |
| extracellular region | UACA CHL1 CSPG4 IL32 LPL **IGF1** ANGPTL2 ECGF1 **TNFRSF11B** CX3CL1 MMP1 FGF2 CXCL13 WNT5B FGF1 CXCL12 COL13A1 LEP **CYR61** IGFBP5 PRL **SERPINE1** PLA2G5 FN1 | 24 | 353 | 0.000014 |
| cytoskeleton | FBLIM1 DIAPH1 UACA **TPM1** STK38L RAPH1 VASP FGD4 FSCN1 CFL2 CALD1 RP11-54H7.1 ACTG2 NEDD9 MICAL2 PDLIM7 PLEKHC1 ACTC CTNNAL1 MYLIP DSP TUBB6 SMTN PALLD | 24 | 363 | 0.0000154 |
| *biological process* | | | | |
| development | HOP CHL1 EBF DDIT4L BDNF FZD4 CYP1B1 CHGN DSCR1L1 **PDLIM5** HDAC9 GLDN CLTCL1 FABP5 FGF1 PDLIM7 HMGA2 TNFRSF12A **CYR61** SORT1 **PPARGC1A** AHNAK PRL DSP CEBPA FBLIM1 CSPG4 EYA1 **IGF1** ANGPTL2 FGD4 ROR2 CAP2 VEGFC PALMD **TNFRSF11B** ECGF1 BHLHB3 FGF2 MAFB ARNT2 WNT5B NEDD9 **KLF6** PLEKHC1 IGFBP5 MYLIP MKX SMTN | 49 | 771 | 4.99 x 10$^{-11}$ |
| signal transduction | CHL1 LRRFIP2 CMKOR1 FZD4 ARHGAP28 **SNF1LK2** ARHGAP29 INPP4B ARL4C DSCR1L1 CX3CL1 **RGS4 RAB20** FGF1 **ANKRD1** SGK3 **PPARGC1A** PRL SERPINB9 CEBPA **PLCB4** DIRAS3 FN1 SPHK1 CSPG4 CD97 STK38L RAPH1 PDE7B **IGF1** FGD4 ROR2 TNS3 **RASD1** CAP2 VEGFC CLIC3 **TNFRSF11B** ECGF1 ADCY7 FGF2 ARNT2 WNT5B TAS2R38 NEDD9 GPR176 RAB3B HMOX1 OXTR CXCL12 GNAL LEP IGFBP5 | 53 | 1170 | 0.0000202 |
| *molecular function* | | | | |
| signal transducer activity | DIAPH1 MICB CMKOR1 LOXL4 BDNF LRP4 FZD4 **PDLIM5** CX3CL1 **RGS4** CLTCL1 FGF1 TNFRSF12A **PPARGC1A** SORT1 PRL **PLCB4** CD97 EVI2A CSPG4 IL32 **IGF1** ANGPTL2 ROR2 GMFG VEGFC ECGF1 **TNFRSF11B** FGF2 CXCL13 WNT5B ARNT2 TAS2R38 GPR176 HMOX1 OXTR CXCL12 GNAL LEP | 39 | 794 | 0.000196 |
| cytoskeletal protein binding | DIAPH1 **TPM1 SYNPO2** STK38L VASP FGD4 FSCN1 GMFG MYLIP CFL2 **CNN1** SMTN **PDLIM5** PALLD CALD1 | 15 | 177 | 0.00208 |

Reliably measured and after initiation of adipogenic transdifferentiation differentially regulated probe sets with at least one P detection call in the compared samples for each experimental set were subjected to GOstat analyses. The total number of regulated and not regulated probe sets detected on the GeneChip served as reference and is given in the respective column. Only over-represented GO classes containing at least 5 genes and a GOstat p-value ≤ 0.1 were considered. The above table shows only a selection of the major over-represented GO classes, complete lists for each time point and transdifferentiation direction are stated in tab. 18 and tab. 19. Adipogenic transdifferentiation exhibited 159 differentially regulated target probe sets that were analysed in reference to all 20,357 reliably measured probe sets for the 3 h time point, 418 target probe sets were referred to 21,892 reliably measured probe sets for the 24 h time point. The GO class of cellular component did not show any relevant over-representation under the stated criteria 3 h after initiation of adipogenic transdifferentiation. Gene symbols are stated according to the HUGO gene nomenclature, those in bold letters rank amongst the top 50 of the bioinformatic scoring depicted in tab. 11.

**Tab. 9    Major over-represented GO classes for osteogenic transdifferentiation – GeneChips HG-U 133 Plus 2.0**

| GO term | Gene symbol | Regulated genes | Genes on array | GOstat p-value |
|---|---|---|---|---|
| **3 h after initiation of osteogenic transdifferentiation** | | | | |
| *cellular component* | | | | |
| extracellular region | MMP3 GDF15 MMP12 **ANGPTL4** COL1A2 | 5 | 344 | 0.0782 |
| *biological process* | | | | |
| cellular carbohydrate metabolism | MMP3 MMP12 **PDK4** EXT1 PCK1 | 5 | 190 | 0.0916 |
| *molecular function* | | | | |
| signal transducer activity | EDG2 ACVR1C GDF15 PBEF1 **PDLIM5 RGS4** FZD4 | 7 | 790 | 0.0938 |
| **24 h after initiation of osteogenic transdifferentiation** | | | | |
| *cellular component* | | | | |
| cytoskeleton | DIAPH1 KIF20A ESPL1 KIF21A TPM4 TUBA1 MPHOSPH1 HIP1 BUB1 VASP AURKA MICAL1 ARPC5 MICAL2 LASP1 PPL CTNNAL1 HSPB1 KIF14 DSP CENPE PALLD PDLIM2 UACA FBLIM1 RAI14 BUB1B **TPM1** LMNB1 KIF11 RAPH1 CKAP2 SPAG5 FSCN1 DBN1 EPB41L2 CALD1 ACTG2 KIF4A LOC146909 TTK NEDD9 RACGAP1 CDC42EP5 CDC20 TPX2 KNS2 KIF23 WDR1 MYLIP NEK2 ANLN EPB41L3 PRC1 SGCD KIF15 SMTN TPM2 KIF2C DLG7 ARHGDIB | 61 | 379 | 2.84 x 10⁻¹¹ |
| extracellular region | MMP13 CHL1 MMP12 **IGFBP1** APOL6 PLAT GLIPR1 YARS GREM2 FSTL3 MFAP5 PRRG4 PDGFA FGF1 SAA2 **CYR61** LAMA4 VEGF CHI3L1 **SERPINE1** COMP CLEC3B COL11A1 FN1 UACA THBS1 ANGPTL2 HAPLN1 PHGDH **TNFRSF11B** CXCL13 WNT5B GDF15 CXCL12 **ANGPTL4** WISP1 LEP COL8A1 SGCD CTGF ADIPOQ | 41 | 362 | 0.00397 |
| chromosome | BUB1B RFC3 MAD2L1 BUB1 TMPO HNRPD MCM2 CDCA5 AURKB ZWILCH RAD50 CBX5 TOP2A PRRX2 SGOL2 HMGA2 KNTC2 MCM7 CHEK1 CENPE CDCA8 KIF2C | 22 | 159 | 0.00628 |
| *biological process* | | | | |
| cell cycle | CDKN3 ESPL1 DDIT3 BUB1 E2F7 AURKB RAD50 PBK E2F8 PDGFA FGF1 MCM5 CDC6 RGC32 MCM6 CHEK1 DIRAS3 HRASLS3 KIF11 MKI67 CKAP2 CEP55 MCM2 BARD1 CDK6 CCND3 YWHAH RACGAP1 CDC20 BRIP1 TPX2 PTTG1 NEK2 ANLN KIF15 KIF2C DLG7 UHRF1 HK2 ZWINT CDCA5 PLK1 CCNB1 AURKA TCF19 CDC2 HDAC9 NUSAP1 SGOL2 MSH2 UBE2C WEE1 VEGF CIT CENPE BUB1B MAD2L1 BRRN1 SPAG5 SPIN3 CCND1 PLK4 VEGFC CCNA2 CCNB2 NEDD9 TTK CCNE2 KIF23 KNTC2 MCM7 PRC1 SESN2 CDCA8 HCAP-G | 75 | 462 | 1.13 x 10⁻¹⁴ |
| cytoskeleton organization and biogenesis | DIAPH1 KIF20A ESPL1 KIF21A TUBA1 ZWINT MPHOSPH1 AURKA ADRA2A MICAL1 ARPC5 NUSAP1 LASP1 UBE2C KIF14 **CNN1** CENPE PALLD BUB1B KIF11 FSCN1 SPAG5 DBN1 EPB41L2 LOC146909 KIF4A YWHAH CDC42EP5 RACGAP1 NEDD9 TTK KNS2 KIF23 CXCL12 KNTC2 PRC1 EPB41L3 SGCD KIF15 KIF2C ARHGDIB | 41 | 201 | 1.45 x 10⁻¹¹ |
| development | EMP1 EBF **IGFBP1** CASC5 FOXC2 BDNF NRCAM SLC3A2 SEMA6D CSRP2 EDNRB NTRK2 TAGLN FGF1 PPL TNFRSF12A LAMA4 **CYR61** **PPARGC1A** IFRD1 CLEC3B COL11A1 **EPHA2** CAP2 DBN1 PHGDH SOX9 **TNFRSF11B** MEOX2 IER3 WNT5B YWHAH LPIN1 RACGAP1 HLF WISP1 MYLIP CTGF CAP1 CHL1 DDIT4L ALDH3A2 GPM6B NRAS FZD4 CYP1B1 TAGLN2 ALPL SEMA3G GHR DLX1 **PDLIM5** CACNB2 PRRX2 HDAC9 TGFBR3 DACT1 HMGA2 FHL3 VEGF CIT DSP MET COMP EFNB2 FBLIM1 THBS1 ANGPTL2 CEBPG SEMA5A SPIN3 VEGFC VLDLR BHLHB3 ARNT2 NEDD9 CDC42EP5 **KLF6** MBNL1 **ANGPTL4** SGCD SMTN KITLG ARHGDIB | 85 | 786 | 0.0000117 |
| signal transduction | CLOCK **IGFBP1** KIT CMKOR1 GKAP1 ITGA3 ARHGAP28 SCG5 AGTR1 INPP4B OPN1SW ARL4C EDNRB PXK ITGA5 **RAB20** NTRK2 PLEKHG2 **DDAH1** PDGFA FGF1 **ANKRD1 PPARGC1A** BAG1 **PLCB4** ILK DIRAS3 CLIC1 **EPHA2** ARHGAP22 **RASD1** IL4R CAP2 FAM13A1 ADCY7 **TNFRSF11B** PRKAR2B RAC2 YWHAH WNT5B TAS2R38 GDF15 RACGAP1 PPP4R1 HMOX1 CXCL12 GNAL WISP1 PBEF1 RHOC CAP1 GNB4 CHL1 ZWINT PLP2 FZD4 **SNF1LK2** AURKA ADRA2A SAV1 MICAL1 TOP2A SLC20A1 MKNK2 **RGS4** FEN1 PTGFR TGFBR3 DACT1 IL18R1 LIFR UBE2C VEGF CIT GEM MET ZYX FN1 BUB1B CD97 RAPH1 PDE7B SPAG5 VEGFC VLDLR TXNRD1 PDE3B RAGE ARNT2 TNFRSF21 NEDD9 ECT2 ARHGEF2 RAB3B FPR1 DEPDC1 ARHGAP18 LEP KNTC2 DAPK3 TGFB1I1 PTGER2 RASL11B KITLG ARHGDIB | 105 | 1228 | 0.0106 |
| *molecular function* | | | | |
| cytoskeletal protein binding | DIAPH1 **TPM1** TPM4 HIP1 VASP FSCN1 NRCAM DBN1 PXK **PDLIM5** EPB41L2 CALD1 YWHAH RACGAP1 TAGLN LASP1 MYLIP WDR1 ANLN EPB41L3 **CNN1** TPM2 SMTN CAP1 PALLD | 25 | 182 | 0.021 |
| nucleotide binding | RFC3 KIF21A REV3L TUBA1 KIT BUB1 DHRS3 AURKB SCG5 PBK RAD50 ARL4C FIGNL1 **RAB20** NTRK2 MCM5 ACACB CDC6 RP11-301I17.1 PC **PPARGC1A** MCM6 CHEK1 TK1 MELK CIRBP MXRA5 ILK DIRAS3 KIF11 ATAD2 **PDK4 EPHA2** GBP1 MKI67 HNRPD MCM2 **RASD1** PRKAR2B RAC2 LOC91461 TRIP13 MCM4 ACTG2 LOC146909 CDK6 FAM83D TPX2 BRIP1 GNAL NEK2 KIF15 RHOC KIF2C KIF20A PCK2 DOCK11 TRIB3 HK2 POR MPHOSPH1 PLK1 DCK LOC81691 **SNF1LK2** AURKA CDC2 YARS TOP2A MKNK2 MSH2 WEE1 EHD1 KIF14 CIT GEM MET CENPE BUB1B RP2 PLK4 RRM1 LARP6 TXNRD1 SPG3A ME1 RAGE KIF4A TTK THNSL1 RAB3B FRY KIF23 MCM7 DAPK3 RASL11B | 96 | 113 | 0.0516 |
| signal transducer activity | CLOCK KIT CMKOR1 ITGA3 BDNF SEMA6D OPN1SW AGTR1 EDNRB GREM2 ITGA5 NTRK2 PDGFA **FGF1** LASP1 TNFRSF12A SAA2 LAMA4 **PPARGC1A** BAG1 **PLCB4** NR1H3 MXRA5 **EPHA2** IL4R NR1D2 **TNFRSF11B** WNT5B YWHAH GDF15 TAS2R38 HMOX1 CXCL12 GNAL PBEF1 RHOC ULBP2 GNB4 DIAPH1 LOXL4 FZD4 ADRA2A GHR SEMA3G YARS **PDLIM5** SLC20A1 **RGS4** TGFBR3 PTGFR LIFR IL18R1 VEGF MET EFNB2 THBS1 EVI2A CD97 ANGPTL2 SEMA5A IGSF4 VLDLR VEGFC CXCL13 PDCD1LG2 TNFRSF21 ARNT2 ECT2 FPR1 LEP KDELR3 TGFB1I1 PTGER2 KITLG ADIPOQ | 75 | 834 | 0.0527 |

Reliably measured and after initiation of osteogenic transdifferentiation differentially regulated probe sets with at least one P detection call in the compared samples for each experimental set were subjected to GOstat analyses. The total number of regulated and not regulated probe sets detected on the GeneChip served as reference and is given in the respective column. Only over-represented GO classes containing at least 5 genes and a GOstat p-value ≤ 0.1 were considered. The above table shows only a selection of the major over-represented GO classes, complete lists for each time point and transdifferentiation direction are stated in tab. 20 and tab. 21. Osteogenic transdifferentiation provided 92 target probe sets 3 h after initiation of transdifferentiation that were analysed to the reference of all 22,634 reliably measured probe sets at this time point, for the 24 h time point 1,196 target probe sets were found and analyzed to the reference of all 24,108 reliably measured probe sets. Gene symbols are stated according to the HUGO gene nomenclature, those in bold letters rank amongst the top 50 of the bioinformatic scoring depicted in tab. 11.

### 4.3.4  Functional grouping of differentially regulated genes

Amongst all reproducibly and at least 2-fold regulated genes that were obtained by employment of the larger GeneChips, members of various signalling pathways were detected (tab. 10). Several genes exhibiting differential regulation shortly after initiation of transdifferentiation were involved in fibroblast growth factor (FGF) signalling, insulin-like growth factor (IGF) signalling, integrin signalling, Wnt/β-catenin signalling, G-protein signalling, and plasminogen activator urokinase (PLAU) signalling. Moreover, some genes correlated with lipid metabolism, adenosine triphosphate (ATP) metabolism, and adipogenesis. Many of these functionally grouped genes also showed reciprocal regulation patterns regarding the different transdifferentiation directions.

## Tab. 10   Regulation of functionally grouped genes

| Gene symbol | Gene name | Regulation during | |
| --- | --- | --- | --- |
| | | adipogenic trans-differentiation | osteogenic trans-differentiation |
| *FGF signalling* | | | |
| FGF1 [b] | fibroblast growth factor 1 | down | up |
| FGF2 | fibroblast growth factor 2 | down | - |
| FGF7 | fibroblast growth factor 7 | - | up |
| BCL2 | B-cell CLL/lymphoma 2 | - | down |
| *IGF signalling* | | | |
| IGF1 [b] | insulin-like growth factor 1 | up | down |
| IGFBP1 [b] | insulin-like growth factor binding protein 1 | - | down |
| IGFBP5 | insulin-like growth factor binding protein 5 | up | - |
| PIK3R3 | phosphoinositide-3-kinase, regulatory subunit 3 (p55, gamma) | up | - |
| YWHAH | tyrosine 3-monooxygenase/tryptophan 5-monooxygenase activation protein, eta polypeptide | - | up |
| CCND1 | cyclin D1 | - | up |
| CCND3 | cyclin D3 | - | up |
| PRKAR2B | protein kinase, cAMP-dependent, regulatory, type II, beta | - | down |
| *integrin signalling* | | | |
| ITGA3 | integrin, alpha 3 | - | up |
| ITGA5 | integrin, alpha 5 | - | up |
| VIL2 [b] | villin 2 (ezrin) | down | up |
| ACTG2 | actin, gamma 2, smooth muscle, enteric | down | up |
| ACTN1 | actinin, alpha 1 | - | up |
| ACTC | actin, alpha, cardiac muscle | down | - |
| CFL2 | cofilin 2 (muscle) | down | up |
| VCL | vinculin | - | up |
| ILK | integrin-linked kinase | - | up |
| CDC2 | cell division cycle 2, G1 to S and G2 to M | - | up |
| YWHAH | tyrosine 3-monooxygenase/tryptophan 5-monooxygenase activation protein, eta polypeptide | - | up |
| IGFBP1 [b] | insulin-like growth factor binding protein 1 | - | down |
| IGFBP5 | insulin-like growth factor binding protein 5 | up | - |
| LAMA4 | laminin, alpha 4 | - | down |
| *Wnt/β-catenin signalling* | | | |
| WNT5B | wingless-type MMTV integration site family, member 5B | down | up |
| BIRC5 | baculoviral IAP repeat-containing 5 | - | up |
| FOSL1 | FOS-like antigen 1 | down | - |
| NRCAM | neuronal cell adhesion molecule | - | down |
| CCND1 | cyclin D1 | - | up |
| ENC1 [a] | ectodermal-neural cortex (with BTB-like domain) | down | - |
| VEGF | vascular endothelial growth factor | up | down |
| TLE1 | transducin-like enhancer of split 1 | - | down |
| TLE3 | transducin-like enhancer of split 3 | up | - |
| ANGPTL4 [a, b] | angiopoietin-like 4 | - | down |
| IGF1 [a, b] | insulin-like growth factor 1 | up | down |
| SFRP2 [a, b] | secreted frizzled-related protein 2 | up | down |
| CYR61 [a, b] | cysteine-rich, angiogenic inducer, 61 | down | up |
| COL11A1 [a] | collagen, type XI, alpha 1 | - | up |
| CTGF [a] | connective tissue growth factor | - | up |
| THBS1 [a] | thrombospondin 1 | down | up |
| TNFRSF11B [a, b] | tumor necrosis factor receptor superfamily, member 11b | down | up |
| WISP1 [a] | WNT1 inducible signalling pathway protein 1 | - | up |
| *G-protein signalling* | | | |
| RGS4 [b] | regulator of G-protein signalling 4 | down | up |
| PLCB4 [b] | phospholipase C, beta 4 | down | up |
| GNB4 | guanine nucleotide binding protein (G protein), beta polypeptide 4 | down | up |
| EDG3 | endothelial differentiation, sphingolipid G-protein-coupled receptor, 3 | up | down |
| PRKAR2B | protein kinase, cAMP-dependent, regulatory, type II, beta | - | down |
| NFATC1 | nuclear factor of activated T-cells, cytoplasmic, calcineurin-dependent 1 | up | - |
| NFATC4 | nuclear factor of activated T-cells, cytoplasmic, calcineurin-dependent 4 | up | - |
| *plasminogen activator, urokinase (PLAU) signalling* | | | |
| PLAUR | plasminogen activator urokinase receptor | - | up |
| SERPINB2 [b] | serpin peptidase inhibitor, clade B (ovalbumin), member 2 | down | - |
| SERPINE1 [b] | serpin peptidase inhibitor, clade E, member 1 | down | up |
| *lipid metabolism* | | | |
| ACACA | acetyl-Coenzyme A carboxylase alpha | - | down |
| ACACB | acetyl-Coenzyme A carboxylase beta | up | down |
| *adenosine triphosphate (ATP) metabolism* | | | |
| PDE4B [b] | phosphodiesterase 4B, cAMP-specific | up | down |
| ADCY7 | adenylate cyclase 7 | down | up |
| *adipogenesis-associated genes* | | | |
| PPARGC1A [b] | peroxisome proliferative activated receptor, gamma, coactivator 1, alpha | up | down |
| FABP4 [b] | fatty acid binding protein 4, adipocyte | up | - |
| LPL | lipoprotein lipase | up | - |
| CEBPA | CCAAT/enhancer binding protein (C/EBP), alpha | up | - |

The regulation patterns for both transdifferentiation pathways are depicted for genes grouped into functional classes. A minus indicates that no expression change was detected under the defined criteria (see materials and methods' section), the superscript 'a' marks genes whose transcription is regulated by WNT3A [Jackson et al., 2005; Si et al., 2006], genes ranking amongst the top 50 of the bioinformatic scoring scheme (see next section) are labelled by the superscript 'b'.

### 4.3.5   Development of a novel bioinformatic scoring scheme for interpretation of microarray results

Due to the high number of at least 2-fold and reproducibly regulated genes during transdifferentiation obtained by employment of the GeneChips HG-U 133 Plus 2.0, a novel empirical scoring system was developed to filter out genes with potential relevance regarding the early events of transdifferentiation.

#### *4.3.5.1  Definition of the criteria for the novel scoring scheme*

In collaboration with Prof. Dr. Ralf Zimmer and Dr. Robert Küffner of the Institute of Informatics at the Ludwig Maximilians University in Munich, the criteria defining the bioinformatic scoring scheme were determined and formulas for the calculation of the bioinformatic score were developed and applied to the sum of 8 compared probe pairs.

The design of the bioinformatic score provided high scores for those genes that were significantly regulated and was further elevated if their regulation was reciprocal regarding the two transdifferentiation pathways. Moreover, the scoring scheme assessed the reproducibility of regulation events in repeated experiments, thus evaluating datasets from different biological samples obtained by different microarray sets. Only those probe sets attributed with an increase or decrease call by the Affymetrix comparison algorithm were taken into account. The signal log ratios obtained from corresponding pairs (signal of transdifferentiated sample versus signal of differentiated control sample) determined the extent of regulation. Furthermore, to incorporate the reliability of the signal intensities, log change p-values were factored in to weight the log changes. The weighted fold changes displayed a unimodal, almost symmetrical distribution. Given the intensity distribution of the individual microarray sets, z-scores of the weighted fold changes were used to empirically quantify the strength of regulation.

The *score*$_S$ calculated the extent of reciprocal regulation for probe set *s* from RNA sample *r*:

$$score_S(s,r) = \left| z_{3h}^{AC:OB}(s,r) - z_{3h}^{OB:AC}(s,r) \right| + \left| z_{24h}^{AC:OB}(s,r) - z_{24h}^{OB:AC}(s,r) \right| + \left| z_{24h-3h}^{AC:OB}(s,r) - z_{24h-3h}^{OB:AC}(s,r) \right|$$

with *AC:OB* = osteogenic transdifferentiation, *OB:AC* = adipogenic transdifferentiation.

Thereby, the combination of z-scores of the respective time points in the first and second summand selected for probe sets with high fold changes and preferably reciprocal regulation

between different transdifferentiation directions. The third summand quantified the reciprocal regulation of weighted log fold changes for the 3 h and 24 h time points of the same transdifferentiation direction.

If several probe set representing the same gene were combined to a set of probe sets $g_{s,r}$ that measures gene $g$ in sample $r$. Accordingly, the single gene score for each microarray set, i.e. for the different biological samples, was calculated by:

$$score_G(g,r) = \frac{1}{\sqrt{|g_{s,r}|}} \sum_{s \in g_{s,r}} score_S(s,r)$$

All single gene scores derived from single RNA samples $r \in R$ were averaged over the set of samples $R$. An uncentred correlation coefficient was employed to weight this average, which resulted in higher scores if time courses in $R$ were reproducible. Thus, genes were ranked by their relevance via:

$$score_{G,R}(g) = ucorr(Z(r_1),Z(r_2)) \cdot \frac{1}{|R|} \sum_{r \in R} score_G(g,r), \text{ with}$$

$$Z(r) = \mathop{++}_{s \in g_{s,r}} < z_{3h}^{AC:OB}(s,r) - z_{3h}^{OB:AC}(s,r), z_{24h}^{AC:OB}(s,r) - z_{24h}^{OB:AC}(s,r), z_{24h-3h}^{AC:OB}(s,r) - z_{24h-3h}^{OB:AC}(s,r) >$$

Thereby, the single gene scores, i.e. $score_G(g,r)$ (named score 1 and score 2 in tab. 11), rank a gene $g$ based on the first and the second measured sample $r$ corresponding to the different biological samples. The combined score, i.e. $score_{G,R}(g)$, quantifies the total relevance of the gene and was used to rank the genes in descending order.

### 4.3.5.2 Ranking of differentially regulated gene products by the novel scoring scheme

The 50 highest-ranking genes are listed in tab. 11 according to their descending bioinformatic score with additional information regarding the regulation patterns detected by microarray analyses and their functional properties. The signal log changes of the 8 highest-ranking genes are plotted in fig. 26. These graphs are representative for many of the highly ranked genes as they exhibit reciprocal regulation between the different transdifferentiation pathways in at least one of the time points examined. Regarding their functional properties, many of the highly ranked genes were associated with signalling pathways, morphology, cell differentiation, lipid metabolism, cellular biosynthesis, and transcription. Moreover, amongst the top 50-ranking genes more than 60% were also detected by GOstat analyses as members of over-represented GO categories (tab. 16, tab. 17, tab. 18, and tab. 19).

**Tab. 11  Top 50 of regulated genes ranked by their bioinformatic scoring**

| # | Regulation in adipogenic transdiff. | Regulation in osteogenic transdiff. | Com-bined score | Corre-lation | Score 1 | Score 2 | # of probe sets | Gene symbol | Gene name | Functions |
|---|---|---|---|---|---|---|---|---|---|---|
| 1 | down | up | 42.47 | 0.89 | 49.37 | 46.12 | 3 | RGS4 | regulator of G-protein signalling 4 | a, g |
| 2 | down | up | 32.28 | 0.94 | 28.62 | 40.21 | 2 | TNFRSF11B | tumor necrosis factor receptor superfamily, member 11b | a, k |
| 3 | down | up | 32.27 | 0.97 | 28.68 | 37.68 | 1 | KRTAP1-5 | keratin associated protein 1-5 | |
| 4 | down | up | 31.07 | 0.79 | 36.14 | 42.40 | 7 | SYNPO2 | synaptopodin 2 | |
| 5 | up | down | 30.93 | 0.82 | -32.98 | -42.65 | 5 | PHLDA1 | pleckstrin homology-like domain, family A, member 1 | |
| 6 | down | up | 29.31 | 0.93 | 24.43 | 38.64 | 2 | PLCB4 | phospholipase C, beta 4 | a, d, g |
| 7 | up | down | 28.64 | 0.95 | -29.83 | -30.33 | 2 | SFRP2 | secreted frizzled-related protein 2 | a, c |
| 8 | up | down | 28.38 | 0.78 | -34.39 | -38.87 | 3 | NR4A2 | nuclear receptor subfamily 4, group A, member 2 | a, f |
| 9 | down | up | 28.11 | 0.99 | 28.35 | 28.47 | 1 | ANKRD1 | ankyrin repeat domain 1 | a |
| 10 | down | up | 28.01 | 0.94 | 28.93 | 30.57 | 1 | KRTHA4 | keratin, hair, acidic, 4 | |
| 11 | up | down | 28.00 | 0.94 | -26.32 | -33.12 | 3 | ARL7 | ADP-ribosylation factor-like 7 | |
| 12 | down | up | 27.98 | 0.99 | 23.83 | 32.64 | 2 | FGF1 | fibroblast growth factor 1 | a, b, c, h |
| 13 | down | up | 27.88 | 0.98 | 23.47 | 33.21 | 1 | MGAM | maltase-glucoamylase | |
| 14 | down | up | 26.90 | 0.85 | 31.80 | 31.70 | 2 | FMN2 | formin 2 | a |
| 15 | down | up | 26.28 | 0.89 | 21.54 | 37.29 | 2 | CYR61 | cysteine-rich, angiogenic inducer, 61 | b |
| 16 | up | down | 25.71 | 0.90 | -19.01 | -38.01 | 2 | ANGPTL4 | angiopoietin-like 4 | b, c, d |
| 17 | down | up | 25.30 | 0.94 | 21.97 | 31.75 | 4 | TPM1 | tropomyosin 1 | a, d, e |
| 18 | up | down | 24.78 | 0.99 | -24.21 | -26.12 | 1 | RASD1 | RAS, dexamethasone-induced 1 | a |
| 19 | up | down | 24.25 | 0.88 | -18.36 | -36.60 | 1 | SLC16A6 | solute carrier family 16, member 6 | |
| 20 | down | up | 23.81 | 0.66 | 51.56 | 20.24 | 2 | B3GALT2 | UDP-Gal:betaGlcNAc beta 1,3-galactosyltransferase, polypeptide 2 | e |
| 21 | up | down | 23.48 | 0.84 | -33.91 | -21.89 | 1 | PDK4 | pyruvate dehydrogenase kinase, isoenzyme 4 | |
| 22 | down | up | 23.33 | 0.97 | 24.12 | 23.94 | 1 | BIRC3 | baculoviral IAP repeat-containing 3 | a, l |
| 23 | down | up | 22.97 | 0.94 | 25.91 | 22.92 | 2 | SERPINE1 | serpin peptidase inhibitor, clade E, member 1 | m |
| 24 | down | up | 22.96 | 0.93 | 30.39 | 19.27 | 4 | VIL2 | villin 2 (ezrin) | b, j |
| 25 | up | down | 22.72 | 1.00 | -21.52 | -24.11 | 1 | DDIT4 | DNA-damage-inducible transcript 4 | |
| 26 | up | (down) | 22.40 | 0.89 | -24.26 | -26.17 | 3 | ID4 | inhibitor of DNA binding 4, dominant negative helix-loop-helix protein | f |
| 27 | down | up | 21.90 | 0.93 | 22.33 | 24.65 | 2 | ALDH1B1 | aldehyde dehydrogenase 1 family, member B1 | |
| 28 | down | up | 21.87 | 0.99 | 22.37 | 21.76 | 1 | SCHIP1 | schwannomin interacting protein 1 | |
| 29 | down | up | 21.86 | 0.86 | 21.13 | 29.76 | 3 | DDAH1 | dimethylarginine dimethylaminohydrolase 1 | a |
| 30 | down | up | 21.74 | 0.97 | 18.56 | 26.15 | 1 | MRVI1 | murine retrovirus integration site 1 homolog | |
| 31 | up | down | 21.08 | 0.79 | -31.70 | -21.40 | 4 | IGF1 | insulin-like growth factor 1 | a, i |
| 32 | down | up | 20.27 | 0.71 | 30.96 | 26.42 | 4 | PDLIM5 | PDZ and LIM domain 5 | b |
| 33 | up | (down) | 19.80 | 1.00 | -19.60 | -20.02 | 1 | FABP4 | fatty acid binding protein 4, adipocyte | o |
| 34 | down | up | 19.75 | 0.99 | 23.27 | 16.84 | 2 | DNAJB4 | DnaJ homolog, subfamily B, member 4 | |
| 35 | down | up | 19.56 | 1.00 | 18.61 | 20.61 | 1 | CNN1 | calponin 1, basic, smooth muscle | |
| 36 | up | down | 19.55 | 0.94 | -17.56 | -24.17 | 2 | PDE4B | phosphodiesterase 4B, cAMP-specific | a, n |
| 37 | down | up | 19.49 | 0.99 | 20.66 | 18.59 | 2 | KLF6 | Kruppel-like factor 6 | b, c, f |
| 38 | up | down | 19.18 | 0.96 | -16.47 | -23.38 | 3 | INSIG1 | insulin induced gene 1 | |
| 39 | down | -- | 19.02 | 1.00 | 17.03 | 21.00 | 1 | CCL3L1 | chemokine ligand 3-like 1 | a |
| 40 | up | down | 18.86 | 1.00 | -18.50 | -19.37 | 1 | RAB20 | RAB20, member RAS oncogene family | a |
| 41 | up | down | 18.75 | 0.80 | -10.55 | -36.58 | 1 | IGFBP1 | insulin-like growth factor binding protein 1 | a, b, i, j |
| 42 | down | up | 18.46 | 0.99 | 21.19 | 16.03 | 2 | TMEM173 | transmembrane protein 173 | |
| 43 | up | down | 18.45 | 0.97 | -21.88 | -16.28 | 2 | SNF1LK2 | SNF1-like kinase 2 | a |
| 44 | up | down | 18.26 | 0.99 | -18.60 | -18.28 | 1 | PPARGC1A | peroxisome proliferative activated receptor, gamma, coactivator 1, alpha | c, d, e, f |
| 45 | (down)* | up* | 18.06 | 0.89 | 17.81 | 22.74 | 1 | EPHA2 | EPH receptor A2 | a |
| 46 | up | down | 18.03 | 0.96 | 15.87 | 21.71 | 1 | 230795_at | 230795_at (transcribed locus) | |
| 47 | up | down | 17.96 | 1.00 | -17.51 | -18.56 | 1 | G0S2 | G0/G1 switch 2 | |
| 48 | down | up | 17.96 | 0.839 | 21.42 | 21.38 | 1 | SERPINB2 | serpin peptidase inhibitor, clade B, member 2 | m |
| 49 | down | up | 17.84 | 0.957 | 17.58 | 19.69 | 1 | LMO7 | LIM domain 7 | |
| 50 | down | up | 17.82 | 0.993 | 16.81 | 19.08 | 1 | PHLDA2 | pleckstrin homology-like domain, family A, member 2 | |

Regulated genes are listed by their descending combined score that quantifies the total relevance of each gene resulting from the correlation of both single gene scores 1 and 2. The number of regulated probe sets that were taken into account for the same gene is stated in the respective column. Additionally, up- or down-regulation of genes in osteogenic and adipogenic transdifferentiation, respectively, is displayed according to the microarray data. Thereby, -- indicates absence of any decrease or increase call, less than 2-fold regulations are stated in parentheses, and the asterisk indicates that this gene only exhibited reciprocal regulation 24 h after initiation of transdifferentiation, whereas the 3 h time point showed no regulation in osteogenic but up-regulation in adipogenic transdifferentiation.

a = signal transduction, b = morphology, c = cell differentiation, d = lipid metabolism, e = cellular biosynthesis, f = transcription, g = G-protein signalling, h = FGF signalling, i = IGF signalling, j = integrin signalling, k = osteoclastogenesis, l = inhibition of apoptosis, m = PLAU signalling, n = ATP metabolism, o = adipogenesis.
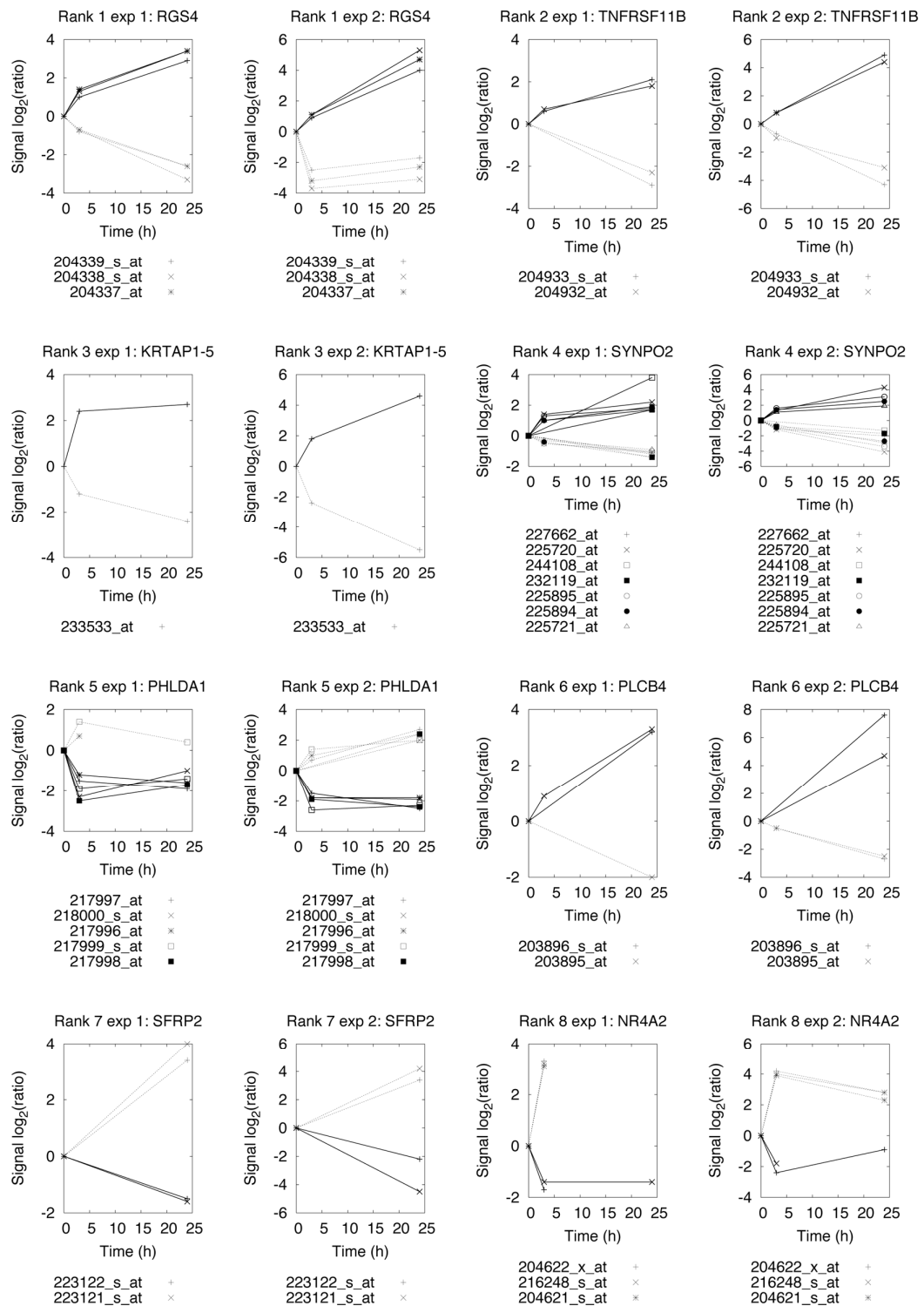
**Fig. 26    Plot of gene regulation patterns of the 8 most highly ranked genes**

Signal $\log_2$ ratios obtained by two microarray experiments (exp 1 and 2) represent changes of gene expression 3 h and 24 h after initiation of transdifferentiation, respectively. Transdifferentiation from adipocytes into osteoblasts is stated by continuous curves, whereas transdifferentiation of pre-osteoblasts into adipocytes is shown by dotted curves. Multiple curves for the same gene in a single transdifferentiation direction show regulation of multiple probe sets for the corresponding gene. Expression levels of transdifferentiated samples were compared to control mRNA levels of differentiated cells. Accordingly, the increase of gene expression is stated by positive values while the decrease of gene expression is given by negative values.

## 4.4   Functional testing of human recombinant proteins during differentiation and transdifferentiation

Amongst the established genes, several genes that had received high ranking by bioinformatic evaluation (see 4.3.5.2) encode for secreted proteins. Prior to functional testing of some of the respective gene products in our cell culture system that were commercially available and produced in our own laboratory, respectively, the regulation patterns of gene expression were evaluated by semi-quantitative RT-PCR (see 4.3.2).

For TNFRSF11B, SFRP2, FGF1, CYR61, and IGF1, reciprocal regulation patterns of gene expression during the different transdifferentiation pathways were detected by microarray analyses and confirmed by semi-quantitative RT-PCR analyses (except for the change of SFRP2 during osteogenic transdifferentiation). While TNFRSF11B and CYR61 declined during adipogenic transdifferentiation and augmented during osteogenic transdifferentiation, SFRP2 and IGF1 showed the reciprocal regulation pattern with decreasing mRNA amounts for osteogenic but increasing mRNA levels for adipogenic transdifferentiation.

Since distinct changes of gene expression during the early events of transdifferentiation should also influence the feasibility of differentiation of MSCs, at first normal adipogenic and osteogenic differentiation were examined in presence of the recombinant proteins encoded by these genes.

### 4.4.1   Secreted proteins tested in differentiation of MSCs without effect

According to the changes of TNFRSF11B and CYR61 mRNA levels shortly after initiation of both transdifferentiation pathways, the corresponding proteins rhTNFRSF11B and rhCYR61 were supposed to decrease adipogenic but to enhance osteogenic differentiation. In contrast, due to the changes of SFRP2 and IGF1 mRNA levels rmSFRP2 and rhIGF1 were expected to increase adipogenic but to reduce osteogenic differentiation.

Differentiation was monitored by staining of lipid vesicle accumulation for adipogenic differentiation whereas osteogenic differentiation was assessed by staining of ALP activity and mineralised extracellular matrix in the cell monolayers. Control samples incubated in the respective differentiation medium without recombinant proteins and with additional protein solvent (0.0005% BSA in PBS), respectively, showed normal adipogenic and osteogenic differentiation of MSCs. Employment of the above-mentioned recombinant proteins in parallel with the respective differentiation factors did not cause noticeable alteration of differentiation in our cell culture system. As an exception, for addition of rmSFRP2 to osteogenic differentiation medium cells were observed to detach within the first days of incubation. For adipogenic differentiation, the application of these recombinant proteins prior to and during incubation with the differentiation factors was tested but yielded no effect either. Moreover, rmSFRP2 was not able to induce adipogenic differentiation in the absence of the

conventional adipogenic differentiation factors. Similarly, TNFRSF11B could not provoke osteogenic differentiation in absence of the conventional osteogenic differentiation supplements.

### 4.4.2   Effect of FGF1 on adipogenic differentiation and transdifferentiation

Distinct changes in mRNA levels for FGF1 early after initiation of transdifferentiation obtained by microarray data and RT-PCR analysis indicated an inhibitory effect of FGF1 protein on adipogenic and an enhancing effect on osteogenic development. At first, the influence of rhFGF1 on adipogenic and osteogenic differentiation was examined.

Addition of 6 - 50 ng/ml rhFGF1 during adipogenic differentiation resulted in significant decrease of adipocyte-specific lipid vesicle accumulation (fig. 27 and fig. 28). This finding was irrespective of the prior incubation of confluent MSCs with sole 6 - 50 ng/ml rhFGF1 followed by simultaneous application of FGF1 and adipogenic supplements. Since gaps in the cell monolayers appeared occasionally after 14 d of incubation during application of 50 ng/ml FGF1 with adipogenic supplements, the semi-quantitative assessment of lipid vesicle accumulation was only performed for the lower concentrations of rhFGF1. Thereby, rhFGF1 had no proliferative effect neither on subconfluent nor on confluent MSCs (fig. 29). Sole pre-incubation with 6 - 50 ng/ml rhFGF1 previous to exposure to adipogenic medium without any rhFGF1 could not inhibit accumulation of lipid vesicles. According to the observed effects of rhFGF1 on adipogenic differentiation, adipogenic transdifferentiation was also clearly diminished by simultaneous addition of 6 - 50 ng/ml rhFGF1 (fig. 30).

Application of 50 ng/ml rhFGF1 in parallel with osteogenic supplements demonstrated no alterations of osteogenic differentiation, neither in the temporal course nor in the amount of ALP activity and mineralisation of extracellular matrix. Incubation with 50 ng/ml rhFGF1 alone, i.e. without osteogenic supplements could not provoke osteogenic differentiation of confluent MSCs either.

Application of heparin alone that is commonly used to enhance the biological activity of FGF1 [Burgess et al., 1994; Wesche et al., 2005] displayed no influence on the conducted experiments.

Attempts to detect FGF1 protein in preparations of intracellular and supernatant protein by Western blotting failed while controls of as little as 25 ng rhFGF1 produced strong bands.
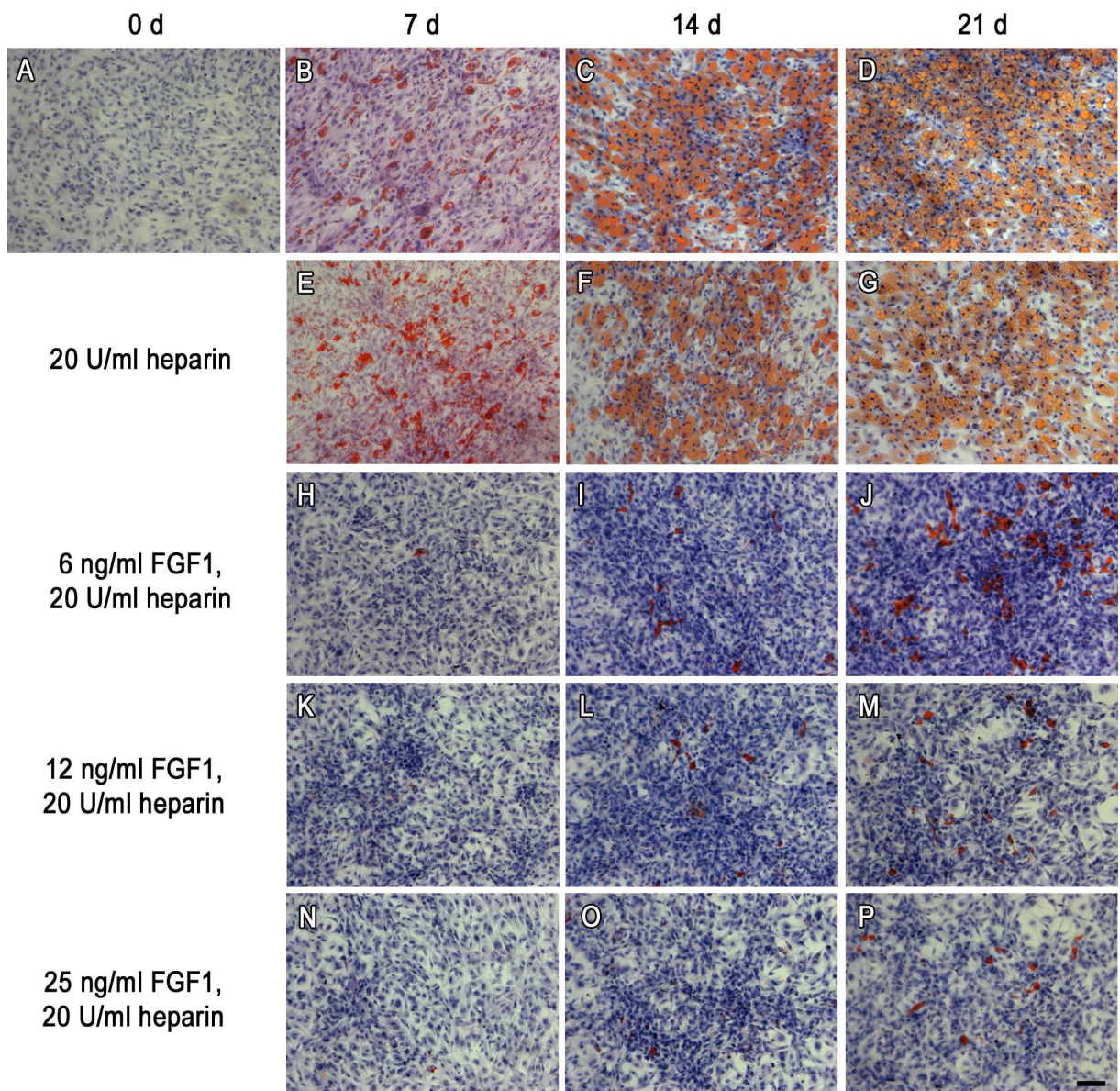
**Fig. 27    Effect of different concentrations of rhFGF1 on adipogenic differentiation**

Representative results are depicted for lipid vesicle accumulation that was visualised for normal adipogenic differentiation of MSCs (A - D) and for incubation in AM supplemented with 20 U/ml heparin alone (E - G) or with 20 U/ml heparin plus different concentrations of FGF1 as stated on the left side (H - P). Thereby, intracellular lipid vesicles were stained by Oilred O and cell nuclei were counterstained with hemalaun as indicated at the beginning of the experiment (0 d) and after 7 d, 14 d, and 21 d of incubation in the respective medium. The accumulation of red lipid vesicles during exposure to adipogenic differentiation medium (B - D) and during incubation in adipogenic differentiation medium supplemented with heparin alone (E - G) showed distinct adipogenic differentiation. Incubation with various concentrations of rhFGF1 strongly reduced lipid vesicle accumulation (H - P). Scale bar = 100 μm.

## Lipid vesicle accumulation
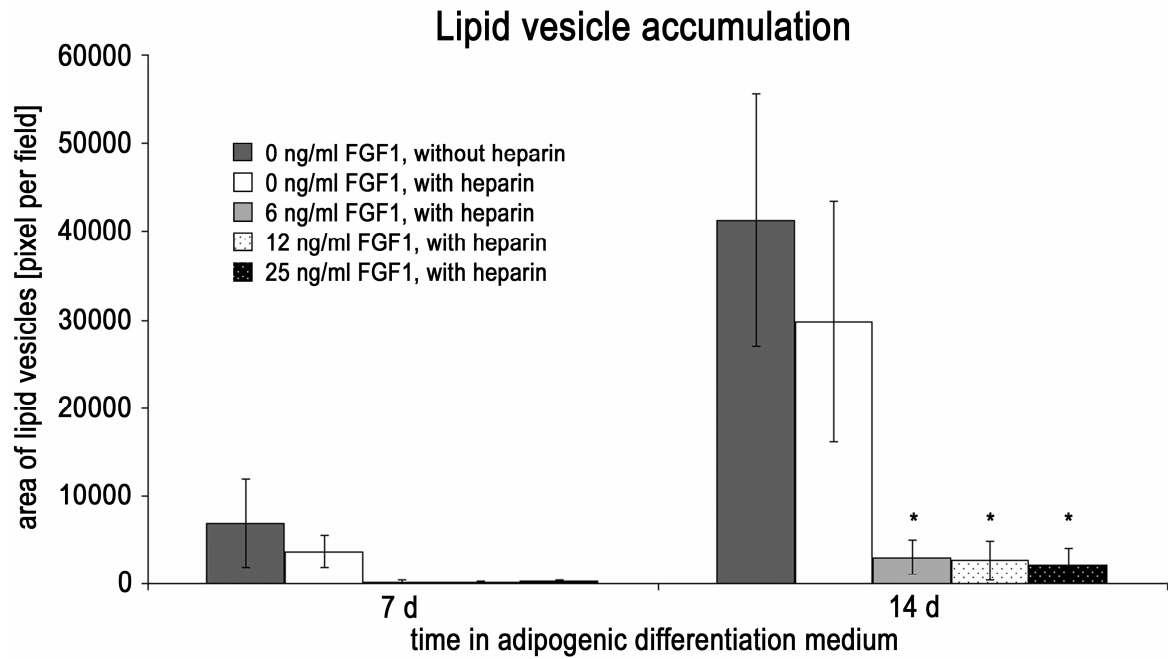


**Fig. 28  Semi-quantitative evaluation of lipid vesicle accumulation during adipogenic incubation and FGF1 treatment**

After 7 d and 14 d of incubation in adipogenic medium with or without heparin and FGF1 as indicated, lipid vesicle-containing area was determined. Mean ± SEM of 3 (7 d) and 4 (14 d) independent experiments with 6 fields analysed per experiment and incubation condition are displayed. The asterisks mark $P < 0.05$ compared to the adipogenic control (0 ng/ml FGF1, without heparin) as well as to the heparin control (0 ng/ml FGF1, with heparin).
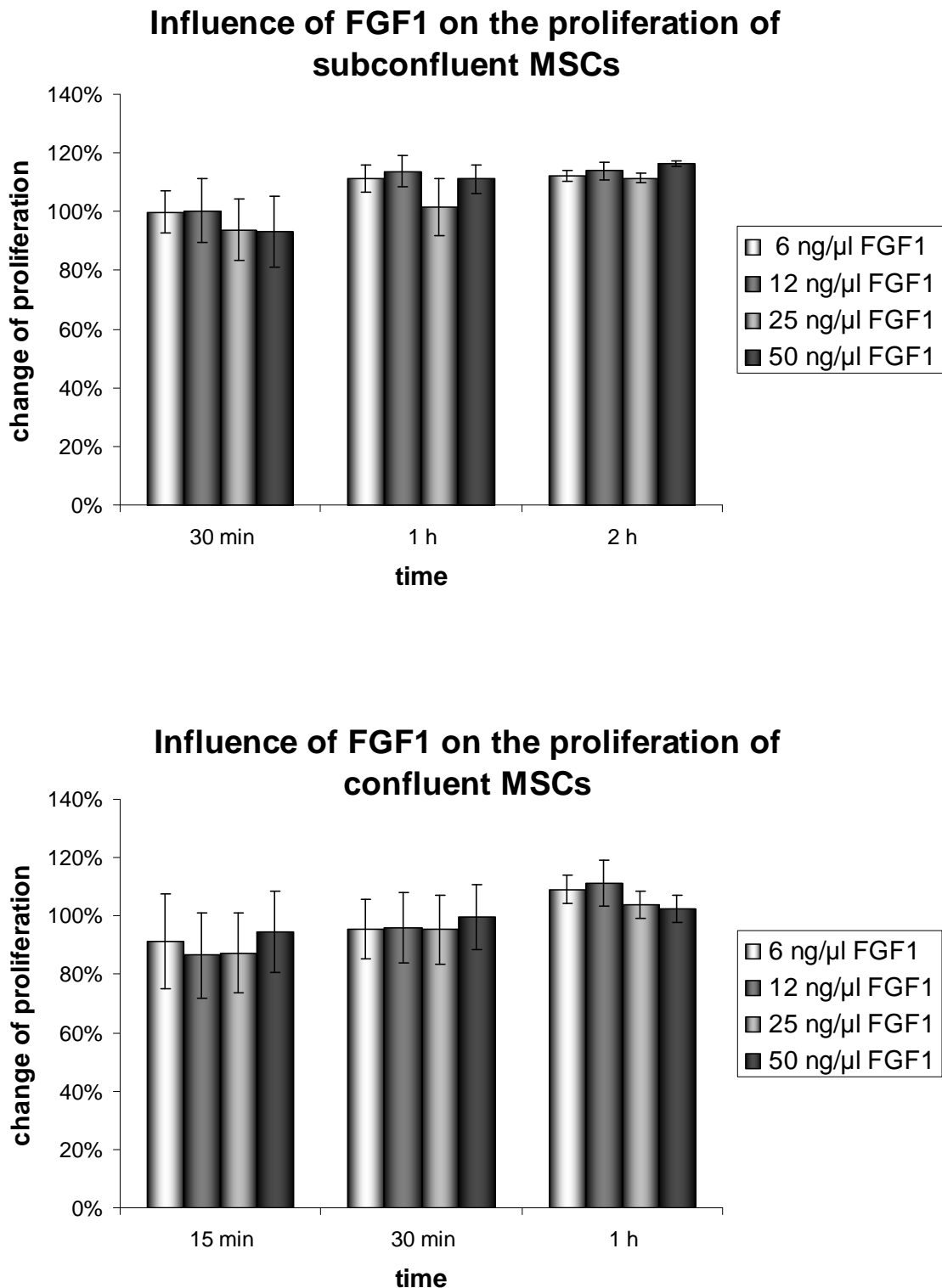
**Fig. 29   Influence of rhFGF1 on proliferation of MSCs**

Different concentrations of rhFGF1 were examined for their potential proliferative effect on subconfluent (n = 3; upper graph) and confluent MSCs (n = 4; lower graph). Proliferation was normalised on proliferation of MSCs incubated in control medium without rhFGF1 for the same time period as indicated. Change of proliferation is given as mean + SEM. Addition of rhFGF1 did not change the proliferation rate of MSCs neither for the subconfluent nor for the confluent assay.
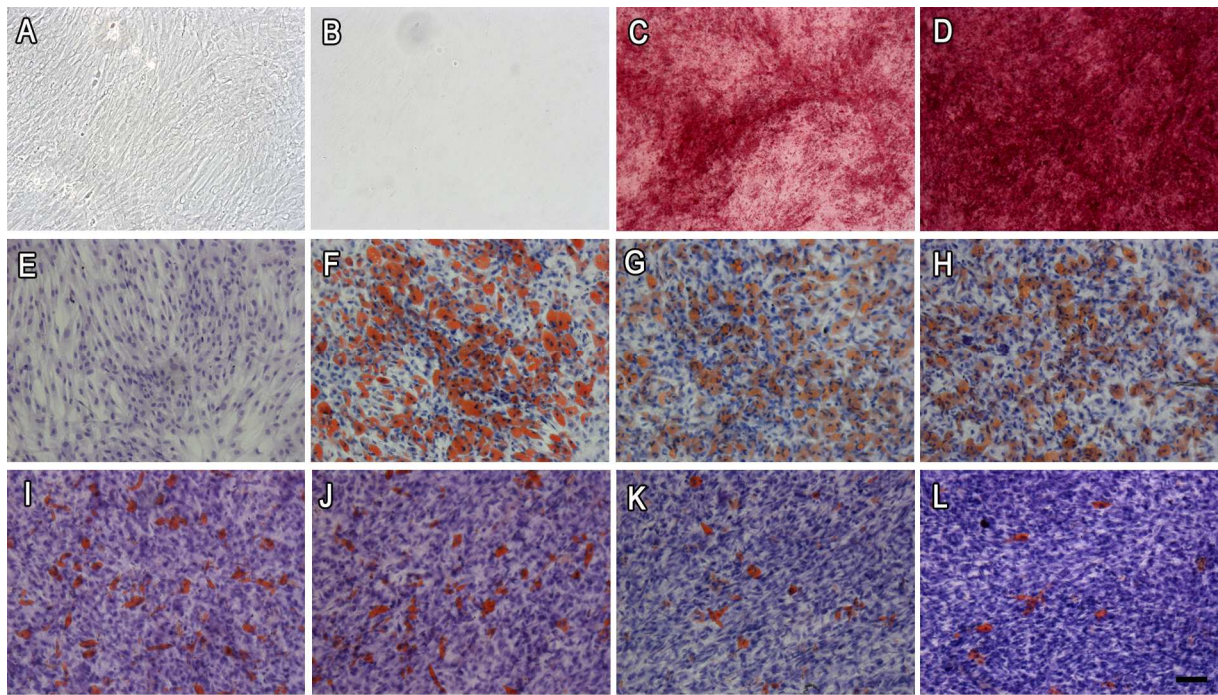
**Fig. 30    Influence of rhFGF1 during adipogenic transdifferentiation**

Representative staining of osteogenic and adipogenic markers is shown for undifferentiated cells as well as for (trans)differentiated cells in presence or absence of FGF1. As controls, MSC monolayers were subjected to normal osteogenic (C = 14 d and D = 28 d) and adipogenic differentiation (F = 14 d) as well as normal adipogenic transdifferentiation (G = 14 d in osteogenic medium + 14 d in adipogenic medium) and adipogenic transdifferentiation in presence of heparin (H = 14 d in osteogenic medium + 14 d in adipogenic medium plus 20 U/ml heparin). Moreover, the effect of different concentrations of rhFGF1 (I = 6 ng/ml, J = 12 ng/ml, K = 25 ng/ml, L = 50 ng/ml) on adipogenic transdifferentiation (14 d in osteogenic medium + 14 d in adipogenic medium plus 20 U/ml heparin and rhFGF1) was assessed.

Alizarin red S staining was performed at day 0 (A phase contrast image, B bright field image) and for controls incubated in normal osteogenic differentiation medium (C and D) to visualise calcium deposition in the extracellular matrix. Pre-osteoblasts, obtained after 14 d of osteogenic differentiation were used to start transdifferentiation experiments (C) To detect lipid vesicle accumulation, Oilred O staining was carried out at day 0 (E) as well as at the end points of incubation for all controls and samples exposed to adipogenic differentiation and transdifferentiation assays (I - L) as stated above. While adipogenic differentiation (F) and transdifferentiation (G) yielded high lipid vesicle accumulation, adipogenic reprogramming was strongly decreased in presence of rhFGF1 (I - L). Application of heparin alone did not alter adipogenic transdifferentiation (H). Scale bar = 100 µm.

# 5 Discussion

The bone marrow and other sites comprise multipotent MSCs that give rise to a variety of mesenchymal lineages as adipocytes and osteoblasts [Barry and Murphy, 2004; Caplan, 1991; Muraglia et al., 2000; Nöth et al., 2002a; Pittenger et al., 1999; Prockop, 1997]. Thereby, osteoblasts play a crucial role for bone remodelling and fracture healing [Krane, 2005; Martin and Sims, 2005]. Since with ageing, an inverse relationship between bone and adipose tissue generation was reported [Beresford et al., 1992; Burkhardt et al., 1987; Gimble et al., 2006; Koo et al., 1998], lack of osteogenic differentiation of MSCs as well as transdifferentiation (reprogramming) of osteoblasts into adipocytes could contribute to this degeneration process. Therefore in the work presented here, bone-marrow derived human MSCs were not only proven to be able to differentiate into adipocytes and osteoblasts as described previously [Schütze et al., 2005b] but also plasticity between the osteogenic and adipogenic lineage was detected and further examined in our cell culture system.

## 5.1 MSCs are capable of adipogenic and osteogenic differentiation and transdifferentiation

Primary MSCs used in our cell culture system were proven to differentiate into adipocytes and osteoblasts, respectively, by incubation in the established differentiation media [Jaiswal et al., 1997; Pittenger et al., 1999]. Moreover, adipocytes and pre-osteoblasts derived from these MSCs were still capable of reprogramming into the respective other lineage simply by application of the respective other differentiation medium. Thereby, differentiation as well as transdifferentiation was accompanied by the expression of the respective lineage-specific marker genes, thus proving the attainment of the adipogenic or osteogenic phenotype.

Conventional osteogenic differentiation was characterised by increasing expression levels of the osteoblast-specific marker mRNAs for ALP and OC as well as by ALP activity and deposition of mineralised matrix in the monolayers (fig. 10, fig. 11, and fig. 12) [Aubin, 1998; Stein et al., 1996]. After 28 d of osteogenic incubation, also weak expression of adipogenic marker mRNAs (PPARγ2 and LPL) was detected. On the one hand, this observation could arise from some pre-osteoblasts that underwent spontaneous transdifferentiation into adipocytes. Hence together with other events, this could also partly account for the age- and disease-related gain of adipose tissue in human bone marrow [Beresford et al., 1992; Koo et al., 1998]. On the other hand, further microarray analyses performed by our group detected low expression levels of PPARγ2 even in undifferentiated MSCs (personal communication with Prof. Dr. F. Jakob). This suggests that expression of PPARγ2 alone is not sufficient to report the adipogenic phenotype but the inductive factors of the adipogenic differentiation medium aid to its adipogenic effect. Moreover, weak expression of PPARγ2 during

osteogenic induction was also reported by Song and Tuan [2004] but did not result in adipocyte-specific lipid vesicle accumulation.

Thus, considering the mRNA levels of osteogenic and adipogenic markers during osteogenic differentiation we employed pre-osteoblasts after up to 15 d of osteogenic incubation for adipogenic transdifferentiation experiments. These pre-osteoblasts expressed OC and from day 10 onwards also ALP while no adipogenic markers were detected during this time frame. Moreover after 14 d of osteogenic incubation, calcium hydrogen phosphate deposition commenced and homogeneous staining for ALP activity all over the monolayer was observed indicating uniform differentiation into pre-osteoblasts. Transdifferentiation of these pre-osteoblast into differentiated adipocytes was obtained after 14 d of incubation in adipogenic differentiation medium with strong expression of the adipogenic mRNA markers (PPARγ2 and LPL) while the osteogenic ones decreased (ALP) and disappeared (OC), respectively (fig. 10). The loss of osteogenic marker expression after adipogenic transdifferentiation and the above mentioned ALP activity stretching homogeneously over the monolayer excluded significant contribution of possibly undifferentiated MSCs to the resulting adipocytes. Furthermore, transdifferentiated adipocytes even displayed larger areas of lipid vesicle accumulation than conventionally differentiated ones derived from undifferentiated MSCs (fig. 17). Again, this supports the hypothesis of spontaneous adipogenic conversion of pre-osteoblasts that is further enhanced by the adipogenic factors of the medium.

Conventional adipogenic differentiation for 14 d yielded adipocytes strongly expressing adipocyte-specific marker mRNAs (PPARγ2 and LPL) and containing intracellular lipid vesicles (fig. 10 and fig. 13) [Pittenger et al., 1999; Rosen et al., 2000]. Hence, osteogenic transdifferentiation was induced in these fully differentiated adipocytes and resulted in the conversion towards osteoblasts after 4 weeks of subsequent incubation in osteogenic differentiation medium (fig. 17 and fig. 18). Transdifferentiated osteoblasts displayed strong expression of osteogenic marker mRNAs (ALP and OC) and mineralisation of their extracellular matrix. However, adipogenic marker mRNA levels (PPARγ2 and LPL) persisted and the monolayers still contained residual lipid vesicles. These findings indicate that the osteogenic transdifferentiation pathway is less efficient than the adipogenic one.

Although the cells employed in our system are derived from a heterogeneous population of MSCs, i.e. not from single cell clones, the sole contribution of possibly undifferentiated MSCs to the formation of the osteogenic phenotype seems unlikely, since adipogenic markers are strongly expressed and the accumulation of at least small lipid vesicles can be observed for the majority of the cells prior to induction of osteogenic transdifferentiation. Moreover in contrast to the adipogenic differentiation medium, the composition of the osteogenic differentiation medium does not differ much from that of the propagation medium also containing one of the osteoinductive components (L-ascorbic acid 2-phosphate) [Jaiswal et

al., 1997; Nöth et al., 2002a]. Thus, while conventional osteogenic differentiation starting from undifferentiated MSCs can be achieved easily [Jaiswal et al., 1997; Nöth et al., 2002a; Schütze et al., 2005b], the factors included in osteogenic differentiation medium might not be sufficient to induce osteogenic transdifferentiation in all cells of the monolayer. Especially considering activation of the complex Wnt signalling pathway which is mandatory for conventional osteogenic differentiation [Gregory et al., 2005; Rawadi et al., 2003] also as a prerequisite for osteogenic transdifferentiation of adipocytes, the osteogenic factors applied with the differentiation medium may not be specific enough in the latter process.

Even though the existence of transdifferentiation *in vivo* has not been proven yet and some work regards changes in lineage phenotype as a consequence of cell fusion or heterogeneity [Orkin and Zon, 2002; Terada et al., 2002; Verfaillie, 2002; Ying et al., 2002] our findings are in accordance with the results of *in vitro* experiments showing plasticity of adipocytes [Park et al., 1999] and osteoblasts [Nuttall et al., 1998; Schiller et al., 2001]. Moreover, transdifferentiation at the single cell level was reported *in vitro* for human MSC-derived osteoblasts, adipocytes, and chondrocytes [Song and Tuan, 2004]. Regarding the progression of transdifferentiation, de-differentiation prior to re-differentiation and a direct change between lineage phenotypes have been considered as possible mechanisms [Song and Tuan, 2004; Verfaillie, 2002].

Regarding the whole organism, fatty degeneration was described to arise with or without relation to age. Independent of age, the muscle tissue of the shoulder's rotator cuff was shown to develop adipogenic conversion after trauma [Goutallier et al., 1994; Moore and Dawson, 1990]. More commonly, age-related increase of adipose tissue in the bone marrow was observed as soon as in the first decade of life in the diaphysis of long bones [Nakagaki et al., 1996; Zawin and Jaramillo, 1993] and more strikingly in older age. The associated simultaneous loss of bone mass is considered to contribute to age-related diseases like osteopenia and osteoporosis [Burkhardt et al., 1987; Gimble et al., 2006; Justesen et al., 2001; Koo et al., 1998; Meunier et al., 1971; Pei and Tontonoz, 2004; Rosen and Bouxsein, 2006]. Therefore, the reprogramming of pre-osteoblasts into adipocytes shown in our *in vitro* experiments could also take place *in vivo* and enhance the above mentioned age- and disease-related changes.

Knowledge about the molecular events initiating adipogenic and osteogenic transdifferentiation, respectively, that are unknown so far could help to understand the mechanisms contributing to the fatty degeneration of bone marrow and provide means to counteract this phenomenon. Thus after establishment of our *in vitro* system allowing for transdifferentiation between the adipogenic and osteogenic lineage, we performed Affymetrix microarray analyses to detect changes in gene expression shortly after initiation transdifferentiation.

## 5.2   Microarray analyses revealed reproducible regulation of a high number of gene products during transdifferentiation

Affymetrix microarray analyses allowed for detection of gene expression patterns shortly after initiation of transdifferentiation comparing mRNA levels of transdifferentiated cells with those of cells further on incubated in the same differentiation medium as before. Thereby, the employment of a single MSC batch together with the smaller GeneChips HG-U 133A that were able to detect differential regulation of 14,500 genes served for the obtainment of a first insight into gene expression changes during adipogenic transdifferentiation and for determination of the reliability of the microarray data regarding our cell culture system. Re-evaluation of microarray data by semi-quantitative RT-PCR for highly regulated genes yielded 91% accordance for identical RNA samples and 45% accordance for both of two additional RNA preparations of further MSC batches (tab. 4 and tab. 5). Moreover, the confirmation of up-regulation for adipocyte-specific gene products (APM1 and FABP4) during adipogenic transdifferentiation met the expectations. These findings stated the general reliability and significance of the Affymetrix microarray data for our cell culture system, but also demonstrated some variations obviously dependent on the different MSC batches.

The more complete Affymetrix GeneChips HG-U 133 Plus 2.0 that represent an extended version of the GeneChips HG-U 133A offered the ability to determine regulation of 38,500 genes considered to represent the whole human genome. As these GeneChips became available, different batches of MSCs were employed to conduct two microarray analyses per transdifferentiation direction, which allowed for detection of reproducibly regulated mRNA species. Thereby, the re-evaluation of changes in mRNA levels 3 h and 24 h after initiation of transdifferentiation for selected genes again confirmed the reliability and significance of microarray data regarding our cell culture system. Regulation of established genes showed high accordance, i.e. in 82% of the examined regulation events (fig. 23 and tab. 6). Since transdifferentiation processes may involve novel genes whose functions are not known so far, additional assessment of at the time point of examination hypothetical gene products was performed for 16 genes in the course of the medical doctorate of Ulrike Meyer. Here, the re-evaluation of regulation patterns yielded slightly less accordance (59%) (tab. 7). This lower consistence could be correlated with uncertainties regarding the respective mRNA sequences of hypothetical genes possibly leading to cross hybridisation on the GeneChips or sub-optimal detection by RT-PCR.

Furthermore, only about 60% of the genes found to be regulated by the first single array analysis for adipogenic transdifferentiation showed reproducible regulation patterns in the subsequent microarray analyses for the same transdifferentiation direction. Due to the higher accordance between microarray data and RT-PCR experiments, this variability seems to originate from differences in MSC batches as observed by examination of additional RNA

samples for re-evaluation of the first microarray analysis. Nevertheless, the larger GeneChips detected reproducible regulation of a high number of genes, amongst them many that could not be assessed by the smaller GeneChips. Many of the reproducibly regulated genes found by usage of the larger GeneChips showed reciprocal regulation patterns regarding the different transdifferentiation directions. Furthermore, osteogenic reprogramming was characterised by increases in gene expression for the majority of regulated genes whereas adipogenic transdifferentiation was accompanied by decreased mRNA levels for the majority of regulated genes. The active induction of gene expression during the osteogenic switch suggests the requirement for active repression of the adipogenic pathway. Concordantly, the activation of nuclear NAD-dependent protein deacetylase sirtuin 1 was reported to decline adipogenic conversion of murine MSCs during osteogenic incubation *in vitro* [Bäckesjö et al., 2006]. Hence, impairment of active repression of the adipogenic pathway in MSCs or pre-osteoblasts could clear the way for adipogenic development and therefore contribute to the adipogenic degeneration of the bone marrow mentioned before.

Since Song et al. [2006] assumed that transdifferentiation of differentiated phenotypes occurs via dedifferentiation into a stem cell like state followed by redifferentiation into another phenotype, they performed microarray analyses that compared differentiated cells (osteoblasts, adipocytes, and chondrocytes) with undifferentiated MSCs and dedifferentiated cells of each lineage, respectively. Whereas in this experimental setting the three groups differed in duration of their cultivation, incubation periods between compared samples were identical in our experiments thus avoiding any possible influence of *in vitro* ageing of the cells on changes in gene expression [Baxter et al., 2004; Bonab et al., 2006; Serakinci et al., 2004]. Regardless of this consideration, some genes were regulated in both studies (e.g. BIRC3, IGFBP5, IGF1, LAMA4, PRKAR2B, RGS2, RGS4, SERPINE1, TNFRSF11B, and YWHAH). This finding might suggest the occurrence of some dedifferentiation events in our cell culture system of transdifferentiation. However, gene regulation patterns between the adipogenic and osteogenic transdifferentiation direction were often reciprocal regarding our cell culture system, which therefore favours the assumption of immediate induction of transdifferentiation.

Further analyses grouped regulated gene products into GO classes according to their association with *cellular components*, *molecular functions*, and *biological processes*. Regarding the single microarray analysis for adipogenic transdifferentiation, regulated genes were affiliated into the subclasses of *molecular function* and *biological process* resulting in separate GO graphs distinguishing between the time point of gene regulation (3 h and 24 h after initiation of adipogenic transdifferentiation, respectively) as well as between up- and down-regulation of mRNA amounts (fig. 24 and fig. 25). Up-regulation of the majority of

genes associated with transcription and signal transduction 3 h after initiation of transdifferentiation indicated the requirement for *de novo* synthesis of gene products and subsequent activation of signalling pathways. The sustainment of regulated genes in the subclass of signal transduction 24 h after initiation of transdifferentiation supported this assumption. Moreover, changes in secretion of proteins at this time point were assumed to occur due to regulation of extracellular region-associated genes while up-regulation of catalytic transporter activity- as well as lipid metabolism-correlated genes pointed at the onset of an adipogenesis-related metabolism. GOstat analyses of reproducibly regulated gene products obtained by usage of the larger GeneChips also resulted in over-representation of genes correlated with signal transduction not only for both time points examined but also for the different transdifferentiation directions (tab. 8 and tab. 9). In accordance with the data for the single microarray analysis mentioned above, transcription-associated genes were only enriched 3 h after initiation of adipogenic transdifferentiation. Moreover, almost all GO classes that showed over-representation for the first microarray analysis were obtained as well after the GO analyses for reproducibly regulated genes. After 24 h, reproducibly regulated genes mainly accumulated in the groups of development, extracellular region, morphogenesis, and cytoskeleton for both transdifferentiation directions. Furthermore, osteogenic transdifferentiation was accompanied by over-representation of genes affiliated to the categories of cell cycle and chromosome. Altogether, these data suggest that transdifferentiation requires alteration of signalling pathways and development-associated gene products. Moreover, adipogenic transdifferentiation begins with early regulation of transcription while genes regarding morphological changes are important for both transdifferentiation directions 24 h after initiation of the reprogramming.

Only a few of the known mRNA markers of adipogenesis were up-regulated during adipogenic transdifferentiation (tab. 10) but none of the osteogenic ones showed differential regulation in neither of the transdifferentiation pathways within the time frame of 24 h after initiation of transdifferentiation. Hence, other genes that have not been related to adipogenesis and osteogenesis or whose functions are unknown so far are likely to be involved in the onset of transdifferentiation events especially regarding the osteogenic switch of adipocytes. Therefore, the development of a novel bioinformatic scoring scheme helped to filter out gene products with possibly high relevance for initiation of transdifferentiation.

## 5.3 The development of a novel bioinformatic scoring scheme improves the detection of gene products potentially important for transdifferentiation

The examination of genome-wide gene expression patterns shortly after initiation of adipogenic and osteogenic transdifferentiation by microarray analyses yielded high numbers of reproducibly regulated genes (fig. 22). Therefore, transdifferentiation seemed to comprise complex mechanisms to abrogate the current lineage phenotype and to switch to the

respective other one involving far more and other genes than described for conventional differentiation.

Our empirical scoring scheme provided a means to prioritise gene products for further analyses due to the reproducibility, extent, and reciprocity of their regulation regarding the adipogenic and osteogenic transdifferentiation direction. Ranking of genes according to their score listed factors with possibly highest relevance for transdifferentiation. Thereby, genes with reciprocal regulation patterns between the reverse transdifferentiation pathways were considered very important and awarded high scores because they might be involved in balancing and controlling adipogenic and osteogenic lineage development. Moreover, a reciprocal correlation between the expression of lineage-specific genes during normal differentiation starting from stem cells was reported to partly inhibit the differentiation into the respective other lineage [Akune et al., 2004; Nuttall and Gimble, 2004]. The value of the bioinformatic score was further confirmed by affiliation of many of the top 50-ranking genes to over-represented GO categories re-emphasising their relevance (tab. 11). Thus, this assessment of the relevance of regulated genes set the stage for further functional evaluation and analysis of several highly ranked genes.

### 5.3.1 Members of several signalling pathways are highly regulated during transdifferentiation

Together with further at least 2-fold regulated genes, several of the top 50-ranking ones were associated with signalling pathways (tab. 10). Amongst them integrin, IGF, Wnt/β-catenin, G-protein, and FGF signalling comprised the highest numbers of members.

Most of the genes associated with integrin signalling showed up-regulation during osteogenic transdifferentiation which pointed towards changes of the actin cytoskeleton that is organised by integrins [Giancotti and Ruoslahti, 1999]. Both, VIL2 and IGFBP1 are ranking amongst the top 50 of the bioinformatic scoring. Thereby, VIL2 is acting as a membrane-cytoskeletal linking protein that governs cell-cell and cell-matrix adhesions [Berryman et al., 1993; Hiscox and Jiang, 1999] and IGFBP1 is recognised by the α5β1 integrin receptor and influences phosphorylation of focal adhesion kinase [Ricort, 2004]. Furthermore, also members of PLAU signalling that has been described to affect integrin signalling and matrix remodelling were differentially regulated [Choong and Nadesapillai, 2003].

Regarding IGF signalling, augmentation of IGF1 mRNA levels shortly after initiation of adipogenic transdifferentiation suggested promotion of the adipogenic lineage as reported for murine and human pre-adipocytes [Boney et al., 1994; Schmidt et al., 1990]. Thereby, besides paracrine signalling also an autocrine function of IGF1 and IGFBPs was assumed that was likely to affect transdifferentiation in our cell culture system [Wabitsch et al., 2000]. IGF1 has also been connected to Wnt signalling since its expression was induced by WNT1 in 3T3-L1 preadipocytes where presence of IGF1 prevented these cells from apoptosis after

serum withdrawal [Gagnon et al., 2001; Longo et al., 2002]. However, since WNT1 gene expression was not altered during the transdifferentiation experiments and only serum-containing incubation conditions were applied, the action of IGF1 as component of Wnt signalling seemed unlikely for reprogramming. Contrary to our expectations, external application of rhIGF1 had no influence on adipogenic and osteogenic differentiation in our cell culture system, but could nevertheless influence transdifferentiation events, which remains to be elucidated.

Also several other gene products correlated with Wnt/β-catenin signalling showed up- or down-regulation during the transdifferentiation processes. For conventional differentiation, activation of this signalling pathway enhances osteogenesis while adipogenesis is prevented [Bennett et al., 2002; MacDougald and Mandrup, 2002; Rawadi et al., 2003; Ross et al., 2000]. High relevance amongst the factors of Wnt/β-catenin signalling was attributed to TNFRSF11B (= OPG), SFRP2, and CYR61 by our bioinformatic scoring.

Application of rhTNFRSF11B in our *in vitro* cell culture system however neither changed adipogenic and osteogenic differentiation nor induced spontaneous osteogenesis in undifferentiated MSCs. Nevertheless, since TNFRSF11B also inhibits the development of osteoclasts [Lacey et al., 1998; Simonet et al., 1997] its function may rather affect the *in vivo* situation, where its up-regulation shortly after osteogenic reprogramming could abolish the bone matrix resorbing function of osteoclasts while its down-regulation during adipogenic transdifferentiation could promote osteoclast function and thus loss of bone mass and concomitant increase of adipose tissue [Justesen et al., 2001; Koo et al., 1998; Meunier et al., 1971; Pei and Tontonoz, 2004; Rosen and Bouxsein, 2006].

SFRP2 was controversially discussed to facilitate or to inhibit osteogenic differentiation depending on the cell culture system [Boland et al., 2004; Oshima et al., 2005]. Our data obtained at the mRNA level support the latter view but this could not be proven by supplementation of culture media with rmSFRP2. While adipogenesis of MSCs was not influenced, the effect of the recombinant protein on osteogenesis could not be determined since cells detached upon addition of rmSFRP2 to the osteogenic differentiation medium. Perhaps the murine recombinant protein could not exactly mimic the effect of its human analogue in the concentration used.

CYR61 is an extracellular matrix-associated signalling protein that is synthesised in various tissues and has been shown to be secreted by osteoblasts but has been mainly related to angiogenesis so far [Lau and Lam, 1999; Lechner et al., 2000; Schütze et al., 2005a; Schütze et al., 2006]. Some recent work using the murine pluripotent mesenchymal stem cell line C3H10T1/2 reported on the up-regulation of CYR61 in response to wingless-type MMTV integration site family member 3A (WNT3A) that has been considered to enhance osteogenic differentiation [Jackson et al., 2005; Si et al., 2006]. Moreover, Si et al. [2006] showed that

silencing of CYR61 expression diminished osteogenesis-specific ALP activity. Although up-regulation of CYR61 was also detected for osteogenic transdifferentiation by our microarray analyses and confirmed by RT-PCR, external addition of rhCYR61 did neither alter osteogenic nor adipogenic differentiation in our cell culture system.

In general, secretion of proteins like CYR61 during transdifferentiation in our cell culture system does not necessarily imply that they function in an autocrine fashion. *In vivo*, secreted proteins may also target neighbouring cells, which in turn respond to this stimulus by signals that influence current differentiation stages. Thus, the effect of a secreted protein on the generation of mature tissues can go beyond differentiation into a single phenotype since it can influence e.g. stimulation of angiogenesis and chemotaxis as reported for CYR61 [Grzeszkiewicz et al., 2002; Lau and Lam, 1999; Schütze et al., 2005a; Schütze et al., 2006]. Interestingly for several of the genes regulated by WNT3A in C3H10T1/2 cells, expression changes were also found in our experiments shortly after initiation of transdifferentiation [Jackson et al., 2005; Si et al., 2006]. Accordingly, regulation patterns in response to WNT3A and after initiation of osteogenic transdifferentiation matched for down-regulation of ANGPTL4, IGF1, and SFRP2 as well as for up-regulation of CYR61, collagen type XI alpha 1 (COL11A1), connective tissue growth factor (CTGF), thrombospondin 1 (THBS1), TNFRSF11B, and WNT1 inducible signalling pathway protein 1 (WISP1). As at the mRNA level neither differential regulation of WNT3A nor of β-catenin was detected during transdifferentiation, their regulation could rather be managed post-transcriptionally at the protein level, e.g. by SFRP2. The down-regulation of SFRP2 in osteogenic and its up-regulation in adipogenic transdifferentiation would meet this assumption, provided that the action of this Wnt antagonist inhibits osteogenesis as reported by Oshima et al. [2005]. Moreover, Wnt signalling could be forwarded via β-catenin-independent mechanisms like the Wnt/G-protein pathway [Kohn and Moon, 2005].

The regulation of several G-protein signalling-associated genes like regulator of G-protein signalling 4 (RGS4) and phospholipase C beta 4 (PLCB4) during transdifferentiation in our cell culture system suggested strong influence of their corresponding proteins on reprogramming either in combination with Wnts or with other factors. Moreover, this indicated the importance of transmembrane signalling during transdifferentiation [Gilman, 1987].

### 5.3.2  FGF1 as one of the potential key factors of transdifferentiation displays inhibitory effects on adipogenic differentiation as well as on transdifferentiation

The FGF signalling pathway was considered important for initiation of transdifferentiation since several of its members displayed changes in gene expression. Furthermore, FGF1 was reciprocally regulated regarding the different transdifferentiation directions and obtained therefore high bioinformatic scoring amongst the top 50 of the ranking. Regarding its functional mechanism, FGF1 was considered to act in an autocrine fashion that enhanced

osteogenic but inhibited adipogenic transdifferentiation. Accordingly, external addition of rhFGF1 proved its strong inhibitory effect on adipogenic differentiation and transdifferentiation (fig. 27, fig. 28, and fig. 30).

Though FGF1 has contrarily been reported to stimulate adipogenesis in human pre-adipocytes [Hutley et al., 2004], these results could be caused by the proliferative effect of FGF1 on subconfluent pre-adipocytes *in vitro*. Unlike in our experiments where (trans)differentiation experiments were conducted with confluent monolayers, FGF1 could accelerate proliferation in subconfluent condition compared to those not subjected to FGF1 treatment. This would simply promote adipogenesis by earlier achievement of confluence which is a prerequisite for the beginning of adipogenic differentiation [Rosen et al., 2000]. We also showed that proliferation was not stimulated by FGF1 in our cell culture system (fig. 29). Since FGF1 can bind to all four types of FGF receptors [Eswarakumar et al., 2005], differential receptor expression or further factors may be involved that guide signalling possibly via another receptor than in the experiments of Hutley et al. [2004] therefore provoking another outcome. Moreover, foetal rat calvarial cells have been reported to respond differently to FGF1 depending on their maturation stage; while early osteoblasts showed enhanced proliferation, later osteoblasts were retarded in maturation and mineralisation [Tang et al., 1996]. Additionally, systemic administration of FGF1 in ovariectomised, osteoporotic rats has been reported to diminish bone loss and to enhance bone formation [Dunstan et al., 1999]. In our cell culture system, rhFGF1 had no effect on osteogenic differentiation when applied simultaneously with the conventional osteogenic differentiation factors, neither regarding the extent of mineralisation nor the temporal course of the formation of osteogenic markers. Nonetheless, this does not abrogate stimulation of osteogenic transdifferentiation of MSC-derived adipocytes by FGF1 possibly involving other mechanisms than conventional osteogenic differentiation.

The finding and confirmation of the unexpected inhibitory function of FGF1 regarding the adipogenic phenotype served as the "proof of principle" that our approach that includes a new bioinformatic scoring scheme is feasible to detect novel regulators of transdifferentiation and differentiation that decide between osteogenesis and adipogenesis. At the same time, it also emphasises the need for functional analyses. Therefore, the bioinformatic ranking served well as a first filtering method to handle huge data amounts. Subsequent analyses must examine whether changes at the transcription level also affect the protein level and therefore control the initiation of transdifferentiation. Thus, novel molecules might be identified from the results of this screen.

## 5.4   Perspective

Given the proof of transdifferentiation between the adipogenic and osteogenic lineage in our cell culture system of human MSCs, the age-related fatty degeneration of human bone marrow that is inversely correlated with the loss of bone mass [Beresford et al., 1992; Burkhardt et al., 1987; Gimble et al., 2006; Koo et al., 1998] may at least partly be caused by adipogenic conversion of osteoblasts. The establishment of our cell culture system that employed primary human MSCs to monitor transdifferentiation between the adipogenic and osteogenic lineage set the stage to examine the molecular events provoking the reprogramming of cells. The examination of global gene expression patterns together with the development of a novel bioinformatic scoring scheme paid special attention to genes displaying reciprocal regulation patterns regarding the different transdifferentiation directions and allowed for elucidation of gene products with potentially high functional relevance regarding initiation of the reprogramming processes. The "proof of principle" for our bioinformatic ranking was provided by verification of the inhibitory effect of FGF1 on adipogenic transdifferentiation. Examples for further reasonable and promising approaches to examine the processes underlying transdifferentiation are stated below.

### *Mechanisms of FGF1 action*

Regarding the mechanisms by which FGF1 exerts its inhibitory effect on adipogenic (trans)differentiation, better understanding of the molecular events taking place during adipogenic transdifferentiation would be desirable. It is not clear whether established FGF signalling components are involved or factors not known yet cause the observed effect. Hence, further examinations could elucidate if or which FGF receptor mediates the signal transduction. Moreover, all FGF receptors are receptor tyrosine kinases that can turn on several intracellular signalling pathways like Ras/MAP kinase signalling and phosphoinositol metabolism-mediated cell signalling resulting in modulation of transcription factor activity [Schlessinger, 2000]. Detailed knowledge about the participating pathways could elucidate novel possibilities in order to specifically address molecules *in vivo* that would inhibit the adipogenic conversion.

### *Effect of FGF1 in animal models*

As a first more empirically *in vivo* attempt, application of FGF1 in an osteopenic mouse model that displays accelerated adipogenesis could be examined [Klein et al., 2004]. Possibly treatment with FGF1 could rescue the osteopenic phenotype of these mice by inhibition of adipogenesis. Moreover together with systemically applied FGF2, the interplay between FGF1 inhibiting adipogenesis and FGF2 accelerating osteogenesis could be assessed in ovariectomised, osteoporotic rats or estrogen receptor α knockout mice [Dunstan et al., 1999; Ling et al., 2006; Parikka et al., 2005; Xiao et al., 2002].

Ovariectomised, osteoporotic rats have already been shown to respond to systemic application of FGF1 with decreased bone loss and increased bone formation but changes in adipose tissue were not examined [Dunstan et al., 1999]. FGF2 as enhancer of osteogenesis was only administered locally in the mentioned study but could possibly act in concert with adipogenesis-inhibiting FGF1 when both were applied systemically.

### *Examination of further highly ranked factors with known or unknown function*

Moreover due to the high number of reproducibly and strongly regulated genes, further functional analyses should be performed. Since our approach proved already functional relevance of a key factor, not only members of known signalling pathways but also hypothetical genes and genes without known function are expected to affect the initiation of transdifferentiation. Methods of choice for functional analyses will thereby depend on the available information regarding the characteristics of each protein that should be addressed. Whereas the influence of some highly ranked secreted proteins was tested *in vitro* in the course of this doctorate by addition of the recombinant proteins to the cell culture media, intracellular proteins could be examined by gene silencing assays using short interference (si)RNAs. Hypothetical genes and such with unknown localisation could be approached by establishment of their over-expression in MSCs. For both, gene silencing and overexpression, lentiviral systems would be suitable since they allow for stable expression of siRNAs and transgenes, respectively [Christian et al., 2005; Saunders et al., 2006].

### *Therapeutic potential of gene products regulated during transdifferentiation*

Altogether, our results emphasise the importance of regulatory mechanisms that balance between the adipogenic and osteogenic lineage and give insight into gene expression changes shortly after initiation of reprogramming. Besides the considerations regarding transdifferentiation, our microarray data may also provide further knowledge about the transcriptome of differentiated cells. When compared to the transcriptome of undifferentiated MSCs, novel factors of relevance for induction and maintenance of the osteogenic versus adipogenic differentiation pathway could be identified. Moreover, since FGF1 acts as a potent inhibitor of adipogenic transdifferentiation and further functional assays are likely to provide more proteins involved in lineage determination, knowledge about the influence of these factors could help to find potential targets for therapeutic interventions that inhibit adipogenic degeneration and simultaneously facilitate osteogenesis *in vivo*, especially with ageing.

# 6   References

Adler C-P. 1983a. Knochenkrankheiten. Stuttgart: Thieme. p 47-72.

Adler C-P. 1983b. Knochenkrankheiten. Stuttgart: Thieme. p 1-10.

Ailhaud G, Amri E, Bardon S, Barcellini-Couget S, Bertrand B, Catalioto RM, Dani C, Doglio A, Forest C, Gaillard D, et al. 1991. Growth and differentiation of regional adipose tissue: molecular and hormonal mechanisms. Int J Obes 15 Suppl 2:87-90.

Ailhaud G, Fukamizu A, Massiera F, Negrel R, Saint-Marc P, Teboul M. 2000. Angiotensinogen, angiotensin II and adipose tissue development. Int J Obes Relat Metab Disord 24 Suppl 4:S33-5.

Akune T, Ohba S, Kamekura S, Yamaguchi M, Chung UI, Kubota N, Terauchi Y, Harada Y, Azuma Y, Nakamura K, Kadowaki T, Kawaguchi H. 2004. PPARgamma insufficiency enhances osteogenesis through osteoblast formation from bone marrow progenitors. J Clin Invest 113:846-55.

Ali AA, Weinstein RS, Stewart SA, Parfitt AM, Manolagas SC, Jilka RL. 2005. Rosiglitazone causes bone loss in mice by suppressing osteoblast differentiation and bone formation. Endocrinology 146:1226-35.

Alliston T, Choy L, Ducy P, Karsenty G, Derynck R. 2001. TGF-beta-induced repression of CBFA1 by Smad3 decreases cbfa1 and osteocalcin expression and inhibits osteoblast differentiation. Embo J 20:2254-72.

Alvarez-Dolado M, Pardal R, Garcia-Verdugo JM, Fike JR, Lee HO, Pfeffer K, Lois C, Morrison SJ, Alvarez-Buylla A. 2003. Fusion of bone-marrow-derived cells with Purkinje neurons, cardiomyocytes and hepatocytes. Nature 425:968-73.

Aubin JE. 1998. Advances in the osteoblast lineage. Biochem Cell Biol 76:899-910.

Bäckesjö CM, Li Y, Lindgren U, Haldosen LA. 2006. Activation of sirt1 decreases adipocyte formation during osteoblast differentiation of mesenchymal stem cells. J Bone Miner Res 21:993-1002.

Balooch G, Balooch M, Nalla RK, Schilling S, Filvaroff EH, Marshall GW, Marshall SJ, Ritchie RO, Derynck R, Alliston T. 2005. TGF-beta regulates the mechanical properties and composition of bone matrix. Proc Natl Acad Sci U S A 102:18813-8.

Barak Y, Nelson MC, Ong ES, Jones YZ, Ruiz-Lozano P, Chien KR, Koder A, Evans RM. 1999. PPAR gamma is required for placental, cardiac, and adipose tissue development. Mol Cell 4:585-95.

Barry FP, Murphy JM. 2004. Mesenchymal stem cells: clinical applications and biological characterization. Int J Biochem Cell Biol 36:568-84.

Bartl R. 2001. Osteoporose. Stuttgart: Thieme. p 1-13.

Battula VL, Bareiss PM, Treml S, Conrad S, Albert I, Hojak S, Abele H, Schewe B, Just L, Skutella T, Buhring HJ. 2007. Human placenta and bone marrow derived MSC cultured in serum-free, b-FGF-containing medium express cell surface frizzled-9 and SSEA-4 and give rise to multilineage differentiation. Differentiation 75:279-91.

Baxter MA, Wynn RF, Jowitt SN, Wraith JE, Fairbairn LJ, Bellantuono I. 2004. Study of telomere length reveals rapid aging of human marrow stromal cells following in vitro expansion. Stem Cells 22:675-82.

Beissbarth T, Speed TP. 2004. GOstat: find statistically overrepresented Gene Ontologies within a group of genes. Bioinformatics 20:1464-5.

Benjamini Y, Hochberg Y. 1995. Controlling the false discovery rate: a practical and powerful approach to multiple testing. J Royal Statistical Soc B 57:289-300.

Bennett CN, Ross SE, Longo KA, Bajnok L, Hemati N, Johnson KW, Harrison SD, MacDougald OA. 2002. Regulation of Wnt signaling during adipogenesis. J Biol Chem 277:30998-1004.

Beresford JN, Bennett JH, Devlin C, Leboy PS, Owen ME. 1992. Evidence for an inverse relationship between the differentiation of adipocytic and osteogenic cells in rat marrow stromal cell cultures. J Cell Sci 102 ( Pt 2):341-51.

Berryman M, Franck Z, Bretscher A. 1993. Ezrin is concentrated in the apical microvilli of a wide variety of epithelial cells whereas moesin is found primarily in endothelial cells. J Cell Sci 105 (Pt 4):1025-43.

Bianco P, Riminucci M, Gronthos S, Robey PG. 2001. Bone marrow stromal stem cells: nature, biology, and potential applications. Stem Cells 19:180-92.

Boland GM, Perkins G, Hall DJ, Tuan RS. 2004. Wnt 3a promotes proliferation and suppresses osteogenic differentiation of adult human mesenchymal stem cells. J Cell Biochem 93:1210-30.

Bonab MM, Alimoghaddam K, Talebian F, Ghaffari SH, Ghavamzadeh A, Nikbin B. 2006. Aging of mesenchymal stem cell in vitro. BMC Cell Biol 7:14.

Boney CM, Moats-Staats BM, Stiles AD, D'Ercole AJ. 1994. Expression of insulin-like growth factor-I (IGF-I) and IGF-binding proteins during adipogenesis. Endocrinology 135:1863-8.

Bradford MM. 1976. A rapid and sensitive method for the quantitation of microgram quantities of protein utilizing the principle of protein-dye binding. Anal Biochem 72:248-54.

Bronner F. 1994. Calcium and osteoporosis. Am J Clin Nutr 60:831-6.

Brügger A. 1980. Die Erkrankungen des Bewegungsapparats und seines Nervensystems: Grundlagen und Differentialdiagnose; ein intedisziplinäres Handbuch für die Praxis. Stuttgart: Gustav Fischer. p 625-627.

Burgess WH, Friesel R, Winkles JA. 1994. Structure-function studies of FGF-1: dissociation and partial reconstitution of certain of its biological activities. Mol Reprod Dev 39:56-60; discussion 60-1.

Burkhardt R, Kettner G, Bohm W, Schmidmeier M, Schlag R, Frisch B, Mallmann B, Eisenmenger W, Gilg T. 1987. Changes in trabecular bone, hematopoiesis and bone marrow vessels in aplastic anemia, primary osteoporosis, and old age: a comparative histomorphometric study. Bone 8:157-64.

Caplan AI. 1991. Mesenchymal stem cells. J Orthop Res 9:641-50.

Caplan AI. 2005. Review: mesenchymal stem cells: cell-based reconstructive therapy in orthopedics. Tissue Eng 11:1198-211.

Choi KY, Kim HJ, Lee MH, Kwon TG, Nah HD, Furuichi T, Komori T, Nam SH, Kim YJ, Kim HJ, Ryoo HM. 2005. Runx2 regulates FGF2-induced Bmp2 expression during cranial bone development. Dev Dyn 233:115-21.

Choong PF, Nadesapillai AP. 2003. Urokinase plasminogen activator system: a multifunctional role in tumor progression and metastasis. Clin Orthop Relat Res:S46-58.

Christian M, Kiskinis E, Debevec D, Leonardsson G, White R, Parker MG. 2005. RIP140-targeted repression of gene expression in adipocytes. Mol Cell Biol 25:9383-91.

Cianflone K, Maslowska M, Sniderman AD. 1999. Acylation stimulating protein (ASP), an adipocyte autocrine: new directions. Semin Cell Dev Biol 10:31-41.

Cousin B, Casteilla L, Dani C, Muzzin P, Revelli JP, Penicaud L. 1993. Adipose tissues from various anatomical sites are characterized by different patterns of gene expression and regulation. Biochem J 292 ( Pt 3):873-6.

Currey JD. 1999. The design of mineralised hard tissues for their mechanical functions. J Exp Biol 202:3285-94.

da Silva Meirelles L, Chagastelles PC, Nardi NB. 2006. Mesenchymal stem cells reside in virtually all post-natal organs and tissues. J Cell Sci 119:2204-13.

de Meis L, Arruda AP, da Costa RM, Benchimol M. 2006. Identification of a Ca2+-ATPase in brown adipose tissue mitochondria: regulation of thermogenesis by ATP and Ca2+. J Biol Chem 281:16384-90.

Ducy P, Schinke T, Karsenty G. 2000. The osteoblast: a sophisticated fibroblast under central surveillance. Science 289:1501-4.

Ducy P, Zhang R, Geoffroy V, Ridall AL, Karsenty G. 1997. Osf2/Cbfa1: a transcriptional activator of osteoblast differentiation. Cell 89:747-54.

Dunstan CR, Boyce R, Boyce BF, Garrett IR, Izbicka E, Burgess WH, Mundy GR. 1999. Systemic administration of acidic fibroblast growth factor (FGF-1) prevents bone loss and increases new bone formation in ovariectomized rats. J Bone Miner Res 14:953-9.

Duplomb L, Dagouassat M, Jourdon P, Heymann D. 2007. Concise review: embryonic stem cells: a new tool to study osteoblast and osteoclast differentiation. Stem Cells 25:544-52.

Ebert R, Schütze N, Schilling T, Seefried L, Weber M, Nöth U, Eulert J, Jakob F. 2007. Influence of hormones on osteogenic differentiation processes of mesenchymal stem cells, Expert Rev Endocrinol Metab 2(1):59-78

Erceg I, Tadic T, Kronenberg MS, Marijanovic I, Lichtler AC. 2003. Dlx5 regulation of mouse osteoblast differentiation mediated by avian retrovirus vector. Croat Med J 44:407-11.

Eswarakumar VP, Lax I, Schlessinger J. 2005. Cellular signaling by fibroblast growth factor receptors. Cytokine Growth Factor Rev 16:139-49.

Farooqi IS, Matarese G, Lord GM, Keogh JM, Lawrence E, Agwu C, Sanna V, Jebb SA, Perna F, Fontana S, Lechler RI, DePaoli AM, O'Rahilly S. 2002. Beneficial effects of leptin on obesity, T cell hyporesponsiveness, and neuroendocrine/metabolic dysfunction of human congenital leptin deficiency. J Clin Invest 110:1093-103.

Franceschi RT, Iyer BS. 1992. Relationship between collagen synthesis and expression of the osteoblast phenotype in MC3T3-E1 cells. J Bone Miner Res 7:235-46.

Frayn KN, Karpe F, Fielding BA, Macdonald IA, Coppack SW. 2003. Integrative physiology of human adipose tissue. Int J Obes Relat Metab Disord 27:875-88.

Fried SK, Russell CD, Grauso NL, Brolin RE. 1993. Lipoprotein lipase regulation by insulin and glucocorticoid in subcutaneous and omental adipose tissues of obese women and men. J Clin Invest 92:2191-8.

Friedenstein AJ, Deriglasova UF, Kulagina NN, Panasuk AF, Rudakowa SF, Luria EA, Ruadkow IA. 1974. Precursors for fibroblasts in different populations of hematopoietic cells as detected by the in vitro colony assay method. Exp Hematol 2:83-92.

Friedenstein AJ, Gorskaja JF, Kulagina NN. 1976. Fibroblast precursors in normal and irradiated mouse hematopoietic organs. Exp Hematol 4:267-74.

Fuller K, Kirstein B, Chambers TJ. 2007. The regulation and enzymatic basis of bone resorption by human osteoclasts. Clin Sci (Lond).

Gagnon A, Dods P, Roustan-Delatour N, Chen CS, Sorisky A. 2001. Phosphatidylinositol-3,4,5-trisphosphate is required for insulin-like growth factor 1-mediated survival of 3T3-L1 preadipocytes. Endocrinology 142:205-12.

Gaskins HR, Hausman GJ, Martin RJ. 1989. Regulation of gene expression during adipocyte differentiation: a review. J Anim Sci 67:2263-72.

Gaur T, Lengner CJ, Hovhannisyan H, Bhat RA, Bodine PV, Komm BS, Javed A, van Wijnen AJ, Stein JL, Stein GS, Lian JB. 2005. Canonical WNT signaling promotes osteogenesis by directly stimulating Runx2 gene expression. J Biol Chem 280:33132-40.

Gelman L, Zhou G, Fajas L, Raspe E, Fruchart JC, Auwerx J. 1999. p300 interacts with the N- and C-terminal part of PPARgamma2 in a ligand-independent and -dependent manner, respectively. J Biol Chem 274:7681-8.

GeneCards. 2006. http://www.genecards.org. 30 March, 2007

Giancotti FG, Ruoslahti E. 1999. Integrin signaling. Science 285:1028-32.

Gilman AG. 1987. G proteins: transducers of receptor-generated signals. Ann Rev Biochem 56:615-49.

Gimble JM, Morgan C, Kelly K, Wu X, Dandapani V, Wang CS, Rosen V. 1995. Bone morphogenetic proteins inhibit adipocyte differentiation by bone marrow stromal cells. J Cell Biochem 58:393-402.

Gimble JM, Zvonic S, Floyd ZE, Kassem M, Nuttall ME. 2006. Playing with bone and fat. J Cell Biochem 98:251-66.

Glass DA, 2nd, Bialek P, Ahn JD, Starbuck M, Patel MS, Clevers H, Taketo MM, Long F, McMahon AP, Lang RA, Karsenty G. 2005. Canonical Wnt signaling in differentiated osteoblasts controls osteoclast differentiation. Dev Cell 8:751-64.

Glass DA, Karsenty G. 2007. In vivo analysis of Wnt signaling. Endocrinology:doi:10.1210/en.2006-1272.

Gori F, Thomas T, Hicok KC, Spelsberg TC, Riggs BL. 1999. Differentiation of human marrow stromal precursor cells: bone morphogenetic protein-2 increases OSF2/CBFA1, enhances osteoblast commitment, and inhibits late adipocyte maturation. J Bone Miner Res 14:1522-35.

Goutallier D, Postel JM, Bernageau J, Lavau L, Voisin MC. 1994. Fatty muscle degeneration in cuff ruptures. Pre- and postoperative evaluation by CT scan. Clin Orthop Relat Res:78-83.

Gregory CA, Gunn WG, Reyes E, Smolarz AJ, Munoz J, Spees JL, Prockop DJ. 2005. How Wnt signaling affects bone repair by mesenchymal stem cells from the bone marrow. Ann N Y Acad Sci 1049:97-106.

Grey A, Bolland M, Gamble G, Wattie D, Horne A, Davidson J, Reid IR. 2007. The Peroxisome Proliferator-Activated Receptor-{gamma} Agonist Rosiglitazone Decreases Bone Formation and Bone Mineral Density in Healthy Postmenopausal Women: A Randomized, Controlled Trial. J Clin Endocrinol Metab 92:1305-10.

Grzeszkiewicz TM, Lindner V, Chen N, Lam SC, Lau LF. 2002. The angiogenic factor cysteine-rich 61 (CYR61, CCN1) supports vascular smooth muscle cell adhesion and stimulates chemotaxis through integrin alpha(6)beta(1) and cell surface heparan sulfate proteoglycans. Endocrinology 143:1441-50.

Guerre-Millo M. 2004. Adipose tissue and adipokines: for better or worse. Diabetes Metab 30:13-9.

Gustafson B, Smith U. 2006. Cytokines promote Wnt signaling and inflammation and impair the normal differentiation and lipid accumulation in 3T3-L1 preadipocytes. J Biol Chem 281:9507-16.

Haynesworth SE, Goshima J, Goldberg VM, Caplan AI. 1992. Characterization of cells with osteogenic potential from human marrow. Bone 13:81-8.

Henriksen K, Leeming DJ, Byrjalsen I, Nielsen RH, Sorensen MG, Dziegiel MH, Martin TJ, Christiansen C, Qvist P, Karsdal MA. 2007. Osteoclasts prefer aged bone. Osteoporos Int:doi:10.1007/s00198-006-0298-4.

Hiscox S, Jiang WG. 1999. Ezrin regulates cell-cell and cell-matrix adhesion, a possible role with E-cadherin/beta-catenin. J Cell Sci 112 Pt 18:3081-90.

Hsu H, Lacey DL, Dunstan CR, Solovyev I, Colombero A, Timms E, Tan HL, Elliott G, Kelley MJ, Sarosi I, Wang L, Xia XZ, Elliott R, Chiu L, Black T, Scully S, Capparelli C, Morony S, Shimamoto G, Bass MB, Boyle WJ. 1999. Tumor necrosis factor receptor family member RANK mediates osteoclast differentiation and activation induced by osteoprotegerin ligand. Proc Natl Acad Sci U S A 96:3540-5.

Hu E, Tontonoz P, Spiegelman BM. 1995. Transdifferentiation of myoblasts by the adipogenic transcription factors PPAR gamma and C/EBP alpha. Proc Natl Acad Sci U S A 92:9856-60.

Hunter GK, Hauschka PV, Poole AR, Rosenberg LC, Goldberg HA. 1996. Nucleation and inhibition of hydroxyapatite formation by mineralized tissue proteins. Biochem J 317 ( Pt 1):59-64.

Hutley L, Shurety W, Newell F, McGeary R, Pelton N, Grant J, Herington A, Cameron D, Whitehead J, Prins J. 2004. Fibroblast growth factor 1: a key regulator of human adipogenesis. Diabetes 53:3097-106.

Ichida F, Nishimura R, Hata K, Matsubara T, Ikeda F, Hisada K, Yatani H, Cao X, Komori T, Yamaguchi A, Yoneda T. 2004. Reciprocal roles of MSX2 in regulation of osteoblast and adipocyte differentiation. J Biol Chem 279:34015-22.

Ito Y, Miyazono K. 2003. RUNX transcription factors as key targets of TGF-beta superfamily signaling. Curr Opin Genet Dev 13:43-7.

Jackson A, Vayssiere B, Garcia T, Newell W, Baron R, Roman-Roman S, Rawadi G. 2005. Gene array analysis of Wnt-regulated genes in C3H10T1/2 cells. Bone 36:585-98.

Jacob AL, Smith C, Partanen J, Ornitz DM. 2006. Fibroblast growth factor receptor 1 signaling in the osteo-chondrogenic cell lineage regulates sequential steps of osteoblast maturation. Dev Biol 296:315-28.

Jaiswal N, Haynesworth SE, Caplan AI, Bruder SP. 1997. Osteogenic differentiation of purified, culture-expanded human mesenchymal stem cells in vitro. J Cell Biochem 64:295-312.

Jaiswal RK, Jaiswal N, Bruder SP, Mbalaviele G, Marshak DR, Pittenger MF. 2000. Adult human mesenchymal stem cell differentiation to the osteogenic or adipogenic lineage is regulated by mitogen-activated protein kinase. J Biol Chem 275:9645-52.

Jeon EJ, Lee KY, Choi NS, Lee MH, Kim HN, Jin YH, Ryoo HM, Choi JY, Yoshida M, Nishino N, Oh BC, Lee KS, Lee YH, Bae SC. 2006. Bone morphogenetic protein-2 stimulates Runx2 acetylation. J Biol Chem 281:16502-11.

Justesen J, Stenderup K, Ebbesen EN, Mosekilde L, Steiniche T, Kassem M. 2001. Adipocyte tissue volume in bone marrow is increased with aging and in patients with osteoporosis. Biogerontology 2:165-71.

Kanazawa A, Tsukada S, Kamiyama M, Yanagimoto T, Nakajima M, Maeda S. 2005. Wnt5b partially inhibits canonical Wnt/beta-catenin signaling pathway and promotes adipogenesis in 3T3-L1 preadipocytes. Biochem Biophys Res Commun 330:505-10.

Kang JS, Alliston T, Delston R, Derynck R. 2005. Repression of Runx2 function by TGF-beta through recruitment of class II histone deacetylases by Smad3. Embo J 24:2543-55.

Khan E, Abu-Amer Y. 2003. Activation of peroxisome proliferator-activated receptor-gamma inhibits differentiation of preosteoblasts. J Lab Clin Med 142:29-34.

Kim JB, Wright HM, Wright M, Spiegelman BM. 1998. ADD1/SREBP1 activates PPARgamma through the production of endogenous ligand. Proc Natl Acad Sci U S A 95:4333-7.

Klein RF, Allard J, Avnur Z, Nikolcheva T, Rotstein D, Carlos AS, Shea M, Waters RV, Belknap JK, Peltz G, Orwoll ES. 2004. Regulation of bone mass in mice by the lipoxygenase gene Alox15. Science 303:229-32.

Kohn AD, Moon RT. 2005. Wnt and calcium signaling: beta-catenin-independent pathways. Cell Calcium 38:439-46.

Koo KH, Dussault R, Kaplan P, Kim R, Ahn IO, Christopher J, Song HR, Wang GJ. 1998. Age-related marrow conversion in the proximal metaphysis of the femur: evaluation with T1-weighted MR imaging. Radiology 206:745-8.

Krane SM. 2005. Identifying genes that regulate bone remodeling as potential therapeutic targets. J Exp Med 201:841-3.

Krug AW, Ehrhart-Bornstein M. 2005. Newly discovered endocrine functions of white adipose tissue: possible relevance in obesity-related diseases. Cell Mol Life Sci 62:1359-62.

Kundu M, Javed A, Jeon JP, Horner A, Shum L, Eckhaus M, Muenke M, Lian JB, Yang Y, Nuckolls GH, Stein GS, Liu PP. 2002. Cbfbeta interacts with Runx2 and has a critical role in bone development. Nat Genet 32:639-44.

Lacey DL, Timms E, Tan HL, Kelley MJ, Dunstan CR, Burgess T, Elliott R, Colombero A, Elliott G, Scully S, Hsu H, Sullivan J, Hawkins N, Davy E, Capparelli C, Eli A, Qian YX, Kaufman S, Sarosi I, Shalhoub V, Senaldi G, Guo J, Delaney J, Boyle WJ. 1998. Osteoprotegerin ligand is a cytokine that regulates osteoclast differentiation and activation. Cell 93:165-76.

Laczka-Osyczka A, Laczka M, Kasugai S, Ohya K. 1998. Behavior of bone marrow cells cultured on three different coatings of gel-derived bioactive glass-ceramics at early stages of cell differentiation. J Biomed Mater Res 42:433-42.

Lau LF, Lam SC. 1999. The CCN family of angiogenic regulators: the integrin connection. Exp Cell Res 248:44-57.

Lechner A, Schütze N, Siggelkow H, Seufert J, Jakob F. 2000. The immediate early gene product hCYR61 localizes to the secretory pathway in human osteoblasts. Bone 27:53-60.

Lecka-Czernik B, Moerman EJ, Grant DF, Lehmann JM, Manolagas SC, Jilka RL. 2002. Divergent effects of selective peroxisome proliferator-activated receptor-gamma 2 ligands on adipocyte versus osteoblast differentiation. Endocrinology 143:2376-84.

Lindl T. 2002. Zell- und Gewebekultur. Heidelberg: Spektrum. p 110-112.

Ling L, Murali S, Dombrowski C, Haupt LM, Stein GS, van Wijnen AJ, Nurcombe V, Cool SM. 2006. Sulfated glycosaminoglycans mediate the effects of FGF2 on the osteogenic potential of rat calvarial osteoprogenitor cells. J Cell Physiol 209:811-25.

Logan CY, Nusse R. 2004. The Wnt signaling pathway in development and disease. Annu Rev Cell Dev Biol 20:781-810.

Longo KA, Kennell JA, Ochocinska MJ, Ross SE, Wright WS, MacDougald OA. 2002. Wnt signaling protects 3T3-L1 preadipocytes from apoptosis through induction of insulin-like growth factors. J Biol Chem 277:38239-44.

MacDougald OA, Lane MD. 1995. Transcriptional regulation of gene expression during adipocyte differentiation. Annu Rev Biochem 64:345-73.

MacDougald OA, Mandrup S. 2002. Adipogenesis: forces that tip the scales. Trends Endocrinol Metab 13:5-11.

Maeda N, Takahashi M, Funahashi T, Kihara S, Nishizawa H, Kishida K, Nagaretani H, Matsuda M, Komuro R, Ouchi N, Kuriyama H, Hotta K, Nakamura T, Shimomura I, Matsuzawa Y. 2001.

PPARgamma ligands increase expression and plasma concentrations of adiponectin, an adipose-derived protein. Diabetes 50:2094-9.

Marie PJ, Coffin JD, Hurley MM. 2005. FGF and FGFR signaling in chondrodysplasias and craniosynostosis. J Cell Biochem 96:888-96.

Martin TJ. 1983. Drug and hormone effects on calcium release from bone. Pharmacol Ther 21:209-28.

Martin TJ, Sims NA. 2005. Osteoclast-derived activity in the coupling of bone formation to resorption. Trends Mol Med 11:76-81.

Mavri A, Alessi MC, Bastelica D, Geel-Georgelin O, Fina F, Sentocnik JT, Stegnar M, Juhan-Vague I. 2001. Subcutaneous abdominal, but not femoral fat expression of plasminogen activator inhibitor-1 (PAI-1) is related to plasma PAI-1 levels and insulin resistance and decreases after weight loss. Diabetologia 44:2025-31.

McLarren KW, Lo R, Grbavec D, Thirunavukkarasu K, Karsenty G, Stifani S. 2000. The mammalian basic helix loop helix protein HES-1 binds to and modulates the transactivating function of the runt-related factor Cbfa1. J Biol Chem 275:530-8.

Meunier P, Aaron J, Edouard C, Vignon G. 1971. Osteoporosis and the replacement of cell populations of the marrow by adipose tissue. A quantitative study of 84 iliac bone biopsies. Clin Orthop Relat Res 80:147-54.

Miller J, Horner A, Stacy T, Lowrey C, Lian JB, Stein G, Nuckolls GH, Speck NA. 2002. The core-binding factor beta subunit is required for bone formation and hematopoietic maturation. Nat Genet 32:645-9.

Miller JR, Hocking AM, Brown JD, Moon RT. 1999. Mechanism and function of signal transduction by the Wnt/beta-catenin and Wnt/Ca2+ pathways. Oncogene 18:7860-72.

Misof BM, Roschger P, Tesch W, Baldock PA, Valenta A, Messmer P, Eisman JA, Boskey AL, Gardiner EM, Fratzl P, Klaushofer K. 2003. Targeted overexpression of vitamin D receptor in osteoblasts increases calcium concentration without affecting structural properties of bone mineral crystals. Calcif Tissue Int 73:251-7.

Miyama K, Yamada G, Yamamoto TS, Takagi C, Miyado K, Sakai M, Ueno N, Shibuya H. 1999. A BMP-inducible gene, dlx5, regulates osteoblast differentiation and mesoderm induction. Dev Biol 208:123-33.

Moerman EJ, Teng K, Lipschitz DA, Lecka-Czernik B. 2004. Aging activates adipogenic and suppresses osteogenic programs in mesenchymal marrow stroma/stem cells: the role of PPAR-gamma2 transcription factor and TGF-beta/BMP signaling pathways. Aging Cell 3:379-89.

Moore SG, Dawson KL. 1990. Red and yellow marrow in the femur: age-related changes in appearance at MR imaging. Radiology 175:219-23.

Muraglia A, Cancedda R, Quarto R. 2000. Clonal mesenchymal progenitors from human bone marrow differentiate in vitro according to a hierarchical model. J Cell Sci 113 ( Pt 7):1161-6.

Nakagaki K, Ozaki J, Tomita Y, Tamai S. 1996. Fatty degeneration in the supraspinatus muscle after rotator cuff tear. J Shoulder Elbow Surg 5:194-200.

Nakashima K, de Crombrugghe B. 2003. Transcriptional mechanisms in osteoblast differentiation and bone formation. Trends Genet 19:458-66.

Nakashima K, Zhou X, Kunkel G, Zhang Z, Deng JM, Behringer RR, de Crombrugghe B. 2002. The novel zinc finger-containing transcription factor osterix is required for osteoblast differentiation and bone formation. Cell 108:17-29.

Nakayama Y, Nakajima Y, Kato N, Takai H, Kim DS, Arai M, Mezawa M, Araki S, Sodek J, Ogata Y. 2006. Insulin-like growth factor-I increases bone sialoprotein (BSP) expression through fibroblast growth factor-2 response element and homeodomain protein-binding site in the proximal promoter of the BSP gene. J Cell Physiol 208:326-35.

Nöth U, Osyczka AM, Tuli R, Hickok NJ, Danielson KG, Tuan RS. 2002a. Multilineage mesenchymal differentiation potential of human trabecular bone-derived cells. J Orthop Res 20:1060-9.

Nöth U, Tuli R, Osyczka AM, Danielson KG, Tuan RS. 2002b. In vitro engineered cartilage constructs produced by press-coating biodegradable polymer with human mesenchymal stem cells. Tissue Eng 8:131-44.

Nuttall ME, Gimble JM. 2004. Controlling the balance between osteoblastogenesis and adipogenesis and the consequent therapeutic implications. Curr Opin Pharmacol 4:290-4.

Nuttall ME, Patton AJ, Olivera DL, Nadeau DP, Gowen M. 1998. Human trabecular bone cells are able to express both osteoblastic and adipocytic phenotype: implications for osteopenic disorders. J Bone Miner Res 13:371-82.

Orkin SH, Zon LI. 2002. Hematopoiesis and stem cells: plasticity versus developmental heterogeneity. Nat Immunol 3:323-8.

Ornitz DM. 2005. FGF signaling in the developing endochondral skeleton. Cytokine Growth Factor Rev 16:205-13.

Oshima T, Abe M, Asano J, Hara T, Kitazoe K, Sekimoto E, Tanaka Y, Shibata H, Hashimoto T, Ozaki S, Kido S, Inoue D, Matsumoto T. 2005. Myeloma cells suppress bone formation by secreting a soluble Wnt inhibitor, sFRP-2. Blood 106:3160-5.

Parikka V, Peng Z, Hentunen T, Risteli J, Elo T, Vaananen HK, Harkonen P. 2005. Estrogen responsiveness of bone formation in vitro and altered bone phenotype in aged estrogen receptor-alpha-deficient male and female mice. Eur J Endocrinol 152:301-14.

Park SR, Oreffo RO, Triffitt JT. 1999. Interconversion potential of cloned human marrow adipocytes in vitro. Bone 24:549-54.

Patel YM, Lane MD. 2000. Mitotic Clonal Expansion during Preadipocyte Differentiation: Calpain-mediated Turnover of p27. J. Biol. Chem. 275:17653-17660.

Pei L, Tontonoz P. 2004. Fat's loss is bone's gain. J Clin Invest 113:805-6.

Pereira RF, Halford KW, O'Hara MD, Leeper DB, Sokolov BP, Pollard MD, Bagasra O, Prockop DJ. 1995. Cultured adherent cells from marrow can serve as long-lasting precursor cells for bone, cartilage, and lung in irradiated mice. Proc Natl Acad Sci U S A 92:4857-61.

Pittenger MF, Mackay AM, Beck SC, Jaiswal RK, Douglas R, Mosca JD, Moorman MA, Simonetti DW, Craig S, Marshak DR. 1999. Multilineage potential of adult human mesenchymal stem cells. Science 284:143-7.

Prockop DJ. 1997. Marrow stromal cells as stem cells for nonhematopoietic tissues. Science 276:71-4.

Qiu Z, Wei Y, Chen N, Jiang M, Wu J, Liao K. 2001. DNA synthesis and mitotic clonal expansion is not a required step for 3T3-L1 preadipocyte differentiation into adipocytes. J Biol Chem 276:11988-95.

Quarto N, Longaker MT. 2006. FGF-2 inhibits osteogenesis in mouse adipose tissue-derived stromal cells and sustains their proliferative and osteogenic potential state. Tissue Eng 12:1405-18.

Rawadi G, Vayssiere B, Dunn F, Baron R, Roman-Roman S. 2003. BMP-2 controls alkaline phosphatase expression and osteoblast mineralization by a Wnt autocrine loop. J Bone Miner Res 18:1842-53.

Ricort JM. 2004. Insulin-like growth factor binding protein (IGFBP) signalling. Growth Horm IGF Res 14:277-86.

Rodic N, Rutenberg MS, Terada N. 2004. Cell fusion and reprogramming: resolving our transdifferences. Trends Mol Med 10:93-6.

Rosen CJ, Bouxsein ML. 2006. Mechanisms of disease: is osteoporosis the obesity of bone? Nat Clin Pract Rheumatol 2:35-43.

Rosen ED, Sarraf P, Troy AE, Bradwin G, Moore K, Milstone DS, Spiegelman BM, Mortensen RM. 1999. PPAR gamma is required for the differentiation of adipose tissue in vivo and in vitro. Mol Cell 4:611-7.

Rosen ED, Walkey CJ, Puigserver P, Spiegelman BM. 2000. Transcriptional regulation of adipogenesis. Genes Dev 14:1293-307.

Ross SE, Erickson RL, Gerin I, DeRose PM, Bajnok L, Longo KA, Misek DE, Kuick R, Hanash SM, Atkins KB, Andresen SM, Nebb HI, Madsen L, Kristiansen K, MacDougald OA. 2002. Microarray analyses during adipogenesis: understanding the effects of Wnt signaling on adipogenesis and the roles of liver X receptor alpha in adipocyte metabolism. Mol Cell Biol 22:5989-99.

Ross SE, Hemati N, Longo KA, Bennett CN, Lucas PC, Erickson RL, MacDougald OA. 2000. Inhibition of adipogenesis by Wnt signaling. Science 289:950-3.

Rössler H, Rüther W. 2000. Orthopädie. Munich: Urban & Fischer. p 3-17.

Rozen S, Skaletsky H. 2000. Primer3 on the WWW for general users and for biologist programmers. Methods Mol Biol 132:365-86.

Rzonca SO, Suva LJ, Gaddy D, Montague DC, Lecka-Czernik B. 2004. Bone is a target for the antidiabetic compound rosiglitazone. Endocrinology 145:401-6.

Sabatakos G, Sims NA, Chen J, Aoki K, Kelz MB, Amling M, Bouali Y, Mukhopadhyay K, Ford K, Nestler EJ, Baron R. 2000. Overexpression of DeltaFosB transcription factor(s) increases bone formation and inhibits adipogenesis. Nat Med 6:985-90.

Sato Y, Araki H, Kato J, Nakamura K, Kawano Y, Kobune M, Sato T, Miyanishi K, Takayama T, Takahashi M, Takimoto R, Iyama S, Matsunaga T, Ohtani S, Matsuura A, Hamada H, Niitsu Y. 2005. Human mesenchymal stem cells xenografted directly to rat liver are differentiated into human hepatocytes without fusion. Blood 106:756-63.

Saunders WB, Bohnsack BL, Faske JB, Anthis NJ, Bayless KJ, Hirschi KK, Davis GE. 2006. Coregulation of vascular tube stabilization by endothelial cell TIMP-2 and pericyte TIMP-3. J Cell Biol 175:179-91.

Schiller PC, D'Ippolito G, Brambilla R, Roos BA, Howard GA. 2001. Inhibition of gap-junctional communication induces the trans-differentiation of osteoblasts to an adipocytic phenotype in vitro. J Biol Chem 276:14133-8.

Schlessinger J. 2000. Cell signaling by receptor tyrosine kinases. Cell 103:211-25.

Schmidt W, Poll-Jordan G, Loffler G. 1990. Adipose conversion of 3T3-L1 cells in a serum-free culture system depends on epidermal growth factor, insulin-like growth factor I, corticosterone, and cyclic AMP. J Biol Chem 265:15489-95.

Schütze N, Kunzi-Rapp K, Wagemanns R, Nöth U, Jatzke S, Jakob F. 2005a. Expression, purification, and functional testing of recombinant CYR61/CCN1. Protein Expr Purif 42:219-25.

Schütze N, Nöth U, Schneidereit J, Hendrich C, Jakob F. 2005b. Differential expression of CCN-family members in primary human bone marrow-derived mesenchymal stem cells during osteogenic, chondrogenic and adipogenic differentiation. Cell Commun Signal 3:5.

Schütze N, Wagemanns R, Schilling T, Jakob F. 2006. CCN1. UCSD-Nature Molecule Pages, doi: 10.1038/mp.a003362.01

Serakinci N, Guldberg P, Burns JS, Abdallah B, Schrodder H, Jensen T, Kassem M. 2004. Adult human mesenchymal stem cell as a target for neoplastic transformation. Oncogene 23:5095-8.

Si W, Kang Q, Luu HH, Park JK, Luo Q, Song WX, Jiang W, Luo X, Li X, Yin H, Montag AG, Haydon RC, He TC. 2006. CCN1/Cyr61 is regulated by the canonical Wnt signal and plays an important role in Wnt3A-induced osteoblast differentiation of mesenchymal stem cells. Mol Cell Biol 26:2955-64.

Simonet WS, Lacey DL, Dunstan CR, Kelley M, Chang MS, Luthy R, Nguyen HQ, Wooden S, Bennett L, Boone T, Shimamoto G, DeRose M, Elliott R, Colombero A, Tan HL, Trail G, Sullivan J, Davy E, Bucay N, Renshaw-Gegg L, Hughes TM, Hill D, Pattison W, Campbell P, Sander S, Van G, Tarpley J, Derby P, Lee R, Boyle WJ. 1997. Osteoprotegerin: a novel secreted protein involved in the regulation of bone density. Cell 89:309-19.

Song L, Tuan RS. 2004. Transdifferentiation potential of human mesenchymal stem cells derived from bone marrow. Faseb J 18:980-2.

Song L, Webb NE, Song Y, Tuan RS. 2006. Identification and Functional Analysis of Candidate Genes Regulating Mesenchymal Stem Cell Self-Renewal and Multipotency. Stem Cells.

Spencer GJ, Utting JC, Etheridge SL, Arnett TR, Genever PG. 2006. Wnt signalling in osteoblasts regulates expression of the receptor activator of NFkappaB ligand and inhibits osteoclastogenesis in vitro. J Cell Sci 119:1283-96.

Spiegelman BM, Choy L, Hotamisligil GS, Graves RA, Tontonoz P. 1993. Regulation of adipocyte gene expression in differentiation and syndromes of obesity/diabetes. J Biol Chem 268:6823-6.

Stein GS, Lian JB, Stein JL, Van Wijnen AJ, Montecino M. 1996. Transcriptional control of osteoblast growth and differentiation. Physiol Rev 76:593-629.

Tadic T, Erceg I, Stover ML, Rowe DW, Lichtler AC. 2001. Dlx5 induces expression of COL1A1 promoter contained in a retrovirus vector. Croat Med J 42:436-9.

Tang KT, Capparelli C, Stein JL, Stein GS, Lian JB, Huber AC, Braverman LE, DeVito WJ. 1996. Acidic fibroblast growth factor inhibits osteoblast differentiation in vitro: altered expression of collagenase, cell growth-related, and mineralization-associated genes. J Cell Biochem 61:152-66.

Terada N, Hamazaki T, Oka M, Hoki M, Mastalerz DM, Nakano Y, Meyer EM, Morel L, Petersen BE, Scott EW. 2002. Bone marrow cells adopt the phenotype of other cells by spontaneous cell fusion. Nature 416:542-5.

Tontonoz P, Graves RA, Budavari AI, Erdjument-Bromage H, Lui M, Hu E, Tempst P, Spiegelman BM. 1994a. Adipocyte-specific transcription factor ARF6 is a heterodimeric complex of two nuclear hormone receptors, PPAR gamma and RXR alpha. Nucleic Acids Res 22:5628-34.

Tontonoz P, Hu E, Graves RA, Budavari AI, Spiegelman BM. 1994b. mPPAR gamma 2: tissue-specific regulator of an adipocyte enhancer. Genes Dev 8:1224-34.

Tontonoz P, Hu E, Spiegelman BM. 1994c. Stimulation of adipogenesis in fibroblasts by PPAR gamma 2, a lipid-activated transcription factor. Cell 79:1147-56.

Tosh D, Slack JM. 2002. How cells change their phenotype. Nat Rev Mol Cell Biol 3:187-94.

Trayhurn P, Bing C, Wood IS. 2006. Adipose tissue and adipokines--energy regulation from the human perspective. J Nutr 136:1935S-1939S.

Väänänen HK, Zhao H, Mulari M, Halleen JM. 2000. The cell biology of osteoclast function. J Cell Sci 113 ( Pt 3):377-81.

Verfaillie CM. 2002. Adult stem cells: assessing the case for pluripotency. Trends Cell Biol 12:502-8.

Wabitsch M, Heinze E, Debatin KM, Blum WF. 2000. IGF-I- and IGFBP-3-expression in cultured human preadipocytes and adipocytes. Horm Metab Res 32:555-9.

Wajchenberg BL. 2000. Subcutaneous and visceral adipose tissue: their relation to the metabolic syndrome. Endocr Rev 21:697-738.

Wee HJ, Huang G, Shigesada K, Ito Y. 2002. Serine phosphorylation of RUNX2 with novel potential functions as negative regulatory mechanisms. EMBO Rep 3:967-74.

Wesche J, Malecki J, Wiedlocha A, Ehsani M, Marcinkowska E, Nilsen T, Olsnes S. 2005. Two nuclear localization signals required for transport from the cytosol to the nucleus of externally added FGF-1 translocated into cells. Biochemistry 44:6071-80.

Wu Z, Rosen ED, Brun R, Hauser S, Adelmant G, Troy AE, McKeon C, Darlington GJ, Spiegelman BM. 1999. Cross-regulation of C/EBP alpha and PPAR gamma controls the transcriptional pathway of adipogenesis and insulin sensitivity. Mol Cell 3:151-8.

Xiao G, Jiang D, Gopalakrishnan R, Franceschi RT. 2002. Fibroblast growth factor 2 induction of the osteocalcin gene requires MAPK activity and phosphorylation of the osteoblast transcription factor, Cbfa1/Runx2. J Biol Chem 277:36181-7.

Yao TP, Ku G, Zhou N, Scully R, Livingston DM. 1996. The nuclear hormone receptor coactivator SRC-1 is a specific target of p300. Proc Natl Acad Sci U S A 93:10626-31.

Ying QL, Nichols J, Evans EP, Smith AG. 2002. Changing potency by spontaneous fusion. Nature 416:545-8.

Yu JG, Javorschi S, Hevener AL, Kruszynska YT, Norman RA, Sinha M, Olefsky JM. 2002. The effect of thiazolidinediones on plasma adiponectin levels in normal, obese, and type 2 diabetic subjects. Diabetes 51:2968-74.

Zawin JK, Jaramillo D. 1993. Conversion of bone marrow in the humerus, sternum, and clavicle: changes with age on MR images. Radiology 188:159-64.

Zhang YW, Yasui N, Ito K, Huang G, Fujii M, Hanai J, Nogami H, Ochi T, Miyazono K, Ito Y. 2000. A RUNX2/PEBP2alpha A/CBFA1 mutation displaying impaired transactivation and Smad interaction in cleidocranial dysplasia. Proc Natl Acad Sci U S A 97:10549-54.

# 7 Appendix

## 7.1 Fold changes of gene regulation after initiation of adipogenic transdifferentiation – GeneChips HG-U 133A

**Tab. 12 Fold changes of gene regulation 3 h after initiation of adipogenic transdifferentiation**

| Gene name | Gene symbol | Affymetrix probe set ID | Fold change + 3 h |
|---|---|---|---|
| ADP-ribosylation factor-like 7 | ARL7 | 202208_s_at | 3.2 |
| ADP-ribosylation factor-like 7 | ARL7 | 202207_at | 2.5 |
| adrenomedullin | ADM | 202912_at | -2.8 |
| amphiregulin (schwannoma-derived growth factor) | AREG | 205239_at | 3.6 |
| ankyrin repeat and SOCS box-containing 1 | ASB1 | 212819_at | -2.9 |
| apolipoprotein L domain containing 1 | APOLD1 | 221031_s_at | 4.5 |
| ATPase, Ca++ transporting, plasma membrane 1 | ATP2B1 | 212930_at | -10.4 |
| ATP-binding cassette, sub-family A (ABC1), member 5 | ABCA5 | 213353_at | -3.9 |
| cAMP responsive element modulator | CREM | 209967_s_at | 8.3 |
| cAMP responsive element modulator | CREM | 207630_s_at | 3.6 |
| cathepsin Z | CTSZ | 210042_s_at | 5.2 |
| cathepsin Z | CTSZ | 212562_s_at | 5.2 |
| Cbp/p300-interacting transactivator, with Glu/Asp-rich carboxy-terminal domain, 2 | CITED2 | 209357_at | -2.8 |
| chemokine (C-X3-C motif) ligand 1 | CX3CL1 | 823_at | -3.3 |
| chemokine (C-X3-C motif) ligand 1 | CX3CL1 | 203687_at | -10.7 |
| chromobox homolog 4 (Pc class homolog, Drosophila) | CBX4 | 206724_at | 2.9 |
| chromosome 6 open reading frame 56 | C6orf56 | 204049_s_at | -2.5 |
| cofactor required for Sp1 transcriptional activation, subunit 9, 33kDa | CRSP9 | 204349_at | -12.0 |
| colon carcinoma related protein | LOC51159 | 220327_at | -2.5 |
| core-binding factor, runt domain, alpha subunit 2; translocated to, 1; cyclin D-related | CBFA2T1 | 205528_s_at | -16.1 |
| cystathionase (cystathionine gamma-lyase) | CTH | 217127_at | 3.8 |
| cystathionase (cystathionine gamma-lyase) | CTH | 206085_s_at | 2.6 |
| cysteine knot superfamily 1, BMP antagonist 1 | CKTSF1B1 | 218469_at | -2.5 |
| cysteine knot superfamily 1, BMP antagonist 1 | CKTSF1B1 | 218468_s_at | -2.5 |
| cysteine-rich, angiogenic inducer, 61 | CYR61 | 210764_s_at | -4.1 |
| cysteine-rich, angiogenic inducer, 61 | CYR61 | 201289_at | -5.2 |
| dapper homolog 1, antagonist of beta-catenin (xenopus) | DACT1 | 219179_at | -2.8 |
| decidual protein induced by progesterone | DEPP | 209182_s_at | -3.1 |
| distal-less homeo box 2 | DLX2 | 207147_at | 2.8 |
| DnaJ (Hsp40) homolog, subfamily B, member 4 | DNAJB4 | 203810_at | -2.5 |
| DnaJ (Hsp40) homolog, subfamily B, member 4 | DNAJB4 | 203811_s_at | -2.7 |
| downregulated in ovarian cancer 1 | DOC1 | 204135_at | -4.1 |
| dual specificity phosphatase 4 | DUSP4 | 204014_at | 3.9 |
| dual specificity phosphatase 6 | DUSP6 | 208891_at | -4.0 |
| dual specificity phosphatase 6 | DUSP6 | 208892_s_at | -4.8 |
| dual specificity phosphatase 7 | DUSP7 | 214793_at | -3.1 |
| dual-specificity tyrosine-(Y)-phosphorylation regulated kinase 1A | DYRK1A | 211541_s_at | 3.9 |
| early growth response 2 (Krox-20 homolog, Drosophila) | EGR2 | 205249_at | -3.8 |
| early growth response 3 | EGR3 | 206115_at | -3.4 |
| ectodermal-neural cortex (with BTB-like domain) | ENC1 | 201341_at | -2.7 |
| GATA binding protein 6 | GATA6 | 210002_at | -2.5 |
| guanine nucleotide binding protein (G protein), alpha activating activity polypeptide, olfactory type | GNAL | 218177_at | 4.9 |
| guanine nucleotide binding protein (G protein), alpha activating activity polypeptide, olfactory type | GNAL | 218178_s_at | 4.1 |
| heme oxygenase (decycling) 1 | HMOX1 | 203665_at | -2.5 |
| HIF-1 responsive RTP801 | RTP801 | 202887_s_at | 3.2 |
| high mobility group AT-hook 2 | HMGA2 | 208025_s_at | -3.2 |
| homeo box A1 | HOXA1 | 214639_s_at | 3.0 |
| human immunodeficiency virus type I enhancer binding protein 1 | HIVEP1 | 204512_at | -2.7 |
| hyaluronan synthase 1 | HAS1 | 207316_at | 3.8 |
| hypothetical protein FLJ22341 | FLJ22341 | 219202_at | 7.3 |
| inhibitor of DNA binding 2, dominant negative helix-loop-helix protein | ID2 | 201566_x_at | 2.8 |
| inhibitor of DNA binding 4, dominant negative helix-loop-helix protein | ID4 | 209293_x_at | 4.9 |
| inhibitor of DNA binding 4, dominant negative helix-loop-helix protein | ID4 | 209292_at | 4.7 |
| inhibitor of DNA binding 4, dominant negative helix-loop-helix protein | ID4 | 209291_at | 3.6 |
| intercellular adhesion molecule 1 (CD54), human rhinovirus receptor | ICAM1 | 202638_s_at | -2.8 |
| intersectin 2 | ITSN2 | 209898_x_at | -10.3 |
| KIAA0701 protein | KIAA0701 | 213118_at | -6.6 |
| KIAA0874 protein | KIAA0874 | 216563_at | -2.7 |
| Kruppel-like factor 4 (gut) | KLF4 | 220266_s_at | 2.8 |
| Kruppel-like factor 5 (intestinal) | KLF5 | 209212_s_at | -2.9 |
| Kruppel-like factor 7 (ubiquitous) | KLF7 | 204334_at | -3.0 |
| leukemia inhibitory factor (cholinergic differentiation factor) | LIF | 205266_at | -2.9 |

| Gene name | Gene symbol | Affymetrix probe set ID | Fold change + 3 h |
|---|---|---|---|
| LIM protein (similar to rat protein kinase C-binding enigma) | LIM | 221994_at | -2.9 |
| matrix metalloproteinase 1 (interstitial collagenase) | MMP1 | 204475_at | -2.9 |
| myosin VI | MYO6 | 210480_s_at | -2.6 |
| myosin VI | MYO6 | 203215_s_at | -3.0 |
| neural precursor cell expressed, developmentally down-regulated 9 | NEDD9 | 202150_s_at | -2.6 |
| nuclear factor of activated T-cells, cytoplasmic, calcineurin-dependent 1 | NFATC1 | 211105_s_at | 2.6 |
| nuclear receptor subfamily 4, group A, member 1 | NR4A1 | 202340_x_at | 2.6 |
| nuclear receptor subfamily 4, group A, member 2 | NR4A2 | 204621_s_at | 9.6 |
| nuclear receptor subfamily 4, group A, member 2 | NR4A2 | 216248_s_at | 9.5 |
| nuclear receptor subfamily 4, group A, member 2 | NR4A2 | 204622_x_at | 7.4 |
| nuclear receptor subfamily 4, group A, member 3 | NR4A3 | 209959_at | 2.7 |
| nuclear receptor subfamily 4, group A, member 3 | NR4A3 | 207978_s_at | 2.5 |
| peptidylprolyl isomerase F (cyclophilin F) | PPIF | 201490_s_at | 2.6 |
| period homolog 1 (Drosophila) | PER1 | 202861_at | 2.9 |
| phosphodiesterase 4B, cAMP-specific (phosphodiesterase E4 dunce homolog, Drosophila) | PDE4B | 203708_at | 5.5 |
| phosphodiesterase 4D, cAMP-specific (phosphodiesterase E3 dunce homolog, Drosophila) | PDE4D | 204491_at | 4.6 |
| phosphodiesterase 4D, cAMP-specific (phosphodiesterase E3 dunce homolog, Drosophila) | PDE4D | 210836_x_at | 3.0 |
| phosphodiesterase 4D, cAMP-specific (phosphodiesterase E3 dunce homolog, Drosophila) | PDE4D | 210837_s_at | 2.7 |
| phospholamban | PLN | 204939_s_at | -2.9 |
| pim-1 oncogene | PIM1 | 209193_at | -3.3 |
| potassium voltage-gated channel, Isk-related family, member 4 | KCNE4 | 222379_at | 5.9 |
| prostaglandin E receptor 4 (subtype EP4) | PTGER4 | 204897_at | -4.0 |
| protein kinase C-like 2 | PRKCL2 | 212628_at | -2.6 |
| protein phosphatase 1, regulatory (inhibitor) subunit 3C | PPP1R3C | 204284_at | 3.2 |
| RAB20, member RAS oncogene family | RAB20 | 219622_at | 2.6 |
| regulator of G-protein signalling 16 | RGS16 | 209324_s_at | -5.7 |
| regulator of G-protein signalling 16 | RGS16 | 209325_s_at | -5.7 |
| regulator of G-protein signalling 2, 24kDa | RGS2 | 202388_at | 6.1 |
| retinoic acid induced 3 | RAI3 | 212444_at | 2.9 |
| SAM domain, SH3 domain and nuclear localisation signals, 1 | SAMSN1 | 220330_s_at | -4.1 |
| serine/threonine kinase 38 like | STK38L | 212572_at | -3.5 |
| serine/threonine kinase 38 like | STK38L | 212565_at | -3.8 |
| signal sequence receptor, gamma (translocon-associated protein gamma) | SSR3 | 217790_s_at | 2.8 |
| solute carrier family 2 (facilitated glucose transporter), member 3 | SLC2A3 | 202499_s_at | 4.7 |
| solute carrier family 2 (facilitated glucose transporter), member 14 | SLC2A14 | 222088_s_at | 3.8 |
| solute carrier family 2 (facilitated glucose transporter), member 3 | SLC2A3 | 202498_s_at | 3.5 |
| solute carrier family 2 (facilitated glucose transporter), member 14 | SLC2A14 | 216236_s_at | 2.9 |
| solute carrier family 2 (facilitated glucose transporter), member 3 | SLC2A3 | 202497_x_at | 2.9 |
| solute carrier family 7 (cationic amino acid transporter, y+ system), member 5 | SLC7A5 | 201195_s_at | 2.9 |
| sprouty homolog 2 (Drosophila) | SPRY2 | 204011_at | -2.5 |
| superoxide dismutase 2, mitochondrial | SOD2 | 215078_at | -3.8 |
| thioredoxin interacting protein | TXNIP | 201008_s_at | -2.6 |
| TNF receptor-associated factor 1 | TRAF1 | 205599_at | -2.9 |
| TNF-induced protein | GG2-1 | 210260_s_at | -2.5 |
| TNF-induced protein | GG2-1 | 208296_x_at | -3.6 |
| topoisomerase (DNA) II alpha 170kDa | TOP2A | 201291_s_at | -2.9 |
| transcription factor 8 (represses interleukin 2 expression) | TCF8 | 208078_s_at | 5.9 |
| translation initiation factor IF2 | IF2 | 201027_s_at | -6.1 |
| tumor rejection antigen (gp96) 1 | TRA1 | 216449_x_at | -2.7 |
| vasopressin-induced transcript | VIP32 | 218631_at | 2.6 |
| zinc finger protein 217 | ZNF217 | 203739_at | -3.6 |
| zinc finger protein 331 | ZNF331 | 219228_at | 7.6 |

Fold change + 3 h = differential gene expression 3 h after initiation of transdifferentiation.


**Tab. 13  Fold changes of gene regulation 24 h after initiation of adipogenic transdifferentiation**

| Gene name | Gene symbol | Affymetrix probe set ID | Fold change + 24 h |
|---|---|---|---|
| 3-hydroxysteroid epimerase | RODH | 205700_at | -3.4 |
| acetyl-Coenzyme A carboxylase beta | ACACB | 43427_at | 3.0 |
| acetyl-Coenzyme A carboxylase beta | ACACB | 49452_at | 3.0 |
| adenosine deaminase | ADA | 204639_at | 2.6 |
| adipose most abundant gene transcript 1 | APM1 | 207175_at | 5.7 |
| ADP-ribosylation factor-like 7 | ARL7 | 202207_at | 3.2 |
| ADP-ribosylation factor-like 7 | ARL7 | 202206_at | 3.1 |
| alcohol dehydrogenase IB (class I), beta polypeptide | ADH1B | 209613_s_at | 3.0 |
| aldehyde dehydrogenase 1 family, member A3 | ALDH1A3 | 203180_at | 2.8 |
| aldehyde dehydrogenase 1 family, member B1 | ALDH1B1 | 209646_x_at | -3.2 |
| aldehyde dehydrogenase 1 family, member B1 | ALDH1B1 | 209645_s_at | -3.8 |
| aldehyde dehydrogenase 2 family (mitochondrial) | ALDH2 | 201425_at | 3.2 |
| aldo-keto reductase family 1, member C1 (dihydrodiol dehydrogenase 1; 20-alpha (3- | AKR1C1 | 216594_x_at | 2.6 |

| Gene name | Gene symbol | Affymetrix probe set ID | Fold change + 24 h |
|---|---|---|---|
| alpha)-hydroxysteroid dehydrogenase) | | | |
| aldo-keto reductase family 1, member C1 (dihydrodiol dehydrogenase 1; 20-alpha (3-alpha)-hydroxysteroid dehydrogenase) | AKR1C1 | 204151_x_at | 2.5 |
| aldo-keto reductase family 1, member C2 (dihydrodiol dehydrogenase 2; bile acid binding protein; 3-alpha hydroxysteroid dehydrogenase, type III) | AKR1C2 | 211653_x_at | 2.5 |
| amine oxidase, copper containing 2 (retina-specific) | AOC2 | 207064_s_at | 6.5 |
| ATP-binding cassette, sub-family A (ABC1), member 1 | ABCA1 | 203504_s_at | 2.7 |
| ATP-binding cassette, sub-family D (ALD), member 2 | ABCD2 | 207583_at | 3.5 |
| atrophin-1 interacting protein 1 | AIP1 | 209737_at | -4.0 |
| atrophin-1 interacting protein 1 | AIP1 | 207702_s_at | -21.6 |
| baculoviral IAP repeat-containing 3 | BIRC3 | 210538_s_at | -12.0 |
| calcium channel, voltage-dependent, beta 2 subunit | CACNB2 | 213714_at | 2.9 |
| caldesmon 1 | CALD1 | 201615_x_at | -2.5 |
| calponin 1, basic, smooth muscle | CNN1 | 203951_at | -3.1 |
| carbohydrate (N-acetylglucosamine 6-O) sulfotransferase 7 | CHST7 | 206756_at | 2.7 |
| cardiac ankyrin repeat protein | CARP | 206029_at | -8.6 |
| catalase | CAT | 201432_at | 3.2 |
| catalase | CAT | 211922_s_at | 3.0 |
| cathepsin Z | CTSZ | 210042_s_at | 2.7 |
| CCAAT/enhancer binding protein (C/EBP), alpha | CEBPA | 204039_at | 10.5 |
| CD97 antigen | CD97 | 202910_s_at | -2.6 |
| cell adhesion molecule with homology to L1CAM (close homolog of L1) | CHL1 | 204591_at | 25.5 |
| chemokine (C-X-C motif) ligand 12 (stromal cell-derived factor 1) | CXCL12 | 203666_at | 3.9 |
| chemokine (C-X-C motif) ligand 5 | CXCL5 | 214974_x_at | 2.5 |
| chloride channel 4 | CLCN4 | 217556_at | 5.8 |
| chloride channel 4 | CLCN4 | 214769_at | 3.2 |
| chloride channel 4 | CLCN4 | 205149_s_at | 2.8 |
| chloride intracellular channel 3 | CLIC3 | 219529_at | -4.1 |
| chondroitin beta1,4 N-acetylgalactosaminyltransferase | ChGn | 219049_at | 2.5 |
| chondroitin sulfate proteoglycan 4 (melanoma-associated) | CSPG4 | 214297_at | -3.5 |
| cysteine and glycine-rich protein 2 | CSRP2 | 207030_s_at | -2.8 |
| cysteine and glycine-rich protein 2 | CSRP2 | 211126_s_at | -3.1 |
| cysteine-rich, angiogenic inducer, 61 | CYR61 | 210764_s_at | -3.1 |
| cytochrome P450, family 1, subfamily B, polypeptide 1 | CYP1B1 | 202434_s_at | 2.8 |
| cytochrome P450, family 1, subfamily B, polypeptide 1 | CYP1B1 | 202436_s_at | 2.5 |
| cytochrome P450, family 1, subfamily B, polypeptide 1 | CYP1B1 | 202437_s_at | 2.5 |
| cytochrome P450, family 7, subfamily B, polypeptide 1 | CYP7B1 | 207386_at | -3.6 |
| D site of albumin promoter (albumin D-box) binding protein | DBP | 209782_s_at | 8.3 |
| dapper homolog 1, antagonist of beta-catenin (xenopus) | DACT1 | 219179_at | -2.5 |
| dedicator of cytokinesis protein 10 | DOCK10 | 219279_at | -2.7 |
| desmoplakin | DSP | 200606_at | -3.0 |
| DnaJ (Hsp40) homolog, subfamily B, member 4 | DNAJB4 | 203811_s_at | -3.0 |
| dual specificity phosphatase 4 | DUSP4 | 204014_at | 2.5 |
| dual-specificity tyrosine-(Y)-phosphorylation regulated kinase 2 | DYRK2 | 202969_at | -2.7 |
| ecotropic viral integration site 2A | EVI2A | 204774_at | 3.5 |
| EH-domain containing 1 | EHD1 | 222221_x_at | -2.5 |
| enigma (LIM domain protein) | ENIGMA | 214266_s_at | -2.6 |
| eyes absent homolog 1 (Drosophila) | EYA1 | 214608_s_at | 2.7 |
| fascin homolog 1, actin-bundling protein (Strongylocentrotus purpuratus) | FSCN1 | 201564_s_at | -3.8 |
| fatty acid binding protein 4, adipocyte | FABP4 | 203980_at | 14.5 |
| fibroblast growth factor 1 (acidic) | FGF1 | 205117_at | -3.2 |
| flavoprotein oxidoreductase MICAL2 | MICAL2 | 212472_at | -2.9 |
| flavoprotein oxidoreductase MICAL2 | MICAL2 | 212473_s_at | -3.3 |
| fusion, derived from t(12;16) malignant liposarcoma | FUS | 200959_at | -2.5 |
| G protein-coupled receptor 49 | GPR49 | 213880_at | -34.1 |
| glutamine-fructose-6-phosphate transaminase 2 | GFPT2 | 205100_at | 2.5 |
| HCV NS3-transactivated protein 2 | NS3TP2 | 218706_s_at | -4.2 |
| hyaluronan synthase 2 | HAS2 | 206432_at | 3.0 |
| hydroxysteroid (11-beta) dehydrogenase 1 | HSD11B1 | 205404_at | 4.3 |
| hypothetical protein CG003 | 13CDNA73 | 204072_s_at | -3.0 |
| hypothetical protein LOC283824 | LOC283824 | 213725_x_at | 3.2 |
| hypothetical protein MGC2827 | MGC2827 | 219142_at | 3.0 |
| hypothetical protein MGC4655 | MGC4655 | 210933_s_at | -2.8 |
| inhibitor of DNA binding 2, dominant negative helix-loop-helix protein | ID2 | 201565_s_at | 2.8 |
| insulin-like growth factor 1 (somatomedin C) | IGF1 | 209540_at | 4.3 |
| insulin-like growth factor 1 (somatomedin C) | IGF1 | 209541_at | 2.8 |
| insulin-like growth factor 1 (somatomedin C) | IGF1 | 211577_s_at | 2.6 |
| insulin-like growth factor binding protein 1 | IGFBP1 | 205302_at | 2.5 |
| insulin-like growth factor binding protein 5 | IGFBP5 | 203424_s_at | 3.5 |
| insulin-like growth factor binding protein 5 | IGFBP5 | 211958_at | 3.5 |
| interleukin 6 (interferon, beta 2) | IL6 | 205207_at | -2.6 |
| interleukin 8 | IL8 | 202859_x_at | -3.1 |
| interleukin 8 | IL8 | 211506_s_at | -3.6 |
| jagged 1 (Alagille syndrome) | JAG1 | 216268_s_at | -2.5 |
| jagged 1 (Alagille syndrome) | JAG1 | 209098_s_at | -3.3 |
| KIAA0537 gene product | ARK5 | 204589_at | -3.6 |

| Gene name | Gene symbol | Affymetrix probe set ID | Fold change + 24 h |
|---|---|---|---|
| KIAA0626 gene product | KIAA0626 | 205442_at | -5.3 |
| KIAA1199 protein | KIAA1199 | 212942_s_at | -5.5 |
| Kruppel-like factor 2 (lung) | KLF2 | 219371_s_at | -3.2 |
| kruppel-like factor 6 | KLF6 | 208961_s_at | -2.6 |
| kruppel-like factor 6 | KLF6 | 208960_s_at | -3.1 |
| leptin (obesity homolog, mouse) | LEP | 207092_at | -4.4 |
| likely ortholog of mouse semaF cytoplasmic domain associated protein 3 | SEMACAP3 | 212915_at | 2.5 |
| LIM and cysteine-rich domains 1 | LMCD1 | 218574_s_at | -3.2 |
| LIM domain only 7 | LMO7 | 202674_s_at | -3.4 |
| LIM protein (similar to rat protein kinase C-binding enigma) | LIM | 203242_s_at | -2.5 |
| LIM protein (similar to rat protein kinase C-binding enigma) | LIM | 211681_s_at | -2.6 |
| LIM protein (similar to rat protein kinase C-binding enigma) | LIM | 216804_s_at | -2.7 |
| lipoprotein lipase | LPL | 203548_s_at | 3.6 |
| lipoprotein lipase | LPL | 203549_s_at | 3.1 |
| mannosidase, alpha, class 1C, member 1 | MAN1C1 | 218918_at | 2.7 |
| matrix metalloproteinase 1 (interstitial collagenase) | MMP1 | 204475_at | -5.0 |
| matrix metalloproteinase 13 (collagenase 3) | MMP13 | 205959_at | -3.2 |
| metastasis suppressor 1 | MTSS1 | 203037_s_at | -3.2 |
| midline 1 (Opitz/BBB syndrome) | MID1 | 203637_s_at | 2.8 |
| monocyte to macrophage differentiation-associated | MMD | 203414_at | 2.8 |
| myosin, heavy polypeptide 11, smooth muscle | MYH11 | 201497_x_at | -2.6 |
| natural killer cell transcript 4 | NK4 | 203828_s_at | -10.1 |
| neural precursor cell expressed, developmentally down-regulated 9 | NEDD9 | 202150_s_at | -3.0 |
| neurexin 3 | NRXN3 | 205795_at | -15.3 |
| nudix (nucleoside diphosphate linked moiety X)-type motif 13 | NUDT13 | 214136_at | 2.7 |
| odd-skipped-related 2A protein | OSR2 | 213568_at | 4.6 |
| oxytocin receptor | OXTR | 206825_at | -3.0 |
| perilipin | PLIN | 205913_at | 21.7 |
| phosphodiesterase 7B | PDE7B | 220343_at | 2.5 |
| phospholamban | PLN | 204939_s_at | -3.1 |
| phospholamban | PLN | 204938_s_at | -3.6 |
| phospholipase A2, group V | PLA2G5 | 215870_s_at | -2.9 |
| prostaglandin I2 (prostacyclin) synthase | PTGIS | 208131_s_at | -3.6 |
| protein tyrosine phosphatase, non-receptor type substrate 1 | PTPNS1 | 202897_at | -3.2 |
| PTPL1-associated RhoGAP 1 | PARG1 | 203910_at | -2.5 |
| putative lymphocyte G0/G1 switch gene | G0S2 | 213524_s_at | 9.6 |
| pyruvate dehydrogenase kinase, isoenzyme 4 | PDK4 | 205960_at | 3.3 |
| RAB3B, member RAS oncogene family | RAB3B | 205924_at | -3.8 |
| rab6 GTPase activating protein (GAP and centrosome-associated) | GAPCENA | 204028_s_at | -3.3 |
| rab6 GTPase activating protein (GAP and centrosome-associated) | GAPCENA | 213313_at | -3.6 |
| Ras association (RalGDS/AF-6) domain family 4 | RASSF4 | 49306_at | 4.6 |
| ras homolog gene family, member I | ARHI | 215506_s_at | 2.7 |
| regulator of G-protein signalling 4 | RGS4 | 204339_s_at | -4.1 |
| regulator of G-protein signalling 4 | RGS4 | 204338_s_at | -7.0 |
| regulator of G-protein signalling 4 | RGS4 | 204337_at | -7.7 |
| S100 calcium binding protein P | S100P | 204351_at | 5.2 |
| serine (or cysteine) proteinase inhibitor, clade E (nexin, plasminogen activator inhibitor type 1), member 1 | SERPINE1 | 202627_s_at | -2.6 |
| serine/threonine kinase 38 like | STK38L | 212572_at | -3.2 |
| serine/threonine kinase 38 like | STK38L | 212565_at | -3.3 |
| serum-inducible kinase | SNK | 201939_at | -2.8 |
| solute carrier family 16 (monocarboxylic acid transporters), member 7 | SLC16A7 | 207057_at | -3.3 |
| solute carrier family 20 (phosphate transporter), member 1 | SLC20A1 | 201920_at | -2.7 |
| solute carrier family 22 (organic cation transporter), member 4 | SLC22A4 | 205896_at | 2.7 |
| sortilin 1 | SORT1 | 212797_at | -2.6 |
| spermidine/spermine N1-acetyltransferase | SAT | 213988_s_at | 2.9 |
| spinocerebellar ataxia 1 (olivopontocerebellar ataxia 1, autosomal dominant, ataxin 1) | SCA1 | 203231_s_at | -2.6 |
| stanniocalcin 1 | STC1 | 204595_s_at | -2.5 |
| stanniocalcin 1 | STC1 | 204597_x_at | -3.2 |
| stanniocalcin 1 | STC1 | 204596_s_at | -4.4 |
| Traf2 and NCK interacting kinase | KIAA0551 | 213107_at | 6.3 |
| tropomyosin 1 (alpha) | TPM1 | 206116_s_at | -2.7 |
| tumor necrosis factor receptor superfamily, member 11b (osteoprotegerin) | TNFRSF11B | 204932_at | -2.9 |
| tumor necrosis factor receptor superfamily, member 11b (osteoprotegerin) | TNFRSF11B | 204933_s_at | -29.4 |
| tumor necrosis factor receptor superfamily, member 12A | TNFRSF12A | 218368_s_at | -4.0 |
| UDP-Gal:betaGlcNAc beta 1,3-galactosyltransferase, polypeptide 2 | B3GALT2 | 210121_at | -38.6 |
| UDP-Gal:betaGlcNAc beta 1,3-galactosyltransferase, polypeptide 2 | B3GALT2 | 217452_at | -50.6 |
| villin 2 (ezrin) | VIL2 | 208623_s_at | -2.7 |
| villin 2 (ezrin) | VIL2 | 208622_s_at | -3.3 |
| v-maf musculoaponeurotic fibrosarcoma oncogene homolog B (avian) | MAFB | 218559_s_at | 2.7 |

Fold change + 24 h = differential gene expression 24 h after initiation of transdifferentiation.

## 7.2 Fold changes of gene regulation after initiation of adipogenic and osteogenic transdifferentiation – GeneChips HG-U 133 Plus 2.0

**Tab. 14 Fold changes of gene expression 3 h after initiation of adipogenic transdifferentiation**

| Gene Title | Gene Symbol | Affymetrix Probe Set ID | + 3 h sample_array 1 versus control_array 1 [fold change] | + 3 h sample_array 2 versus control_array 2 [fold change] |
|---|---|---|---|---|
| --- | --- | 242856_at | 2.46 | 3.36 |
| --- | --- | 242228_at | -2.87 | -2.01 |
| ADP-ribosylation factor-like 7 | ARL7 | 202207_at | 2.39 | 5.03 |
| arginine vasopressin-induced 1 | AVPI1 | 218631_at | 2.31 | 4.03 |
| baculoviral IAP repeat-containing 3 | BIRC3 | 210538_s_at | -2.38 | -2.89 |
| BCL2-like 11 (apoptosis facilitator) | BCL2L11 | 225606_at | 2.16 | 4.11 |
| cAMP responsive element modulator | CREM | 214508_x_at | 3.23 | 3.05 |
| cAMP responsive element modulator | CREM | 209967_s_at | 4.00 | 3.43 |
| cAMP responsive element modulator | CREM | 207630_s_at | 2.87 | 3.03 |
| Cas-Br-M (murine) ecotropic retroviral transforming sequence b | CBLB | 227900_at | -2.20 | -2.28 |
| CDNA clone IMAGE:4514712, partial cds | --- | 225842_at | 3.39 | 2.93 |
| CDNA clone IMAGE:4514712, partial cds | --- | 217999_s_at | 2.68 | 2.55 |
| CDNA clone IMAGE:6025865, partial cds | --- | 212444_at | 4.38 | 17.88 |
| CDNA FLJ11397 fis, clone HEMBA1000622 | --- | 236251_at | -2.68 | -3.25 |
| CDNA FLJ11397 fis, clone HEMBA1000622 | --- | 232797_at | -2.35 | -4.29 |
| chemokine (C-C motif) ligand 20 | CCL20 | 205476_at | -2.75 | -2.83 |
| chemokine (C-C motif) ligand 3 /// chemokine (C-C motif) ligand 3-like 1 /// chemokine (C-C motif) ligand 3-like, centromeric | CCL3 /// CCL3L1 /// MGC12815 | 205114_s_at | -7.31 | -48.50 |
| chemokine (C-X-C motif) ligand 1 (melanoma growth stimulating activity, alpha) | CXCL1 | 204470_at | -2.10 | -5.28 |
| chromatin modifying protein 1B | CHMP1B | 218178_s_at | 3.41 | 3.10 |
| chromatin modifying protein 1B | CHMP1B | 218177_at | 4.14 | 2.46 |
| chromobox homolog 4 (Pc class homolog, Drosophila) | CBX4 | 227558_at | 2.08 | 5.13 |
| Chromodomain helicase DNA binding protein 1 | CHD1 | 235791_x_at | 2.17 | 2.01 |
| chromodomain helicase DNA binding protein 1 | CHD1 | 204258_at | 2.16 | 2.22 |
| chromosome 11 open reading frame 17 /// chromosome 11 open reading frame 17 /// likely ortholog of rat SNF1/AMP-activated protein kinase /// likely ortholog of rat SNF1/AMP-activated protein kinase | C11orf17 /// SNARK | 220987_s_at | -3.61 | -5.28 |
| chromosome 14 open reading frame 31 | C14orf31 | 225481_at | -2.06 | -3.29 |
| chromosome 8 open reading frame 13 | C8orf13 | 226614_s_at | 2.89 | 2.69 |
| cystathionase (cystathionine gamma-lyase) | CTH | 217127_at | 3.63 | 2.68 |
| cystathionase (cystathionine gamma-lyase) | CTH | 206085_s_at | 3.34 | 2.43 |
| cysteine-rich, angiogenic inducer, 61 | CYR61 | 210764_s_at | -3.78 | -3.81 |
| cysteine-rich, angiogenic inducer, 61 | CYR61 | 201289_at | -2.95 | -3.66 |
| distal-less homeo box 2 | DLX2 | 207147_at | 2.93 | 2.58 |
| distal-less homeo box 5 | DLX5 | 213707_s_at | 2.55 | 9.65 |
| DNA-damage-inducible transcript 4 | DDIT4 | 202887_s_at | 2.69 | 9.32 |
| DnaJ (Hsp40) homolog, subfamily B, member 4 | DNAJB4 | 203811_s_at | -2.53 | -2.06 |
| downregulated in ovarian cancer 1 | DOC1 | 204135_at | -5.28 | -6.63 |
| downregulated in ovarian cancer 1 | DOC1 | 1554966_a_at | -4.56 | -5.86 |
| dual specificity phosphatase 4 | DUSP4 | 204014_at | 3.43 | 3.12 |
| dual specificity phosphatase 6 | DUSP6 | 208892_s_at | -3.14 | -56.10 |
| dual specificity phosphatase 6 | DUSP6 | 208891_at | -4.47 | -24.42 |
| Dynamin 3 | DNM3 | 232090_at | -2.41 | -3.07 |
| early B-cell factor 3 | EBF3 | 227243_s_at | 2.64 | 2.55 |
| early B-cell factor 3 | EBF3 | 227242_s_at | 2.93 | 3.14 |
| early growth response 2 (Krox-20 homolog, Drosophila) | EGR2 | 205249_at | -4.23 | -7.26 |
| early growth response 3 | EGR3 | 206115_at | -3.39 | -2.04 |
| ectodermal-neural cortex (with BTB-like domain) | ENC1 | 201341_at | -2.22 | -3.86 |
| ectodermal-neural cortex (with BTB-like domain) | ENC1 | 201340_s_at | -3.46 | -4.29 |
| EPH receptor A2 | EPHA2 | 203499_at | 3.29 | 23.75 |
| EPH receptor B3 | EPHB3 | 1438_at | 3.51 | 11.00 |
| Fibroblast growth factor 18 | FGF18 | 231382_at | 2.33 | 4.82 |
| FLJ46041 protein | FLJ46041 | 1559263_s_at | -2.35 | -3.66 |
| formin 2 | FMN2 | 1555471_a_at | -11.96 | -4.53 |
| Full length insert cDNA clone YP08F12 | --- | 237031_at | 4.50 | 4.59 |
| FYVE, RhoGEF and PH domain containing 4 | FGD4 | 230559_x_at | -4.06 | -3.94 |
| FYVE, RhoGEF and PH domain containing 4 | FGD4 | 227948_at | -2.71 | -3.16 |
| G protein-coupled receptor 157 | GPR157 | 227970_at | 2.85 | 2.75 |
| G protein-coupled receptor, family C, group 5, member A | GPCR5A | 203108_at | 2.62 | 11.00 |
| glucocorticoid induced transcript 1 | GLCCI1 | 227525_at | 2.41 | 2.36 |

| Gene Title | Gene Symbol | Affymetrix Probe Set ID | + 3 h sample_array 1 versus control_array 1 [fold change] | + 3 h sample_array 2 versus control_array 2 [fold change] |
|---|---|---|---|---|
| glucocorticoid induced transcript 1 | GLCCI1 | 225706_at | 2.31 | 2.30 |
| growth arrest-specific 1 | GAS1 | 204456_s_at | 2.00 | 3.07 |
| H2.0-like homeo box 1 (Drosophila) | HLX1 | 214438_at | -2.20 | -2.36 |
| HCV NS3-transactivated protein 2 | NS3TP2 | 238049_at | -14.22 | -4.99 |
| high mobility group AT-hook 2 /// high mobility group AT-hook 2 | HMGA2 | 208025_s_at | -4.44 | -9.06 |
| Homo sapiens, clone IMAGE:3881549, mRNA | --- | 226034_at | 3.53 | 3.32 |
| Homo sapiens, clone IMAGE:4096273, mRNA | --- | 1555832_s_at | -2.19 | -2.10 |
| Homo sapiens, clone IMAGE:4794726, mRNA | --- | 226189_at | -2.53 | -4.72 |
| human immunodeficiency virus type I enhancer binding protein 1 | HIVEP1 | 204512_at | -2.55 | -2.81 |
| hyaluronan synthase 1 | HAS1 | 207316_at | 3.56 | 5.94 |
| hypothetical protein DKFZp434F0318 /// hypothetical protein DKFZp434F0318 | DKFZP434F0318 | 221031_s_at | 6.06 | 2.91 |
| Hypothetical protein FLJ13815 | FLJ13815 | 242245_at | -3.53 | -3.53 |
| Hypothetical protein FLJ25715 | FLJ25715 | 231952_at | 2.33 | 2.38 |
| hypothetical protein FLJ36031 | FLJ36031 | 229521_at | -3.05 | -6.23 |
| Hypothetical protein FLJ36031 | FLJ36031 | 226756_at | -2.81 | -6.77 |
| hypothetical protein LOC144347 | LOC144347 | 227320_at | -2.11 | -2.31 |
| hypothetical protein LOC157693 | LOC157693 | 1559141_s_at | 9.51 | 4.20 |
| hypothetical protein LOC157693 | LOC157693 | 1559140_at | 7.31 | 2.39 |
| inhibitor of DNA binding 2, dominant negative helix-loop-helix protein | ID2 | 201565_s_at | 2.14 | 4.23 |
| inhibitor of DNA binding 2, dominant negative helix-loop-helix protein /// inhibitor of DNA binding 2B, dominant negative helix-loop-helix protein | ID2 /// ID2B | 201566_x_at | 2.41 | 5.66 |
| Inhibitor of DNA binding 4, dominant negative helix-loop-helix protein | ID4 | 226933_s_at | 2.99 | 14.03 |
| inhibitor of DNA binding 4, dominant negative helix-loop-helix protein | ID4 | 209293_x_at | 3.73 | 11.47 |
| Inhibitor of DNA binding 4, dominant negative helix-loop-helix protein | ID4 | 209292_at | 4.99 | 7.84 |
| inhibitor of DNA binding 4, dominant negative helix-loop-helix protein | ID4 | 209291_at | 3.25 | 12.21 |
| intercellular adhesion molecule 1 (CD54), human rhinovirus receptor | ICAM1 | 202638_s_at | -2.69 | -2.19 |
| intercellular adhesion molecule 1 (CD54), human rhinovirus receptor | ICAM1 | 202637_s_at | -2.57 | -2.31 |
| interleukin 8 | IL8 | 211506_s_at | -2.36 | -7.26 |
| kelch-like 15 (Drosophila) | KLHL15 | 226370_at | 3.58 | 2.23 |
| keratin associated protein 1-1 /// keratin associated protein 1-1 | KRTAP1-1 | 220976_s_at | -3.36 | -10.56 |
| keratin associated protein 1-5 | KRTAP1-5 | 233533_at | -2.33 | -5.28 |
| keratin associated protein 2-1 /// keratin associated protein 2-4 | KRTAP2-1 /// KRTAP2-4 | 1555673_at | -5.10 | -4.32 |
| KIAA1726 protein | KIAA1726 | 231899_at | -2.62 | -4.11 |
| Kruppel-like factor 4 (gut) | KLF4 | 221841_s_at | 2.06 | 4.44 |
| Kruppel-like factor 4 (gut) | KLF4 | 220266_s_at | 3.18 | 3.27 |
| Kruppel-like factor 5 (intestinal) | KLF5 | 209211_at | -4.89 | -3.84 |
| Kruppel-like factor 6 | KLF6 | 208961_s_at | -2.03 | -2.11 |
| Kruppel-like factor 6 | KLF6 | 208960_s_at | -2.20 | -2.53 |
| Kruppel-like factor 7 (ubiquitous) | KLF7 | 204334_at | -2.71 | -2.16 |
| leucine-rich repeats and immunoglobulin-like domains 3 | LRIG3 | 226908_at | -2.04 | -3.61 |
| leukemia inhibitory factor (cholinergic differentiation factor) | LIF | 205266_at | -3.76 | -5.90 |
| LIM and senescent cell antigen-like domains 3 | LIMS3 | 223800_s_at | 2.46 | 2.14 |
| matrix metalloproteinase 1 (interstitial collagenase) | MMP1 | 204475_at | -3.78 | -3.63 |
| musculin (activated B-cell factor-1) | MSC | 209928_s_at | -2.87 | -5.06 |
| nuclear factor of activated T-cells, cytoplasmic, calcineurin-dependent 1 | NFATC1 | 211105_s_at | 2.85 | 2.60 |
| nuclear receptor subfamily 4, group A, member 1 | NR4A1 | 202340_x_at | 2.55 | 3.81 |
| nuclear receptor subfamily 4, group A, member 2 | NR4A2 | 216248_s_at | 9.25 | 15.78 |
| nuclear receptor subfamily 4, group A, member 2 | NR4A2 | 204622_x_at | 10.06 | 17.75 |
| nuclear receptor subfamily 4, group A, member 2 | NR4A2 | 204621_s_at | 8.40 | 15.24 |
| nuclear receptor subfamily 4, group A, member 3 | NR4A3 | 209959_at | 3.34 | 2.73 |
| nuclear receptor subfamily 4, group A, member 3 | NR4A3 | 207978_s_at | 3.46 | 3.20 |
| peptidylprolyl isomerase F (cyclophilin F) | PPIF | 201490_s_at | 2.31 | 2.43 |
| peptidylprolyl isomerase F (cyclophilin F) | PPIF | 201489_at | 2.08 | 2.27 |
| period homolog 1 (Drosophila) | PER1 | 202861_at | 3.10 | 4.69 |
| Phosphatidylinositol transfer protein, cytoplasmic 1 | PITPNC1 | 239808_at | 11.71 | 9.99 |
| phosphatidylinositol transfer protein, cytoplasmic 1 | PITPNC1 | 238649_at | 2.91 | 7.41 |
| phosphatidylinositol transfer protein, cytoplasmic 1 | PITPNC1 | 219155_at | 2.16 | 4.32 |
| phosphodiesterase 4B, cAMP-specific (phosphodiesterase E4 dunce homolog, Drosophila) | PDE4B | 203708_at | 3.53 | 6.32 |
| phosphodiesterase 4D, cAMP-specific | PDE4D | 210837_s_at | 2.03 | 11.63 |

| Gene Title | Gene Symbol | Affymetrix Probe Set ID | + 3 h sample_array 1 versus control_array 1 [fold change] | + 3 h sample_array 2 versus control_array 2 [fold change] |
|---|---|---|---|---|
| (phosphodiesterase E3 dunce homolog, Drosophila) | | | | |
| Phosphodiesterase 4D, cAMP-specific (phosphodiesterase E3 dunce homolog, Drosophila) | PDE4D | 204491_at | 4.03 | 30.91 |
| phosphoinositide-3-kinase, regulatory subunit 3 (p55, gamma) | PIK3R3 | 202743_at | 2.58 | 3.58 |
| Potassium voltage-gated channel, Isk-related family, member 4 | KCNE4 | 222379_at | 4.69 | 7.11 |
| potassium voltage-gated channel, Isk-related family, member 4 | KCNE4 | 1552508_at | 6.06 | 8.82 |
| potassium voltage-gated channel, Isk-related family, member 4 | KCNE4 | 1552507_at | 4.82 | 7.01 |
| prostaglandin E receptor 4 (subtype EP4) | PTGER4 | 204897_at | -5.58 | -6.96 |
| RAB20, member RAS oncogene family | RAB20 | 219622_at | 3.68 | 7.06 |
| RAS, dexamethasone-induced 1 | RASD1 | 223467_at | 3.41 | 16.11 |
| regulator of G-protein signalling 2, 24kDa | RGS2 | 202388_at | 6.11 | 10.34 |
| RGM domain family, member B | RGMB | 227339_at | -3.14 | -3.16 |
| Runt-related transcription factor 1; translocated to, 1 (cyclin D-related) | RUNX1T1 | 228827_at | -2.07 | -2.27 |
| sema domain, immunoglobulin domain (Ig), transmembrane domain (TM) and short cytoplasmic domain, (semaphorin) 4C | SEMA4C | 46665_at | 2.93 | 4.59 |
| serine (or cysteine) proteinase inhibitor, clade B (ovalbumin), member 2 | SERPINB2 | 204614_at | -3.18 | -23.75 |
| serine (or cysteine) proteinase inhibitor, clade E (nexin, plasminogen activator inhibitor type 1), member 1 | SERPINE1 | 1568765_at | -3.73 | -2.30 |
| serine/threonine kinase 38 like | STK38L | 212572_at | -3.56 | -2.41 |
| Shroom-related protein | ShrmL | 225548_at | -2.27 | -2.53 |
| sine oculis homeobox homolog 2 (Drosophila) | SIX2 | 206510_at | 2.48 | 2.91 |
| SNF1-like kinase /// SNF1-like kinase | SNF1LK | 208078_s_at | 6.41 | 11.24 |
| solute carrier family 19 (thiamine transporter), member 2 | SLC19A2 | 209681_at | 2.06 | 2.85 |
| solute carrier family 2 (facilitated glucose transporter), member 3 | SLC2A3 | 202499_s_at | 4.86 | 3.41 |
| solute carrier family 2 (facilitated glucose transporter), member 3 | SLC2A3 | 202498_s_at | 3.51 | 3.25 |
| solute carrier family 2 (facilitated glucose transporter), member 3 | SLC2A3 | 202497_x_at | 2.87 | 2.87 |
| solute carrier family 2 (facilitated glucose transporter), member 3 /// solute carrier family 2 (facilitated glucose transporter), member 14 | SLC2A3 /// SLC2A14 | 222088_s_at | 4.08 | 3.29 |
| solute carrier family 2 (facilitated glucose transporter), member 3 /// solute carrier family 2 (facilitated glucose transporter), member 14 | SLC2A3 /// SLC2A14 | 216236_s_at | 2.85 | 2.85 |
| solute carrier family 7 (cationic amino acid transporter, y+ system), member 5 | SLC7A5 | 201195_s_at | 2.64 | 4.53 |
| ST3 beta-galactoside alpha-2,3-sialyltransferase 5 | ST3GAL5 | 203217_s_at | 2.43 | 2.85 |
| TGFB-induced factor (TALE family homeobox) | TGIF | 203313_s_at | 2.19 | 3.97 |
| toll-like receptor 4 | TLR4 | 232068_s_at | -4.26 | -10.70 |
| toll-like receptor 4 /// toll-like receptor 4 | TLR4 | 224341_x_at | -2.79 | -4.69 |
| toll-like receptor 4 /// toll-like receptor 4 | TLR4 | 221060_at | -2.10 | -2.95 |
| Transcribed locus | --- | 241470_x_at | -23.43 | -9.00 |
| Transcribed locus, weakly similar to XP_548293.1 similar to Flotillin-2 (Reggie-1) (REG-1) [Canis familiaris] | --- | 240432_x_at | -2.75 | -2.79 |
| transducer of ERBB2, 1 | TOB1 | 228834_at | 2.20 | 4.50 |
| transmembrane protein 46 | TMEM46 | 230493_at | 4.53 | 6.06 |
| tumor necrosis factor receptor superfamily, member 1B | TNFRSF1B | 203508_at | 2.79 | 4.63 |
| tumor necrosis factor, alpha-induced protein 8 | TNFAIP8 | 210260_s_at | -2.85 | -3.68 |
| tumor necrosis factor, alpha-induced protein 8 | TNFAIP8 | 208296_x_at | -2.73 | -3.18 |
| vascular endothelial growth factor | VEGF | 211527_x_at | 2.01 | 2.17 |
| v-ets erythroblastosis virus E26 oncogene homolog 1 (avian) | ETS1 | 224833_at | -2.08 | -2.06 |
| zinc finger protein 217 | ZNF217 | 203739_at | -2.25 | -5.90 |
| zinc finger protein 281 | ZNF281 | 228785_at | -2.03 | -4.76 |
| zinc finger protein 295 | ZNF295 | 225539_at | -2.27 | -2.25 |
| zinc finger protein 331 | ZNF331 | 227613_at | 11.55 | 9.19 |
| zinc finger protein 331 | ZNF331 | 219228_at | 9.65 | 7.94 |

Transdifferentiated samples were compared to differentiated controls. Fold changes for transcripts with reproducible regulation directions regarding two different MSC charges (array 1 and array 2) are listed by gene name. + 3 h = 3 h after initiation of adipogenic transdifferentiation.

**Tab. 15 Fold changes of gene expression 24 h after initiation of adipogenic transdifferentiation**

| Gene title | Gene symbol | Affymetrix probe set ID | + 24 h sample_array 1 versus control_array 1 [fold change] | + 24 h sample_array 2 versus control_array 2 [fold change] |
|---|---|---|---|---|
| --- | --- | 225207_at | 7.94 | 8.40 |
| --- | --- | 231075_x_at | -2.10 | -2.10 |
| --- | --- | 229669_at | -6.15 | -3.97 |
| --- | --- | 227088_at | -2.19 | -4.08 |
| --- | --- | 224929_at | -2.43 | -2.99 |
| --- | --- | 212565_at | -2.73 | -2.17 |
| acetyl-Coenzyme A carboxylase beta | ACACB | 49452_at | 5.31 | 5.31 |
| acetyl-Coenzyme A carboxylase beta | ACACB | 43427_at | 4.14 | 5.17 |
| actin, alpha, cardiac muscle | ACTC | 205132_at | -5.17 | -6.68 |
| actin, gamma 2, smooth muscle, enteric | ACTG2 | 202274_at | -3.01 | -3.48 |
| adenomatosis polyposis coli down-regulated 1 | APCDD1 | 225016_at | 3.81 | 2.39 |
| adenosine deaminase | ADA | 204639_at | 2.16 | 4.63 |
| adenylate cyclase 7 | ADCY7 | 203741_s_at | -2.11 | -2.85 |
| ADP-ribosylation factor-like 7 | ARL7 | 202208_at | 2.81 | 6.77 |
| ADP-ribosylation factor-like 7 | ARL7 | 202207_at | 3.51 | 5.06 |
| ADP-ribosylation factor-like 7 | ARL7 | 202206_at | 3.07 | 5.54 |
| aggrecan 1 (chondroitin sulfate proteoglycan 1, large aggregating proteoglycan, antigen identified by monoclonal antibody A0122) | AGC1 | 207692_s_at | -2.08 | -2.35 |
| AHNAK nucleoprotein (desmoyokin) | AHNAK | 235281_x_at | -2.28 | -2.46 |
| aldehyde dehydrogenase 1 family, member B1 | ALDH1B1 | 209646_x_at | -3.43 | -6.28 |
| aldehyde dehydrogenase 1 family, member B1 | ALDH1B1 | 209645_s_at | -5.82 | -7.36 |
| aldehyde dehydrogenase 2 family (mitochondrial) | ALDH2 | 201425_at | 3.14 | 2.55 |
| aldo-keto reductase family 1, member C2 (dihydrodiol dehydrogenase 2; bile acid binding protein; 3-alpha hydroxysteroid dehydrogenase, type III) | AKR1C2 | 209699_x_at | 2.13 | 2.03 |
| Aldo-keto reductase family 1, member C2 (dihydrodiol dehydrogenase 2; bile acid binding protein; 3-alpha hydroxysteroid dehydrogenase, type III) | AKR1C2 | 1555854_at | 2.89 | 20.39 |
| aldo-keto reductase family 1, member C2 (dihydrodiol dehydrogenase 2; bile acid binding protein; 3-alpha hydroxysteroid dehydrogenase, type III) /// aldo-keto reductase family 1, member C2 (dihydrodiol dehydrogenase 2; bile acid binding protein; 3-alpha hydroxysteroid dehydrogenase, type III) | AKR1C2 | 211653_x_at | 2.31 | 2.10 |
| aldo-keto reductase family 1, member C3 (3-alpha hydroxysteroid dehydrogenase, type II) | AKR1C3 | 209160_at | 2.39 | 2.46 |
| alpha-kinase 2 | ALPK2 | 228367_at | -2.17 | -6.77 |
| amphoterin induced gene 2 | AMIGO2 | 222108_at | -4.44 | -2.66 |
| amyotrophic lateral sclerosis 2 (juvenile) chromosome region, candidate 13 | ALS2CR13 | 226431_at | 2.07 | 2.28 |
| angiopoietin-like 2 | ANGPTL2 | 213004_at | 2.51 | 2.46 |
| angiopoietin-like 2 | ANGPTL2 | 213001_at | 2.55 | 2.81 |
| ankyrin repeat domain 1 (cardiac muscle) | ANKRD1 | 206029_at | -6.36 | -20.82 |
| arrestin domain containing 3 | ARRDC3 | 224797_at | 3.03 | 4.56 |
| aryl-hydrocarbon receptor nuclear translocator 2 | ARNT2 | 202986_at | -2.51 | -3.81 |
| ATPase, Class I, type 8B, member 1 | ATP8B1 | 226302_at | -5.35 | -4.06 |
| ATP-binding cassette, sub-family A (ABC1), member 1 | ABCA1 | 203505_at | 3.66 | 4.26 |
| ATP-binding cassette, sub-family A (ABC1), member 1 | ABCA1 | 203504_s_at | 3.41 | 4.26 |
| atrophin-1 interacting protein 1 | AIP1 | 209737_at | -3.39 | -3.20 |
| atrophin-1 interacting protein 1 | AIP1 | 207702_s_at | -5.50 | -11.79 |
| basic helix-loop-helix domain containing, class B, 3 | BHLHB3 | 221530_s_at | 4.66 | 15.14 |
| BCL2-like 11 (apoptosis facilitator) | BCL2L11 | 225606_at | 3.76 | 6.06 |
| beta 3-glycosyltransferase-like | B3GTL | 227083_at | -2.27 | -2.10 |
| BMP-binding endothelial regulator precursor protein | BMPER | 241986_at | 2.64 | 2.14 |
| brain-derived neurotrophic factor | BDNF | 206382_s_at | -2.14 | -4.69 |
| brother of CDO | BOC | 225990_at | 3.73 | 3.66 |
| brother of CDO | BOC | 224184_s_at | 4.72 | 3.20 |
| caldesmon 1 | CALD1 | 201615_x_at | -2.31 | -3.20 |
| calponin 1, basic, smooth muscle | CNN1 | 203951_at | -3.12 | -6.06 |
| CAP, adenylate cyclase-associated protein, 2 (yeast) | CAP2 | 212554_at | -2.73 | -2.10 |
| carbohydrate (N-acetylglucosamine 6-O) sulfotransferase 7 | CHST7 | 206756_at | 2.17 | 2.16 |
| carboxypeptidase M | CPM | 243403_x_at | -2.60 | -4.44 |
| carboxypeptidase M | CPM | 241765_at | -3.34 | -3.05 |
| carboxypeptidase M | CPM | 235706_at | -3.03 | -3.23 |
| carboxypeptidase M | CPM | 235019_at | -2.81 | -3.94 |
| carboxypeptidase M | CPM | 206100_at | -2.28 | -2.91 |
| catenin (cadherin-associated protein), alpha-like 1 | CTNNAL1 | 202468_s_at | -2.60 | -4.06 |
| Cbl-interacting protein Sts-1 | STS-1 | 238462_at | -2.25 | -3.10 |
| CCAAT/enhancer binding protein (C/EBP), alpha | CEBPA | 204039_at | 5.62 | 24.93 |
| CD24 antigen (small cell lung carcinoma cluster 4 | CD24 | 209772_s_at | -2.46 | -2.11 |

| Gene title | Gene symbol | Affymetrix probe set ID | + 24 h sample_array 1 versus control_array 1 [fold change] | + 24 h sample_array 2 versus control_array 2 [fold change] |
|---|---|---|---|---|
| antigen) | | | | |
| CD97 antigen | CD97 | 202910_s_at | -2.11 | -2.28 |
| CDC14 cell division cycle 14 homolog B (S. cerevisiae) /// CDC14 cell division cycle 14 homolog B (S. cerevisiae) | CDC14B | 208022_s_at | -2.11 | -2.19 |
| CDNA FLJ10145 fis, clone HEMBA1003322 | --- | 232795_at | -3.29 | -2.57 |
| CDNA FLJ10145 fis, clone HEMBA1003322 | --- | 1557286_at | -5.28 | -3.86 |
| CDNA FLJ14392 fis, clone HEMBA1003166 | --- | 239866_at | 2.41 | 4.32 |
| CDNA FLJ26242 fis, clone DMC00770 | --- | 239262_at | 2.00 | 2.30 |
| CDNA FLJ34013 fis, clone FCBBF2002111 | --- | 225710_at | -2.23 | -3.23 |
| CDNA FLJ90295 fis, clone NT2RP2000240. | --- | 229190_at | 2.25 | 2.17 |
| CDNA: FLJ22256 fis, clone HRC02860 | --- | 233814_at | 2.14 | 2.64 |
| cell adhesion molecule with homology to L1CAM (close homolog of L1) | CHL1 | 204591_at | 5.03 | 3.51 |
| chemokine (C-X3-C motif) ligand 1 | CX3CL1 | 823_at | -2.19 | -2.57 |
| chemokine (C-X-C motif) ligand 12 (stromal cell-derived factor 1) | CXCL12 | 209687_at | 2.16 | 2.01 |
| chemokine (C-X-C motif) ligand 12 (stromal cell-derived factor 1) | CXCL12 | 203666_at | 3.76 | 2.89 |
| chemokine (C-X-C motif) ligand 13 (B-cell chemoattractant) | CXCL13 | 205242_at | 2.60 | 3.05 |
| chemokine orphan receptor 1 | CMKOR1 | 212977_at | 2.60 | 5.10 |
| chemokine-like factor super family 8 | CKLFSF8 | 235099_at | 2.93 | 3.10 |
| Chloride channel 4 | CLCN4 | 214769_at | 4.26 | 3.97 |
| chloride channel 4 | CLCN4 | 205148_s_at | 2.43 | 2.39 |
| chloride intracellular channel 3 | CLIC3 | 219529_at | -4.56 | -4.35 |
| cholesterol 25-hydroxylase | CH25H | 206932_at | 2.25 | 2.38 |
| chondroitin beta1,4 N-acetylgalactosaminyltransferase | ChGn | 219049_at | 2.55 | 3.27 |
| Chondroitin sulfate proteoglycan 4 (melanoma-associated) | CSPG4 | 214297_at | -3.71 | -7.11 |
| chondroitin sulfate proteoglycan 4 (melanoma-associated) | CSPG4 | 204736_s_at | -2.77 | -3.43 |
| chromatin modifying protein 1B | CHMP1B | 218177_at | 2.00 | 2.30 |
| Chromobox homolog 5 (HP1 alpha homolog, Drosophila) | CBX5 | 231862_at | -2.27 | -2.10 |
| chromosome 10 open reading frame 48 | C10orf48 | 241902_at | -2.95 | -2.81 |
| chromosome 10 open reading frame 48 | C10orf48 | 239468_at | -2.71 | -3.56 |
| chromosome 5 open reading frame 13 | C5orf13 | 201309_x_at | -2.11 | -3.71 |
| chromosome 5 open reading frame 4 | C5orf4 | 220751_s_at | 2.89 | 2.14 |
| Chromosome 6 open reading frame 188 | C6orf188 | 232217_at | -2.43 | -2.28 |
| Chromosome 6 open reading frame 188 | C6orf188 | 230254_at | -2.19 | -2.39 |
| chromosome 6 open reading frame 32 | C6orf32 | 209829_at | 2.27 | 3.36 |
| chromosome 6 open reading frame 85 | C6orf85 | 223194_s_at | 4.32 | 6.68 |
| clathrin, heavy polypeptide-like 1 | CLTCL1 | 205944_s_at | -2.46 | -4.26 |
| COBL-like 1 | COBLL1 | 203642_s_at | -2.58 | -3.05 |
| cofilin 2 (muscle) /// cofilin 2 (muscle) | CFL2 | 224352_s_at | -2.01 | -2.16 |
| coiled-coil domain containing 3 | CCDC3 | 223316_at | -2.04 | -3.03 |
| collagen, type XIII, alpha 1 | COL13A1 | 211343_s_at | -2.38 | -2.91 |
| collomin | COLM | 230360_at | -4.63 | -2.11 |
| cysteine-rich, angiogenic inducer, 61 | CYR61 | 210764_s_at | -2.87 | -24.25 |
| cytidine monophosphate-N-acetylneuraminic acid hydroxylase (CMP-N-acetylneuraminate monooxygenase) | CMAH | 205518_s_at | -2.17 | -3.01 |
| cytochrome P450, family 1, subfamily B, polypeptide 1 | CYP1B1 | 202436_s_at | 2.33 | 2.06 |
| cytochrome P450, family 1, subfamily B, polypeptide 1 | CYP1B1 | 202435_s_at | 2.48 | 2.38 |
| cytochrome P450, family 1, subfamily B, polypeptide 1 | CYP1B1 | 202434_s_at | 2.77 | 2.66 |
| cytochrome P450, family 19, subfamily A, polypeptide 1 | CYP19A1 | 203475_at | -3.12 | -2.31 |
| cytochrome P450, family 7, subfamily B, polypeptide 1 | CYP7B1 | 207386_at | -2.58 | -4.41 |
| dedicator of cytokinesis 10 | DOCK10 | 219279_at | -3.10 | -2.51 |
| dehydrogenase/reductase (SDR family) member 3 | DHRS3 | 202481_at | 2.31 | 2.39 |
| deleted in bladder cancer 1 | DBC1 | 205818_at | 2.77 | 8.75 |
| desmoplakin | DSP | 200606_at | -3.03 | -5.03 |
| diaphanous homolog 1 (Drosophila) | DIAPH1 | 209190_s_at | -2.27 | -2.23 |
| diaphanous homolog 2 (Drosophila) | DIAPH2 | 205603_s_at | -2.51 | -3.61 |
| dimethylarginine dimethylaminohydrolase 1 | DDAH1 | 1553565_s_at | -4.79 | -8.75 |
| DIRAS family, GTP-binding RAS-like 3 | DIRAS3 | 215506_s_at | 2.45 | 3.05 |
| DKFZP434C171 protein | DKFZP434C171 | 212886_at | 2.97 | 3.36 |
| DKFZP434C171 protein | DKFZP434C171 | 1553102_a_at | 2.81 | 3.46 |
| DKFZP564J0863 protein | DKFZP564J0863 | 223453_s_at | -2.35 | -2.14 |
| DNA-damage-inducible transcript 4-like | DDIT4L | 228057_at | 3.20 | 3.89 |
| DnaJ (Hsp40) homolog, subfamily B, member 4 | DNAJB4 | 203811_s_at | -3.58 | -3.39 |
| DnaJ (Hsp40) homolog, subfamily B, member 4 | DNAJB4 | 203810_at | -2.69 | -3.27 |
| Down syndrome critical region gene 1-like 1 | DSCR1L1 | 203498_at | -2.89 | -2.03 |
| downregulated in ovarian cancer 1 | DOC1 | 1554966_a_at | -4.72 | -2.93 |

| Gene title | Gene symbol | Affymetrix probe set ID | + 24 h sample_array 1 versus control_array 1 [fold change] | + 24 h sample_array 2 versus control_array 2 [fold change] |
|---|---|---|---|---|
| dual specificity phosphatase 5 | DUSP5 | 209457_at | -2.91 | -3.56 |
| Dual specificity phosphatase 7 | DUSP7 | 213848_at | -2.10 | -2.48 |
| dystrophia myotonica-protein kinase | DMPK | 37996_s_at | -3.39 | -2.93 |
| early B-cell factor | EBF | 232204_at | 2.57 | 2.25 |
| Early B-cell factor | EBF | 227646_at | 2.39 | 2.13 |
| ecotropic viral integration site 2A | EVI2A | 204774_at | 3.10 | 2.83 |
| EH domain binding protein 1-like 1 | EHBP1L1 | 221755_at | -2.77 | -12.21 |
| EH-domain containing 4 | EHD4 | 229074_at | -2.33 | -2.73 |
| EH-domain containing 4 | EHD4 | 209536_s_at | -3.20 | -2.83 |
| enabled homolog (Drosophila) | ENAH | 222434_at | -2.30 | -2.64 |
| endothelial cell growth factor 1 (platelet-derived) | ECGF1 | 204858_s_at | -2.11 | -2.38 |
| endothelial differentiation, sphingolipid G-protein-coupled receptor, 3 | EDG3 | 231741_at | 2.13 | 7.01 |
| endothelial differentiation, sphingolipid G-protein-coupled receptor, 3 | EDG3 | 228176_at | 3.86 | 20.53 |
| eyes absent homolog 1 (Drosophila) | EYA1 | 214608_s_at | 2.97 | 4.17 |
| family with sequence similarity 13, member C1 | FAM13C1 | 1554547_at | 6.77 | 3.01 |
| Family with sequence similarity 20, member A | FAM20A | 243221_at | 2.11 | 2.71 |
| family with sequence similarity 20, member A | FAM20A | 242945_at | 2.01 | 2.71 |
| family with sequence similarity 20, member A | FAM20A | 226804_at | 2.31 | 3.39 |
| family with sequence similarity 43, member A | FAM43A | 227410_at | 4.03 | 4.99 |
| fascin homolog 1, actin-bundling protein (Strongylocentrotus purpuratus) | FSCN1 | 201564_s_at | -2.28 | -3.48 |
| fatty acid binding protein 4, adipocyte | FABP4 | 203980_at | 19.97 | 62.25 |
| fatty acid binding protein 5 (psoriasis-associated) | FABP5 | 202345_s_at | 2.25 | 2.35 |
| FCH and double SH3 domains 2 | FCHSD2 | 203620_s_at | -2.06 | -2.11 |
| fibroblast growth factor 1 (acidic) | FGF1 | 208240_s_at | -2.66 | -6.02 |
| fibroblast growth factor 1 (acidic) | FGF1 | 205117_at | -3.20 | -7.26 |
| fibroblast growth factor 1 (acidic) | FGF1 | 1552721_a_at | -3.97 | -9.58 |
| fibroblast growth factor 2 (basic) | FGF2 | 204421_s_at | -2.55 | -2.55 |
| fibroblast growth factor 5 | FGF5 | 208378_x_at | -5.70 | -2.03 |
| Fibronectin 1 | FN1 | 235629_at | -3.84 | -2.77 |
| fibronectin 1 | FN1 | 1558199_at | -2.14 | -3.76 |
| filamin-binding LIM protein-1 | FBLP-1 | 1555480_a_at | -2.43 | -2.77 |
| FLJ46041 protein | FLJ46041 | 1559263_s_at | -3.05 | -3.01 |
| formin 2 | FMN2 | 223618_at | -2.36 | -6.96 |
| formin 2 | FMN2 | 1555471_a_at | -9.19 | -6.73 |
| FOS-like antigen 1 | FOSL1 | 204420_at | -2.60 | -2.48 |
| frizzled homolog 4 (Drosophila) | FZD4 | 218665_at | 2.07 | 2.91 |
| Full open reading frame cDNA clone RZPDo834C0824D for gene HIST2H4, histone 2, H4; complete cds, incl. stopcodon | --- | 230795_at | 2.91 | 8.75 |
| FYVE, RhoGEF and PH domain containing 4 | FGD4 | 242445_at | -2.75 | -4.41 |
| FYVE, RhoGEF and PH domain containing 4 | FGD4 | 230559_x_at | -2.79 | -2.36 |
| FYVE, RhoGEF and PH domain containing 4 | FGD4 | 227948_at | -4.59 | -3.20 |
| glia maturation factor, gamma | GMFG | 204220_at | -2.03 | -2.17 |
| glucosaminyl (N-acetyl) transferase 1, core 2 (beta-1,6-N-acetylglucosaminyltransferase) | GCNT1 | 239761_at | -2.17 | -2.57 |
| glutaminase | GLS | 223079_s_at | -3.53 | -4.11 |
| glutaminase | GLS | 221510_s_at | -2.41 | -3.05 |
| glutamine-fructose-6-phosphate transaminase 2 | GFPT2 | 205100_at | 2.45 | 3.01 |
| guanine nucleotide binding protein (G protein), beta polypeptide 4 | GNB4 | 223487_x_at | -2.87 | -3.16 |
| guanylate binding protein 1, interferon-inducible, 67kDa | GBP1 | 231577_s_at | -2.27 | -2.79 |
| HCV NS3-transactivated protein 2 | NS3TP2 | 218706_s_at | -4.47 | -3.94 |
| heat shock 27kDa protein 2 | HSPB2 | 205824_at | -2.27 | -3.10 |
| heat shock 27kDa protein family, member 7 (cardiovascular) | HSPB7 | 218934_s_at | -3.25 | -2.28 |
| heme oxygenase (decycling) 1 | HMOX1 | 203665_at | 2.30 | 12.04 |
| hexokinase 2 | HK2 | 202934_at | 2.73 | 3.94 |
| high mobility group AT-hook 2 /// high mobility group AT-hook 2 | HMGA2 | 208025_s_at | -2.07 | -2.77 |
| histone 1, H2ac | HIST1H2AC | 215071_s_at | 2.14 | 7.06 |
| histone 1, H2bd | HIST1H2BD | 209911_x_at | 2.11 | 2.77 |
| histone deacetylase 9 | HDAC9 | 205659_at | -9.45 | -8.88 |
| homeodomain-only protein /// homeodomain-only protein | HOP | 211597_s_at | -2.91 | -3.61 |
| Homo sapiens, clone IMAGE:4096273, mRNA | --- | 224606_at | -2.03 | -2.93 |
| Homo sapiens, clone IMAGE:4454331, mRNA | --- | 227396_at | -2.11 | -3.23 |
| Homo sapiens, clone IMAGE:5309572, mRNA | --- | 238463_at | 2.10 | 2.20 |
| hyaluronan synthase 3 | HAS3 | 223541_at | -3.53 | -4.03 |
| hydroxysteroid (11-beta) dehydrogenase 1 | HSD11B1 | 205404_at | 4.17 | 2.62 |
| Hypothetical gene supported by BC008048 | --- | 238727_at | 3.78 | 2.36 |
| hypothetical protein CG003 | 13CDNA73 | 204072_s_at | -2.53 | -2.85 |

| Gene title | Gene symbol | Affymetrix probe set ID | + 24 h sample_array 1 versus control_array 1 [fold change] | + 24 h sample_array 2 versus control_array 2 [fold change] |
|---|---|---|---|---|
| Hypothetical protein DKFZp434D2328 | LOC91526 | 226641_at | -2.31 | -2.79 |
| hypothetical protein FLJ10159 | FLJ10159 | 218974_at | 2.31 | 4.14 |
| hypothetical protein FLJ11000 | FLJ11000 | 218999_at | 2.48 | 2.64 |
| hypothetical protein FLJ13391 | FLJ13391 | 227828_s_at | -2.75 | -3.68 |
| hypothetical protein FLJ20010 | FLJ20010 | 218789_s_at | 2.04 | 2.87 |
| hypothetical protein FLJ20152 | FLJ20152 | 218532_s_at | 2.23 | 4.00 |
| hypothetical protein FLJ21062 | FLJ21062 | 1554919_s_at | 3.76 | 3.23 |
| hypothetical protein FLJ21986 | FLJ21986 | 228728_at | -3.61 | -3.92 |
| hypothetical protein FLJ21986 | FLJ21986 | 220032_at | -2.55 | -2.00 |
| hypothetical protein FLJ23322 | FLJ23322 | 231846_at | 2.10 | 3.84 |
| Hypothetical protein FLJ36031 | FLJ36031 | 226756_at | -2.22 | -2.23 |
| hypothetical protein LOC144347 | LOC144347 | 227320_at | -3.03 | -2.87 |
| hypothetical protein LOC253981 | LOC253981 | 226430_at | 2.16 | 2.85 |
| hypothetical protein LOC283824 | LOC283824 | 213725_x_at | 2.83 | 2.79 |
| hypothetical protein LOC340061 | LOC340061 | 224916_at | -2.95 | -2.36 |
| hypothetical protein LOC54103 | LOC54103 | 213142_x_at | -2.45 | -3.48 |
| hypothetical protein MGC26963 | MGC26963 | 242963_at | -2.85 | -2.28 |
| hypothetical protein MGC26963 | MGC26963 | 227038_at | -2.39 | -2.58 |
| hypothetical protein MGC45780 | MGC45780 | 235849_at | 7.57 | 8.11 |
| Hypothetical protein MGC45780 | MGC45780 | 229839_at | 8.22 | 13.93 |
| hypothetical protein MGC48998 | MGC48998 | 1554960_at | -2.20 | -24.76 |
| IBR domain containing 2 | IBRDC2 | 228153_at | -2.89 | -2.85 |
| immediate early response 2 | IER2 | 202081_at | -2.41 | -2.43 |
| inositol polyphosphate-4-phosphatase, type II, 105kDa | INPP4B | 205376_at | -2.08 | -3.56 |
| insulin-like growth factor 1 (somatomedin C) | IGF1 | 211577_at | 2.75 | 5.10 |
| insulin-like growth factor 1 (somatomedin C) | IGF1 | 209542_x_at | 2.81 | 17.39 |
| insulin-like growth factor 1 (somatomedin C) | IGF1 | 209541_at | 2.79 | 7.21 |
| insulin-like growth factor 1 (somatomedin C) | IGF1 | 209540_at | 4.03 | 8.34 |
| insulin-like growth factor binding protein 5 | IGFBP5 | 211959_at | 2.87 | 33.82 |
| insulin-like growth factor binding protein 5 | IGFBP5 | 211958_at | 4.20 | 10.27 |
| insulin-like growth factor binding protein 5 | IGFBP5 | 203424_s_at | 5.03 | 13.74 |
| insulin-like growth factor binding protein 5 | IGFBP5 | 1555997_s_at | 2.99 | 13.09 |
| interleukin 1 receptor-like 1 | IL1RL1 | 207526_s_at | -2.00 | -2.25 |
| interleukin 27 receptor, alpha | IL27RA | 222062_at | -11.63 | -7.94 |
| interleukin 32 /// interleukin 32 | IL32 | 203828_s_at | -5.13 | -5.66 |
| interleukin 8 | IL8 | 211506_s_at | -3.92 | -2.38 |
| Jagged 1 (Alagille syndrome) | JAG1 | 231183_s_at | -2.36 | -6.45 |
| jagged 1 (Alagille syndrome) | JAG1 | 216268_s_at | -2.48 | -8.82 |
| jagged 1 (Alagille syndrome) | JAG1 | 209099_x_at | -2.41 | -9.00 |
| jagged 1 (Alagille syndrome) | JAG1 | 209098_s_at | -2.83 | -9.45 |
| junctophilin 2 | JPH2 | 229578_at | -2.62 | -11.31 |
| kelch repeat and BTB (POZ) domain containing 2 | KBTBD2 | 234233_s_at | -2.03 | -3.43 |
| keratin 7 | KRT7 | 209016_s_at | -2.07 | -2.73 |
| keratin associated protein 1-5 | KRTAP1-5 | 233533_at | -5.39 | -44.32 |
| keratin associated protein 2-1 /// keratin associated protein 2-4 | KRTAP2-1 /// KRTAP2-4 | 1555673_at | -7.57 | -2.60 |
| KIAA0114 gene product | KIAA0114 | 224870_at | 3.25 | 2.89 |
| KIAA1199 | KIAA1199 | 1554685_a_at | -6.06 | -2.43 |
| KIAA1212 | KIAA1212 | 225045_at | -2.14 | -2.08 |
| KIAA1217 | KIAA1217 | 1554438_at | 2.22 | 3.61 |
| KIAA1754 | KIAA1754 | 225582_at | 2.01 | 2.17 |
| Kinase suppressor of ras | KSR | 235252_at | 2.20 | 2.66 |
| Kruppel-like factor 2 (lung) | KLF2 | 219371_s_at | -2.95 | -3.86 |
| Kruppel-like factor 5 (intestinal) | KLF5 | 209211_at | -2.38 | -2.64 |
| Kruppel-like factor 6 | KLF6 | 208961_s_at | -2.19 | -3.07 |
| Kruppel-like factor 6 | KLF6 | 208960_s_at | -2.27 | -3.18 |
| kynureninase (L-kynurenine hydrolase) | KYNU | 217388_s_at | 2.73 | 2.01 |
| leptin (obesity homolog, mouse) | LEP | 207092_at | -3.63 | -2.20 |
| leucine rich repeat (in FLII) interacting protein 2 | LRRFIP2 | 220610_s_at | -2.14 | -2.13 |
| leucine rich repeat neuronal 3 | LRRN3 | 209841_s_at | -2.62 | -2.99 |
| leucine rich repeat neuronal 3 | LRRN3 | 209840_s_at | -3.36 | -4.79 |
| leucine zipper, putative tumor suppressor 1 | LZTS1 | 47550_at | -2.11 | -2.64 |
| leucine-rich repeat-containing G protein-coupled receptor 5 | LGR5 | 213880_at | -5.13 | -7.52 |
| likely ortholog of chicken tsukushi | TSK | 218245_at | 2.50 | 2.57 |
| LIM and cysteine-rich domains 1 | LMCD1 | 242767_at | -4.11 | -10.41 |
| LIM and cysteine-rich domains 1 | LMCD1 | 218574_s_at | -3.25 | -6.50 |
| LIM domain 7 | LMO7 | 242722_at | -5.62 | -8.00 |
| LIM domain 7 | LMO7 | 202674_s_at | -3.34 | -9.85 |
| lipoprotein lipase | LPL | 203549_s_at | 3.05 | 5.82 |
| lipoprotein lipase | LPL | 203548_s_at | 3.20 | 6.36 |
| low density lipoprotein receptor-related protein 4 | LRP4 | 212850_s_at | 2.45 | 3.23 |
| lysyl oxidase-like 4 | LOXL4 | 227145_at | -4.08 | -4.79 |
| Male sterility domain containing 1 | MLSTD1 | 239108_at | -8.28 | -2.19 |

| Gene title | Gene symbol | Affymetrix probe set ID | + 24 h sample_array 1 versus control_array 1 [fold change] | + 24 h sample_array 2 versus control_array 2 [fold change] |
|---|---|---|---|---|
| maltase-glucoamylase (alpha-glucosidase) | MGAM | 206522_at | -11.88 | -54.57 |
| MARCKS-like 1 | MARCKSL1 | 200644_at | 3.12 | 5.10 |
| matrix metalloproteinase 1 (interstitial collagenase) | MMP1 | 204475_at | -37.27 | -4.89 |
| Mdm2, transformed 3T3 cell double minute 2, p53 binding protein (mouse) | MDM2 | 211832_s_at | -8.94 | -2.11 |
| MHC class I polypeptide-related sequence B | MICB | 206247_at | -2.11 | -2.58 |
| microtubule associated monoxygenase, calponin and LIM domain containing 2 | MICAL2 | 212473_s_at | -3.39 | -4.63 |
| microtubule associated monoxygenase, calponin and LIM domain containing 2 | MICAL2 | 212472_at | -3.36 | -4.76 |
| microtubule associated monoxygenase, calponin and LIM domain containing 2 | MICAL2 | 206275_s_at | -3.27 | -2.60 |
| MRNA; cDNA DKFZp586O0724 (from clone DKFZp586O0724) | --- | 231929_at | -2.06 | -3.29 |
| MRNA; cDNA DKFZp686E22185 (from clone DKFZp686E22185) | --- | 235438_at | -2.23 | -4.20 |
| murine retrovirus integration site 1 homolog | MRVI1 | 230214_at | -3.56 | -8.22 |
| Murine retrovirus integration site 1 homolog | MRVI1 | 226047_at | -4.11 | -6.19 |
| murine retrovirus integration site 1 homolog | MRVI1 | 224550_s_at | -2.89 | -16.68 |
| muscleblind-like (Drosophila) | MBNL1 | 1555594_a_at | -2.11 | -2.46 |
| myeloid cell leukemia sequence 1 (BCL2-related) | MCL1 | 200796_s_at | -2.16 | -2.13 |
| Myosin heavy chain Myr 8 | MYR8 | 215119_at | -16.34 | -38.85 |
| Myosin heavy chain Myr 8 | MYR8 | 1557720_s_at | -4.08 | -3.51 |
| myosin regulatory light chain interacting protein | MYLIP | 228098_s_at | 3.07 | 3.07 |
| myosin regulatory light chain interacting protein | MYLIP | 223130_s_at | 3.05 | 2.99 |
| myosin regulatory light chain interacting protein | MYLIP | 223129_x_at | 3.14 | 5.06 |
| myosin regulatory light chain interacting protein | MYLIP | 220319_s_at | 2.53 | 2.30 |
| neural precursor cell expressed, developmentally down-regulated 9 | NEDD9 | 202150_s_at | -2.83 | -3.61 |
| neural precursor cell expressed, developmentally down-regulated 9 | NEDD9 | 202149_at | -2.01 | -3.10 |
| nexilin (F actin binding protein) | NEXN | 226103_at | -2.13 | -4.63 |
| nexilin (F actin binding protein) | NEXN | 1552309_a_at | -2.14 | -4.56 |
| nuclear factor of activated T-cells, cytoplasmic, calcineurin-dependent 4 | NFATC4 | 236270_at | 2.43 | 2.19 |
| odd-skipped related 2 (Drosophila) | OSR2 | 213568_at | 4.50 | 2.60 |
| oxytocin receptor | OXTR | 206825_at | -6.15 | -3.51 |
| palladin | KIAA0992 | 200906_s_at | -2.19 | -3.73 |
| palmdelphin | PALMD | 222725_s_at | 3.07 | 4.29 |
| PDZ and LIM domain 5 | PDLIM5 | 221994_at | -3.84 | -5.86 |
| PDZ and LIM domain 5 | PDLIM5 | 216804_s_at | -2.97 | -3.66 |
| PDZ and LIM domain 5 | PDLIM5 | 213684_s_at | -3.51 | -3.48 |
| PDZ and LIM domain 5 | PDLIM5 | 212412_at | -2.20 | -2.38 |
| PDZ and LIM domain 5 | PDLIM5 | 203243_s_at | -2.14 | -2.62 |
| PDZ and LIM domain 5 | PDLIM5 | 203242_at | -2.77 | -3.10 |
| PDZ and LIM domain 5 /// PDZ and LIM domain 5 | PDLIM5 | 211681_s_at | -2.89 | -3.81 |
| PDZ and LIM domain 7 (enigma) | PDLIM7 | 214121_x_at | -2.08 | -2.36 |
| peroxisome proliferative activated receptor, gamma, coactivator 1, alpha | PPARGC1A | 219195_at | 6.45 | 7.78 |
| phosphodiesterase 4B, cAMP-specific (phosphodiesterase E4 dunce homolog, Drosophila) | PDE4B | 203708_at | 3.03 | 5.90 |
| phosphodiesterase 7B | PDE7B | 243438_at | 5.86 | 3.10 |
| phosphodiesterase 7B | PDE7B | 230109_at | 3.56 | 3.14 |
| phosphodiesterase 7B | PDE7B | 220343_at | 2.27 | 2.62 |
| phosphoglucomutase 3 | PGM3 | 210041_s_at | -2.33 | -2.06 |
| phospholipase A2, group V | PLA2G5 | 206178_at | -2.31 | -2.10 |
| phospholipase C, beta 4 | PLCB4 | 203895_at | -4.11 | -5.78 |
| Platelet-derived growth factor alpha polypeptide | PDGFA | 229830_at | -2.06 | -10.78 |
| pleckstrin homology domain containing, family C (with FERM domain) member 1 | PLEKHC1 | 214212_x_at | -2.22 | -2.71 |
| pleckstrin homology domain containing, family C (with FERM domain) member 1 | PLEKHC1 | 209209_s_at | -2.07 | -2.50 |
| pleckstrin homology, Sec7 and coiled-coil domains 3 | PSCD3 | 243752_s_at | -2.64 | -2.19 |
| pleckstrin homology-like domain, family A, member 2 | PHLDA2 | 209803_s_at | -2.01 | -3.41 |
| Plexin A4 | PLXNA4 | 228104_at | 3.48 | 4.50 |
| potassium channel tetramerisation domain containing 12 | KCTD12 | 212192_at | 2.17 | 2.01 |
| PRKC, apoptosis, WT1, regulator | PAWR | 204004_at | -2.01 | -3.71 |
| prolactin | PRL | 205445_at | 2.55 | 3.92 |
| proline-serine-threonine phosphatase interacting protein 2 | PSTPIP2 | 219938_s_at | -2.89 | -3.66 |
| prostaglandin I2 (prostacyclin) synthase /// prostaglandin I2 (prostacyclin) synthase | PTGIS | 208131_s_at | -3.18 | -5.46 |
| protein phosphatase 1, regulatory (inhibitor) subunit 13 like | PPP1R13L | 218849_s_at | -3.32 | -3.53 |
| protein phosphatase 2C, magnesium-dependent, | PPM2C | 222572_at | -2.25 | -2.01 |

| Gene title | Gene symbol | Affymetrix probe set ID | + 24 h sample_array 1 versus control_array 1 [fold change] | + 24 h sample_array 2 versus control_array 2 [fold change] |
|---|---|---|---|---|
| catalytic subunit | | | | |
| PTPL1-associated RhoGAP 1 | PARG1 | 203910_at | -2.48 | -2.01 |
| putative G protein coupled receptor | GPR | 206673_at | -2.19 | -2.13 |
| putative lymphocyte G0/G1 switch gene | G0S2 | 213524_s_at | 9.58 | 19.29 |
| pyruvate dehydrogenase kinase, isoenzyme 4 | PDK4 | 205960_at | 24.42 | 5.39 |
| RAB20, member RAS oncogene family | RAB20 | 219622_at | 2.69 | 4.69 |
| RAB27B, member RAS oncogene family | RAB27B | 228708_at | 3.23 | 2.22 |
| RAB3B, member RAS oncogene family | RAB3B | 239202_at | -3.76 | -5.78 |
| RAB3B, member RAS oncogene family | RAB3B | 227123_at | -2.97 | -4.32 |
| RAB3B, member RAS oncogene family | RAB3B | 205924_at | -2.85 | -6.92 |
| Ras association (RalGDS/AF-6) and pleckstrin homology domains 1 | RAPH1 | 225189_s_at | -2.55 | -3.32 |
| Ras association (RalGDS/AF-6) and pleckstrin homology domains 1 | RAPH1 | 225188_at | -2.06 | -3.23 |
| Ras association (RalGDS/AF-6) and pleckstrin homology domains 1 | RAPH1 | 225186_at | -2.81 | -3.39 |
| ras homolog gene family, member B | RHOB | 1553962_s_at | -2.51 | -3.86 |
| RAS, dexamethasone-induced 1 | RASD1 | 223467_at | 4.38 | 7.52 |
| receptor tyrosine kinase-like orphan receptor 2 | ROR2 | 205578_at | 2.66 | 2.08 |
| Regulating synaptic membrane exocytosis 1 | RIMS1 | 231986_at | -3.73 | -20.39 |
| regulator of G-protein signalling 4 | RGS4 | 204339_s_at | -6.15 | -3.18 |
| regulator of G-protein signalling 4 | RGS4 | 204338_s_at | -10.13 | -8.63 |
| regulator of G-protein signalling 4 | RGS4 | 204337_at | -6.15 | -5.03 |
| REV3-like, catalytic subunit of DNA polymerase zeta (yeast) | REV3L | 208070_s_at | 2.30 | 2.66 |
| Rho GTPase activating protein 28 | ARHGAP28 | 227911_at | 2.28 | 5.50 |
| ring finger protein 144 | RNF144 | 204040_at | 2.51 | 5.35 |
| schwannomin interacting protein 1 | SCHIP1 | 204030_s_at | -3.86 | -7.11 |
| secreted frizzled-related protein 2 | SFRP2 | 223122_at | 10.56 | 10.78 |
| secreted frizzled-related protein 2 | SFRP2 | 223121_s_at | 16.45 | 18.25 |
| secretory protein LOC284013 | LOC284013 | 235751_s_at | 2.30 | 35.51 |
| sema domain, transmembrane domain (TM), and cytoplasmic domain, (semaphorin) 6D | SEMA6D | 226492_at | 2.22 | 5.54 |
| serine (or cysteine) proteinase inhibitor, clade B (ovalbumin), member 2 | SERPINB2 | 204614_at | -2.36 | -2.36 |
| serine (or cysteine) proteinase inhibitor, clade B (ovalbumin), member 9 | SERPINB9 | 209723_at | -2.36 | -2.17 |
| serine (or cysteine) proteinase inhibitor, clade E (nexin, plasminogen activator inhibitor type 1), member 1 | SERPINE1 | 202628_s_at | -2.13 | -3.58 |
| serine (or cysteine) proteinase inhibitor, clade E (nexin, plasminogen activator inhibitor type 1), member 1 | SERPINE1 | 202627_s_at | -2.46 | -4.00 |
| serine (or cysteine) proteinase inhibitor, clade E (nexin, plasminogen activator inhibitor type 1), member 1 | SERPINE1 | 1568765_at | -2.03 | -4.82 |
| serine active site containing 1 | SERAC1 | 232183_at | -2.23 | -2.35 |
| serine/threonine kinase 38 like | STK38L | 212572_at | -4.82 | -2.07 |
| serum/glucocorticoid regulated kinase-like | SGKL | 220038_at | -2.31 | -3.18 |
| SHB (Src homology 2 domain containing) adaptor protein B | SHB | 1557458_s_at | -2.41 | -2.04 |
| Shroom-related protein | ShrmL | 225548_at | -2.69 | -4.41 |
| signal sequence receptor, gamma (translocon-associated protein gamma) | SSR3 | 217790_s_at | -3.46 | -2.25 |
| similar to AVLV472 | MGC23985 | 1554195_a_at | -3.36 | -3.07 |
| smoothelin | SMTN | 209427_at | -2.23 | -2.01 |
| SNF1-like kinase 2 | SNF1LK2 | 213221_s_at | 2.31 | 2.97 |
| solute carrier family 16 (monocarboxylic acid transporters), member 7 | SLC16A7 | 207057_at | -2.57 | -2.38 |
| solute carrier family 19, member 3 | SLC19A3 | 239345_at | 2.14 | 4.00 |
| solute carrier family 19, member 3 | SLC19A3 | 220736_at | 2.36 | 4.11 |
| solute carrier family 8 (sodium/calcium exchanger), member 1 | SLC8A1 | 241752_at | -4.44 | -4.82 |
| solute carrier family 8 (sodium/calcium exchanger), member 1 | SLC8A1 | 235518_at | -3.53 | -4.69 |
| sortilin 1 | SORT1 | 212797_at | -2.17 | -3.94 |
| sphingosine kinase 1 | SPHK1 | 219257_s_at | -2.53 | -2.89 |
| SPOC domain containing 1 | SPOCD1 | 235417_at | -2.13 | -3.32 |
| sprouty homolog 4 (Drosophila) | SPRY4 | 221489_s_at | -2.60 | -2.71 |
| ST3 beta-galactoside alpha-2,3-sialyltransferase 5 | ST3GAL5 | 203217_s_at | 4.23 | 3.53 |
| stanniocalcin 1 | STC1 | 204596_s_at | -3.05 | -2.01 |
| sushi, nidogen and EGF-like domains 1 | SNED1 | 213493_at | 2.07 | 3.68 |
| synaptopodin 2 | SYNPO2 | 232119_at | -2.69 | -3.23 |
| synaptopodin 2 | SYNPO2 | 227662_at | -2.08 | -4.11 |
| synaptopodin 2 | SYNPO2 | 225894_at | -2.58 | -6.68 |
| Synaptopodin 2 | SYNPO2 | 225720_at | -2.10 | -17.51 |

| Gene title | Gene symbol | Affymetrix probe set ID | + 24 h sample_array 1 versus control_array 1 [fold change] | + 24 h sample_array 2 versus control_array 2 [fold change] |
|---|---|---|---|---|
| TBC1 (tre-2/USP6, BUB2, cdc16) domain family, member 1 | TBC1D1 | 227945_at | -2.38 | -3.01 |
| TBC1 (tre-2/USP6, BUB2, cdc16) domain family, member 1 | TBC1D1 | 212350_at | -2.11 | -2.66 |
| TBC1 domain family, member 2 | TBC1D2 | 222173_s_at | -2.91 | -2.10 |
| tensin-like SH2 domain containing 1 | TENS1 | 217853_at | -2.03 | -2.28 |
| Thrombospondin 1 | THBS1 | 235086_at | -2.17 | -2.04 |
| thymus high mobility group box protein TOX | TOX | 204529_s_at | -2.27 | -3.58 |
| Transcribed locus | --- | 241560_at | 4.32 | 4.29 |
| Transcribed locus | --- | 229795_at | 2.28 | 2.04 |
| Transcribed locus | --- | 235046_at | -3.18 | -3.25 |
| Transcribed locus | --- | 229479_at | -6.06 | -3.07 |
| Transcribed locus, moderately similar to XP_517655.1 similar to KIAA0825 protein [Pan troglodytes] | --- | 229641_at | -3.66 | -5.90 |
| Transcribed locus, strongly similar to NP_065910.1 Shroom-related protein [Homo sapiens] | --- | 228400_at | -3.68 | -5.66 |
| transcription elongation factor A (SII), 3 | TCEA3 | 226388_at | -2.10 | -2.64 |
| transducin-like enhancer of split 3 (E(sp1) homolog, Drosophila) | TLE3 | 228340_at | 2.04 | 2.22 |
| transient receptor potential cation channel, subfamily V, member 2 | TRPV2 | 222855_s_at | -2.10 | -3.16 |
| transient receptor potential cation channel, subfamily V, member 2 | TRPV2 | 219282_s_at | -2.03 | -3.71 |
| transmembrane 4 L six family member 1 | TM4SF1 | 209387_s_at | -2.60 | -2.73 |
| transmembrane 4 L six family member 1 | TM4SF1 | 209386_at | -2.17 | -2.51 |
| transmembrane protein 35 | TMEM35 | 219685_at | 2.20 | 2.58 |
| transmembrane protein 37 | TMEM37 | 227190_at | 2.14 | 19.70 |
| tripartite motif-containing 2 | TRIM2 | 202342_s_at | 2.38 | 3.05 |
| tropomyosin 1 (alpha) | TPM1 | 206117_at | -2.75 | -7.36 |
| tropomyosin 1 (alpha) | TPM1 | 206116_s_at | -2.28 | -5.31 |
| TSC22 domain family 1 | TGFB1I4 | 235315_at | -2.08 | -2.19 |
| tubulin, beta 2 /// tubulin, beta polypeptide paralog | TUBB2 /// RP11-506K6.1 | 209372_x_at | -2.20 | -3.18 |
| tubulin, beta 6 | TUBB6 | 209191_at | -2.19 | -2.71 |
| tumor necrosis factor receptor superfamily, member 11b (osteoprotegerin) | TNFRSF11B | 204933_s_at | -7.36 | -19.16 |
| tumor necrosis factor receptor superfamily, member 11b (osteoprotegerin) | TNFRSF11B | 204932_at | -5.06 | -8.88 |
| tumor necrosis factor receptor superfamily, member 12A | TNFRSF12A | 218368_s_at | -3.97 | -4.76 |
| tumor necrosis factor receptor superfamily, member 21 | TNFRSF21 | 218856_at | 2.01 | 2.66 |
| tumor protein D52-like 1 | TPD52L1 | 203786_s_at | -2.38 | -4.66 |
| tumor-associated calcium signal transducer 2 | TACSTD2 | 202286_s_at | -3.43 | -4.86 |
| ubiquitin-like, containing PHD and RING finger domains, 1 | UHRF1 | 225655_at | -2.20 | -2.03 |
| UDP-Gal:betaGlcNAc beta 1,3-galactosyltransferase, polypeptide 2 | B3GALT2 | 217452_s_at | -6.19 | -6.54 |
| UDP-Gal:betaGlcNAc beta 1,3-galactosyltransferase, polypeptide 2 | B3GALT2 | 210121_at | -44.02 | -4.20 |
| UDP-N-acetyl-alpha-D-galactosamine:polypeptide N-acetylgalactosaminyltransferase 3 (GalNAc-T3) | GALNT3 | 203397_s_at | -3.41 | -5.54 |
| uveal autoantigen with coiled-coil domains and ankyrin repeats | UACA | 223279_s_at | -3.12 | -2.50 |
| vascular endothelial growth factor C | VEGFC | 209946_at | -2.14 | -2.73 |
| vasodilator-stimulated phosphoprotein | VASP | 202205_at | -2.08 | -2.08 |
| villin 2 (ezrin) | VIL2 | 217234_s_at | -3.03 | -2.77 |
| villin 2 (ezrin) | VIL2 | 208622_s_at | -2.39 | -3.86 |
| villin 2 (ezrin) | VIL2 | 208621_s_at | -3.16 | -3.20 |
| v-maf musculoaponeurotic fibrosarcoma oncogene homolog B (avian) | MAFB | 218559_s_at | 2.11 | 2.41 |
| WD repeat domain 1 | WDR1 | 210935_s_at | -2.08 | -4.89 |
| wingless-type MMTV integration site family, member 5B | WNT5B | 223537_s_at | -2.17 | -2.64 |
| Zinc finger, BED domain containing 3 | ZBED3 | 235109_at | 2.46 | 5.21 |

Transdifferentiated samples were compared to differentiated controls. Fold changes for transcripts with reproducible regulation directions regarding two different MSC charges (array 1 and array 2) are listed by gene name. + 24 h = 24 h after initiation of adipogenic transdifferentiation.

**Tab. 16  Fold changes of gene expression 3 h after initiation of osteogenic transdifferentiation**

| Gene title | Gene symbol | Affymetrix probe set ID | + 3 h sample_array 1 versus control_array 1 [fold change] | + 3 h sample_array 2 versus control_array 2 [fold change] |
|---|---|---|---|---|
| --- | --- | 206078_at | 2.57 | 5.82 |
| --- | --- | 226136_at | 2.43 | 2.03 |
| --- | --- | 235579_at | 2.33 | 2.68 |
| --- | --- | 241773_at | 2.64 | 3.43 |
| --- | --- | 242157_at | 2.36 | 2.87 |
| --- | --- | 225207_at | -3.92 | -3.10 |
| --- | --- | 244025_at | -2.51 | -3.34 |
| A disintegrin-like and metalloprotease (reprolysin type) with thrombospondin type 1 motif, 15 | ADAMTS15 | 229004_at | -3.81 | -4.06 |
| activin A receptor, type IC | ACVR1C | 1552519_at | -2.16 | -2.50 |
| angiopoietin-like 4 | ANGPTL4 | 221009_s_at | -3.07 | -4.11 |
| angiopoietin-like 4 | ANGPTL4 | 223333_s_at | -3.53 | -4.50 |
| armadillo repeat containing 8 | ARMC8 | 219094_at | 2.07 | 2.69 |
| ARP3 actin-related protein 3 homolog (yeast) | ACTR3 | 228603_at | 2.89 | 2.89 |
| baculoviral IAP repeat-containing 3 | BIRC3 | 210538_s_at | 2.27 | 2.51 |
| B-cell CLL/lymphoma 10 | BCL10 | 1557257_at | 2.83 | 2.46 |
| B-cell CLL/lymphoma 2 | BCL2 | 203685_at | -2.04 | -2.23 |
| bicaudal D homolog 1 (Drosophila) | BICD1 | 1554020_at | 3.56 | 3.36 |
| calponin 1, basic, smooth muscle | CNN1 | 203951_at | 2.45 | 3.36 |
| CDNA clone IMAGE:4514712, partial cds | --- | 217999_s_at | -3.68 | -5.98 |
| CDNA clone IMAGE:4514712, partial cds | --- | 225842_at | -2.79 | -5.86 |
| chromosome 9 open reading frame 65 | C9orf65 | 1552455_at | 2.23 | 6.68 |
| Collagen, type I, alpha 2 | COL1A2 | 229218_at | 2.39 | 3.23 |
| deleted in liver cancer 1 | DLC1 | 224822_at | -2.01 | -2.08 |
| deleted in lymphocytic leukemia, 2 /// BCMS upstream neighbor-like | DLEU2 /// BCMSUNL | 215629_s_at | 2.23 | 2.77 |
| DNA-damage-inducible transcript 4 | DDIT4 | 202887_s_at | -4.29 | -4.20 |
| dual specificity phosphatase 4 | DUSP4 | 204014_at | -2.06 | -2.68 |
| Dynamin 3 | DNM3 | 232090_at | 2.30 | 2.22 |
| Exostoses (multiple) 1 | EXT1 | 232174_at | 2.31 | 2.50 |
| family with sequence similarity 46, member B | FAM46B | 229518_at | 2.87 | 2.45 |
| fibroblast growth factor 7 (keratinocyte growth factor) | FGF7 | 1555103_s_at | 2.23 | 2.20 |
| frizzled homolog 4 (Drosophila) | FZD4 | 218665_at | -2.41 | -2.25 |
| glucocorticoid induced transcript 1 | GLCCI1 | 225706_at | -2.14 | -3.03 |
| glucocorticoid induced transcript 1 | GLCCI1 | 227525_at | -2.93 | -3.34 |
| Glucosaminyl (N-acetyl) transferase 1, core 2 (beta-1,6-N-acetylglucosaminyltransferase) | GCNT1 | 240076_at | 2.06 | 3.56 |
| growth differentiation factor 15 | GDF15 | 221577_x_at | -2.28 | -2.13 |
| guanylate binding protein 1, interferon-inducible, 67kDa | GBP1 | 231577_s_at | 2.45 | 2.81 |
| guanylate binding protein 1, interferon-inducible, 67kDa /// guanylate binding protein 1, interferon-inducible, 67kDa | GBP1 | 202269_x_at | 2.23 | 2.81 |
| guanylate binding protein 1, interferon-inducible, 67kDa /// guanylate binding protein 1, interferon-inducible, 67kDa | GBP1 | 202270_at | 2.31 | 2.38 |
| HECT domain containing 2 | HECTD2 | 238803_at | 2.75 | 3.97 |
| hepatocyte growth factor (hepapoietin A; scatter factor) | HGF | 210755_at | 2.55 | 5.90 |
| Heterogeneous nuclear ribonucleoprotein D (AU-rich element RNA binding protein 1, 37kDa) | HNRPD | 213359_at | -2.71 | -3.61 |
| hypothetical gene supported by BC062741 | LOC401151 | 237465_at | 3.32 | 3.89 |
| hypothetical protein BC007901 | LOC91461 | 225380_at | -2.53 | -2.16 |
| hypothetical protein DKFZp566D1346 | DKFZP566D1346 | 1556361_s_at | 3.32 | 3.32 |
| Hypothetical protein FLJ10154 | FLJ10154 | 227448_at | 2.20 | 3.32 |
| hypothetical protein FLJ37034 | FLJ37034 | 229622_at | 7.94 | 3.73 |
| hypothetical protein LOC284454 | LOC284454 | 1555847_a_at | 2.20 | 2.58 |
| keratin associated protein 1-5 | KRTAP1-5 | 233533_at | 5.13 | 3.51 |
| keratin, hair, acidic, 4 | KRTHA4 | 206969_at | 24.42 | 14.22 |
| KIAA1387 protein | KIAA1387 | 222270_at | 2.06 | 2.23 |
| KIAA1609 protein | KIAA1609 | 221843_s_at | 8.94 | 2.46 |
| KIAA1754 | KIAA1754 | 225582_at | -2.35 | -2.93 |
| KIAA1913 | KIAA1913 | 234994_at | 2.19 | 2.13 |
| Kruppel-like factor 6 | KLF6 | 208960_s_at | 2.36 | 2.25 |
| Leucine rich repeat (in FLII) interacting protein 2 | LRRFIP2 | 230082_at | 2.08 | 2.28 |
| LOC150368 protein | LOC150368 | 226504_at | 2.22 | 2.01 |
| LOC440476 | --- | 1555976_s_at | 2.53 | 4.00 |
| matrix metalloproteinase 12 (macrophage elastase) | MMP12 | 204580_at | 5.50 | 3.12 |
| matrix metalloproteinase 3 (stromelysin 1, progelatinase) | MMP3 | 205828_at | 2.73 | 2.19 |
| Muscleblind-like (Drosophila) | MBNL1 | 1558111_at | 3.27 | 4.44 |
| Muscleblind-like (Drosophila) | MBNL1 | 235879_at | 2.99 | 3.43 |
| myosin regulatory light chain interacting protein | MYLIP | 220319_s_at | -2.57 | -2.39 |
| myosin regulatory light chain interacting protein | MYLIP | 223129_x_at | -2.91 | -2.19 |

| Gene title | Gene symbol | Affymetrix probe set ID | + 3 h sample_array 1 versus control_array 1 [fold change] | + 3 h sample_array 2 versus control_array 2 [fold change] |
|---|---|---|---|---|
| myosin regulatory light chain interacting protein | MYLIP | 223130_s_at | -2.20 | -2.19 |
| myosin regulatory light chain interacting protein | MYLIP | 228098_s_at | -2.22 | -2.17 |
| nuclear receptor subfamily 4, group A, member 2 | NR4A2 | 204622_x_at | -3.32 | -5.39 |
| nuclear receptor subfamily 4, group A, member 3 | NR4A3 | 209959_at | -2.11 | -3.05 |
| PDZ and LIM domain 5 | PDLIM5 | 213684_s_at | 3.01 | 3.68 |
| PDZ and LIM domain 5 | PDLIM5 | 221994_at | 3.43 | 2.99 |
| phosphoenolpyruvate carboxykinase 1 (soluble) | PCK1 | 208383_s_at | -4.08 | -4.35 |
| phospholamban | PLN | 204939_s_at | 2.69 | 40.79 |
| phospholamban | PLN | 204940_at | 3.41 | 3.76 |
| pleckstrin homology-like domain, family A, member 1 | PHLDA1 | 217996_at | -2.31 | -3.41 |
| pleckstrin homology-like domain, family A, member 1 | PHLDA1 | 217997_at | -2.77 | -2.93 |
| pleckstrin homology-like domain, family A, member 1 | PHLDA1 | 217998_at | -5.70 | -3.63 |
| pleckstrin homology-like domain, family A, member 1 | PHLDA1 | 218000_s_at | -4.79 | -3.36 |
| pleckstrin homology-like domain, family A, member 2 | PHLDA2 | 209803_s_at | 2.60 | 2.38 |
| Pre-B-cell colony enhancing factor 1 | PBEF1 | 243296_at | -2.10 | -3.10 |
| pyruvate dehydrogenase kinase, isoenzyme 4 | PDK4 | 205960_at | -4.11 | -3.66 |
| RAB20, member RAS oncogene family | RAB20 | 219622_at | -2.50 | -2.22 |
| RAS, dexamethasone-induced 1 | RASD1 | 223467_at | -3.53 | -4.08 |
| regulator of G-protein signalling 4 | RGS4 | 204337_at | 2.64 | 2.13 |
| regulator of G-protein signalling 4 | RGS4 | 204338_s_at | 2.50 | 2.08 |
| solute carrier family 16 (monocarboxylic acid transporters), member 6 | SLC16A6 | 207038_at | -2.06 | -4.32 |
| Splicing factor, arginine/serine-rich 3 | SFRS3 | 235324_at | 2.28 | 2.81 |
| superoxide dismutase 2, mitochondrial | SOD2 | 215078_at | 2.36 | 2.51 |
| suppressor of variegation 4-20 homolog 1 (Drosophila) | SUV420H1 | 222759_at | 3.16 | 3.43 |
| Synaptopodin 2 | SYNPO2 | 225720_at | 2.71 | 2.46 |
| synaptopodin 2 | SYNPO2 | 225895_at | 2.43 | 2.95 |
| Transcribed locus | --- | 229479_at | 2.06 | 2.41 |
| Transcribed locus | --- | 231098_at | 3.20 | 3.76 |
| Transcribed locus | --- | 235693_at | 2.01 | 2.75 |

Transdifferentiated samples were compared to differentiated controls. Fold changes for transcripts with reproducible regulation directions regarding two different MSC charges (array 1 and array 2) are listed by gene name. + 3 h = 3 h after initiation of osteogenic transdifferentiation.

**Tab. 17  Changes of gene expression 24 h after initiation of osteogenic transdifferentiation**

| Gene title | Gene symbol | Affymetrix probe set ID | + 24 h sample_array 1 versus control_array 1 [fold change] | + 24 h sample_array 2 versus control_array 2 [fold change] |
|---|---|---|---|---|
| --- | --- | 203817_at | 2.17 | 3.97 |
| --- | --- | 204886_at | 3.48 | 4.89 |
| --- | --- | 214806_at | 2.31 | 2.00 |
| --- | --- | 217211_at | 2.01 | 2.36 |
| --- | --- | 222606_at | 2.51 | 3.32 |
| --- | --- | 222802_at | 3.51 | 4.35 |
| --- | --- | 224929_at | 4.63 | 5.62 |
| --- | --- | 225782_at | 2.22 | 3.41 |
| --- | --- | 225790_at | 2.25 | 3.61 |
| --- | --- | 226136_at | 3.32 | 3.48 |
| --- | --- | 228407_at | 3.48 | 3.29 |
| --- | --- | 229669_at | 5.66 | 6.50 |
| --- | --- | 230165_at | 2.75 | 3.32 |
| --- | --- | 230494_at | 2.39 | 2.69 |
| --- | --- | 236304_at | 5.46 | 11.24 |
| --- | --- | 242856_at | 2.79 | 4.69 |
| --- | --- | 1557236_at | -2.48 | -2.93 |
| --- | --- | 1558044_s_at | -2.27 | -2.83 |
| --- | --- | 210524_x_at | -2.17 | -4.20 |
| --- | --- | 214584_x_at | -2.43 | -4.47 |
| --- | --- | 219800_s_at | -2.46 | -2.30 |
| --- | --- | 225207_at | -5.94 | -4.59 |
| --- | --- | 227246_at | -2.27 | -2.20 |
| --- | --- | 235050_at | -20.97 | -2.57 |
| --- | --- | 239907_at | -2.58 | -3.29 |
| --- | --- | 244353_s_at | -9.06 | -4.00 |
| 3-hydroxy-3-methylglutaryl-Coenzyme A reductase | HMGCR | 202540_s_at | -2.20 | -3.14 |

| Gene title | Gene symbol | Affymetrix probe set ID | + 24 h sample_array 1 versus control_array 1 [fold change] | + 24 h sample_array 2 versus control_array 2 [fold change] |
|---|---|---|---|---|
| 3'-phosphoadenosine 5'-phosphosulfate synthase 2 | PAPSS2 | 203060_s_at | 2.01 | 2.14 |
| 4-aminobutyrate aminotransferase | ABAT | 209459_s_at | 2.25 | 2.89 |
| 4-aminobutyrate aminotransferase | ABAT | 209460_at | 3.07 | 2.83 |
| 7-dehydrocholesterol reductase | DHCR7 | 201790_s_at | -2.38 | -3.48 |
| 7-dehydrocholesterol reductase | DHCR7 | 201791_s_at | -2.23 | -2.68 |
| A disintegrin-like and metalloprotease (reprolysin type) with thrombospondin type 1 motif, 15 | ADAMTS15 | 229004_at | -10.63 | -17.15 |
| acetyl-Coenzyme A carboxylase alpha | ACACA | 212186_at | -2.69 | -2.73 |
| acetyl-Coenzyme A carboxylase beta | ACACB | 1552615_at | -2.17 | -3.20 |
| acetyl-Coenzyme A carboxylase beta | ACACB | 1552616_a_at | -2.43 | -4.41 |
| acetyl-Coenzyme A carboxylase beta | ACACB | 221928_at | -2.11 | -3.39 |
| acetyl-Coenzyme A carboxylase beta | ACACB | 43427_at | -2.27 | -4.20 |
| acetyl-Coenzyme A carboxylase beta | ACACB | 49452_at | -2.23 | -4.69 |
| acheron | FLJ11196 | 218651_s_at | -3.07 | -2.13 |
| acidic (leucine-rich) nuclear phosphoprotein 32 family, member E /// acidic (leucine-rich) nuclear phosphoprotein 32 family, member E | ANP32E | 208103_s_at | 2.17 | 2.19 |
| actin related protein 2/3 complex, subunit 5, 16kDa | ARPC5 | 1555797_a_at | 2.39 | 2.99 |
| actin related protein 2/3 complex, subunit 5, 16kDa | ARPC5 | 211963_s_at | 2.36 | 2.55 |
| actin, gamma 2, smooth muscle, enteric | ACTG2 | 202274_at | 4.92 | 5.39 |
| actinin, alpha 1 | ACTN1 | 208637_x_at | 2.16 | 2.31 |
| actinin, alpha 1 | ACTN1 | 211160_x_at | 2.04 | 2.17 |
| activating transcription factor 4 (tax-responsive enhancer element B67) | ATF4 | 200779_at | -2.13 | -2.93 |
| adaptor-related protein complex 4, sigma 1 subunit | AP4S1 | 210278_s_at | 2.20 | 2.55 |
| additional sex combs like 1 (Drosophila) | ASXL1 | 244519_at | 2.45 | 2.03 |
| adenomatosis polyposis coli down-regulated 1 | APCDD1 | 225016_at | -2.89 | -2.46 |
| adenosine deaminase, RNA-specific, B1 (RED1 homolog rat) | ADARB1 | 203865_s_at | 2.33 | 3.03 |
| adenylate cyclase 7 | ADCY7 | 203741_s_at | 5.21 | 6.59 |
| adiponectin, C1Q and collagen domain containing | ADIPOQ | 207175_at | -2.03 | -2.46 |
| adipose differentiation-related protein | ADFP | 209122_at | -2.08 | -4.03 |
| adlican | DKFZp564I1922 | 209596_at | 3.86 | 6.59 |
| ADP-ribosylation factor-like 7 | ARL7 | 202206_at | -3.51 | -4.66 |
| ADP-ribosylation factor-like 7 | ARL7 | 202207_at | -3.53 | -4.82 |
| ADP-ribosylation factor-like 7 | ARL7 | 202208_s_at | -2.89 | -5.82 |
| adrenergic, alpha-2A-, receptor /// adrenergic, alpha-2A-, receptor | ADRA2A | 209869_at | -3.68 | -4.11 |
| adrenergic, beta, receptor kinase 2 | ADRBK2 | 204184_s_at | -2.73 | -2.07 |
| adrenergic, beta, receptor kinase 2 | ADRBK2 | 228771_at | -3.07 | -2.62 |
| AER61 glycosyltransferase | AER61 | 221935_s_at | 2.46 | 3.58 |
| alcohol dehydrogenase 1A (class I), alpha polypeptide /// alcohol dehydrogenase IB (class I), beta polypeptide /// alcohol dehydrogenase 1C (class I), gamma polypeptide | ADH1A /// ADH1B /// ADH1C | 209614_at | -2.91 | -3.51 |
| alcohol dehydrogenase IB (class I), beta polypeptide | ADH1B | 209612_s_at | -3.23 | -5.43 |
| alcohol dehydrogenase IB (class I), beta polypeptide | ADH1B | 209613_s_at | -3.51 | -4.92 |
| aldehyde dehydrogenase 1 family, member A3 | ALDH1A3 | 203180_at | -3.63 | -2.91 |
| aldehyde dehydrogenase 1 family, member B1 | ALDH1B1 | 209645_s_at | 3.61 | 5.58 |
| aldehyde dehydrogenase 1 family, member B1 | ALDH1B1 | 209646_x_at | 2.73 | 2.89 |
| aldehyde dehydrogenase 1 family, member L1 | ALDH1L1 | 205208_at | -2.11 | -2.89 |
| aldehyde dehydrogenase 3 family, member A2 | ALDH3A2 | 202053_s_at | -2.27 | -3.03 |
| aldehyde dehydrogenase 3 family, member A2 | ALDH3A2 | 202054_s_at | -3.03 | -4.56 |
| aldehyde dehydrogenase 3 family, member A2 | ALDH3A2 | 210544_s_at | -2.68 | -4.53 |
| aldo-keto reductase family 1, member C1 (dihydrodiol dehydrogenase 1; 20-alpha (3-alpha)-hydroxysteroid dehydrogenase) /// aldo-keto reductase family 1, member C2 (dihydrodiol dehydrogenase 2; bile acid binding protein; 3-alpha hydroxysteroid dehydrogenase, type III) | AKR1C1 /// AKR1C2 | 217626_at | -3.03 | -7.62 |
| Aldo-keto reductase family 1, member C2 (dihydrodiol dehydrogenase 2; bile acid binding protein; 3-alpha hydroxysteroid dehydrogenase, type III) | AKR1C2 | 1555854_at | -2.99 | -5.82 |
| alkaline phosphatase, liver/bone/kidney | ALPL | 215783_s_at | 2.14 | 2.46 |
| ALL1-fused gene from chromosome 1q /// ALL1-fused gene from chromosome 1q | AF1Q | 211071_s_at | 2.51 | 4.06 |
| alpha-kinase 2 | ALPK2 | 228367_at | 2.79 | 5.62 |
| amphoterin induced gene 2 | AMIGO2 | 222108_at | 2.17 | 3.25 |
| amyotrophic lateral sclerosis 2 (juvenile) chromosome region, candidate 13 | ALS2CR13 | 226431_at | -2.30 | -2.25 |
| angiopoietin-like 2 | ANGPTL2 | 213001_at | -3.29 | -4.82 |
| angiopoietin-like 2 | ANGPTL2 | 213004_at | -2.93 | -2.58 |
| angiopoietin-like 2 | ANGPTL2 | 219514_at | -2.30 | -2.77 |
| angiopoietin-like 4 | ANGPTL4 | 221009_s_at | -4.66 | -6.45 |
| angiopoietin-like 4 | ANGPTL4 | 223333_s_at | -5.94 | -9.38 |
| angiotensin II receptor, type 1 | AGTR1 | 205357_s_at | -2.95 | -7.62 |

| Gene title | Gene symbol | Affymetrix probe set ID | + 24 h sample_array 1 versus control_array 1 [fold change] | + 24 h sample_array 2 versus control_array 2 [fold change] |
|---|---|---|---|---|
| angiotensin II receptor, type 1 | AGTR1 | 208016_s_at | -3.07 | -7.73 |
| anillin, actin binding protein (scraps homolog, Drosophila) | ANLN | 1552619_a_at | 5.90 | 6.92 |
| anillin, actin binding protein (scraps homolog, Drosophila) | ANLN | 222608_s_at | 4.99 | 7.16 |
| ankyrin 2, neuronal | ANK2 | 202920_at | -2.39 | -2.48 |
| ankyrin repeat domain 1 (cardiac muscle) | ANKRD1 | 206029_at | 15.56 | 20.11 |
| ankyrin repeat domain 6 | ANKRD6 | 204671_s_at | 2.48 | 3.25 |
| antigen identified by monoclonal antibody Ki-67 | MKI67 | 212020_s_at | 3.10 | 2.39 |
| antigen identified by monoclonal antibody Ki-67 | MKI67 | 212022_s_at | 3.84 | 3.39 |
| antigen identified by monoclonal antibody Ki-67 | MKI67 | 212023_s_at | 4.32 | 3.92 |
| apical protein-like (Xenopus laevis) | APXL | 204967_at | 3.41 | 5.50 |
| apolipoprotein B mRNA editing enzyme, catalytic polypeptide-like 3B | APOBEC3B | 206632_s_at | 5.13 | 7.57 |
| apolipoprotein L, 6 | APOL6 | 219716_at | -2.85 | -2.73 |
| apoptosis-inducing factor (AIF)-like mitochondrion-associated inducer of death | AMID | 228445_at | -2.60 | -2.23 |
| apoptosis-inducing factor (AIF)-like mitochondrion-associated inducer of death /// apoptosis-inducing factor (AIF)-like mitochondrion-associated inducer of death | AMID | 224461_s_at | -2.66 | -2.14 |
| aquaporin 3 | AQP3 | 39248_at | -5.58 | -6.11 |
| aquaporin 7 | AQP7 | 206955_at | -2.48 | -2.95 |
| arginase, type II | ARG2 | 203946_s_at | -3.51 | -3.73 |
| Armadillo repeat containing, X-linked 4 | ARMCX4 | 227444_at | 2.41 | 2.53 |
| ARP3 actin-related protein 3 homolog (yeast) | ACTR3 | 200996_at | 2.14 | 2.22 |
| arrestin domain containing 2 | ARRDC2 | 226055_at | 2.38 | 2.01 |
| arrestin domain containing 3 | ARRDC3 | 224797_at | -2.13 | -2.58 |
| aryl-hydrocarbon receptor nuclear translocator 2 | ARNT2 | 202986_at | 4.32 | 6.73 |
| arylsulfatase J | ARSJ | 219973_at | 3.07 | 5.28 |
| ASF1 anti-silencing function 1 homolog B (S. cerevisiae) | ASF1B | 218115_at | 2.69 | 5.24 |
| asp (abnormal spindle)-like, microcephaly associated (Drosophila) | ASPM | 219918_s_at | 5.21 | 4.32 |
| asparagine synthetase | ASNS | 205047_s_at | -5.21 | -5.74 |
| ATPase family, AAA domain containing 2 | ATAD2 | 218782_s_at | 2.41 | 3.66 |
| ATPase family, AAA domain containing 2 | ATAD2 | 222740_at | 2.91 | 3.58 |
| ATPase family, AAA domain containing 2 | ATAD2 | 228401_at | 2.85 | 4.66 |
| ATPase family, AAA domain containing 2 | ATAD2 | 235266_at | 2.77 | 3.89 |
| ATPase, Class I, type 8B, member 1 | ATP8B1 | 226302_at | 4.00 | 6.63 |
| ATPase, Na+/K+ transporting, beta 1 polypeptide | ATP1B1 | 201242_s_at | 3.25 | 9.71 |
| ATPase, Na+/K+ transporting, beta 1 polypeptide | ATP1B1 | 201243_s_at | 3.27 | 5.74 |
| aurora kinase B | AURKB | 209464_at | 5.10 | 4.41 |
| baculoviral IAP repeat-containing 3 | BIRC3 | 210538_s_at | 4.26 | 10.93 |
| baculoviral IAP repeat-containing 5 (survivin) | BIRC5 | 202095_s_at | 5.13 | 7.06 |
| baculoviral IAP repeat-containing 5 (survivin) | BIRC5 | 210334_x_at | 3.20 | 5.28 |
| BAI1-associated protein 2-like 1 | BAIAP2L1 | 227372_s_at | 2.85 | 2.45 |
| barren homolog (Drosophila) | BRRN1 | 212949_at | 11.08 | 4.66 |
| basic helix-loop-helix domain containing, class B, 3 | BHLHB3 | 221530_s_at | -2.68 | -4.79 |
| B-cell CLL/lymphoma 2 | BCL2 | 203685_at | -4.50 | -3.86 |
| B-cell translocation gene 1, anti-proliferative | BTG1 | 200921_s_at | -2.00 | -2.27 |
| BCL2-associated athanogene | BAG1 | 211475_s_at | -2.06 | -2.20 |
| BCL2-like 11 (apoptosis facilitator) | BCL2L11 | 1553096_s_at | -2.14 | -2.01 |
| BCL2-like 11 (apoptosis facilitator) | BCL2L11 | 1555372_at | -3.20 | -2.89 |
| BCL2-like 11 (apoptosis facilitator) | BCL2L11 | 1558143_a_at | -4.17 | -4.29 |
| BCL2-like 11 (apoptosis facilitator) | BCL2L11 | 225606_at | -4.92 | -5.43 |
| BCL6 co-repressor | BCOR | 223916_s_at | 12.30 | 3.68 |
| beta 3-glycosyltransferase-like | B3GTL | 227083_at | 2.06 | 2.10 |
| beta 3-glycosyltransferase-like | B3GTL | 227100_at | 2.38 | 2.50 |
| brain acyl-CoA hydrolase | BACH | 208002_s_at | 2.01 | 3.05 |
| brain-derived neurotrophic factor | BDNF | 206382_s_at | 2.77 | 6.19 |
| BRCA1 associated RING domain 1 | BARD1 | 205345_at | 3.18 | 3.36 |
| BRCA1 associated RING domain 1 | BARD1 | 227545_at | 3.12 | 4.14 |
| BRCA1 interacting protein C-terminal helicase 1 | BRIP1 | 235609_at | 3.84 | 5.17 |
| BRCA1 interacting protein C-terminal helicase 1 /// BRCA1 interacting protein C-terminal helicase 1 | BRIP1 | 221703_at | 7.26 | 16.80 |
| brother of CDO | BOC | 224184_s_at | -4.69 | -3.56 |
| brother of CDO | BOC | 225990_at | -4.86 | -3.25 |
| BUB1 budding uninhibited by benzimidazoles 1 homolog (yeast) | BUB1 | 209642_at | 4.20 | 4.92 |
| BUB1 budding uninhibited by benzimidazoles 1 homolog (yeast) | BUB1 | 215509_s_at | 5.70 | 4.00 |
| BUB1 budding uninhibited by benzimidazoles 1 homolog beta (yeast) | BUB1B | 203755_at | 4.41 | 5.74 |
| butyrobetaine (gamma), 2-oxoglutarate dioxygenase (gamma-butyrobetaine hydroxylase) 1 | BBOX1 | 205363_at | -4.53 | -2.71 |
| C1GALT1-specific chaperone 1 | C1GALT1C1 | 238989_at | -2.19 | -2.13 |

| Gene title | Gene symbol | Affymetrix probe set ID | + 24 h sample_array 1 versus control_array 1 [fold change] | + 24 h sample_array 2 versus control_array 2 [fold change] |
|---|---|---|---|---|
| calcium channel, voltage-dependent, beta 2 subunit | CACNB2 | 213714_at | -2.07 | -3.23 |
| caldesmon 1 | CALD1 | 201615_x_at | 2.64 | 3.53 |
| caldesmon 1 | CALD1 | 201616_s_at | 2.23 | 3.07 |
| caldesmon 1 | CALD1 | 205525_at | 2.68 | 4.56 |
| calponin 1, basic, smooth muscle | CNN1 | 203951_at | 5.21 | 7.78 |
| calponin 2 | CNN2 | 201605_x_at | 2.07 | 2.14 |
| cAMP responsive element binding protein 3-like 1 | CREB3L1 | 213059_at | 2.71 | 3.34 |
| cancer susceptibility candidate 5 | CASC5 | 228323_at | 4.26 | 3.97 |
| CAP, adenylate cyclase-associated protein 1 (yeast) | CAP1 | 213798_s_at | 2.17 | 2.22 |
| CAP, adenylate cyclase-associated protein, 2 (yeast) | CAP2 | 212554_at | 3.48 | 4.47 |
| cartilage oligomeric matrix protein | COMP | 205713_s_at | -2.08 | -2.68 |
| Catalase | CAT | 238363_at | -3.78 | -2.87 |
| catalase /// catalase | CAT | 211922_s_at | -2.04 | -2.19 |
| catenin (cadherin-associated protein), alpha-like 1 | CTNNAL1 | 202468_s_at | 2.46 | 4.26 |
| cathepsin C | CTSC | 225646_at | -2.20 | -2.08 |
| Cbl-interacting protein Sts-1 | STS-1 | 238462_at | 2.83 | 7.94 |
| CCAAT/enhancer binding protein (C/EBP), gamma | CEBPG | 225527_at | -2.07 | -2.13 |
| CD24 antigen (small cell lung carcinoma cluster 4 antigen) | CD24 | 208650_s_at | 2.48 | 4.14 |
| CD24 antigen (small cell lung carcinoma cluster 4 antigen) | CD24 | 209771_x_at | 2.68 | 2.71 |
| CD24 antigen (small cell lung carcinoma cluster 4 antigen) | CD24 | 216379_x_at | 2.62 | 2.99 |
| CD24 antigen (small cell lung carcinoma cluster 4 antigen) | CD24 | 266_s_at | 2.33 | 3.01 |
| CD97 antigen | CD97 | 202910_s_at | 2.83 | 2.66 |
| CDC20 cell division cycle 20 homolog (S. cerevisiae) | CDC20 | 202870_s_at | 4.72 | 4.32 |
| CDC42 effector protein (Rho GTPase binding) 5 | CDC42EP5 | 227850_x_at | 2.23 | 2.60 |
| CDC6 cell division cycle 6 homolog (S. cerevisiae) | CDC6 | 203967_at | 4.50 | 6.32 |
| CDC6 cell division cycle 6 homolog (S. cerevisiae) | CDC6 | 203968_s_at | 4.44 | 5.50 |
| CDNA clone IMAGE:4184613, partial cds | --- | 225220_at | -2.36 | -2.41 |
| CDNA clone IMAGE:4514712, partial cds | --- | 217999_s_at | -2.68 | -4.79 |
| CDNA clone IMAGE:4514712, partial cds | --- | 225842_at | -2.99 | -2.68 |
| CDNA clone IMAGE:5263177, partial cds | --- | 228108_at | -3.27 | -4.66 |
| CDNA clone IMAGE:5263177, partial cds | --- | 228457_at | -4.89 | -4.79 |
| CDNA clone IMAGE:5263177, partial cds | --- | 229506_at | -3.81 | -4.76 |
| CDNA clone IMAGE:5286843, partial cds | --- | 235174_at | -2.31 | -2.97 |
| CDNA clone IMAGE:6724444, with apparent retained intron | --- | 235533_at | -2.41 | -2.07 |
| CDNA FLJ10145 fis, clone HEMBA1003322 | --- | 1557286_at | 3.05 | 3.03 |
| CDNA FLJ11381 fis, clone HEMBA1000501 | --- | 227350_at | 3.53 | 5.74 |
| CDNA FLJ13266 fis, clone OVARC1000960 | --- | 235274_at | -3.89 | -2.73 |
| CDNA FLJ14942 fis, A-PLACE1011185 | --- | 226223_at | 2.46 | 5.66 |
| CDNA FLJ26242 fis, clone DMC00770 | --- | 239262_at | -5.74 | -6.59 |
| CDNA FLJ30156 fis, clone BRACE2000487 | --- | 235134_at | -2.30 | -2.57 |
| CDNA FLJ30652 fis, clone DFNES2000011 | --- | 224811_at | 2.04 | 2.43 |
| CDNA FLJ34013 fis, clone FCBBF2002111 | --- | 225710_at | 3.20 | 3.10 |
| CDNA FLJ34374 fis, clone FEBRA2017502 | --- | 236856_x_at | 2.08 | 2.19 |
| CDNA FLJ34734 fis, clone MESAN2006971 | --- | 1558847_at | 2.14 | 3.41 |
| CDNA FLJ37828 fis, clone BRSSN2006575 | --- | 227719_at | 3.71 | 3.63 |
| CDNA FLJ39947 fis, clone SPLEN2024232 | --- | 1557116_at | -3.27 | -2.81 |
| CDNA FLJ44429 fis, clone UTERU2015653 | --- | 227061_at | 2.28 | 3.23 |
| CDNA FLJ44441 fis, clone UTERU2020242 | --- | 229121_at | 3.43 | 6.73 |
| CDNA: FLJ22631 fis, clone HSI06451 | --- | 1564358_at | -3.86 | -6.96 |
| cell adhesion molecule with homology to L1CAM (close homolog of L1) | CHL1 | 204591_at | -3.20 | -3.23 |
| Cell division cycle 2, G1 to S and G2 to M | CDC2 | 203213_at | 4.92 | 5.17 |
| cell division cycle 2, G1 to S and G2 to M | CDC2 | 203214_x_at | 5.13 | 4.99 |
| cell division cycle 2, G1 to S and G2 to M | CDC2 | 210559_s_at | 4.86 | 5.06 |
| cell division cycle associated 1 | CDCA1 | 223381_at | 4.99 | 6.82 |
| cell division cycle associated 3 | CDCA3 | 223307_at | 4.76 | 4.44 |
| cell division cycle associated 3 /// cell division cycle associated 3 | CDCA3 | 221436_s_at | 3.97 | 2.30 |
| cell division cycle associated 4 | CDCA4 | 218399_s_at | 2.66 | 2.04 |
| cell division cycle associated 5 | CDCA5 | 224753_at | 4.08 | 3.43 |
| cell division cycle associated 7 /// cell division cycle associated 7 | CDCA7 | 224428_s_at | 2.28 | 5.43 |
| cell division cycle associated 8 | CDCA8 | 221520_s_at | 11.47 | 20.39 |
| centromere protein A, 17kDa | CENPA | 204962_s_at | 4.03 | 3.94 |
| centromere protein E, 312kDa | CENPE | 205046_at | 3.73 | 3.58 |
| centromere protein F, 350/400ka (mitosin) | CENPF | 207828_s_at | 3.66 | 2.25 |
| ceruloplasmin (ferroxidase) | CP | 1558034_s_at | -3.16 | -3.18 |
| CG016 | LOC88523 | 214748_at | -2.04 | -2.53 |
| chemokine (C-X-C motif) ligand 12 (stromal cell-derived factor 1) | CXCL12 | 203666_at | -5.35 | -4.23 |

| Gene title | Gene symbol | Affymetrix probe set ID | + 24 h sample_array 1 versus control_array 1 [fold change] | + 24 h sample_array 2 versus control_array 2 [fold change] |
|---|---|---|---|---|
| chemokine (C-X-C motif) ligand 13 (B-cell chemoattractant) | CXCL13 | 205242_at | -2.43 | -2.06 |
| chemokine orphan receptor 1 | CMKOR1 | 212977_at | -2.91 | -3.48 |
| chitinase 3-like 1 (cartilage glycoprotein-39) | CHI3L1 | 209395_at | -2.30 | -4.47 |
| chitinase 3-like 1 (cartilage glycoprotein-39) | CHI3L1 | 209396_s_at | -2.58 | -5.31 |
| CHK1 checkpoint homolog (S. pombe) | CHEK1 | 205393_s_at | 3.86 | 2.66 |
| CHK1 checkpoint homolog (S. pombe) | CHEK1 | 205394_at | 2.62 | 2.68 |
| chloride channel 3 | CLCN3 | 201733_at | -2.11 | -2.43 |
| chloride channel 4 | CLCN4 | 205148_s_at | -2.39 | -2.85 |
| Chloride channel 4 | CLCN4 | 214769_at | -3.18 | -4.38 |
| Chloride channel 4 | CLCN4 | 217556_at | -2.95 | -4.50 |
| chloride intracellular channel 1 | CLIC1 | 208659_at | 2.75 | 2.11 |
| cholesterol 25-hydroxylase | CH25H | 206932_at | -2.57 | -2.87 |
| choline kinase alpha | CHKA | 204266_s_at | -2.20 | -2.17 |
| chondroitin sulfate proteoglycan 4 (melanoma-associated) | CSPG4 | 204736_s_at | 15.24 | 22.94 |
| choroideremia-like (Rab escort protein 2) | CHML | 1565951_s_at | 2.62 | 2.97 |
| choroideremia-like (Rab escort protein 2) | CHML | 226350_at | 2.38 | 2.91 |
| chromatin modifying protein 1B | CHMP1B | 218177_at | -2.11 | -2.20 |
| chromobox homolog 5 (HP1 alpha homolog, Drosophila) | CBX5 | 209715_at | 2.89 | 2.27 |
| chromosome 1 open reading frame 24 | C1orf24 | 217966_s_at | -6.15 | -6.45 |
| chromosome 1 open reading frame 24 | C1orf24 | 217967_s_at | -7.78 | -6.77 |
| chromosome 10 open reading frame 104 | C10orf104 | 224664_at | -2.06 | -2.07 |
| chromosome 10 open reading frame 104 | C10orf104 | 229145_at | -2.27 | -2.85 |
| chromosome 10 open reading frame 3 | C10orf3 | 218542_at | 6.15 | 6.82 |
| chromosome 10 open reading frame 45 | C10orf45 | 223058_at | -2.46 | -2.08 |
| chromosome 15 open reading frame 17 | C15orf17 | 224798_s_at | -2.43 | -2.46 |
| chromosome 16 open reading frame 34 | C16orf34 | 212115_at | 2.45 | 2.36 |
| chromosome 18 open reading frame 54 | C18orf54 | 229442_at | 2.41 | 2.22 |
| Chromosome 18 open reading frame 54 | C18orf54 | 241733_at | 2.89 | 2.36 |
| chromosome 19 open reading frame 12 | C19orf12 | 223983_s_at | -2.31 | -2.08 |
| chromosome 19 open reading frame 12 | C19orf12 | 225863_s_at | -2.57 | -2.33 |
| Chromosome 19 open reading frame 12 | C19orf12 | 227704_at | -3.05 | -2.08 |
| chromosome 20 open reading frame 129 | C20orf129 | 225687_at | 5.31 | 6.23 |
| chromosome 20 open reading frame 139 | C20orf139 | 225252_at | -2.51 | -2.25 |
| chromosome 20 open reading frame 172 | C20orf172 | 219512_at | 2.55 | 2.31 |
| chromosome 20 open reading frame 35 | C20orf35 | 218094_s_at | 4.06 | 4.76 |
| chromosome 20 open reading frame 59 | C20orf59 | 219559_at | 3.43 | 3.07 |
| chromosome 21 open reading frame 5 | C21orf5 | 205248_at | 2.71 | 3.14 |
| chromosome 21 open reading frame 7 | C21orf7 | 221211_s_at | 3.56 | 3.14 |
| chromosome 5 open reading frame 13 | C5orf13 | 201309_x_at | 4.82 | 4.63 |
| chromosome 5 open reading frame 13 | C5orf13 | 201310_s_at | 4.03 | 3.61 |
| Chromosome 5 open reading frame 13 | C5orf13 | 222344_at | 7.11 | 9.78 |
| chromosome 5 open reading frame 13 | C5orf13 | 230424_at | 3.81 | 3.92 |
| chromosome 6 open reading frame 115 | C6orf115 | 223361_at | 2.46 | 2.41 |
| chromosome 6 open reading frame 173 | C6orf173 | 226936_at | 2.85 | 3.14 |
| Chromosome 6 open reading frame 188 | C6orf188 | 230254_at | 2.35 | 2.45 |
| Chromosome 6 open reading frame 188 | C6orf188 | 232217_at | 2.46 | 2.95 |
| chromosome 6 open reading frame 32 | C6orf32 | 209829_at | -6.06 | -4.47 |
| Chromosome 6 open reading frame 66 | C6orf66 | 227559_at | -2.01 | -2.55 |
| chromosome 6 open reading frame 85 | C6orf85 | 223194_s_at | -3.25 | -5.24 |
| chromosome 7 open reading frame 10 | C7orf10 | 219655_at | 2.68 | 2.83 |
| Chromosome 9 open reading frame 3 | C9orf3 | 232270_at | 2.45 | 2.20 |
| chromosome 9 open reading frame 88 | C9orf88 | 223019_at | 2.20 | 2.45 |
| chromosome condensation protein G | HCAP-G | 218662_s_at | 4.29 | 4.29 |
| chromosome condensation protein G | HCAP-G | 218663_at | 4.44 | 6.50 |
| citron (rho-interacting, serine/threonine kinase 21) | CIT | 212801_at | 2.14 | 2.13 |
| claudin 23 | CLDN23 | 228706_s_at | -4.56 | -2.57 |
| claudin 23 | CLDN23 | 228707_at | -4.23 | -5.43 |
| Clock homolog (mouse) | CLOCK | 230657_at | -2.46 | -2.33 |
| cofilin 2 (muscle) | CFL2 | 224663_s_at | 2.00 | 2.28 |
| cofilin 2 (muscle) | CFL2 | 233496_s_at | 2.14 | 2.45 |
| cold inducible RNA binding protein | CIRBP | 225191_at | -2.06 | -2.04 |
| collagen, type IV, alpha 3 (Goodpasture antigen) binding protein | COL4A3BP | 219625_s_at | -2.66 | -3.10 |
| collagen, type IV, alpha 3 (Goodpasture antigen) binding protein | COL4A3BP | 223465_at | -2.23 | -3.12 |
| collagen, type IV, alpha 3 (Goodpasture antigen) binding protein | COL4A3BP | 223466_x_at | -2.08 | -2.97 |
| Collagen, type IV, alpha 3 (Goodpasture antigen) binding protein | COL4A3BP | 226277_at | -2.30 | -3.05 |
| collagen, type VIII, alpha 1 | COL8A1 | 214587_at | 3.36 | 11.55 |
| Collagen, type VIII, alpha 1 | COL8A1 | 226237_at | 3.05 | 9.19 |
| Collagen, type XI, alpha 1 | COL11A1 | 232805_at | 3.29 | 3.39 |

| Gene title | Gene symbol | Affymetrix probe set ID | + 24 h sample_array 1 versus control_array 1 [fold change] | + 24 h sample_array 2 versus control_array 2 [fold change] |
|---|---|---|---|---|
| connective tissue growth factor | CTGF | 209101_at | 2.48 | 10.85 |
| C-type lectin domain family 3, member B | CLEC3B | 205200_at | 3.46 | 5.31 |
| CUE domain containing 1 | CUEDC1 | 219468_s_at | 2.27 | 2.60 |
| cyclin A2 | CCNA2 | 203418_at | 4.41 | 4.14 |
| Cyclin A2 | CCNA2 | 213226_at | 3.58 | 4.23 |
| cyclin B1 | CCNB1 | 214710_s_at | 3.86 | 3.56 |
| cyclin B1 | CCNB1 | 228729_at | 3.89 | 4.59 |
| cyclin B2 | CCNB2 | 202705_at | 4.47 | 4.56 |
| cyclin D1 (PRAD1: parathyroid adenomatosis 1) | CCND1 | 208711_s_at | 2.73 | 5.13 |
| cyclin D1 (PRAD1: parathyroid adenomatosis 1) | CCND1 | 208712_at | 3.29 | 5.78 |
| cyclin D3 | CCND3 | 201700_at | 2.08 | 2.23 |
| cyclin E2 | CCNE2 | 205034_at | 5.78 | 10.70 |
| cyclin E2 | CCNE2 | 211814_s_at | 5.90 | 19.43 |
| cyclin-dependent kinase 2 | CDK2 | 204252_at | 2.75 | 2.58 |
| cyclin-dependent kinase 6 | CDK6 | 224847_at | 3.03 | 3.58 |
| cyclin-dependent kinase 6 | CDK6 | 224848_at | 2.81 | 2.99 |
| cyclin-dependent kinase 6 | CDK6 | 224851_at | 3.16 | 3.84 |
| cyclin-dependent kinase 6 | CDK6 | 235287_at | 3.68 | 3.32 |
| cyclin-dependent kinase inhibitor 3 (CDK2-associated dual specificity phosphatase) | CDKN3 | 1555758_a_at | 2.89 | 3.14 |
| cyclin-dependent kinase inhibitor 3 (CDK2-associated dual specificity phosphatase) | CDKN3 | 209714_s_at | 2.81 | 3.12 |
| cystathionase (cystathionine gamma-lyase) | CTH | 217127_at | -3.61 | -2.39 |
| cysteine and glycine-rich protein 1 | CSRP1 | 200621_at | 2.10 | 3.63 |
| cysteine and glycine-rich protein 2 | CSRP2 | 207030_s_at | 3.41 | 3.10 |
| cysteine and glycine-rich protein 2 | CSRP2 | 211126_s_at | 2.75 | 3.01 |
| Cysteine dioxygenase, type I | CDO1 | 243706_at | -2.30 | -3.25 |
| cysteine sulfinic acid decarboxylase | CSAD | 221139_s_at | -2.95 | -3.14 |
| Cysteine-rich motor neuron 1 | CRIM1 | 233073_at | 3.23 | 2.07 |
| cysteine-rich protein 2 | CRIP2 | 208978_at | 3.46 | 4.29 |
| cysteine-rich, angiogenic inducer, 61 | CYR61 | 201289_at | 2.50 | 9.65 |
| cysteine-rich, angiogenic inducer, 61 | CYR61 | 210764_s_at | 3.14 | 13.64 |
| cytidine monophosphate-N-acetylneuraminic acid hydroxylase (CMP-N-acetylneuraminate monooxygenase) | CMAH | 205518_s_at | 3.23 | 4.06 |
| cytidine monophosphate-N-acetylneuraminic acid hydroxylase (CMP-N-acetylneuraminate monooxygenase) | CMAH | 210571_s_at | 3.36 | 3.03 |
| cytochrome b, ascorbate dependent 3 | CYBASC3 | 224735_at | -2.20 | -3.66 |
| cytochrome b-561 | CYB561 | 209163_at | 2.23 | 2.46 |
| cytochrome c, somatic | CYCS | 229415_at | -2.48 | -3.46 |
| cytochrome c, somatic | CYCS | 244546_at | -2.11 | -3.27 |
| cytochrome P450, family 1, subfamily B, polypeptide 1 | CYP1B1 | 202434_s_at | -3.48 | -6.15 |
| cytochrome P450, family 1, subfamily B, polypeptide 1 | CYP1B1 | 202435_s_at | -2.20 | -2.97 |
| cytoskeleton associated protein 2 | CKAP2 | 218252_at | 2.07 | 2.81 |
| dapper homolog 1, antagonist of beta-catenin (xenopus) | DACT1 | 219179_at | 3.51 | 2.57 |
| death-associated protein kinase 3 | DAPK3 | 203890_s_at | 2.25 | 2.53 |
| decay accelerating factor for complement (CD55, Cromer blood group system) | DAF | 1555950_a_at | -2.38 | -2.13 |
| dedicator of cytokinesis 10 | DOCK10 | 219279_at | 5.62 | 5.17 |
| dedicator of cytokinesis 11 | DOCK11 | 226875_at | -4.92 | -4.53 |
| dedicator of cytokinesis 11 | DOCK11 | 238356_at | -6.63 | -3.36 |
| dehydrogenase/reductase (SDR family) member 3 | DHRS3 | 202481_at | -3.12 | -3.20 |
| deoxycytidine kinase | DCK | 203302_at | 2.13 | 2.53 |
| DEP domain containing 1 | DEPDC1 | 220295_x_at | 5.21 | 3.92 |
| DEP domain containing 1 | DEPDC1 | 222958_s_at | 6.15 | 5.31 |
| DEP domain containing 1 | DEPDC1 | 232278_s_at | 4.69 | 6.19 |
| DEP domain containing 1 | DEPDC1 | 235545_at | 2.62 | 5.70 |
| desmoplakin | DSP | 200606_at | 3.53 | 5.24 |
| diaphanous homolog 1 (Drosophila) | DIAPH1 | 209190_s_at | 3.89 | 3.58 |
| differential display and activated by p53 | DDA3 | 201896_s_at | 3.27 | 2.62 |
| dihydrofolate reductase-like 1 | DHFRL1 | 235675_at | -2.07 | -2.04 |
| dimethylarginine dimethylaminohydrolase 1 | DDAH1 | 1553565_s_at | 5.24 | 11.08 |
| dimethylarginine dimethylaminohydrolase 1 | DDAH1 | 209094_at | 3.10 | 8.17 |
| Dimethylarginine dimethylaminohydrolase 1 | DDAH1 | 229456_s_at | 2.85 | 6.28 |
| DIRAS family, GTP-binding RAS-like 3 | DIRAS3 | 215506_s_at | 3.48 | 5.43 |
| discoidin, CUB and LCCL domain containing 1 | DCBLD1 | 226609_at | 2.16 | 2.87 |
| discs, large homolog 7 (Drosophila) | DLG7 | 203764_at | 4.06 | 4.03 |
| distal-less homeo box 1 | DLX1 | 242138_at | 2.48 | 2.00 |
| DKFZP434C171 protein | DKFZP434C171 | 1553102_a_at | -2.46 | -3.18 |
| DKFZP434C171 protein | DKFZP434C171 | 212886_at | -2.36 | -2.69 |
| DNA cross-link repair 1B (PSO2 homolog, S. cerevisiae) | DCLRE1B | 222889_at | 2.23 | 3.23 |
| DNA replication complex GINS protein PSF2 | Pfs2 | 221521_s_at | 5.62 | 4.82 |

| Gene title | Gene symbol | Affymetrix probe set ID | + 24 h sample_array 1 versus control_array 1 [fold change] | + 24 h sample_array 2 versus control_array 2 [fold change] |
|---|---|---|---|---|
| DNA-damage-inducible transcript 3 | DDIT3 | 209383_at | -5.94 | -8.82 |
| DNA-damage-inducible transcript 4 | DDIT4 | 202887_s_at | -4.79 | -8.51 |
| DNA-damage-inducible transcript 4-like | DDIT4L | 228057_at | -7.46 | -7.67 |
| DnaJ (Hsp40) homolog, subfamily B, member 4 | DNAJB4 | 203810_at | 2.43 | 2.73 |
| DnaJ (Hsp40) homolog, subfamily B, member 4 | DNAJB4 | 203811_s_at | 3.29 | 2.45 |
| DnaJ (Hsp40) homolog, subfamily C, member 9 | DNAJC9 | 213088_s_at | 2.71 | 2.89 |
| DnaJ (Hsp40) homolog, subfamily C, member 9 | DNAJC9 | 213092_x_at | 3.32 | 3.14 |
| Doublecortin and CaM kinase-like 1 | DCAMKL1 | 229800_at | 3.39 | 2.25 |
| downstream neighbor of SON | DONSON | 221677_s_at | 2.28 | 2.58 |
| DRE1 protein | DRE1 | 221986_s_at | -2.08 | -3.23 |
| drebrin 1 | DBN1 | 202806_at | 2.31 | 2.46 |
| drebrin 1 | DBN1 | 217025_s_at | 2.22 | 2.81 |
| Dual specificity phosphatase 7 | DUSP7 | 213848_at | 2.81 | 3.23 |
| dystrobrevin, alpha | DTNA | 205741_s_at | 4.08 | 8.00 |
| dystrobrevin, alpha | DTNA | 227084_at | 2.30 | 2.83 |
| E2F transcription factor 7 | E2F7 | 228033_at | 2.89 | 2.28 |
| E74-like factor 4 (ets domain transcription factor) | ELF4 | 31845_at | 2.16 | 2.10 |
| Early B-cell factor | EBF | 227646_at | -2.28 | -2.81 |
| Early B-cell factor | EBF | 229487_at | -2.35 | -3.01 |
| early B-cell factor | EBF | 232204_at | -2.43 | -2.93 |
| Early B-cell factor | EBF | 233261_at | -2.01 | -2.57 |
| Early growth response 1 | EGR1 | 227404_s_at | 5.17 | 4.50 |
| ecotropic viral integration site 2A | EVI2A | 204774_at | -4.66 | -7.57 |
| EF hand domain family, member D1 | EFHD1 | 209343_at | 3.05 | 3.39 |
| EGF, latrophilin and seven transmembrane domain containing 1 | ELTD1 | 219134_at | 2.03 | 3.84 |
| EH domain binding protein 1-like 1 | EHBP1L1 | 221755_at | 20.25 | 5.24 |
| EH domain binding protein 1-like 1 | EHBP1L1 | 91703_at | 3.48 | 3.92 |
| EH-domain containing 1 | EHD1 | 209037_s_at | 2.83 | 3.32 |
| EH-domain containing 1 | EHD1 | 209039_x_at | 3.63 | 2.25 |
| EH-domain containing 1 | EHD1 | 222221_x_at | 3.46 | 3.39 |
| EH-domain containing 4 | EHD4 | 209536_s_at | 3.16 | 5.66 |
| EH-domain containing 4 | EHD4 | 229074_at | 3.29 | 5.28 |
| EH-domain containing 4 | EHD4 | 233660_at | 2.50 | 2.36 |
| embryonal Fyn-associated substrate | EFS | 204400_at | 2.71 | 2.62 |
| endothelial differentiation, sphingolipid G-protein-coupled receptor, 3 | EDG3 | 228176_at | -3.58 | -3.05 |
| endothelin receptor type B | EDNRB | 204271_s_at | -2.64 | -2.36 |
| endothelin receptor type B | EDNRB | 204273_at | -4.17 | -3.01 |
| endothelin receptor type B | EDNRB | 206701_x_at | -2.93 | -2.45 |
| enolase 1, (alpha) | ENO1 | 240258_at | -8.75 | -2.14 |
| EPH receptor A2 | EPHA2 | 203499_at | 3.07 | 3.51 |
| ephrin-B2 | EFNB2 | 202668_at | 2.14 | 3.81 |
| ephrin-B2 | EFNB2 | 202669_s_at | 2.08 | 2.85 |
| epithelial cell transforming sequence 2 oncogene | ECT2 | 219787_s_at | 2.64 | 5.03 |
| epithelial membrane protein 1 | EMP1 | 213895_at | 3.27 | 2.99 |
| epithelial membrane protein 2 | EMP2 | 225078_at | -2.13 | -3.23 |
| erythrocyte membrane protein band 4.1-like 2 | EPB41L2 | 201718_s_at | 2.17 | 2.46 |
| erythrocyte membrane protein band 4.1-like 2 | EPB41L2 | 201719_s_at | 3.14 | 2.58 |
| erythrocyte membrane protein band 4.1-like 3 | EPB41L3 | 206710_s_at | -6.50 | -4.03 |
| erythrocyte membrane protein band 4.1-like 3 | EPB41L3 | 212681_at | -7.67 | -4.03 |
| erythrocyte membrane protein band 4.1-like 3 /// erythrocyte membrane protein band 4.1-like 3 | EPB41L3 | 211776_s_at | -6.59 | -3.43 |
| exonuclease NEF-sp /// exonuclease NEF-sp | LOC81691 | 208107_s_at | 2.55 | 3.12 |
| Exosome component 6 | EXOSC6 | 227696_at | -2.16 | -2.64 |
| exosome component 9 | EXOSC9 | 205061_s_at | 2.06 | 3.01 |
| Exportin 1 (CRM1 homolog, yeast) | XPO1 | 230729_at | -2.11 | -2.35 |
| extra spindle poles like 1 (S. cerevisiae) | ESPL1 | 38158_at | 2.43 | 2.22 |
| family with sequence similarity 13, member A1 | FAM13A1 | 202972_at | -2.68 | -2.25 |
| family with sequence similarity 13, member A1 | FAM13A1 | 202973_x_at | -2.38 | -2.33 |
| family with sequence similarity 13, member A1 | FAM13A1 | 217047_s_at | -2.46 | -2.22 |
| family with sequence similarity 20, member A | FAM20A | 241981_at | -2.25 | -2.89 |
| family with sequence similarity 43, member A | FAM43A | 227410_at | -3.78 | -7.11 |
| family with sequence similarity 46, member B | FAM46B | 229518_at | 3.16 | 5.78 |
| family with sequence similarity 54, member A | FAM54A | 228069_at | 3.12 | 4.03 |
| fascin homolog 1, actin-bundling protein (Strongylocentrotus purpuratus) | FSCN1 | 201564_s_at | 4.50 | 5.74 |
| fascin homolog 1, actin-bundling protein (Strongylocentrotus purpuratus) | FSCN1 | 210933_s_at | 3.56 | 3.36 |
| fatty acid desaturase 1 | FADS1 | 208963_x_at | -2.25 | -4.20 |
| F-box and leucine-rich repeat protein 5 | FBXL5 | 209004_s_at | 2.16 | 2.39 |
| F-box and leucine-rich repeat protein 5 | FBXL5 | 209005_at | 2.71 | 2.85 |
| F-box protein 5 | FBXO5 | 218875_s_at | 3.71 | 4.38 |
| F-box protein 5 | FBXO5 | 234863_x_at | 3.43 | 4.14 |

| Gene title | Gene symbol | Affymetrix probe set ID | + 24 h sample_array 1 versus control_array 1 [fold change] | + 24 h sample_array 2 versus control_array 2 [fold change] |
|---|---|---|---|---|
| fibroblast growth factor 1 (acidic) | FGF1 | 1552721_a_at | 7.62 | 16.22 |
| fibroblast growth factor 1 (acidic) | FGF1 | 205117_at | 6.19 | 22.32 |
| fibroblast growth factor 5 | FGF5 | 208378_x_at | 2.79 | 29.86 |
| fibronectin 1 | FN1 | 1558199_at | 3.43 | 3.53 |
| fibronectin 1 | FN1 | 214702_at | 2.62 | 2.50 |
| Fibronectin 1 | FN1 | 235629_at | 3.56 | 3.61 |
| fibronectin leucine rich transmembrane protein 2 | FLRT2 | 204359_at | -2.03 | -2.99 |
| fidgetin-like 1 | FIGNL1 | 222843_at | 2.48 | 3.46 |
| filamin-binding LIM protein-1 | FBLP-1 | 1555480_a_at | 3.05 | 2.48 |
| flap structure-specific endonuclease 1 | FEN1 | 204767_s_at | 3.01 | 3.12 |
| flap structure-specific endonuclease 1 | FEN1 | 204768_s_at | 3.25 | 3.25 |
| FLJ20160 protein | FLJ20160 | 225325_at | 2.27 | 2.07 |
| FLJ22794 protein | FLJ22794 | 218248_at | 2.66 | 2.11 |
| FLJ23311 protein | FLJ23311 | 219990_at | 4.69 | 16.68 |
| FLJ35696 protein | FLJ35696 | 227963_at | -4.23 | -2.99 |
| follistatin | FST | 204948_s_at | 2.25 | 3.23 |
| follistatin-like 3 (secreted glycoprotein) | FSTL3 | 203592_s_at | 2.11 | 3.48 |
| Forkhead box C2 (MFH-1, mesenchyme forkhead 1) | FOXC2 | 239058_at | 3.76 | 3.07 |
| forkhead box M1 | FOXM1 | 202580_x_at | 3.10 | 3.39 |
| formin 2 | FMN2 | 1555471_a_at | 8.46 | 29.24 |
| formin 2 | FMN2 | 223618_at | 8.51 | 10.56 |
| formyl peptide receptor 1 /// formyl peptide receptor 1 | FPR1 | 205119_s_at | 2.17 | 2.00 |
| four and a half LIM domains 3 | FHL3 | 218818_at | 2.50 | 2.46 |
| frizzled homolog 4 (Drosophila) | FZD4 | 218665_at | -3.03 | -3.84 |
| FSH primary response (LRPR1 homolog, rat) 1 | FSHPRH1 | 214804_at | 4.96 | 4.17 |
| Full length insert cDNA clone ZD42A08 | --- | 227526_at | -2.19 | -2.51 |
| Full length insert cDNA YH77E09 | --- | 213750_at | -2.58 | -3.39 |
| Full open reading frame cDNA clone RZPDo834C0824D for gene HIST2H4, histone 2, H4; complete cds, incl. stopcodon | --- | 230795_at | -4.59 | -7.11 |
| Full-length cDNA clone CS0DI029YI16 of Placenta Cot 25-normalized of Homo sapiens (human) /// Homo sapiens, clone IMAGE:5249006, mRNA | --- | 241745_at | -2.55 | -3.84 |
| fusion (involved in t(12;16) in malignant liposarcoma) | FUS | 200959_at | 2.01 | 2.01 |
| G kinase anchoring protein 1 | GKAP1 | 234192_s_at | -4.29 | -2.01 |
| G-2 and S-phase expressed 1 | GTSE1 | 204318_s_at | 4.47 | 5.43 |
| G-2 and S-phase expressed 1 | GTSE1 | 215942_s_at | 12.38 | 2.58 |
| GA binding protein transcription factor, beta subunit 2, 47kDa | GABPB2 | 227406_at | -2.48 | -2.19 |
| GABA(A) receptor-associated protein like 1 /// GABA(A) receptors associated protein like 3 | GABARAPL1 /// GABARAPL3 | 211458_s_at | -2.03 | -2.19 |
| GAJ protein | GAJ | 223700_at | 2.73 | 3.63 |
| galactose mutarotase (aldose 1-epimerase) | GALM | 235256_s_at | -3.73 | -2.14 |
| GDP-mannose pyrophosphorylase B | GMPPB | 219920_s_at | 2.08 | 3.14 |
| GLI pathogenesis-related 1 (glioma) | GLIPR1 | 204221_x_at | 2.38 | 2.85 |
| GLI pathogenesis-related 1 (glioma) | GLIPR1 | 204222_s_at | 2.95 | 3.12 |
| GLI pathogenesis-related 1 (glioma) | GLIPR1 | 214085_x_at | 2.38 | 2.51 |
| GLI pathogenesis-related 1 (glioma) | GLIPR1 | 226142_at | 2.13 | 2.97 |
| glucocorticoid induced transcript 1 | GLCCI1 | 227525_at | -2.16 | -2.35 |
| glucosaminyl (N-acetyl) transferase 1, core 2 (beta-1,6-N-acetylglucosaminyltransferase) | GCNT1 | 205505_at | 2.66 | 5.35 |
| glucosaminyl (N-acetyl) transferase 1, core 2 (beta-1,6-N-acetylglucosaminyltransferase) | GCNT1 | 239761_at | 2.95 | 4.69 |
| Glutamate-cysteine ligase, modifier subunit | GCLM | 234986_at | -3.63 | -2.85 |
| glutamic pyruvate transaminase (alanine aminotransferase) 2 | GPT2 | 224839_s_at | -2.11 | -2.14 |
| glutaminase | GLS | 221510_s_at | 2.31 | 2.81 |
| glutaminase | GLS | 223079_s_at | 3.16 | 3.27 |
| glycerol-3-phosphate acyltransferase, mitochondrial | GPAM | 225420_at | -2.43 | -3.34 |
| glycerol-3-phosphate acyltransferase, mitochondrial | GPAM | 225424_at | -2.16 | -3.07 |
| glycerol-3-phosphate dehydrogenase 1 (soluble) | GPD1 | 204997_at | -2.38 | -3.68 |
| glycogenin 2 | GYG2 | 210963_s_at | -2.48 | -2.11 |
| glycogenin 2 | GYG2 | 210964_s_at | -2.38 | -2.60 |
| glycogenin 2 | GYG2 | 215695_s_at | -2.48 | -2.27 |
| glycoprotein M6B | GPM6B | 209167_at | 2.39 | 2.55 |
| glycoprotein M6B | GPM6B | 209168_at | 2.27 | 3.29 |
| glycoprotein M6B | GPM6B | 209169_at | 3.34 | 3.97 |
| glycoprotein M6B | GPM6B | 209170_s_at | 2.27 | 2.68 |
| gremlin 2 homolog, cysteine knot superfamily (Xenopus laevis) | GREM2 | 220794_at | 4.03 | 3.23 |
| Gremlin 2 homolog, cysteine knot superfamily (Xenopus laevis) | GREM2 | 240509_s_at | 11.55 | 18.77 |
| growth and transformation-dependent protein | E2IG5 | 220942_x_at | -2.25 | -2.07 |
| growth and transformation-dependent protein | E2IG5 | 223193_x_at | -2.20 | -2.16 |
| growth and transformation-dependent protein /// growth | E2IG5 | 224345_x_at | -2.17 | -2.10 |

| Gene title | Gene symbol | Affymetrix probe set ID | + 24 h sample_array 1 versus control_array 1 [fold change] | + 24 h sample_array 2 versus control_array 2 [fold change] |
|---|---|---|---|---|
| and transformation-dependent protein | | | | |
| growth arrest-specific 5 | GAS5 | 224741_x_at | -2.16 | -3.07 |
| growth arrest-specific 5 | GAS5 | 224841_x_at | -2.17 | -3.14 |
| growth differentiation factor 15 | GDF15 | 221577_x_at | -8.57 | -5.98 |
| growth hormone receptor | GHR | 205498_at | -2.55 | -2.35 |
| GTP binding protein overexpressed in skeletal muscle | GEM | 204472_at | -2.48 | -2.17 |
| guanine nucleotide binding protein (G protein), beta polypeptide 4 | GNB4 | 223488_s_at | 3.16 | 2.64 |
| guanylate binding protein 1, interferon-inducible, 67kDa | GBP1 | 231577_s_at | 2.99 | 4.53 |
| guanylate binding protein 1, interferon-inducible, 67kDa /// guanylate binding protein 1, interferon-inducible, 67kDa | GBP1 | 202269_x_at | 3.03 | 3.63 |
| guanylate binding protein 1, interferon-inducible, 67kDa /// guanylate binding protein 1, interferon-inducible, 67kDa | GBP1 | 202270_at | 2.75 | 5.50 |
| guanylate binding protein 3 | GBP3 | 223434_at | 2.20 | 2.60 |
| H2A histone family, member X | H2AFX | 205436_s_at | 2.30 | 2.36 |
| HCV NS3-transactivated protein 2 | NS3TP2 | 218706_s_at | 3.84 | 4.32 |
| HCV NS3-transactivated protein 2 | NS3TP2 | 238049_at | 2.50 | 2.00 |
| heat shock 27kDa protein 1 | HSPB1 | 201841_s_at | 2.51 | 2.43 |
| heat shock 27kDa protein 2 | HSPB2 | 205824_at | 2.68 | 3.23 |
| helicase, lymphoid-specific | HELLS | 220085_at | 2.11 | 3.73 |
| helicase, lymphoid-specific | HELLS | 223556_at | 2.06 | 5.35 |
| heme oxygenase (decycling) 1 | HMOX1 | 203665_at | -2.41 | -11.96 |
| heparan sulfate (glucosamine) 3-O-sulfotransferase 2 | HS3ST2 | 219697_at | -2.71 | -2.41 |
| hepatic leukemia factor | HLF | 204753_s_at | -5.54 | -3.48 |
| hepatic leukemia factor | HLF | 204755_x_at | -3.97 | -2.03 |
| heterogeneous nuclear ribonucleoprotein D (AU-rich element RNA binding protein 1, 37kDa) | HNRPD | 221480_at | 2.53 | 2.57 |
| hexokinase 2 | HK2 | 202934_at | -2.10 | -4.17 |
| high mobility group AT-hook 2 /// high mobility group AT-hook 2 | HMGA2 | 208025_s_at | 2.87 | 3.36 |
| histone deacetylase 9 | HDAC9 | 205659_at | 2.89 | 8.17 |
| Homo sapiens, clone IMAGE:3344506, mRNA, partial cds | --- | 216189_at | -5.24 | -3.63 |
| Homo sapiens, clone IMAGE:3881549, mRNA | --- | 226034_at | -2.04 | -3.12 |
| Homo sapiens, clone IMAGE:4096273, mRNA | --- | 1555832_s_at | 2.69 | 2.91 |
| Homo sapiens, clone IMAGE:4096273, mRNA | --- | 224606_at | 2.58 | 2.68 |
| Homo sapiens, clone IMAGE:4285253, mRNA | --- | 1562098_at | 3.43 | 2.19 |
| Homo sapiens, clone IMAGE:4403366, mRNA, partial cds | --- | 1558404_at | -10.63 | -4.44 |
| Homo sapiens, clone IMAGE:4794011, mRNA | --- | 226873_at | 2.39 | 3.03 |
| Homo sapiens, clone IMAGE:4819775, mRNA | --- | 1558605_at | -2.30 | -2.51 |
| Homo sapiens, clone IMAGE:5218412, mRNA | --- | 235152_at | 2.17 | 2.11 |
| Homo sapiens, clone IMAGE:5403381, mRNA | --- | 1561418_at | 2.81 | 17.15 |
| Homo sapiens, Similar to diaphanous homolog 3 (Drosophila), clone IMAGE:5277415, mRNA | --- | 229097_at | 5.98 | 7.11 |
| Homo sapiens, Similar to hypothetical protein FLJ20489, clone IMAGE:5261717, mRNA | --- | 1568983_a_at | -3.18 | -2.85 |
| HRAS-like suppressor 3 | HRASLS3 | 209581_at | -2.22 | -2.41 |
| huntingtin interacting protein 1 | HIP1 | 205425_at | 2.00 | 2.10 |
| Huntingtin interacting protein 1 | HIP1 | 226364_at | 2.28 | 2.19 |
| hyaluronan and proteoglycan link protein 1 | HAPLN1 | 205523_at | 4.17 | 16.68 |
| hyaluronan and proteoglycan link protein 1 | HAPLN1 | 205524_s_at | 3.94 | 15.45 |
| Hyaluronan and proteoglycan link protein 1 | HAPLN1 | 230204_at | 2.45 | 4.63 |
| hyaluronan synthase 3 | HAS3 | 223541_at | 2.81 | 2.48 |
| hyaluronan-mediated motility receptor (RHAMM) | HMMR | 207165_at | 5.43 | 6.15 |
| hyaluronan-mediated motility receptor (RHAMM) | HMMR | 209709_s_at | 4.47 | 4.00 |
| hydroxy-delta-5-steroid dehydrogenase, 3 beta- and steroid delta-isomerase 7 | HSD3B7 | 222817_at | 3.14 | 3.43 |
| hydroxysteroid (17-beta) dehydrogenase 6 | HSD17B6 | 37512_at | 10.41 | 13.36 |
| hypothetical gene supported by AL713721 | LOC441109 | 230405_at | -3.27 | -3.20 |
| Hypothetical gene supported by BC008048 | --- | 238727_at | -2.89 | -7.41 |
| hypothetical gene supported by BC009447 | MGC15887 | 226448_at | -2.48 | -2.13 |
| hypothetical gene supported by BC013438 | LOC375295 | 228564_at | 2.57 | 2.19 |
| Hypothetical LOC285711 | --- | 1564474_at | -2.79 | -7.06 |
| Hypothetical LOC344887 | --- | 241418_at | -2.55 | -2.17 |
| Hypothetical LOC401093 | --- | 232298_at | 3.12 | 3.94 |
| hypothetical LOC401093 | LOC401093 | 235173_at | 2.97 | 2.43 |
| hypothetical protein | LOC387882 | 225105_at | 2.69 | 2.99 |
| hypothetical protein BC007901 | LOC91461 | 225380_at | -2.62 | -3.12 |
| hypothetical protein CG003 | 13CDNA73 | 204072_s_at | 3.66 | 5.94 |
| hypothetical protein DKFZP761M1511 | DKFZP761M1511 | 225355_at | 3.29 | 4.38 |
| hypothetical protein DKFZp761O2018 | DKFZp761O2018 | 232313_at | -3.05 | -2.22 |
| hypothetical protein DKFZp762C1112 | DKFZp762C1112 | 242338_at | -2.39 | -2.22 |

| Gene title | Gene symbol | Affymetrix probe set ID | + 24 h sample_array 1 versus control_array 1 [fold change] | + 24 h sample_array 2 versus control_array 2 [fold change] |
|---|---|---|---|---|
| hypothetical protein DKFZp762E1312 | DKFZp762E1312 | 218726_at | 4.11 | 6.06 |
| hypothetical protein FLJ10094 | FLJ10094 | 219501_at | -2.85 | -2.13 |
| hypothetical protein FLJ10156 | FLJ10156 | 221591_s_at | 4.29 | 3.32 |
| hypothetical protein FLJ10719 | FLJ10719 | 213007_at | 2.45 | 3.27 |
| hypothetical protein FLJ10719 | FLJ10719 | 213008_at | 4.69 | 3.25 |
| hypothetical protein FLJ11000 | FLJ11000 | 218999_at | -4.99 | -4.20 |
| Hypothetical protein FLJ11029 | FLJ11029 | 228273_at | 4.41 | 4.50 |
| hypothetical protein FLJ11151 | FLJ11151 | 222686_s_at | 2.35 | 3.07 |
| hypothetical protein FLJ11336 | FLJ11336 | 205796_at | 2.13 | 2.41 |
| hypothetical protein FLJ13391 | FLJ13391 | 227828_s_at | 4.11 | 19.43 |
| Hypothetical protein FLJ13710 | FLJ13710 | 222835_at | 2.77 | 5.86 |
| hypothetical protein FLJ13912 | FLJ13912 | 45633_at | 2.36 | 3.01 |
| hypothetical protein FLJ20364 | FLJ20364 | 221685_s_at | 2.60 | 2.30 |
| hypothetical protein FLJ20920 | FLJ20920 | 218844_at | -2.69 | -2.95 |
| hypothetical protein FLJ21062 | FLJ21062 | 1554919_s_at | -6.54 | -3.03 |
| hypothetical protein FLJ21062 | FLJ21062 | 219455_at | -8.46 | -3.78 |
| hypothetical protein FLJ22104 | FLJ22104 | 222209_s_at | -2.60 | -2.75 |
| hypothetical protein FLJ22390 | FLJ22390 | 218865_at | -2.30 | -2.45 |
| hypothetical protein FLJ32549 | FLJ32549 | 1554067_at | -2.06 | -2.06 |
| hypothetical protein FLJ34922 | FLJ34922 | 226743_at | 3.58 | 3.36 |
| hypothetical protein FLJ37034 | FLJ37034 | 229622_at | 4.96 | 19.29 |
| hypothetical protein FLJ39653 | FLJ39653 | 1553145_at | -3.25 | -2.69 |
| hypothetical protein FLJ40629 | FLJ40629 | 229610_at | 4.89 | 8.40 |
| hypothetical protein from clone 643 | LOC57228 | 209679_s_at | 4.17 | 2.97 |
| hypothetical protein KIAA1164 | KIAA1164 | 214691_x_at | 2.08 | 2.38 |
| Hypothetical protein KIAA1164 | KIAA1164 | 221711_at | 2.39 | 2.93 |
| hypothetical protein LOC139886 | LOC139886 | 228654_at | 2.57 | 2.81 |
| hypothetical protein LOC144347 | LOC144347 | 227320_at | 3.86 | 3.92 |
| hypothetical protein LOC144874 | LOC144874 | 1556021_at | 2.58 | 2.48 |
| hypothetical protein LOC146909 | LOC146909 | 222039_at | 4.00 | 5.98 |
| hypothetical protein LOC148189 | LOC148189 | 235191_at | -2.22 | -2.97 |
| hypothetical protein LOC202781 | LOC202781 | 235587_at | -2.99 | -2.97 |
| hypothetical protein LOC221981 | LOC221981 | 214920_at | -4.38 | -13.36 |
| Hypothetical protein LOC253039 | LOC253039 | 231828_at | -2.81 | -2.16 |
| hypothetical protein LOC283666 | LOC283666 | 226682_at | -2.13 | -2.71 |
| hypothetical protein LOC283824 | LOC283824 | 213725_x_at | -4.06 | -3.84 |
| hypothetical protein LOC339924 | LOC339924 | 226158_at | -2.22 | -2.83 |
| hypothetical protein LOC340061 | LOC340061 | 224916_at | 6.23 | 5.54 |
| hypothetical protein LOC92270 | LOC92270 | 228816_at | -2.19 | -2.43 |
| hypothetical protein MGC11266 | MGC11266 | 226118_at | 4.00 | 3.94 |
| hypothetical protein MGC16037 | MGC16037 | 229050_s_at | -2.91 | -2.17 |
| hypothetical protein MGC24665 | MGC24665 | 226456_at | 2.43 | 10.06 |
| Hypothetical protein MGC45780 | MGC45780 | 229839_at | -3.01 | -3.61 |
| hypothetical protein MGC4677 /// hypothetical LOC541471 protein | MGC4677 /// LOC541471 | 225799_at | 2.25 | 2.10 |
| hypothetical protein PRO1855 | PRO1855 | 222231_s_at | 2.13 | 2.25 |
| hypoxia-inducible protein 2 | HIG2 | 1554452_a_at | -3.12 | -3.66 |
| hypoxia-inducible protein 2 | HIG2 | 218507_at | -2.39 | -3.29 |
| immediate early response 3 | IER3 | 201631_s_at | 3.43 | 2.46 |
| Immunoglobulin superfamily, member 4 | IGSF4 | 209031_at | -2.66 | -9.00 |
| immunoglobulin superfamily, member 4 | IGSF4 | 209032_s_at | -2.04 | -7.01 |
| Inner centromere protein antigens 135/155kDa | INCENP | 242787_at | 2.22 | 2.20 |
| inositol polyphosphate-4-phosphatase, type II, 105kDa | INPP4B | 205376_at | 3.29 | 3.53 |
| insulin induced gene 1 | INSIG1 | 201625_s_at | -2.68 | -5.43 |
| insulin induced gene 1 | INSIG1 | 201626_at | -2.04 | -3.12 |
| insulin induced gene 1 | INSIG1 | 201627_s_at | -2.71 | -4.99 |
| Insulin receptor | INSR | 226450_at | -2.10 | -2.06 |
| insulin-like growth factor 1 (somatomedin C) | IGF1 | 209541_at | -6.15 | -2.58 |
| insulin-like growth factor binding protein 1 | IGFBP1 | 205302_at | -6.92 | -13.74 |
| integrin, alpha 3 (antigen CD49C, alpha 3 subunit of VLA-3 receptor) | ITGA3 | 201474_s_at | 2.43 | 3.81 |
| integrin, alpha 5 (fibronectin receptor, alpha polypeptide) | ITGA5 | 201389_at | 3.94 | 3.71 |
| integrin-linked kinase | ILK | 201234_at | 2.50 | 2.77 |
| inter-alpha (globulin) inhibitor H5 | ITIH5 | 1553243_at | -2.71 | -2.73 |
| Interferon gamma receptor 1 | IFNGR1 | 242903_at | -2.22 | -2.55 |
| interferon-related developmental regulator 1 | IFRD1 | 202146_at | -2.77 | -2.51 |
| interferon-related developmental regulator 1 | IFRD1 | 202147_s_at | -2.73 | -2.41 |
| interleukin 18 receptor 1 | IL18R1 | 206618_at | -2.81 | -2.03 |
| interleukin 4 receptor | IL4R | 203233_at | 2.58 | 2.07 |
| IQ motif containing GTPase activating protein 3 | IQGAP3 | 229490_s_at | 3.46 | 19.70 |
| IQ motif containing GTPase activating protein 3 | IQGAP3 | 229538_s_at | 3.03 | 2.79 |
| jagged 1 (Alagille syndrome) | JAG1 | 209098_s_at | 2.79 | 3.92 |
| jagged 1 (Alagille syndrome) | JAG1 | 209099_x_at | 2.00 | 5.06 |

| Gene title | Gene symbol | Affymetrix probe set ID | + 24 h sample_array 1 versus control_array 1 [fold change] | + 24 h sample_array 2 versus control_array 2 [fold change] |
|---|---|---|---|---|
| jagged 1 (Alagille syndrome) | JAG1 | 216268_s_at | 2.13 | 6.02 |
| Junction-mediating and regulatory protein | JMY | 226352_at | -2.13 | -2.10 |
| junctophilin 2 | JPH2 | 229578_at | 4.29 | 12.30 |
| juxtaposed with another zinc finger gene 1 | JAZF1 | 225798_at | 2.33 | 2.69 |
| juxtaposed with another zinc finger gene 1 | JAZF1 | 225800_at | 2.57 | 2.19 |
| katanin p60 subunit A-like 1 | KATNAL1 | 227713_at | 2.25 | 2.23 |
| KDEL (Lys-Asp-Glu-Leu) endoplasmic reticulum protein retention receptor 3 | KDELR3 | 204017_at | 2.57 | 3.01 |
| KDEL (Lys-Asp-Glu-Leu) endoplasmic reticulum protein retention receptor 3 | KDELR3 | 207264_at | 2.95 | 4.89 |
| KDEL (Lys-Asp-Glu-Leu) endoplasmic reticulum protein retention receptor 3 | KDELR3 | 207265_s_at | 2.53 | 2.95 |
| kelch-like 7 (Drosophila) | KLHL7 | 220239_at | 2.10 | 2.33 |
| keratin 7 | KRT7 | 209016_s_at | 4.23 | 3.23 |
| keratin associated protein 1-5 | KRTAP1-5 | 233533_at | 6.45 | 23.59 |
| keratin associated protein 2-1 /// keratin associated protein 2-4 | KRTAP2-1 /// KRTAP2-4 | 1555673_at | 13.18 | 5.35 |
| keratin, hair, acidic, 4 | KRTHA4 | 206969_at | 6.77 | 14.12 |
| KIAA0101 | KIAA0101 | 202503_s_at | 3.56 | 3.46 |
| KIAA0146 protein | KIAA0146 | 228325_at | -2.41 | -2.89 |
| KIAA0186 gene product | KIAA0186 | 206102_at | 3.53 | 4.14 |
| KIAA0500 protein | KIAA0500 | 213839_at | -2.79 | -2.77 |
| KIAA0543 protein | KIAA0543 | 226808_at | -2.39 | -2.17 |
| KIAA0802 | KIAA0802 | 213358_at | 2.16 | 2.99 |
| KIAA1026 protein | KIAA1026 | 229144_at | -2.28 | -2.07 |
| KIAA1199 | KIAA1199 | 1554685_a_at | 2.89 | 3.84 |
| KIAA1199 | KIAA1199 | 212942_s_at | 2.25 | 3.89 |
| KIAA1462 | KIAA1462 | 231841_s_at | 2.25 | 2.46 |
| KIAA1524 | KIAA1524 | 1553810_a_at | 2.60 | 2.73 |
| KIAA1671 protein | KIAA1671 | 225525_at | 2.93 | 2.71 |
| KIAA1906 protein | KIAA1906 | 236824_at | -2.55 | -2.03 |
| KIAA1913 | KIAA1913 | 234994_at | 2.38 | 2.28 |
| KIAA1949 | KIAA1949 | 224927_at | 2.36 | 2.50 |
| kinesin 2 60/70kDa | KNS2 | 212877_at | 2.04 | 2.04 |
| kinesin family member 11 | KIF11 | 204444_at | 3.56 | 5.06 |
| kinesin family member 14 | KIF14 | 206364_at | 5.98 | 4.92 |
| Kinesin family member 14 | KIF14 | 236641_at | 3.48 | 3.36 |
| kinesin family member 15 | KIF15 | 219306_at | 3.29 | 2.48 |
| kinesin family member 20A | KIF20A | 218755_at | 4.20 | 3.16 |
| kinesin family member 21A | KIF21A | 226003_at | -2.22 | -2.04 |
| kinesin family member 23 | KIF23 | 204709_s_at | 8.22 | 8.94 |
| kinesin family member 2C | KIF2C | 209408_at | 4.41 | 3.05 |
| kinesin family member 2C | KIF2C | 211519_s_at | 3.51 | 2.55 |
| kinesin family member 4A | KIF4A | 218355_at | 5.31 | 7.21 |
| kinetochore associated 2 | KNTC2 | 204162_at | 5.43 | 5.43 |
| KIT ligand | KITLG | 207029_at | -3.43 | -2.20 |
| KIT ligand | KITLG | 211124_s_at | -2.93 | -2.45 |
| KIT ligand | KITLG | 226534_at | -3.36 | -2.06 |
| Kruppel-like factor 15 | KLF15 | 231015_at | -2.31 | -4.00 |
| Kruppel-like factor 2 (lung) | KLF2 | 219371_s_at | 4.79 | 3.07 |
| Kruppel-like factor 6 | KLF6 | 208960_s_at | 3.23 | 2.79 |
| Kruppel-like factor 6 | KLF6 | 208961_s_at | 2.62 | 2.53 |
| kynureninase (L-kynurenine hydrolase) | KYNU | 210663_s_at | -4.20 | -5.43 |
| kynureninase (L-kynurenine hydrolase) | KYNU | 217388_s_at | -3.12 | -4.53 |
| L-3-hydroxyacyl-Coenzyme A dehydrogenase, short chain | HADHSC | 201035_s_at | -2.10 | -2.25 |
| lamin B1 | LMNB1 | 203276_at | 5.35 | 6.02 |
| lamin B2 | LMNB2 | 216952_s_at | 2.30 | 2.08 |
| Laminin, alpha 4 | LAMA4 | 1556935_at | -3.58 | -3.05 |
| laminin, alpha 4 | LAMA4 | 202202_s_at | -2.20 | -2.03 |
| laminin, alpha 4 | LAMA4 | 210990_s_at | -2.30 | -2.58 |
| leptin (obesity homolog, mouse) | LEP | 207092_at | 2.89 | 6.77 |
| LETM1 domain containing 1 | LETMD1 | 207170_s_at | -2.46 | -2.99 |
| Leucine rich repeat (in FLII) interacting protein 2 | LRRFIP2 | 230082_at | 2.23 | 2.27 |
| leucine rich repeat containing 8 | LRRC8 | 233487_s_at | 3.76 | 2.22 |
| leucine zipper protein FKSG14 | FKSG14 | 222848_at | 5.46 | 6.45 |
| leucyl/cystinyl aminopeptidase | LNPEP | 236728_at | -2.03 | -3.53 |
| leukemia inhibitory factor receptor | LIFR | 205876_at | -2.11 | -2.33 |
| Leukemia inhibitory factor receptor | LIFR | 225571_at | -3.05 | -2.27 |
| Leukemia inhibitory factor receptor | LIFR | 225575_at | -2.41 | -2.08 |
| Leukemia inhibitory factor receptor | LIFR | 227771_at | -2.57 | -2.08 |
| likely ortholog of chicken tsukushi | TSK | 218245_at | -2.48 | -2.85 |
| LIM and cysteine-rich domains 1 | LMCD1 | 218574_s_at | 2.95 | 8.57 |
| LIM and cysteine-rich domains 1 | LMCD1 | 242767_at | 2.43 | 8.51 |

| Gene title | Gene symbol | Affymetrix probe set ID | + 24 h sample_array 1 versus control_array 1 [fold change] | + 24 h sample_array 2 versus control_array 2 [fold change] |
|---|---|---|---|---|
| LIM and SH3 protein 1 | LASP1 | 200618_at | 2.17 | 2.48 |
| LIM domain 7 | LMO7 | 202674_s_at | 6.19 | 8.82 |
| LIM domain 7 | LMO7 | 242722_at | 8.34 | 22.16 |
| LIM domain containing preferred translocation partner in lipoma | LPP | 202822_at | 2.04 | 2.06 |
| LIM domain only 4 | LMO4 | 209205_s_at | -2.07 | -2.62 |
| lipase, hormone-sensitive | LIPE | 208186_s_at | -3.41 | -2.33 |
| lipase, hormone-sensitive | LIPE | 213855_s_at | -2.66 | -2.46 |
| lipin 1 | LPIN1 | 212272_at | -2.38 | -3.81 |
| lipin 1 | LPIN1 | 212274_at | -2.57 | -4.44 |
| lipin 1 | LPIN1 | 212276_at | -2.53 | -4.20 |
| lipoic acid synthetase | LIAS | 214045_at | -2.35 | -2.85 |
| LOC150368 protein | LOC150368 | 226504_at | 2.89 | 2.16 |
| loss of heterozygosity, 3, chromosomal region 2, gene A | LOH3CR2A | 220244_at | 2.50 | 4.08 |
| low density lipoprotein receptor (familial hypercholesterolemia) | LDLR | 202068_s_at | -2.03 | -3.84 |
| low density lipoprotein receptor (familial hypercholesterolemia) | LDLR | 217173_s_at | -2.38 | -2.22 |
| lysyl oxidase-like 4 | LOXL4 | 227145_at | 3.29 | 3.14 |
| MAD2 mitotic arrest deficient-like 1 (yeast) | MAD2L1 | 1554768_a_at | 3.18 | 3.86 |
| MAD2 mitotic arrest deficient-like 1 (yeast) | MAD2L1 | 203362_s_at | 2.30 | 4.08 |
| Malic enzyme 1, NADP(+)-dependent, cytosolic | ME1 | 240788_at | -3.51 | -2.08 |
| maltase-glucoamylase (alpha-glucosidase) | MGAM | 206522_at | 8.94 | 41.07 |
| mannose-6-phosphate receptor binding protein 1 | M6PRBP1 | 202122_s_at | 2.30 | 2.46 |
| mannosidase, alpha, class 1C, member 1 | MAN1C1 | 218918_at | -3.61 | -3.86 |
| MAP kinase interacting serine/threonine kinase 2 | MKNK2 | 218205_s_at | -4.23 | -3.84 |
| MAP kinase interacting serine/threonine kinase 2 | MKNK2 | 223199_at | -3.07 | -3.01 |
| maternal embryonic leucine zipper kinase | MELK | 204825_at | 4.11 | 6.15 |
| matrin 3 | MATR3 | 1564907_s_at | -2.11 | -2.08 |
| matrix metalloproteinase 12 (macrophage elastase) | MMP12 | 204580_at | 2.62 | 3.92 |
| matrix metalloproteinase 13 (collagenase 3) /// matrix metalloproteinase 13 (collagenase 3) | MMP13 | 205959_at | 2.50 | 2.77 |
| MCM10 minichromosome maintenance deficient 10 (S. cerevisiae) | MCM10 | 220651_s_at | 7.78 | 19.43 |
| MCM2 minichromosome maintenance deficient 2, mitotin (S. cerevisiae) | MCM2 | 202107_s_at | 3.03 | 2.35 |
| MCM4 minichromosome maintenance deficient 4 (S. cerevisiae) | MCM4 | 222036_s_at | 2.13 | 2.45 |
| MCM5 minichromosome maintenance deficient 5, cell division cycle 46 (S. cerevisiae) | MCM5 | 201755_at | 3.41 | 16.80 |
| MCM5 minichromosome maintenance deficient 5, cell division cycle 46 (S. cerevisiae) | MCM5 | 216237_s_at | 6.54 | 6.87 |
| MCM6 minichromosome maintenance deficient 6 (MIS5 homolog, S. pombe) (S. cerevisiae) | MCM6 | 201930_at | 2.22 | 2.27 |
| MCM7 minichromosome maintenance deficient 7 (S. cerevisiae) | MCM7 | 208795_s_at | 2.51 | 2.17 |
| MCM7 minichromosome maintenance deficient 7 (S. cerevisiae) | MCM7 | 210983_s_at | 2.27 | 2.31 |
| melanocortin 2 receptor accessory protein | MRAP | 1554044_a_at | -2.39 | -2.79 |
| melanocortin 2 receptor accessory protein | MRAP | 1555740_a_at | -2.58 | -2.35 |
| mesenchymal stem cell protein DSC54 | LOC51334 | 1554867_a_at | 2.66 | 3.25 |
| mesenchymal stem cell protein DSC54 | LOC51334 | 220014_at | 2.48 | 4.72 |
| Mesenchymal stem cell protein DSC96 | --- | 227167_s_at | 2.19 | 3.73 |
| Mesenchymal stem cell protein DSC96 | --- | 230466_s_at | 2.41 | 2.89 |
| mesenchyme homeo box 2 (growth arrest-specific homeo box) | MEOX2 | 206201_s_at | 2.13 | 6.77 |
| met proto-oncogene (hepatocyte growth factor receptor) | MET | 203510_at | 2.23 | 3.97 |
| metallothionein 1F (functional) | MT1F | 213629_x_at | -2.53 | -4.56 |
| metallothionein 1K | MT1K | 217546_at | -3.29 | -5.39 |
| methionine sulfoxide reductase B3 | MSRB3 | 1554127_s_at | 2.57 | 3.89 |
| methionine sulfoxide reductase B3 | MSRB3 | 238583_at | 2.38 | 2.73 |
| methylenetetrahydrofolate dehydrogenase (NADP+ dependent) 2, methenyltetrahydrofolate cyclohydrolase | MTHFD2 | 201761_at | -2.07 | -2.31 |
| microfibrillar associated protein 5 | MFAP5 | 209758_s_at | 3.84 | 5.03 |
| microfibrillar associated protein 5 | MFAP5 | 213764_s_at | 5.06 | 15.45 |
| microfibrillar associated protein 5 | MFAP5 | 213765_at | 4.38 | 7.78 |
| Microsomal glutathione S-transferase 1 | MGST1 | 239001_at | -2.62 | -2.60 |
| microtubule associated monooxygenase, calponin and LIM domain containing 1 | MICAL1 | 218376_s_at | 3.12 | 3.01 |
| microtubule associated monooxygenase, calponin and LIM domain containing 2 | MICAL2 | 212472_at | 5.17 | 7.84 |
| microtubule associated monooxygenase, calponin and LIM domain containing 2 | MICAL2 | 212473_s_at | 4.56 | 7.11 |
| mindbomb homolog 2 (Drosophila) | MIB2 | 226644_at | -6.50 | -3.07 |
| mitochondrial ribosomal protein S25 | MRPS25 | 224015_s_at | -2.85 | -2.77 |

| Gene title | Gene symbol | Affymetrix probe set ID | + 24 h sample_array 1 versus control_array 1 [fold change] | + 24 h sample_array 2 versus control_array 2 [fold change] |
|---|---|---|---|---|
| mitochondrial ribosomal protein S25 | MRPS25 | 224873_s_at | -2.43 | -2.53 |
| Mitochondrial ribosomal protein S30 | MRPS30 | 231207_at | -2.14 | -2.60 |
| MLF1 interacting protein | MLF1IP | 218883_s_at | 2.73 | 3.39 |
| molybdenum cofactor synthesis 1 /// molybdenum cofactor synthesis 1 | MOCS1 | 211673_s_at | -2.01 | -2.11 |
| monoglyceride lipase | MGLL | 225102_at | 3.34 | 4.76 |
| monoglyceride lipase /// monoglyceride lipase | MGLL | 211026_s_at | 4.72 | 5.70 |
| more than blood homolog | MTB | 219588_s_at | 3.18 | 3.53 |
| M-phase phosphoprotein 1 | MPHOSPH1 | 205235_s_at | 2.10 | 3.36 |
| murine retrovirus integration site 1 homolog | MRVI1 | 224550_s_at | 10.70 | 20.82 |
| Murine retrovirus integration site 1 homolog | MRVI1 | 226047_at | 4.99 | 29.86 |
| murine retrovirus integration site 1 homolog | MRVI1 | 230214_at | 4.59 | 8.88 |
| muscleblind-like (Drosophila) | MBNL1 | 201152_s_at | 2.14 | 2.20 |
| mutS homolog 2, colon cancer, nonpolyposis type 1 (E. coli) | MSH2 | 209421_at | 2.22 | 2.27 |
| myeloid-associated differentiation marker | MYADM | 224920_x_at | 2.83 | 3.16 |
| myeloid-associated differentiation marker | MYADM | 225673_at | 4.41 | 4.69 |
| myosin regulatory light chain interacting protein | MYLIP | 223130_s_at | -2.04 | -2.69 |
| Myosin, heavy polypeptide 11, smooth muscle | MYH11 | 227249_at | 2.66 | 3.18 |
| nanos homolog 1 (Drosophila) | NANOS1 | 228523_at | -6.77 | -4.79 |
| nei endonuclease VIII-like 3 (E. coli) | NEIL3 | 219502_at | 2.53 | 3.76 |
| neural precursor cell expressed, developmentally down-regulated 4 | NEDD4 | 213012_at | 2.41 | 2.14 |
| neural precursor cell expressed, developmentally down-regulated 9 | NEDD9 | 202150_s_at | 2.04 | 2.51 |
| neuroblastoma RAS viral (v-ras) oncogene homolog | NRAS | 202647_s_at | 2.45 | 2.27 |
| neuroligin 4, X-linked | NLGN4X | 221933_at | -3.29 | -3.73 |
| neurolysin (metallopeptidase M3 family) | NLN | 225943_at | 2.11 | 2.41 |
| neuron navigator 3 | NAV3 | 1552658_a_at | 2.30 | 2.31 |
| neuron navigator 3 | NAV3 | 204823_at | 2.33 | 2.33 |
| neuronal cell adhesion molecule | NRCAM | 204105_s_at | -5.66 | -2.57 |
| neuronal PAS domain protein 2 | NPAS2 | 39549_at | -2.45 | -2.16 |
| neuronal pentraxin II | NPTX2 | 213479_at | -2.64 | -3.12 |
| neurotrophic tyrosine kinase, receptor, type 2 | NTRK2 | 221795_at | -2.35 | -2.11 |
| nexilin (F actin binding protein) | NEXN | 1552309_a_at | 2.23 | 4.50 |
| nexilin (F actin binding protein) | NEXN | 226103_at | 2.25 | 4.72 |
| NIMA (never in mitosis gene a)-related kinase 2 | NEK2 | 204641_at | 3.56 | 4.32 |
| NOL1/NOP2/Sun domain family, member 6 | NSUN6 | 242239_at | -2.22 | -6.77 |
| non-metastatic cells 7, protein expressed in (nucleoside-diphosphate kinase) | NME7 | 227556_at | 2.93 | 4.14 |
| Nuclear factor I/B | NFIB | 209289_at | -2.08 | -2.07 |
| Nuclear factor I/B | NFIB | 213032_at | -2.38 | -2.35 |
| nuclear receptor subfamily 1, group D, member 2 | NR1D2 | 209750_at | -2.50 | -2.87 |
| nuclear receptor subfamily 1, group D, member 2 | NR1D2 | 225768_at | -2.48 | -2.58 |
| nuclear receptor subfamily 1, group H, member 3 | NR1H3 | 203920_at | -2.28 | -2.46 |
| nucleolar and spindle associated protein 1 | NUSAP1 | 218039_at | 4.66 | 4.26 |
| nucleolar and spindle associated protein 1 | NUSAP1 | 219978_s_at | 3.53 | 2.71 |
| nucleoside phosphorylase | NP | 201695_s_at | 2.30 | 2.28 |
| OCIA domain containing 2 | OCIAD2 | 225314_at | 2.97 | 3.71 |
| odd-skipped related 2 (Drosophila) | OSR2 | 213568_at | -3.46 | -2.45 |
| odz, odd Oz/ten-m homolog 2 (Drosophila) | ODZ2 | 231867_at | 2.95 | 5.94 |
| odz, odd Oz/ten-m homolog 4 (Drosophila) | ODZ4 | 213273_at | -3.16 | -3.20 |
| Opsin 1 (cone pigments), short-wave-sensitive (color blindness, tritan) | OPN1SW | 229549_at | 2.28 | 2.17 |
| P450 (cytochrome) oxidoreductase | POR | 208928_at | -2.20 | -2.38 |
| paired related homeobox 2 | PRRX2 | 219729_at | 2.06 | 2.11 |
| palladin | KIAA0992 | 200906_s_at | 2.71 | 4.63 |
| palladin | KIAA0992 | 200907_s_at | 2.39 | 3.84 |
| palmdelphin | PALMD | 218736_s_at | -4.99 | -4.23 |
| palmdelphin | PALMD | 222725_s_at | -5.43 | -5.24 |
| pancreatic lipase-related protein 3 | PNLIPRP3 | 1558846_at | -3.03 | -22.32 |
| patatin-like phospholipase domain containing 2 | PNPLA2 | 212705_x_at | -2.75 | -2.38 |
| patatin-like phospholipase domain containing 2 | PNPLA2 | 39854_r_at | -2.48 | -2.11 |
| PAX transcription activation domain interacting protein 1 like | PAXIP1L | 228243_at | -2.08 | -2.04 |
| PDZ and LIM domain 2 (mystique) | PDLIM2 | 219165_at | 2.13 | 2.68 |
| PDZ and LIM domain 4 | PDLIM4 | 211564_s_at | 2.36 | 2.71 |
| PDZ and LIM domain 4 | PDLIM4 | 218691_at | 2.33 | 3.73 |
| PDZ and LIM domain 5 | PDLIM5 | 203242_s_at | 2.62 | 3.76 |
| PDZ and LIM domain 5 | PDLIM5 | 213684_s_at | 3.34 | 4.96 |
| PDZ and LIM domain 5 | PDLIM5 | 216804_s_at | 2.55 | 3.97 |
| PDZ and LIM domain 5 | PDLIM5 | 221994_at | 3.76 | 10.85 |
| PDZ and LIM domain 5 /// PDZ and LIM domain 5 | PDLIM5 | 211681_s_at | 2.85 | 3.53 |
| PDZ and LIM domain 7 (enigma) | PDLIM7 | 203370_s_at | 2.58 | 6.32 |
| PDZ binding kinase | PBK | 219148_at | 3.97 | 4.82 |

| Gene title | Gene symbol | Affymetrix probe set ID | + 24 h sample_array 1 versus control_array 1 [fold change] | + 24 h sample_array 2 versus control_array 2 [fold change] |
|---|---|---|---|---|
| periostin, osteoblast specific factor | POSTN | 1555778_a_at | 3.16 | 4.66 |
| periostin, osteoblast specific factor | POSTN | 210809_s_at | 2.51 | 3.01 |
| Periostin, osteoblast specific factor | POSTN | 228481_at | 5.98 | 14.12 |
| periplakin | PPL | 203407_at | -4.03 | -13.64 |
| peroxisome proliferative activated receptor, gamma, coactivator 1, alpha | PPARGC1A | 219195_at | -4.66 | -5.78 |
| PHD finger protein 19 | PHF19 | 227212_s_at | 3.16 | 2.11 |
| phosphatidylinositol transfer protein, cytoplasmic 1 | PITPNC1 | 219155_at | -2.22 | -2.00 |
| phosphodiesterase 3B, cGMP-inhibited | PDE3B | 208591_s_at | -3.97 | -5.17 |
| phosphodiesterase 3B, cGMP-inhibited | PDE3B | 214582_at | -4.26 | -5.58 |
| Phosphodiesterase 3B, cGMP-inhibited | PDE3B | 222317_at | -5.03 | -6.11 |
| Phosphodiesterase 3B, cGMP-inhibited | PDE3B | 222330_at | -4.92 | -121.94 |
| phosphodiesterase 4B, cAMP-specific (phosphodiesterase E4 dunce homolog, Drosophila) | PDE4B | 203708_at | -2.75 | -4.82 |
| phosphodiesterase 4B, cAMP-specific (phosphodiesterase E4 dunce homolog, Drosophila) | PDE4B | 211302_s_at | -2.19 | -3.63 |
| Phosphodiesterase 4D, cAMP-specific (phosphodiesterase E3 dunce homolog, Drosophila) | PDE4D | 204491_at | -2.93 | -2.87 |
| phosphodiesterase 7B | PDE7B | 220343_at | -2.45 | -2.31 |
| phosphodiesterase 7B | PDE7B | 230109_at | -3.68 | -2.53 |
| phosphoenolpyruvate carboxykinase 2 (mitochondrial) | PCK2 | 202847_at | -3.03 | -2.55 |
| phosphoglucomutase 2 | PGM2 | 225366_at | 2.39 | 2.19 |
| phosphoglucomutase 2 | PGM2 | 225367_at | 2.17 | 2.43 |
| phosphoglucomutase 3 | PGM3 | 210041_s_at | 2.01 | 2.38 |
| phosphogluconate dehydrogenase /// phosphogluconate dehydrogenase | PGD | 201118_at | -2.53 | -3.01 |
| phosphoglycerate dehydrogenase | PHGDH | 201397_at | -2.77 | -5.39 |
| phospholipase C, beta 4 | PLCB4 | 203895_at | 9.78 | 26.35 |
| phospholipase C, beta 4 | PLCB4 | 203896_s_at | 9.19 | 195.36 |
| Phospholipase C, epsilon 1 | PLCE1 | 205112_at | 3.03 | 2.14 |
| phospholipase D1, phophatidylcholine-specific | PLD1 | 226636_at | -2.25 | -2.51 |
| phosphoserine aminotransferase 1 | PSAT1 | 220892_s_at | -5.98 | -9.51 |
| phosphoserine aminotransferase 1 | PSAT1 | 223062_s_at | -6.06 | -7.84 |
| phosphoserine phosphatase | PSPH | 205048_s_at | -2.16 | -2.01 |
| pituitary tumor-transforming 1 | PTTG1 | 203554_x_at | 2.36 | 2.36 |
| plakophilin 2 | PKP2 | 207717_s_at | -2.73 | -2.85 |
| plasminogen activator, tissue | PLAT | 201860_s_at | 2.93 | 5.10 |
| plasminogen activator, urokinase receptor | PLAUR | 210845_s_at | 2.33 | 2.19 |
| plasticity related gene 1 | LPPR4 | 213496_at | -3.27 | -6.15 |
| platelet-derived growth factor alpha polypeptide | PDGFA | 205463_s_at | 3.20 | 2.45 |
| Platelet-derived growth factor alpha polypeptide | PDGFA | 229830_at | 2.07 | 4.00 |
| pleckstrin homology domain containing, family G (with RhoGef domain) member 2 | PLEKHG2 | 225979_at | 2.01 | 3.14 |
| pleckstrin homology-like domain, family A, member 1 | PHLDA1 | 217996_at | -3.10 | -3.56 |
| pleckstrin homology-like domain, family A, member 1 | PHLDA1 | 217997_at | -3.63 | -5.62 |
| pleckstrin homology-like domain, family A, member 1 | PHLDA1 | 217998_at | -3.14 | -5.31 |
| pleckstrin homology-like domain, family A, member 1 | PHLDA1 | 218000_s_at | -2.04 | -3.63 |
| pleckstrin homology-like domain, family A, member 2 | PHLDA2 | 209803_s_at | 5.43 | 10.06 |
| Plexin A4 | PLXNA4 | 228104_at | -2.33 | -2.97 |
| polo-like kinase 1 (Drosophila) | PLK1 | 202240_at | 2.60 | 2.22 |
| polo-like kinase 4 (Drosophila) | PLK4 | 204887_s_at | 3.43 | 14.03 |
| polo-like kinase 4 (Drosophila) /// polo-like kinase 4 (Drosophila) | PLK4 | 211088_s_at | 39.12 | 6.36 |
| polymerase (DNA directed), epsilon 2 (p59 subunit) | POLE2 | 205909_at | 4.11 | 4.76 |
| potassium channel tetramerisation domain containing 10 | KCTD10 | 223208_at | 2.19 | 2.19 |
| potassium channel, subfamily K, member 3 | KCNK3 | 205952_at | -3.71 | -5.46 |
| Potassium channel, subfamily K, member 3 | KCNK3 | 235108_at | -4.17 | -5.46 |
| potassium channel, subfamily K, member 6 | KCNK6 | 223658_at | 2.91 | 3.76 |
| potassium large conductance calcium-activated channel, subfamily M, beta member 1 | KCNMB1 | 209948_at | 5.35 | 3.63 |
| PR domain containing 16 | PRDM16 | 232424_at | -2.38 | -3.27 |
| pre-B-cell colony enhancing factor 1 | PBEF1 | 1555167_s_at | -3.46 | -5.21 |
| pre-B-cell colony enhancing factor 1 | PBEF1 | 217738_at | -4.86 | -5.90 |
| pre-B-cell colony enhancing factor 1 | PBEF1 | 217739_s_at | -3.84 | -4.14 |
| Pre-B-cell colony enhancing factor 1 | PBEF1 | 243296_at | -4.99 | -5.86 |
| primase, polypeptide 2A, 58kDa | PRIM2A | 215708_s_at | 2.36 | 2.45 |
| PRKC, apoptosis, WT1, regulator | PAWR | 204004_at | 2.08 | 4.20 |
| PRKC, apoptosis, WT1, regulator | PAWR | 204005_s_at | 2.14 | 4.44 |
| programmed cell death 1 ligand 2 | PDCD1LG2 | 220049_s_at | 8.69 | 14.93 |
| programmed cell death 1 ligand 2 /// programmed cell death 1 ligand 2 | PDCD1LG2 | 224399_at | 4.44 | 8.94 |
| Proline rich Gla (G-carboxyglutamic acid) 4 (transmembrane) | PRRG4 | 238513_at | 2.69 | 3.23 |
| proline-serine-threonine phosphatase interacting protein | PSTPIP2 | 219938_s_at | 2.36 | 2.62 |

| Gene title | Gene symbol | Affymetrix probe set ID | + 24 h sample_array 1 versus control_array 1 [fold change] | + 24 h sample_array 2 versus control_array 2 [fold change] |
|---|---|---|---|---|
| 2 | | | | |
| proprotein convertase subtilisin/kexin type 1 | PCSK1 | 205825_at | -2.66 | -3.18 |
| Proprotein convertase subtilisin/kexin type 7 | PCSK7 | 226523_at | 2.69 | 17.03 |
| prostaglandin E receptor 2 (subtype EP2), 53kDa | PTGER2 | 206631_at | 2.50 | 2.20 |
| prostaglandin F receptor (FP) | PTGFR | 1555097_a_at | -2.69 | -3.81 |
| prostaglandin F receptor (FP) | PTGFR | 207177_at | -3.27 | -3.78 |
| prostaglandin I2 (prostacyclin) synthase /// prostaglandin I2 (prostacyclin) synthase | PTGIS | 208131_s_at | 2.83 | 2.71 |
| protein kinase, cAMP-dependent, regulatory, type II, beta | PRKAR2B | 203680_at | -3.66 | -4.41 |
| protein phosphatase 1, regulatory (inhibitor) subunit 13 like | PPP1R13L | 218849_s_at | 2.13 | 5.06 |
| protein phosphatase 1, regulatory (inhibitor) subunit 14A | PPP1R14A | 227006_at | 2.45 | 17.75 |
| protein phosphatase 2 (formerly 2A), regulatory subunit A (PR 65), beta isoform | PPP2R1B | 202884_s_at | -2.03 | -2.14 |
| protein phosphatase 2 (formerly 2A), regulatory subunit A (PR 65), beta isoform | PPP2R1B | 222351_at | -3.84 | -4.06 |
| protein phosphatase 2, regulatory subunit B (B56), alpha isoform | PPP2R5A | 202187_s_at | -2.57 | -2.27 |
| protein phosphatase 2C, magnesium-dependent, catalytic subunit | PPM2C | 218273_s_at | 2.50 | 2.22 |
| protein phosphatase 2C, magnesium-dependent, catalytic subunit | PPM2C | 222572_at | 2.68 | 2.58 |
| protein phosphatase 4, regulatory subunit 1 | PPP4R1 | 201594_s_at | 2.03 | 2.08 |
| protein regulator of cytokinesis 1 | PRC1 | 218009_s_at | 5.43 | 6.11 |
| protein tyrosine phosphatase, non-receptor type 22 (lymphoid) | PTPN22 | 206060_s_at | 47.84 | 6.59 |
| proteolipid protein 2 (colonic epithelium-enriched) | PLP2 | 201136_at | 2.62 | 2.57 |
| putative small membrane protein NID67 | NID67 | 223276_at | -2.48 | -2.30 |
| PX domain containing serine/threonine kinase | PXK | 1552274_at | -2.10 | -2.64 |
| PX domain containing serine/threonine kinase | PXK | 1552275_s_at | -2.20 | -2.35 |
| PX domain containing serine/threonine kinase | PXK | 225796_at | -2.36 | -2.43 |
| pyruvate carboxylase | PC | 204476_s_at | -2.31 | -2.33 |
| pyruvate dehydrogenase kinase, isoenzyme 4 | PDK4 | 205960_at | -4.99 | -6.02 |
| RAB20, member RAS oncogene family | RAB20 | 219622_at | -3.18 | -5.21 |
| RAB23, member RAS oncogene family | RAB23 | 220955_x_at | 2.17 | 2.43 |
| RAB23, member RAS oncogene family | RAB23 | 229504_at | 2.10 | 3.20 |
| RAB33A, member RAS oncogene family | RAB33A | 206039_at | -3.89 | -4.76 |
| RAB3B, member RAS oncogene family | RAB3B | 205924_at | 2.38 | 8.63 |
| RAB3B, member RAS oncogene family | RAB3B | 205925_s_at | 3.73 | 2.22 |
| RAB3B, member RAS oncogene family | RAB3B | 227123_at | 5.28 | 6.06 |
| RAB3B, member RAS oncogene family | RAB3B | 239202_at | 3.12 | 6.82 |
| Rac GTPase activating protein 1 | RACGAP1 | 222077_s_at | 2.95 | 3.05 |
| RAD51 associated protein 1 | RAD51AP1 | 204146_at | 4.06 | 4.66 |
| RAD51 homolog (RecA homolog, E. coli) (S. cerevisiae) | RAD51 | 205024_s_at | 2.69 | 7.57 |
| rai-like protein | RaLP | 230538_at | 3.32 | 5.86 |
| RA-regulated nuclear matrix-associated protein | RAMP | 218585_s_at | 4.96 | 7.78 |
| RA-regulated nuclear matrix-associated protein | RAMP | 222680_s_at | 6.06 | 7.84 |
| Ras association (RalGDS/AF-6) and pleckstrin homology domains 1 | RAPH1 | 225186_at | 2.69 | 5.31 |
| Ras association (RalGDS/AF-6) and pleckstrin homology domains 1 | RAPH1 | 225188_at | 2.62 | 4.89 |
| Ras association (RalGDS/AF-6) and pleckstrin homology domains 1 | RAPH1 | 225189_s_at | 2.77 | 5.21 |
| ras homolog gene family, member C | RHOC | 200885_at | 2.46 | 3.01 |
| RAS, dexamethasone-induced 1 | RASD1 | 223467_at | -4.06 | -5.78 |
| RAS-like, family 11, member B | RASL11B | 219142_at | -3.84 | -4.38 |
| ras-related C3 botulinum toxin substrate 2 (rho family, small GTP binding protein Rac2) | RAC2 | 213603_s_at | 2.39 | 2.60 |
| Ras-related GTP binding D | RRAGD | 221523_s_at | -2.48 | -4.06 |
| regulating synaptic membrane exocytosis 3 | RIMS3 | 204730_at | -2.38 | -10.63 |
| regulator of G-protein signalling 4 | RGS4 | 204337_at | 10.85 | 25.63 |
| regulator of G-protein signalling 4 | RGS4 | 204338_s_at | 10.27 | 39.95 |
| regulator of G-protein signalling 4 | RGS4 | 204339_s_at | 7.62 | 16.00 |
| renal tumor antigen | RAGE | 205130_at | 4.96 | 3.43 |
| replication factor C (activator 1) 3, 38kDa | RFC3 | 204127_at | 2.04 | 3.07 |
| replication factor C (activator 1) 3, 38kDa | RFC3 | 204128_s_at | 2.79 | 3.71 |
| response gene to complement 32 | RGC32 | 218723_s_at | -2.79 | -3.46 |
| reticulon 4 receptor-like 1 | RTN4RL1 | 230700_at | -2.39 | -2.55 |
| retinitis pigmentosa 2 (X-linked recessive) | RP2 | 205191_at | 2.20 | 3.07 |
| retinoic acid induced 14 | RAI14 | 202052_s_at | 2.22 | 3.58 |
| retinol dehydrogenase 10 (all-trans) | RDH10 | 226021_at | -4.06 | -2.46 |
| REV3-like, catalytic subunit of DNA polymerase zeta (yeast) | REV3L | 208070_s_at | -3.10 | -2.22 |
| REV3-like, catalytic subunit of DNA polymerase zeta | REV3L | 238736_at | -4.41 | -2.60 |

| Gene title | Gene symbol | Affymetrix probe set ID | + 24 h sample_array 1 versus control_array 1 [fold change] | + 24 h sample_array 2 versus control_array 2 [fold change] |
|---|---|---|---|---|
| (yeast) | | | | |
| Rho GDP dissociation inhibitor (GDI) beta | ARHGDIB | 201288_at | 2.64 | 5.94 |
| Rho GTPase activating protein 18 | ARHGAP18 | 225166_at | 3.27 | 3.10 |
| Rho GTPase activating protein 18 | ARHGAP18 | 225171_at | 2.41 | 4.03 |
| Rho GTPase activating protein 18 | ARHGAP18 | 225173_at | 2.10 | 2.68 |
| Rho GTPase activating protein 22 | ARHGAP22 | 206298_at | 15.14 | 2.23 |
| Rho GTPase activating protein 28 | ARHGAP28 | 227911_at | -2.62 | -2.43 |
| rho/rac guanine nucleotide exchange factor (GEF) 2 | ARHGEF2 | 207629_s_at | -2.25 | -2.51 |
| rhomboid, veinlet-like 2 (Drosophila) | RHBDL2 | 1552502_s_at | 4.72 | 6.59 |
| rhomboid, veinlet-like 2 (Drosophila) | RHBDL2 | 1554897_s_at | 4.89 | 23.10 |
| ribonuclease H2, large subunit | RNASEH2A | 203022_at | 2.45 | 2.64 |
| ribonucleotide reductase M1 polypeptide | RRM1 | 201476_s_at | 2.28 | 2.66 |
| ribonucleotide reductase M1 polypeptide | RRM1 | 201477_s_at | 2.36 | 2.97 |
| ribonucleotide reductase M2 polypeptide | RRM2 | 201890_at | 4.69 | 8.34 |
| ribonucleotide reductase M2 polypeptide | RRM2 | 209773_s_at | 4.38 | 7.26 |
| ribosomal L1 domain containing 1 | RSL1D1 | 212019_at | -2.35 | -3.20 |
| ribosomal protein L31 | RPL31 | 200962_at | -2.45 | -2.93 |
| ribosomal protein L37 | RPL37 | 224763_at | -2.16 | -3.20 |
| ribosomal protein L37 | RPL37 | 224767_at | -2.62 | -3.41 |
| ring finger and WD repeat domain 3 | RFWD3 | 218564_at | 2.50 | 2.23 |
| ring finger protein 144 | RNF144 | 204040_at | -2.69 | -2.87 |
| RNA binding motif (RNP1, RRM) protein 3 | RBM3 | 208319_s_at | 2.01 | 2.19 |
| S100 calcium binding protein A16 | S100A16 | 227998_at | 2.28 | 2.20 |
| S100 calcium binding protein A3 | S100A3 | 206027_at | 2.22 | 4.89 |
| salvador homolog 1 (Drosophila) | SAV1 | 218276_s_at | -2.33 | -2.85 |
| salvador homolog 1 (Drosophila) | SAV1 | 234491_s_at | -2.27 | -2.19 |
| SAM and SH3 domain containing 1 | SASH1 | 213236_at | -2.04 | -2.01 |
| sarcoglycan, delta (35kDa dystrophin-associated glycoprotein) | SGCD | 210329_s_at | 2.20 | 2.36 |
| Sarcoglycan, delta (35kDa dystrophin-associated glycoprotein) | SGCD | 213543_at | 2.58 | 3.81 |
| sarcoglycan, delta (35kDa dystrophin-associated glycoprotein) | SGCD | 214492_at | 3.07 | 4.29 |
| sarcoglycan, delta (35kDa dystrophin-associated glycoprotein) | SGCD | 228602_at | 2.79 | 4.96 |
| sarcoglycan, delta (35kDa dystrophin-associated glycoprotein) | SGCD | 230730_at | 2.89 | 4.06 |
| schwannomin interacting protein 1 | SCHIP1 | 204030_s_at | 9.13 | 11.96 |
| sec1 family domain containing 2 | SCFD2 | 236834_at | 2.11 | 2.23 |
| secreted frizzled-related protein 2 | SFRP2 | 223121_s_at | -3.05 | -22.47 |
| secreted frizzled-related protein 2 | SFRP2 | 223122_s_at | -2.79 | -4.50 |
| secretory granule, neuroendocrine protein 1 (7B2 protein) | SGNE1 | 203889_at | 4.96 | 5.03 |
| sema domain, seven thrombospondin repeats (type 1 and type 1-like), transmembrane domain (TM) and short cytoplasmic domain, (semaphorin) 5A | SEMA5A | 205405_at | -2.69 | -2.06 |
| sema domain, transmembrane domain (TM), and cytoplasmic domain, (semaphorin) 6D | SEMA6D | 226492_at | -5.58 | -6.50 |
| sema domain, transmembrane domain (TM), and cytoplasmic domain, (semaphorin) 6D | SEMA6D | 233801_s_at | -4.82 | -4.29 |
| sema domain, transmembrane domain (TM), and cytoplasmic domain, (semaphorin) 6D | SEMA6D | 233882_s_at | -2.08 | -5.35 |
| semaphorin sem2 | LOC56920 | 219689_at | -2.57 | -2.57 |
| sequestosome 1 | SQSTM1 | 201471_s_at | -2.04 | -3.10 |
| serine (or cysteine) proteinase inhibitor, clade E (nexin, plasminogen activator inhibitor type 1), member 1 | SERPINE1 | 1568765_at | 7.57 | 14.62 |
| serine (or cysteine) proteinase inhibitor, clade E (nexin, plasminogen activator inhibitor type 1), member 1 | SERPINE1 | 202627_s_at | 6.32 | 7.21 |
| serine (or cysteine) proteinase inhibitor, clade E (nexin, plasminogen activator inhibitor type 1), member 1 | SERPINE1 | 202628_s_at | 9.45 | 12.82 |
| serine palmitoyltransferase, long chain base subunit 2 | SPTLC2 | 216202_s_at | 2.71 | 2.45 |
| serine/threonine kinase 6 | STK6 | 204092_s_at | 3.66 | 2.79 |
| serine/threonine kinase 6 | STK6 | 208079_s_at | 5.17 | 3.16 |
| serum amyloid A1 | SAA1 | 214456_x_at | 2.89 | 2.04 |
| serum amyloid A1 /// serum amyloid A1 /// serum amyloid A2 /// serum amyloid A2 | SAA1 /// SAA2 | 208607_s_at | 2.99 | 2.38 |
| serum deprivation response (phosphatidylserine binding protein) | SDPR | 222717_at | 5.39 | 2.97 |
| sestrin 2 | SESN2 | 223195_s_at | -3.05 | -2.75 |
| sestrin 2 | SESN2 | 223196_s_at | -2.41 | -2.50 |
| SHC SH2-domain binding protein 1 | SHCBP1 | 219493_at | 5.62 | 7.21 |
| Shroom-related protein | ShrmL | 225548_at | 3.07 | 2.81 |
| shugoshin-like 2 (S. pombe) | SGOL2 | 235425_at | 2.57 | 2.79 |
| similar to Cytochrome c, somatic | MGC12965 | 1554609_at | -2.48 | -2.17 |
| similar to hypothetical protein FLJ10883 | LOC115294 | 232382_s_at | -2.01 | -2.04 |
| similar to mouse 1700027M21Rik gene | LOC493861 | 231292_at | 3.14 | 6.36 |

| Gene title | Gene symbol | Affymetrix probe set ID | + 24 h sample_array 1 versus control_array 1 [fold change] | + 24 h sample_array 2 versus control_array 2 [fold change] |
|---|---|---|---|---|
| Similar to protein of fungal metazoan origin like (11.1 kD) (2C514) | --- | 228096_at | -7.26 | -13.45 |
| similar to RIKEN 4933428I03 | LOC401494 | 244050_at | 2.20 | 2.19 |
| Similar to RIKEN cDNA 2700049P18 gene | MGC57827 | 225834_at | 5.94 | 4.82 |
| similar to Six transmembrane epithelial antigen of prostate | MGC87042 | 217553_at | 2.57 | 3.48 |
| Similar to tripartite motif-containing 16; estrogen-responsive B box protein | --- | 1559681_a_at | -5.06 | -3.18 |
| SMC4 structural maintenance of chromosomes 4-like 1 (yeast) | SMC4L1 | 201663_s_at | 2.41 | 2.87 |
| smoothelin | SMTN | 207390_s_at | 4.32 | 4.00 |
| smoothelin | SMTN | 209427_at | 2.83 | 4.14 |
| SNF1-like kinase 2 | SNF1LK2 | 1557459_at | -2.89 | -3.07 |
| SNF1-like kinase 2 | SNF1LK2 | 213221_s_at | -3.20 | -2.45 |
| SNF1-like kinase 2 | SNF1LK2 | 223430_at | -3.43 | -2.91 |
| SNF1-like kinase 2 | SNF1LK2 | 233648_at | -2.03 | -2.30 |
| solute carrier family 16 (monocarboxylic acid transporters), member 3 | SLC16A3 | 202855_s_at | 2.55 | 2.45 |
| solute carrier family 16 (monocarboxylic acid transporters), member 3 | SLC16A3 | 202856_s_at | 2.13 | 2.28 |
| solute carrier family 16 (monocarboxylic acid transporters), member 6 | SLC16A6 | 207038_at | -21.26 | -58.08 |
| solute carrier family 16 (monocarboxylic acid transporters), member 6 /// similar to solute carrier family 16, member 6; monocarboxylate transporter 6 | SLC16A6 /// LOC440459 | 230748_at | -8.94 | -17.27 |
| solute carrier family 19, member 3 | SLC19A3 | 220736_at | -8.88 | -9.99 |
| solute carrier family 19, member 3 | SLC19A3 | 239345_at | -6.87 | -8.88 |
| solute carrier family 20 (phosphate transporter), member 1 | SLC20A1 | 201920_at | 3.39 | 2.91 |
| solute carrier family 3 (activators of dibasic and neutral amino acid transport), member 2 | SLC3A2 | 200924_s_at | -2.48 | -4.59 |
| Solute carrier family 38, member 1 | SLC38A1 | 224579_at | -2.06 | -4.66 |
| solute carrier family 38, member 5 | SLC38A5 | 234973_at | 3.43 | 4.08 |
| solute carrier family 40 (iron-regulated transporter), member 1 | SLC40A1 | 223044_at | -6.06 | -6.02 |
| solute carrier family 6 (neurotransmitter transporter, taurine), member 6 | SLC6A6 | 205920_at | -2.97 | -2.77 |
| solute carrier family 6 (neurotransmitter transporter, taurine), member 6 | SLC6A6 | 205921_s_at | -3.84 | -2.64 |
| solute carrier family 7 (cationic amino acid transporter, y+ system), member 5 | SLC7A5 | 201195_s_at | -2.41 | -5.06 |
| solute carrier family 7, (cationic amino acid transporter, y+ system) member 11 | SLC7A11 | 207528_s_at | -3.14 | -6.63 |
| solute carrier family 7, (cationic amino acid transporter, y+ system) member 11 | SLC7A11 | 209921_at | -10.56 | -22.47 |
| solute carrier family 7, (cationic amino acid transporter, y+ system) member 11 | SLC7A11 | 217678_at | -10.27 | -13.74 |
| solute carrier family 8 (sodium/calcium exchanger), member 1 | SLC8A1 | 241752_at | 2.43 | 19.29 |
| sorting nexin 9 | SNX9 | 223027_at | -2.22 | -3.03 |
| spastic paraplegia 3A (autosomal dominant) | SPG3A | 223340_at | 2.41 | 2.22 |
| sperm associated antigen 5 | SPAG5 | 203145_at | 2.79 | 2.57 |
| spindle pole body component 24 homolog (S. cerevisiae) | SPBC24 | 235572_at | 2.33 | 3.46 |
| spindle pole body component 25 homolog (S. cerevisiae) | SPBC25 | 209891_at | 5.17 | 4.32 |
| spindlin family, member 3 | SPIN3 | 1555882_at | -2.25 | -2.22 |
| spondin 1, extracellular matrix protein | SPON1 | 209437_s_at | -2.03 | -2.30 |
| spondin 1, extracellular matrix protein | SPON1 | 213993_at | -2.31 | -2.46 |
| sprouty homolog 4 (Drosophila) | SPRY4 | 221489_s_at | 2.20 | 2.99 |
| SRY (sex determining region Y)-box 9 (campomelic dysplasia, autosomal sex-reversal) | SOX9 | 202935_s_at | -2.45 | -5.58 |
| SRY (sex determining region Y)-box 9 (campomelic dysplasia, autosomal sex-reversal) | SOX9 | 202936_s_at | -2.77 | -6.77 |
| ST8 alpha-N-acetyl-neuraminide alpha-2,8-sialyltransferase 4 | ST8SIA4 | 230836_at | -3.10 | -3.01 |
| stanniocalcin 2 | STC2 | 203439_s_at | -2.79 | -2.64 |
| stathmin 1/oncoprotein 18 | STMN1 | 200783_s_at | 3.84 | 2.83 |
| steroid sensitive gene 1 | URB | 243864_at | 2.60 | 3.39 |
| Stonin 2 | STN2 | 227461_at | -2.36 | -4.66 |
| Stonin 2 | STN2 | 235852_at | -5.58 | -6.15 |
| sushi, nidogen and EGF-like domains 1 | SNED1 | 213488_at | -2.22 | -2.53 |
| SWAP-70 protein | SWAP70 | 209306_s_at | 2.01 | 2.43 |
| synapsin II | SYN2 | 229039_at | -2.39 | -2.10 |
| Synaptopodin 2 | SYNPO2 | 225720_at | 4.59 | 19.84 |
| Synaptopodin 2 | SYNPO2 | 225721_at | 3.36 | 3.73 |
| synaptopodin 2 | SYNPO2 | 225894_at | 3.81 | 5.66 |

| Gene title | Gene symbol | Affymetrix probe set ID | + 24 h sample_array 1 versus control_array 1 [fold change] | + 24 h sample_array 2 versus control_array 2 [fold change] |
|---|---|---|---|---|
| synaptopodin 2 | SYNPO2 | 225895_at | 3.46 | 8.40 |
| TAL1 (SCL) interrupting locus | SIL | 205339_at | 2.71 | 3.97 |
| TBC1 (tre-2/USP6, BUB2, cdc16) domain family, member 1 | TBC1D1 | 212350_at | 2.77 | 3.14 |
| TBC1 domain family, member 2 | TBC1D2 | 222173_s_at | 2.06 | 2.03 |
| TBC1 domain family, member 4 | TBC1D4 | 203386_at | 2.41 | 3.94 |
| TBC1 domain family, member 4 | TBC1D4 | 203387_s_at | 2.53 | 3.41 |
| TBC1 domain family, member 8 (with GRAM domain) | TBC1D8 | 1556054_at | -2.04 | -2.16 |
| T-cell activation protein phosphatase 2C | TA-PP2C | 235744_at | -2.41 | -2.01 |
| Tenascin C (hexabrachion) | TNC | 216005_at | 2.81 | 4.99 |
| Tenascin C (hexabrachion) | TNC | 241272_at | 2.07 | 2.99 |
| testis derived transcript (3 LIM domains) | TES | 202719_s_at | 2.11 | 2.51 |
| tetraspanin 14 /// tetraspanin 14 | TSPAN14 | 221002_s_at | -2.06 | -2.93 |
| tetraspanin 2 | TSPAN2 | 227236_at | 5.21 | 5.06 |
| Tetraspanin similiar to uroplakin 1 | LOC90139 | 227307_at | 2.55 | 16.00 |
| thioredoxin reductase 1 | TXNRD1 | 201266_at | -2.13 | -2.01 |
| THO complex 4 | THOC4 | 226320_at | 2.20 | 2.10 |
| thrombospondin 1 | THBS1 | 201107_s_at | 2.57 | 4.50 |
| Thrombospondin 1 | THBS1 | 235086_at | 4.79 | 13.36 |
| thymic stromal lymphopoietin | TSLP | 235737_at | -2.95 | -3.23 |
| thymidine kinase 1, soluble | TK1 | 1554408_a_at | 2.97 | 2.50 |
| thymidine kinase 1, soluble | TK1 | 202338_at | 3.43 | 4.89 |
| thymidylate synthetase | TYMS | 1554696_s_at | 4.38 | 3.36 |
| thymidylate synthetase | TYMS | 202589_at | 3.63 | 3.36 |
| thymopoietin | TMPO | 203432_at | 2.99 | 2.95 |
| thymopoietin | TMPO | 209753_s_at | 2.39 | 3.07 |
| thymopoietin | TMPO | 209754_s_at | 2.51 | 3.97 |
| Thymopoietin | TMPO | 224944_at | 2.64 | 3.16 |
| thyroid hormone receptor interactor 13 | TRIP13 | 204033_at | 3.61 | 4.76 |
| thyrotrophic embryonic factor | TEF | 225840_at | -2.81 | -2.46 |
| TIGA1 | TIGA1 | 225698_at | -2.46 | -3.32 |
| toll-like receptor adaptor molecule 2 | TICAM2 | 228234_at | 2.13 | 2.14 |
| topoisomerase (DNA) II alpha 170kDa | TOP2A | 201291_s_at | 3.81 | 4.50 |
| topoisomerase (DNA) II alpha 170kDa | TOP2A | 201292_at | 4.08 | 3.76 |
| TPX2, microtubule-associated protein homolog (Xenopus laevis) | TPX2 | 210052_s_at | 3.20 | 4.53 |
| Transcribed locus | --- | 229479_at | 19.03 | 17.75 |
| Transcribed locus | --- | 230127_at | 3.61 | 3.92 |
| Transcribed locus | --- | 231098_at | 5.06 | 3.39 |
| Transcribed locus | --- | 235046_at | 2.55 | 3.63 |
| Transcribed locus | --- | 237290_at | 2.87 | 82.71 |
| Transcribed locus | --- | 238467_at | -2.17 | -2.46 |
| Transcribed locus | --- | 238726_at | -4.53 | -4.53 |
| Transcribed locus | --- | 244293_at | -2.55 | -3.18 |
| Transcribed locus, moderately similar to NP_055301.1 neuronal thread protein AD7c-NTP [Homo sapiens] | --- | 228346_at | -2.69 | -2.45 |
| Transcribed locus, moderately similar to XP_510104.1 similar to hypothetical protein FLJ25224 [Pan troglodytes] | --- | 217604_at | -2.69 | -2.50 |
| Transcribed locus, moderately similar to XP_512541.1 similar to hypothetical protein [Pan troglodytes] | --- | 229926_at | 2.50 | 2.17 |
| Transcribed locus, moderately similar to XP_517454.1 similar to hypothetical protein MGC45438 [Pan troglodytes] | --- | 242629_at | 5.82 | 6.77 |
| Transcribed locus, weakly similar to NP_060190.1 signal-transducing adaptor protein-2 [Homo sapiens] | --- | 243584_at | -5.82 | -3.05 |
| Transcribed locus, weakly similar to XP_347139.1 LOC363435 [Rattus norvegicus] | --- | 228049_x_at | -2.17 | -2.91 |
| Transcribed locus, weakly similar to XP_517655.1 similar to KIAA0825 protein [Pan troglodytes] | --- | 229866_at | -2.20 | -4.69 |
| transcription elongation factor A (SII), 3 | TCEA3 | 226388_at | 2.95 | 2.55 |
| transcription factor 19 (SC1) | TCF19 | 223274_at | 4.99 | 5.50 |
| Transducin-like enhancer of split 1 (E(sp1) homolog, Drosophila) | TLE1 | 228284_at | -3.25 | -2.19 |
| transferrin receptor (p90, CD71) | TFRC | 207332_s_at | -2.23 | -2.19 |
| transferrin receptor (p90, CD71) | TFRC | 237215_s_at | -2.45 | -2.64 |
| transforming growth factor beta 1 induced transcript 1 | TGFB1I1 | 209651_at | 4.72 | 6.19 |
| transforming growth factor, beta receptor III (betaglycan, 300kDa) | TGFBR3 | 204731_at | -3.32 | -3.84 |
| Transforming growth factor, beta receptor III (betaglycan, 300kDa) | TGFBR3 | 226625_at | -3.46 | -3.43 |
| transforming, acidic coiled-coil containing protein 3 | TACC3 | 218308_at | 3.01 | 3.29 |
| transgelin 2 | TAGLN2 | 200916_at | 2.16 | 2.20 |
| transgelin 2 | TAGLN2 | 210978_s_at | 2.31 | 2.43 |
| transient receptor potential cation channel, subfamily C, member 4 | TRPC4 | 224219_s_at | 3.07 | 11.63 |

| Gene title | Gene symbol | Affymetrix probe set ID | + 24 h sample_array 1 versus control_array 1 [fold change] | + 24 h sample_array 2 versus control_array 2 [fold change] |
|---|---|---|---|---|
| transient receptor potential cation channel, subfamily V, member 2 | TRPV2 | 219282_s_at | 3.53 | 3.27 |
| transient receptor potential cation channel, subfamily V, member 2 | TRPV2 | 222855_s_at | 3.92 | 4.32 |
| translocase of inner mitochondrial membrane 8 homolog B (yeast) | TIMM8B | 223478_at | -2.03 | -2.31 |
| transmembrane protein 16C | TMEM16C | 215241_at | 3.03 | 7.67 |
| transmembrane protein 38B | TMEM38B | 218772_x_at | -2.50 | -2.53 |
| transmembrane protein 38B | TMEM38B | 222735_at | -2.46 | -2.33 |
| transmembrane protein 38B | TMEM38B | 222736_s_at | -2.31 | -2.66 |
| tribbles homolog 3 (Drosophila) | TRIB3 | 1555788_a_at | -5.35 | -5.82 |
| tribbles homolog 3 (Drosophila) | TRIB3 | 218145_at | -4.44 | -6.68 |
| tripartite motif-containing 16 | TRIM16 | 204341_at | -2.55 | -2.14 |
| tripartite motif-containing 59 | TRIM59 | 227801_at | 5.13 | 5.31 |
| tripartite motif-containing 59 | TRIM59 | 235476_at | 3.12 | 5.66 |
| tropomyosin 1 (alpha) | TPM1 | 206116_s_at | 4.14 | 6.28 |
| tropomyosin 1 (alpha) | TPM1 | 206117_at | 5.74 | 10.27 |
| tropomyosin 1 (alpha) | TPM1 | 210986_s_at | 2.20 | 4.29 |
| tropomyosin 1 (alpha) | TPM1 | 210987_x_at | 2.95 | 4.79 |
| tropomyosin 2 (beta) | TPM2 | 212654_at | 2.58 | 4.38 |
| tropomyosin 3 | TPM3 | 222976_s_at | 2.31 | 2.16 |
| tropomyosin 4 | TPM4 | 212481_s_at | 2.10 | 3.41 |
| TSC22 domain family 1 | TGFB1I4 | 235315_at | 2.46 | 3.84 |
| TSC22 domain family 3 | TSC22D3 | 208763_s_at | -2.22 | -3.39 |
| TTK protein kinase | TTK | 204822_at | 4.66 | 6.96 |
| TU12B1-TY protein | TU12B1-TY | 218786_at | 2.10 | 6.02 |
| tubulin, alpha 1 (testis specific) | TUBA1 | 212242_at | 2.07 | 2.69 |
| tubulin, alpha 3 | TUBA3 | 209118_s_at | 2.04 | 3.10 |
| tubulin, beta 2 /// tubulin, beta polypeptide paralog | TUBB2 /// RP11-506K6.1 | 209372_x_at | 2.00 | 2.73 |
| tubulin, epsilon 1 | TUBE1 | 226181_at | -3.14 | -2.11 |
| tumor necrosis factor receptor superfamily, member 11b (osteoprotegerin) | TNFRSF11B | 204932_at | 3.61 | 21.56 |
| tumor necrosis factor receptor superfamily, member 11b (osteoprotegerin) | TNFRSF11B | 204933_s_at | 4.29 | 29.45 |
| tumor necrosis factor receptor superfamily, member 12A | TNFRSF12A | 218368_s_at | 4.03 | 6.36 |
| tumor necrosis factor receptor superfamily, member 21 | TNFRSF21 | 214581_x_at | -2.55 | -2.01 |
| tyrosine 3-monooxygenase/tryptophan 5-monooxygenase activation protein, eta polypeptide | YWHAH | 201020_at | 3.73 | 3.73 |
| tyrosyl-tRNA synthetase | YARS | 212048_s_at | -2.03 | -2.25 |
| ubiquitin specific protease 1 | USP1 | 202412_s_at | 2.27 | 2.38 |
| ubiquitin specific protease 1 | USP1 | 202413_s_at | 2.04 | 2.36 |
| ubiquitin specific protease 15 | USP15 | 231990_at | 2.30 | 3.39 |
| ubiquitin-conjugating enzyme E2C | UBE2C | 202954_at | 5.82 | 4.35 |
| ubiquitin-conjugating enzyme E2S | UBE2S | 202779_s_at | 2.13 | 2.27 |
| ubiquitin-conjugating enzyme E2T (putative) | UBE2T | 223229_at | 3.25 | 3.03 |
| ubiquitin-like, containing PHD and RING finger domains, 1 | UHRF1 | 225655_at | 8.51 | 12.21 |
| UDP-Gal:betaGlcNAc beta 1,3-galactosyltransferase, polypeptide 2 | B3GALT2 | 210121_at | 138.14 | 26.35 |
| UDP-glucose dehydrogenase | UGDH | 203343_at | 2.41 | 2.28 |
| UDP-N-acetyl-alpha-D-galactosamine:polypeptide N-acetylgalactosaminyltransferase 10 (GalNAc-T10) | GALNT10 | 207357_s_at | 2.14 | 2.99 |
| UDP-N-acetyl-alpha-D-galactosamine:polypeptide N-acetylgalactosaminyltransferase 10 (GalNAc-T10) | GALNT10 | 212256_at | 2.55 | 3.86 |
| UDP-N-acetyl-alpha-D-galactosamine:polypeptide N-acetylgalactosaminyltransferase 3 (GalNAc-T3) | GALNT3 | 203397_s_at | 9.92 | 8.69 |
| UDP-N-acteylglucosamine pyrophosphorylase 1 | UAP1 | 209340_at | 2.13 | 2.28 |
| UL16 binding protein 2 | ULBP2 | 238542_at | 2.73 | 3.03 |
| uveal autoantigen with coiled-coil domains and ankyrin repeats | UACA | 223279_s_at | 4.72 | 7.06 |
| uveal autoantigen with coiled-coil domains and ankyrin repeats | UACA | 238868_at | 3.29 | 3.14 |
| V-abl Abelson murine leukemia viral oncogene homolog 2 (arg, Abelson-related gene) | ABL2 | 226893_at | 2.00 | 2.68 |
| vascular endothelial growth factor | VEGF | 210512_s_at | -2.45 | -2.64 |
| vascular endothelial growth factor | VEGF | 211527_x_at | -2.41 | -3.12 |
| vascular endothelial growth factor | VEGF | 212171_x_at | -2.04 | -2.93 |
| vascular endothelial growth factor C | VEGFC | 209946_at | 3.36 | 4.29 |
| vasodilator-stimulated phosphoprotein | VASP | 202205_at | 2.58 | 4.50 |
| very low density lipoprotein receptor | VLDLR | 209822_s_at | -4.63 | -4.66 |
| villin 2 (ezrin) | VIL2 | 208621_s_at | 8.17 | 2.69 |
| villin 2 (ezrin) | VIL2 | 208622_s_at | 3.78 | 2.35 |
| villin 2 (ezrin) | VIL2 | 208623_s_at | 3.16 | 2.51 |
| villin 2 (ezrin) | VIL2 | 217234_s_at | 4.47 | 2.55 |

| Gene title | Gene symbol | Affymetrix probe set ID | + 24 h sample_array 1 versus control_array 1 [fold change] | + 24 h sample_array 2 versus control_array 2 [fold change] |
|---|---|---|---|---|
| vinculin | VCL | 200931_s_at | 2.28 | 2.91 |
| vitamin K epoxide reductase complex, subunit 1-like 1 | VKORC1L1 | 224881_at | -2.16 | -2.39 |
| v-kit Hardy-Zuckerman 4 feline sarcoma viral oncogene homolog | KIT | 205051_s_at | -3.94 | -7.31 |
| v-maf musculoaponeurotic fibrosarcoma oncogene homolog F (avian) | MAFF | 36711_at | 2.62 | 2.71 |
| v-myb myeloblastosis viral oncogene homolog (avian)-like 1 | MYBL1 | 213906_at | 11.16 | 15.67 |
| WD repeat and HMG-box DNA binding protein 1 | WDHD1 | 204728_s_at | 2.81 | 3.03 |
| WD repeat and HMG-box DNA binding protein 1 | WDHD1 | 216228_s_at | 2.28 | 3.01 |
| WD repeat domain 1 | WDR1 | 200609_s_at | 2.35 | 3.05 |
| WD repeat domain 1 | WDR1 | 200611_s_at | 2.43 | 3.92 |
| WD repeat domain 1 | WDR1 | 210935_s_at | 2.53 | 4.20 |
| WEE1 homolog (S. pombe) | WEE1 | 212533_at | 3.20 | 3.56 |
| wingless-type MMTV integration site family, member 5B | WNT5B | 223537_s_at | 2.87 | 3.81 |
| wingless-type MMTV integration site family, member 5B /// wingless-type MMTV integration site family, member 5B | WNT5B | 221029_s_at | 3.53 | 5.17 |
| WNT1 inducible signaling pathway protein 1 | WISP1 | 206796_at | 2.57 | 2.23 |
| WNT1 inducible signaling pathway protein 1 | WISP1 | 211312_s_at | 2.79 | 2.81 |
| Wolf-Hirschhorn syndrome candidate 1 | WHSC1 | 209053_s_at | 2.30 | 2.62 |
| zinc and ring finger 2 | ZNRF2 | 226261_at | -2.25 | -2.20 |
| zinc finger homeobox 1b | ZFHX1B | 235593_at | -3.58 | -2.19 |
| Zinc finger protein 302 | ZNF302 | 228392_at | -2.04 | -2.36 |
| zinc finger protein 354A | ZNF354A | 205427_at | -2.25 | -2.00 |
| zinc finger protein 36, C3H type-like 1 | ZFP36L1 | 211962_s_at | -2.19 | -2.14 |
| zinc finger protein 367 | ZNF367 | 229551_x_at | 8.17 | 10.34 |
| zinc finger protein 423 | ZNF423 | 214761_at | -2.16 | -2.00 |
| zinc finger protein 436 | ZNF436 | 226113_at | -2.50 | -2.66 |
| zinc finger protein 436 | ZNF436 | 226114_at | -2.04 | -2.43 |
| zinc finger, CCHC domain containing 14 | ZCCHC14 | 212655_at | -2.03 | -2.06 |
| ZW10 interactor | ZWINT | 204026_s_at | 4.03 | 5.74 |
| Zwilch | FLJ10036 | 218349_s_at | 3.48 | 3.66 |
| zyxin | ZYX | 200808_s_at | 2.28 | 3.29 |
| zyxin | ZYX | 215706_x_at | 2.38 | 4.66 |

Transdifferentiated samples were compared to differentiated controls. Fold changes for transcripts with reproducible regulation directions regarding two different MSC charges (array 1 and array 2) are listed by gene name. + 24 h = 24 h after initiation of adipogenic transdifferentiation.

## 7.3   GOstat analyses of gene products regulated during transdifferentiation

**Tab. 18   GOstat analysis – 3 h after initiation of adipogenic transdifferentiation**

| GO term | Gene symbol | Regulated genes | Genes on array | GOstat p-value |
|---|---|---|---|---|
| *biological process* | | | | |
| development | EPHA2 APOLD1 SLC2A14 SIX2 ENC1 EGR2 KLF6 CXCL1 LIF DLX5 HMGA2 HLX1 KLF4 SEMA4C CYR61 EGR3 BICD1 TGIF | 18 | 736 | 0.000858 |
| regulation of transcription, DNA-dependent | NR4A2 SIX2 KLF7 CBX4 CREM ZNF281 ID4 EGR2 KLF6 ZNF331 HIVEP1 CHD1 DLX5 KLF4 HLX1 HMGA2 ZNF217 EGR3 TCF8 TGIF MSC | 21 | 958 | 0.000858 |
| regulation of cellular physiological process | STK38L GAS1 SERPINB2 DUSP6 NR4A2 SIX2 KLF7 CREM CBX4 EGR2 ID4 ZNF281 KLF6 LIF ZNF331 CXCL1 HIVEP1 CHD1 DLX5 HMGA2 HLX1 KLF4 CYR61 EGR3 ZNF217 TNFAIP8 TCF8 TGIF MSC | 29 | 1581 | 0.000858 |
| regulation of cellular process | STK38L GAS1 SERPINB2 DUSP6 NR4A2 SIX2 KLF7 CREM CBX4 EGR2 ID4 ZNF281 KLF6 LIF HIVEP1 ZNF331 CXCL1 CHD1 DLX5 HMGA2 HLX1 KLF4 CYR61 EGR3 ZNF217 TNFAIP8 TCF8 TGIF MSC | 30 | 1695 | 0.000858 |
| regulation of physiological process | STK38L GAS1 SERPINB2 DUSP6 NR4A2 SIX2 KLF7 CREM CBX4 EGR2 ID4 ZNF281 KLF6 LIF ZNF331 CXCL1 HIVEP1 CHD1 DLX5 HMGA2 HLX1 KLF4 CYR61 EGR3 ZNF217 TNFAIP8 TCF8 TGIF MSC | 29 | 16189 | 0.000858 |
| G-protein coupled receptor protein signaling pathway | RGS2 GPRC5A PTGER4 CXCL1 GNAL RASD1 CCL3 GPR157 | 8 | 130 | 0.000858 |
| transcription, DNA-dependent | NR4A2 SIX2 KLF7 CBX4 CREM ZNF281 ID4 EGR2 KLF6 ZNF331 HIVEP1 CHD1 DLX5 KLF4 HLX1 HMGA2 ZNF217 EGR3 TCF8 TGIF MSC | 21 | 995 | 0.000858 |
| cell surface receptor linked signal transduction | RGS2 GPRC5A PTGER4 EPHB3 EPHA2 CXCL1 LIF TNFRSF1B GNAL RASD1 ITGAV CCL3 GPR157 | 13 | 378 | 0.000858 |
| regulation of biological process | STK38L GAS1 SERPINB2 DUSP6 NR4A2 SIX2 KLF7 CREM CBX4 EGR2 ID4 ZNF281 RGS2 KLF6 LIF HIVEP1 ZNF331 CXCL1 CHD1 DLX5 HMGA2 HLX1 KLF4 CYR61 EGR3 ZNF217 TNFAIP8 CCL3 TCF8 TGIF MSC | 31 | 1798 | 0.000858 |
| regulation of transcription | NR4A2 SIX2 KLF7 CBX4 CREM ZNF281 ID4 EGR2 KLF6 ZNF331 HIVEP1 CHD1 DLX5 KLF4 HLX1 HMGA2 ZNF217 EGR3 TCF8 TGIF MSC | 21 | 1013 | 0.00109 |
| regulation of nucleobase, nucleoside, nucleotide and nucleic acid metabolism | NR4A2 SIX2 KLF7 CBX4 CREM ZNF281 ID4 EGR2 KLF6 ZNF331 HIVEP1 CHD1 DLX5 KLF4 HLX1 HMGA2 ZNF217 EGR3 TCF8 TGIF MSC | 21 | 1033 | 0.0015 |
| transcription | NR4A2 SIX2 KLF7 CBX4 CREM ZNF281 ID4 EGR2 KLF6 ZNF331 HIVEP1 CHD1 DLX5 KLF4 HLX1 HMGA2 ZNF217 EGR3 TCF8 TGIF MSC | 21 | 1064 | 0.0025 |
| regulation of cellular metabolism | NR4A2 SIX2 KLF7 CBX4 CREM ZNF281 ID4 EGR2 KLF6 ZNF331 HIVEP1 CHD1 DLX5 KLF4 HLX1 HMGA2 ZNF217 EGR3 TCF8 TGIF MSC | 21 | 1111 | 0.00536 |
| behavior | CCL20 CXCL1 CCL3 EGR2 CYR61 | 5 | 66 | 0.00763 |
| regulation of metabolism | NR4A2 SIX2 KLF7 CBX4 CREM ZNF281 ID4 EGR2 KLF6 ZNF331 HIVEP1 CHD1 DLX5 KLF4 HLX1 HMGA2 ZNF217 EGR3 TCF8 TGIF MSC | 21 | 1144 | 0.00797 |
| negative regulation of biological process | RGS2 CXCL1 KLF4 GAS1 SERPINB2 DUSP6 TNFAIP8 TCF8 CBX4 TGIF ID4 ZNF281 | 12 | 437 | 0.00797 |
| transcription from RNA polymerase II promoter | CHD1 HLX1 TCF8 KLF7 SIX2 TGIF MSC ZNF281 ID4 | 9 | 278 | 0.0138 |
| negative regulation of cellular process | RGS2 CXCL1 KLF4 GAS1 SERPINB2 TNFAIP8 TCF8 CBX4 TGIF ID4 ZNF281 | 11 | 413 | 0.0162 |
| negative regulation of cellular physiological process | CXCL1 KLF4 GAS1 SERPINB2 TNFAIP8 TCF8 TGIF CBX4 ID4 ZNF281 | 10 | 385 | 0.0253 |
| negative regulation of physiological process | CXCL1 KLF4 GAS1 SERPINB2 TNFAIP8 TCF8 TGIF CBX4 ID4 ZNF281 | 10 | 394 | 0.0287 |
| signal transduction | EPHB3 EPHA2 CCL20 STK38L TNFRSF1B DUSP6 RASD1 NR4A2 CREM GPR157 RGS2 RAB20 GPRC5A PTGER4 CXCL1 LIF GNAL ITGAV CCL3 | 19 | 1117 | 0.0342 |
| regulation of transcription from RNA polymerase II promoter | CHD1 TCF8 KLF7 TGIF ID4 ZNF281 | 6 | 161 | 0.0352 |
| immune response | NR4A2 PTGER4 CCL20 KLF6 CCL3 CXCL1 LIF TCF8 | 8 | 282 | 0.0372 |
| negative regulation of transcription | TCF8 KLF4 TGIF ID4 ZNF281 | 5 | 120 | 0.0447 |
| negative regulation of nucleobase, nucleoside, nucleotide and nucleic acid metabolism | TCF8 KLF4 TGIF ID4 ZNF281 | 5 | 125 | 0.0494 |
| defense response | NR4A2 PTGER4 CCL20 KLF6 CCL3 CXCL1 LIF TCF8 | 8 | 306 | 0.0509 |
| cell communication | EPHB3 EPHA2 CCL20 STK38L TNFRSF1B DUSP6 RASD1 NR4A2 CREM GPR157 RGS2 RAB20 GPRC5A PTGER4 CXCL1 LIF GNAL ITGAV CCL3 | 19 | 1195 | 0.0682 |
| response to biotic stimulus | NR4A2 PTGER4 CCL20 KLF6 CCL3 CXCL1 LIF TCF8 | 8 | 328 | 0.0714 |
| negative regulation of | TCF8 KLF4 TGIF ID4 ZNF281 | 5 | 144 | 0.0753 |

| GO term | Gene symbol | Regulated genes | Genes on array | GOstat p-value |
|---------|-------------|-----------------|----------------|----------------|
| cellular metabolism | | | | |
| nervous system development | CXCL1 DLX5 ENC1 EGR2 SEMA4C | 5 | 152 | 0.0905 |
| system development | CXCL1 DLX5 ENC1 EGR2 SEMA4C | 5 | 154 | 0.0905 |
| negative regulation of metabolism | TCF8 KLF4 TGIF ID4 ZNF281 | 5 | 157 | 0.0952 |
| *molecular function* | | | | |
| transcription regulator activity | NR4A2 KLF7 SIX2 CBX4 CREM ZNF281 ID4 EGR2 KLF6 DLX5 HLX1 KLF4 EGR3 ZNF217 TCF8 TGIF MSC | 17 | 588 | 0.0000595 |
| transcription factor activity | DLX5 HLX1 KLF4 ZNF217 NR4A2 EGR3 TCF8 SIX2 KLF7 CREM TGIF EGR2 MSC | 13 | 358 | 0.00131 |
| sequence-specific DNA binding | DLX5 HMGA2 HLX1 NR4A2 TCF8 SIX2 TGIF CREM | 8 | 158 | 0.00529 |
| DNA binding | NR4A2 SIX2 KLF7 CREM ZNF281 EGR2 KLF6 ZNF331 HIVEP1 CHD1 DLX5 KLF4 HMGA2 HLX1 EGR3 ZNF217 TCF8 TGIF MSC | 19 | 923 | 0.00544 |
| transcription corepressor activity | TCF8 TGIF CBX4 ID4 MSC | 5 | 60 | 0.00857 |
| transcriptional repressor activity | TCF8 KLF4 TGIF CBX4 ID4 MSC | 6 | 102 | 0.00998 |
| signal transducer activity | RGS2 GPRC5A PTGER4 EPHB3 EPHA2 CCL20 CXCL1 LIF TNFRSF1B GNAL SEMA4C NR4A2 ITGAV CCL3 GPR157 | 15 | 773 | 0.0339 |
| transcription cofactor activity | TCF8 KLF7 TGIF CBX4 ID4 MSC | 6 | 160 | 0.0467 |
| receptor activity | GPRC5A PTGER4 EPHB3 EPHA2 TNFRSF1B SEMA4C NR4A2 ITGAV GPR157 | 9 | 368 | 0.0658 |
| transmembrane receptor activity | GPRC5A PTGER4 EPHB3 EPHA2 TNFRSF1B GPR157 | 6 | 194 | 0.0921 |

Reliably measured and 3 h after initiation of adipogenic transdifferentiation differentially regulated probe sets with at least one P detection call in the compared samples for each experimental set were subjected to GOstat analyses. The total number of regulated and not regulated probe sets detected on the GeneChip served as reference and is given in the respective column. Only over-represented GO classes containing at least 5 genes and a GOstat p-value ≤ 0.1 were considered. Adipogenic transdifferentiation exhibited 159 differentially regulated target probe sets that were analyzed in reference to all 20,357 reliably measured probe sets for the 3 h time point. The GO class of cellular component did not show any relevant over-representation 3 h after initiation of adipogenic transdifferentiation under the criteria stated above. Gene symbols are stated according to the HUGO gene nomenclature.

**Tab. 19   GOstat analysis – 24 h after initiation of adipogenic transdifferentiation**

| GO term | Gene symbol | Regulated genes | Genes on array | GOstat p-value |
|---------|-------------|-----------------|----------------|----------------|
| *cellular component* | | | | |
| extracellular region | UACA CHL1 CSPG4 IL32 LPL IGF1 ANGPTL2 ECGF1 TNFRSF11B CX3CL1 MMP1 FGF2 CXCL13 WNT5B FGF1 CXCL12 COL13A1 LEP CYR61 IGFBP5 PRL SERPINE1 PLA2G5 FN1 | 24 | 353 | 0.000014 |
| cytoskeleton | FBLIM1 DIAPH1 UACA TPM1 STK38L RAPH1 VASP FGD4 FSCN1 CFL2 CALD1 RP11-54H7.1 ACTG2 NEDD9 MICAL2 PDLIM7 PLEKHC1 ACTC CTNNAL1 MYLIP DSP TUBB6 SMTN PALLD | 24 | 363 | 0.0000154 |
| actin cytoskeleton | ACTG2 RP11-54H7.1 TPM1 STK38L VASP ACTC PLEKHC1 FSCN1 CTNNAL1 SMTN PALLD | 11 | 101 | 0.00198 |
| extracellular region part | CHL1 CSPG4 IL32 LPL ANGPTL2 ECGF1 CX3CL1 MMP1 FGF2 CXCL13 FGF1 CXCL12 COL13A1 LEP PRL FN1 | 16 | 253 | 0.00293 |
| extracellular space | FGF1 IL32 LPL CXCL12 ANGPTL2 LEP PRL ECGF1 CX3CL1 CXCL13 MMP1 FGF2 | 12 | 152 | 0.00919 |
| microsome | CYP1B1 CYP19A1 HMOX1 SSR3 CYP7B1 HSD11B1 | 6 | 49 | 0.0307 |
| cell fraction | CYP19A1 SPHK1 CLCN4 SSR3 CH25H FABP4 CYP1B1 GALNT3 ECGF1 CHGN PDLIM5 CYP7B1 CXCL13 ABCA1 HMOX1 PRL HSD11B1 | 17 | 335 | 0.0307 |
| vesicular fraction | CYP1B1 CYP19A1 HMOX1 SSR3 CYP7B1 HSD11B1 | 6 | 51 | 0.0307 |
| *biological process* | | | | |
| development | HOP CHL1 EBF DDIT4L BDNF FZD4 CYP1B1 CHGN DSCR1L1 PDLIM5 HDAC9 GLDN CLTCL1 FABP5 FGF1 PDLIM7 HMGA2 TNFRSF12A CYR61 SORT1 PPARGC1A AHNAK PRL DSP CEBPA FBLIM1 CSPG4 EYA1 IGF1 ANGPTL2 FGD4 ROR2 CAP2 VEGFC PALMD TNFRSF11B ECGF1 BHLHB3 FGF2 MAFB ARNT2 WNT5B NEDD9 KLF6 PLEKHC1 IGFBP5 MYLIP MKX SMTN | 49 | 771 | $4.99 \times 10^{-11}$ |
| organ development | CSPG4 DDIT4L IGF1 VEGFC CYP1B1 BHLHB3 ECGF1 TNFRSF11B PDLIM5 FGF2 MAFB HDAC9 KLF6 FGF1 PDLIM7 TNFRSF12A SORT1 PRL CEBPA MKX SMTN | 21 | 244 | 0.000000296 |
| cell differentiation | CHL1 CSPG4 VEGFC BHLHB3 ECGF1 MAFB FGF2 ARNT2 HDAC9 GLDN KLF6 FGF1 PDLIM7 TNFRSF12A PPARGC1A SORT1 PRL | 19 | 217 | 0.000000903 |

| GO term | Gene symbol | Regulated genes | Genes on array | GOstat p-value |
|---|---|---|---|---|
| | DSP CEBPA | | | |
| organismal physiological process | DIAPH1 TPM1 CD97 MICB EYA1 IL32 PDE7B IGF1 LPL DHRS3 FOSL1 CYP1B1 SLC8A1 CX3CL1 CXCL13 CALD1 ADA HDAC9 TAS2R38 AKR1C2 KLF6 GPR176 OXTR PDLIM7 CXCL12 PPARGC1A SORT1 PRL HSPB7 SERPINE1 CNN1 SMTN FN1 | 33 | 568 | 0.00000906 |
| signal transduction | CHL1 LRRFIP2 CMKOR1 FZD4 ARHGAP28 SNF1LK2 ARHGAP29 INPP4B ARL4C DSCR1L1 CX3CL1 RGS4 RAB20 FGF1 ANKRD1 SGK3 PPARGC1A PRL SERPINB9 CEBPA PLCB4 DIRAS3 FN1 SPHK1 CSPG4 STK38L RAPH1 PDE7B IGF1 FGD4 ROR2 TNS3 RASD1 CAP2 VEGFC CLIC3 TNFRSF11B ECGF1 ADCY7 FGF2 ARNT2 WNT5B TAS2R38 NEDD9 GPR176 RAB3B HMOX1 OXTR CXCL12 GNAL LEP IGFBP5 | 53 | 1170 | 0.0000202 |
| cell communication | CHL1 LRRFIP2 CMKOR1 FZD4 ARHGAP28 SNF1LK2 ARHGAP29 INPP4B ARL4C DSCR1L1 CX3CL1 RGS4 RAB20 FGF1 ANKRD1 SGK3 PPARGC1A PRL SERPINB9 CEBPA PLCB4 DIRAS3 FN1 SPHK1 CSPG4 STK38L CD97 RAPH1 PDE7B IGF1 FGD4 ROR2 TNS3 RASD1 CAP2 VEGFC CLIC3 TNFRSF11B ECGF1 ADCY7 SLC8A1 CXCL13 FGF2 ARNT2 WNT5B TAS2R38 NEDD9 GPR176 RAB3B HMOX1 OXTR CXCL12 GNAL LEP IGFBP5 | 55 | 1258 | 0.0000382 |
| morphogenesis | FBLIM1 CSPG4 DDIT4L EYA1 FGD4 PALMD CAP2 VEGFC ECGF1 BHLHB3 CHGN PDLIM5 FGF2 NEDD9 CLTCL1 FGF1 TNFRSF12A PLEKHC1 CYR61 IGFBP5 | 20 | 289 | 0.0000836 |
| G-protein coupled receptor protein signaling pathway | TAS2R38 GPR176 SPHK1 CD97 OXTR CMKOR1 CXCL12 GNAL FZD4 RASD1 CAP2 ADCY7 RGS4 | 13 | 126 | 0.00105 |
| angiogenesis | VEGFC FGF1 ECGF1 CSPG4 DDIT4L TNFRSF12A FGF2 | 7 | 33 | 0.00172 |
| cell surface receptor linked signal transduction | SPHK1 LRRFIP2 CD97 CMKOR1 FZD4 RASD1 SNF1LK2 CAP2 ECGF1 ADCY7 CX3CL1 RGS4 WNT5B NEDD9 TAS2R38 GPR176 OXTR CXCL12 GNAL PRL CEBPA FN1 | 22 | 388 | 0.00172 |
| blood vessel development | VEGFC FGF1 ECGF1 CSPG4 DDIT4L TNFRSF12A FGF2 | 7 | 35 | 0.00185 |
| blood vessel morphogenesis | VEGFC FGF1 ECGF1 CSPG4 DDIT4L TNFRSF12A FGF2 | 7 | 35 | 0.00185 |
| vasculature development | VEGFC FGF1 ECGF1 CSPG4 DDIT4L TNFRSF12A FGF2 | 7 | 36 | 0.002 |
| cell adhesion | FBLIM1 NEDD9 CHL1 AGC1 CD97 DDIT4L IL32 CXCL12 PLEKHC1 TNFRSF12A CTNNAL1 CYR61 BOC CX3CL1 FN1 | 15 | 232 | 0.00439 |
| taxis | FOSL1 ECGF1 CXCL12 CX3CL1 FGF2 CXCL13 CYR61 | 7 | 50 | 0.0102 |
| chemotaxis | FOSL1 ECGF1 CXCL12 CX3CL1 FGF2 CXCL13 CYR61 | 7 | 50 | 0.0102 |
| locomotory behavior | FOSL1 ECGF1 CXCL12 CX3CL1 FGF2 CXCL13 CYR61 | 7 | 51 | 0.0108 |
| response to external stimulus | HDAC9 CD97 MICB CXCL12 CYR61 PPARGC1A FOSL1 ECGF1 SERPINE1 CX3CL1 CXCL13 FGF2 FN1 | 13 | 177 | 0.0117 |
| cell motility | TPM1 CD97 VASP IGF1 TNFRSF12A VEGFC MYLIP CX3CL1 CALD1 FN1 | 10 | 115 | 0.0145 |
| locomotion | TPM1 CD97 VASP IGF1 TNFRSF12A VEGFC MYLIP CX3CL1 CALD1 FN1 | 10 | 115 | 0.0145 |
| localization of cell | TPM1 CD97 VASP IGF1 TNFRSF12A VEGFC MYLIP CX3CL1 CALD1 FN1 | 10 | 115 | 0.0145 |
| behavior | FOSL1 ECGF1 CXCL12 CX3CL1 FGF2 CXCL13 CYR61 | 7 | 61 | 0.0222 |
| muscle contraction | TPM1 CNN1 OXTR SMTN SLC8A1 CALD1 | 6 | 44 | 0.0223 |
| organ morphogenesis | VEGFC BHLHB3 ECGF1 FGF1 CSPG4 DDIT4L PDLIM5 TNFRSF12A FGF2 | 9 | 103 | 0.0234 |
| response to chemical stimulus | ARNT2 DNAJB4 HSPB2 CXCL12 CYR61 FOSL1 HSPB7 ECGF1 CX3CL1 CXCL13 FGF2 | 11 | 159 | 0.0371 |
| hemopoiesis | HDAC9 PRL KLF6 CEBPA MAFB | 5 | 39 | 0.0663 |
| hemopoietic or lymphoid organ development | HDAC9 PRL KLF6 CEBPA MAFB | 5 | 40 | 0.0706 |
| response to abiotic stimulus | ARNT2 DNAJB4 HSPB2 CXCL12 CYR61 FOSL1 HSPB7 ECGF1 CX3CL1 CXCL13 FGF2 | 11 | 181 | 0.0829 |
| actin cytoskeleton organization and biogenesis | DIAPH1 NEDD9 CNN1 CXCL12 PLEKHC1 FGD4 FSCN1 | 7 | 83 | 0.0829 |
| response to stimulus | DIAPH1 DNAJB4 CD97 MICB REV3L IL32 HSPB2 EYA1 IGF1 DHRS3 FOSL1 CYP1B1 ECGF1 CX3CL1 FGF2 CXCL13 HDAC9 ADA ARNT2 TAS2R38 KLF6 ANKRD1 CXCL12 SGK3 CYR61 PPARGC1A HSPB7 SERPINE1 UHRF1 FN1 | 30 | 784 | 0.0984 |
| actin filament-based process | DIAPH1 NEDD9 CNN1 CXCL12 PLEKHC1 FGD4 FSCN1 | 7 | 88 | 0.0984 |
| response to wounding | HDAC9 CD97 MICB CXCL12 FOSL1 SERPINE1 CX3CL1 CXCL13 FN1 | 9 | 137 | 0.0984 |
| nervous system development | ARNT2 CHL1 GLDN BDNF AHNAK MYLIP CHGN DSCR1L1 MAFB FGF2 | 10 | 163 | 0.0984 |
| *molecular function* | | | | |
| signal transducer activity | DIAPH1 MICB CMKOR1 LOXL4 BDNF LRP4 FZD4 PDLIM5 CX3CL1 RGS4 CLTCL1 FGF1 TNFRSF12A PPARGC1A SORT1 PRL PLCB4 CD97 EVI2A CSPG4 IL32 IGF1 ANGPTL2 ROR2 GMFG VEGFC ECGF1 TNFRSF11B FGF2 CXCL13 WNT5B ARNT2 TAS2R38 GPR176 HMOX1 OXTR CXCL12 GNAL LEP | 39 | 794 | 0.000196 |
| receptor binding | DIAPH1 IL32 BDNF IGF1 ANGPTL2 VEGFC GMFG ECGF1 TNFRSF11B CX3CL1 FGF2 CXCL13 ARNT2 FGF1 CXCL12 PPARGC1A LEP PRL | 18 | 247 | 0.000196 |
| actin binding | DIAPH1 TPM1 SYNPO2 STK38L VASP FGD4 FSCN1 GMFG CFL2 CNN1 SMTN PDLIM5 CALD1 | 13 | 114 | 0.00054 |
| cytoskeletal protein | DIAPH1 TPM1 SYNPO2 STK38L VASP FGD4 FSCN1 GMFG MYLIP | 15 | 177 | 0.00208 |

| GO term | Gene symbol | Regulated genes | Genes on array | GOstat p-value |
|---|---|---|---|---|
| binding | CFL2 CNN1 SMTN PDLIM5 PALLD CALD1 | | | |
| growth factor activity | VEGFC GMFG ECGF1 FGF1 CXCL12 BDNF IGF1 FGF2 | 8 | 64 | 0.0127 |
| carbohydrate binding | AGC1 FGF1 DDIT4L LPL CYR61 GFPT2 GALNT3 FGF2 FN1 | 9 | 87 | 0.0157 |
| glycosaminoglycan binding | AGC1 FGF1 LPL FGF2 CYR61 FN1 | 6 | 44 | 0.0299 |
| polysaccharide binding | AGC1 FGF1 LPL FGF2 CYR61 FN1 | 6 | 44 | 0.0299 |
| pattern binding | AGC1 FGF1 LPL FGF2 CYR61 FN1 | 6 | 46 | 0.0332 |
| G-protein coupled receptor activity | TAS2R38 GPR176 CD97 OXTR CMKOR1 SORT1 FZD4 | 7 | 68 | 0.0417 |
| heparin binding | FGF1 LPL FGF2 CYR61 FN1 | 5 | 34 | 0.0419 |
| cytokine activity | PRL ECGF1 TNFRSF11B IL32 CXCL12 CX3CL1 CXCL13 | 7 | 77 | 0.0553 |
| protein binding | DNAJB4 EBF BDNF CFL2 CHGN ABCA1 FABP5 FGF1 PDLIM7 TNFRSF12A PPARGC1A CYR61 PRL CNN1 SERPINE1 PALLD CSPG4 STK38L IGF1 FOSL1 CLIC3 LMO7 TNFRSF11B SLC8A1 PPP1R13L FGF2 ACTG2 CXCL12 ACTC BOC MYLIP IGFBP5 HSPB7 UHRF1 DIAPH1 CHL1 LRRFIP2 MICB HSPB2 VASP MDM2 CX3CL1 PDLIM5 DSCR1L1 RGS4 HDAC9 SGK3 CTNNAL1 DSP SERPINB9 CEBPA MARCKSL1 PAWR FN1 FBLIM1 TPM1 SYNPO2 RNF144 CD97 IL32 ANGPTL2 SSR3 FGD4 FSCN1 VEGFC GMFG MAGI2 IBRDC2 ECGF1 MAFB CXCL13 CALD1 ARNT2 NEDD9 PLEKHC1 LEP SMTN | 77 | 2552 | 0.083 |
| transmembrane receptor activity | TAS2R38 GPR176 CD97 EVI2A MICB OXTR CMKOR1 LOXL4 ROR2 SORT1 FZD4 | 11 | 189 | 0.083 |
| enzyme binding | DIAPH1 MDM2 FGD4 MAGI2 SERPINE1 DSCR1L1 PDLIM5 PAWR | 8 | 115 | 0.0913 |
| binding | EBF BDNF CFL2 PPM2C CLTCL1 ABCA1 FABP5 ANKRD1 PPARGC1A SORT1 SLC19A3 SERPINE1 TUBB6 DIRAS3 CYP19A1 CSPG4 STK38L EYA1 IGF1 LMO7 GALNT3 TNFRSF11B ADCY7 PPP1R13L FGF2 ACTG2 AGC1 HMOX1 CXCL12 GNAL MYLIP HSPB7 UHRF1 DIAPH1 CHL1 LRRFIP2 SNED1 HK2 DDIT4L MICB LOXL4 CLCN4 HSPB2 VASP SNF1LK2 CX3CL1 DSCR1L1 RGS4 MICAL2 SGK3 CTNNAL1 DSP MARCKSL1 PAWR SYNPO2 IL32 ANGPTL2 LPL FGD4 VEGFC GMFG IBRDC2 BHLHB3 KLF2 CXCL13 NEDD9 FRY OXTR LEP TSC22D1 HOP DNAJB4 REV3L DHRS3 FABP4 ARL4C CHGN RAB20 FGF1 PDLIM7 TNFRSF12A CYR61 PRL CNN1 PLCB4 PALLD PDK4 SPHK1 RASD1 FOSL1 CLIC3 SLC8A1 CYP7B1 MMP1 AKR1C2 ACTC IGFBP5 OSR2 BOC PLA2G5 MDM2 CH25H LRP4 CYP1B1 GFPT2 LMCD1 SERAC1 PDLIM5 HDAC9 RP11-54H7.1 HMGA2 SERPINB9 CEBPA FN1 FBLIM1 TPM1 RNF144 CD97 HIST1H2BD SSR3 ROR2 FSCN1 MAGI2 ECGF1 CALD1 MAFB ARNT2 RAB3B KLF6 PLEKHC1 ARRDC3 B3GALT2 MKX SMTN | 134 | 5062 | 0.0913 |
| calmodulin binding | CNN1 MARCKSL1 SLC8A1 CALD1 RGS4 | 5 | 51 | 0.0984 |

GOstat analysis results for genes showing differential regulation 24 h after initiation of adipogenic transdifferentiation are depicted under the same prerequisites as described for tab. 18. Altogether, 418 target probe sets were referred to 21,892 reliably measured probe sets for the 24 h time point.

**Tab. 20   GOstat analysis 3 h after initiation of osteogenic transdifferentiation**

| GO term | Gene symbol | Regulated genes | Genes on array | GOstat p-value |
|---|---|---|---|---|
| *cellular component* | | | | |
| extracellular region | MMP3 GDF15 MMP12 ANGPTL4 COL1A2 | 5 | 344 | 0.0782 |
| *biological process* | | | | |
| cellular carbohydrate metabolism | MMP3 MMP12 PDK4 EXT1 PCK1 | 5 | 190 | 0.0916 |
| *molecular function* | | | | |
| signal transducer activity | EDG2 ACVR1C GDF15 PBEF1 PDLIM5 RGS4 FZD4 | 7 | 790 | 0.0938 |

GOstat analysis results for genes showing differential regulation 3 h after initiation of osteogenic transdifferentiation are depicted under the same prerequisites as described for tab. 18. Altogether, 92 target probe sets were obtained 3 h after initiation of transdifferentiation and analysed to the reference of all 22,634 reliably measured probe sets at this time point.

**Tab. 21  GOstat analysis 24 h after initiation of osteogenic transdifferentiation**

| GO term | Gene symbol | Regulated genes | Genes on array | GOstat p-value |
|---|---|---|---|---|
| *cellular component* | | | | |
| cytoskeleton | DIAPH1 KIF20A ESPL1 KIF21A TPM4 TUBA1 MPHOSPH1 HIP1 BUB1 VASP AURKA MICAL1 ARPC5 MICAL2 LASP1 PPL CTNNAL1 HSPB1 KIF14 DSP CENPE PALLD PDLIM2 UACA FBLIM1 RAI14 BUB1B TPM1 LMNB1 KIF11 RAPH1 CKAP2 SPAG5 FSCN1 DBN1 EPB41L2 CALD1 ACTG2 KIF4A LOC146909 TTK NEDD9 RACGAP1 CDC42EP5 CDC20 TPX2 KNS2 KIF23 WDR1 MYLIP NEK2 ANLN EPB41L3 PRC1 SGCD KIF15 SMTN TPM2 KIF2C DLG7 ARHGDIB | 61 | 379 | $2.84 \times 10^{-11}$ |
| cytoskeletal part | KIF20A ESPL1 KIF21A TUBA1 MPHOSPH1 BUB1 AURKA MICAL1 ARPC5 LASP1 KIF14 DSP CENPE PALLD BUB1B TPM1 LMNB1 KIF11 CKAP2 SPAG5 DBN1 EPB41L2 LOC146909 ACTG2 KIF4A RACGAP1 TTK NEDD9 CDC20 TPX2 KNS2 KIF23 NEK2 ANLN PRC1 KIF15 TPM2 KIF2C DLG7 | 39 | 203 | $6.16 \times 10^{-10}$ |
| microtubule cytoskeleton | BUB1B KIF20A ESPL1 KIF21A KIF11 TUBA1 MPHOSPH1 BUB1 CKAP2 SPAG5 AURKA LOC146909 KIF4A RACGAP1 NEDD9 TTK CDC20 KNS2 TPX2 KIF23 KIF14 NEK2 PRC1 CENPE KIF15 KIF2C DLG7 | 27 | 141 | 0.00000083 |
| intracellular non-membrane-bound organelle | RFC3 ESPL1 KIF21A TPM4 TUBA1 BUB1 TMPO AURKB RAD50 CBX5 ARPC5 KRR1 LASP1 PPL HSPB1 CHEK1 PALLD KIF11 MRPS25 MKI67 HNRPD CKAP2 MCM2 ZWILCH DBN1 EPB41L2 LOC146909 ACTG2 RACGAP1 CDC20 KNS2 TPX2 MYLIP NEK2 ANLN EPB41L3 KIF15 KIF2C DLG7 KIF20A DIAPH1 MPHOSPH1 HIP1 CDCA5 VASP AURKA MICAL1 TOP2A PRRX2 SGOL2 MICAL2 HMGA2 CTNNAL1 KIF14 DSP CENPE EXOSC9 PDLIM2 UACA BUB1B RAI14 FBLIM1 TPM1 LMNB1 MAD2L1 RAPH1 FSCN1 SPAG5 CALD1 KIF4A NEDD9 TTK CDC42EP5 KIF23 KNTC2 MCM7 WDR1 PRC1 RPL31 SGCD TPM2 SMTN CDCA8 ARHGDIB | 84 | 746 | 0.00000083 |
| non-membrane-bound organelle | RFC3 ESPL1 KIF21A TPM4 TUBA1 BUB1 TMPO AURKB RAD50 CBX5 ARPC5 KRR1 LASP1 PPL HSPB1 CHEK1 PALLD KIF11 MRPS25 MKI67 HNRPD CKAP2 MCM2 ZWILCH DBN1 EPB41L2 LOC146909 ACTG2 RACGAP1 CDC20 KNS2 TPX2 MYLIP NEK2 ANLN EPB41L3 KIF15 KIF2C DLG7 KIF20A DIAPH1 MPHOSPH1 HIP1 CDCA5 VASP AURKA MICAL1 TOP2A PRRX2 SGOL2 MICAL2 HMGA2 CTNNAL1 KIF14 DSP CENPE EXOSC9 PDLIM2 UACA BUB1B RAI14 FBLIM1 TPM1 LMNB1 MAD2L1 RAPH1 FSCN1 SPAG5 CALD1 KIF4A NEDD9 TTK CDC42EP5 KIF23 KNTC2 MCM7 WDR1 PRC1 RPL31 SGCD TPM2 SMTN CDCA8 ARHGDIB | 84 | 746 | 0.00000083 |
| spindle | BUB1B KIF4A NEDD9 TTK CDC20 KIF11 BUB1 TPX2 KIF23 AURKA PRC1 DLG7 | 12 | 33 | 0.00021 |
| chromosome, pericentric region | BUB1B SGOL2 MAD2L1 BUB1 KNTC2 AURKB ZWILCH CENPE CDCA8 KIF2C | 10 | 31 | 0.00252 |
| extracellular region | MMP13 CHL1 MMP12 IGFBP1 APOL6 PLAT GLIPR1 YARS GREM2 FSTL3 MFAP5 PRRG4 PDGFA FGF1 SAA2 CYR61 LAMA4 VEGF CHI3L1 SERPINE1 COMP CLEC3B COL11A1 FN1 UACA THBS1 ANGPTL2 HAPLN1 PHGDH TNFRSF11B CXCL13 WNT5B GDF15 CXCL12 ANGPTL4 WISP1 LEP COL8A1 SGCD CTGF ADIPOQ | 41 | 362 | 0.00397 |
| microtubule | KIF4A KIF20A RACGAP1 KIF21A KIF11 TUBA1 KNS2 MPHOSPH1 CKAP2 KIF23 SPAG5 KIF14 PRC1 KIF15 CENPE KIF2C | 16 | 96 | 0.0047 |
| microtubule associated complex | KIF4A KIF20A LOC146909 KIF21A KIF11 MPHOSPH1 KNS2 KIF23 KIF14 CENPE KIF15 KIF2C | 12 | 54 | 0.00628 |
| chromosome | BUB1B RFC3 MAD2L1 BUB1 TMPO HNRPD MCM2 CDCA5 AURKB ZWILCH RAD50 CBX5 TOP2A PRRX2 SGOL2 HMGA2 KNTC2 MCM7 CHEK1 CENPE CDCA8 KIF2C | 22 | 159 | 0.00628 |
| kinesin complex | KIF11 KNS2 KIF15 KIF23 KIF2C | 5 | 9 | 0.0135 |
| chromosomal part | BUB1B RFC3 SGOL2 MAD2L1 BUB1 HNRPD HMGA2 MCM2 CDCA5 KNTC2 AURKB MCM7 RAD50 ZWILCH CBX5 CENPE CDCA8 KIF2C | 18 | 128 | 0.015 |
| kinetochore | BUB1B ZWILCH MAD2L1 CENPE BUB1 | 5 | 17 | 0.0877 |
| *biological process* | | | | |
| mitosis | ESPL1 BUB1 PLK1 CDCA5 CCNB1 AURKB AURKA PBK CDC2 NUSAP1 UBE2C CDC6 WEE1 CIT CENPE BUB1B KIF11 MAD2L1 BRRN1 CEP55 SPAG5 CCNA2 YWHAH CCNB2 NEDD9 TTK CDC20 TPX2 PTTG1 KIF23 KNTC2 NEK2 ANLN KIF15 CDCA8 HCAP-G KIF2C DLG7 | 38 | 117 | $2.57 \times 10^{-20}$ |
| M phase of mitotic cell cycle | ESPL1 BUB1 PLK1 CDCA5 CCNB1 AURKB AURKA PBK CDC2 NUSAP1 UBE2C CDC6 WEE1 CIT CENPE BUB1B KIF11 MAD2L1 BRRN1 CEP55 SPAG5 CCNA2 YWHAH CCNB2 NEDD9 TTK CDC20 TPX2 PTTG1 KIF23 KNTC2 NEK2 ANLN KIF15 CDCA8 HCAP-G KIF2C DLG7 | 38 | 119 | $3.57 \times 10^{-20}$ |
| M phase | ESPL1 BUB1 PLK1 CDCA5 CCNB1 AURKB AURKA RAD50 PBK CDC2 NUSAP1 UBE2C CDC6 WEE1 CIT CHEK1 CENPE BUB1B KIF11 MAD2L1 BRRN1 CEP55 SPAG5 CCNA2 YWHAH CCNB2 NEDD9 TTK CDC20 TPX2 PTTG1 KIF23 KNTC2 NEK2 ANLN KIF15 CDCA8 KIF2C HCAP-G DLG7 | 40 | 136 | $2.5 \times 10^{-19}$ |
| mitotic cell cycle | CDKN3 ESPL1 BUB1 PLK1 CDCA5 CCNB1 AURKB AURKA PBK CDC2 NUSAP1 UBE2C CDC6 WEE1 CIT CENPE BUB1B KIF11 MAD2L1 BRRN1 CEP55 SPAG5 CCND1 CCNA2 CDK6 YWHAH CCNB2 NEDD9 TTK CDC20 TPX2 KIF23 PTTG1 KNTC2 NEK2 ANLN PRC1 KIF15 CDCA8 KIF2C HCAP-G DLG7 | 42 | 157 | $5.35 \times 10^{-18}$ |
| cell division | ESPL1 BUB1 CDCA5 CCNB1 AURKB CDC2 NUSAP1 SGOL2 UBE2C CDC6 WEE1 CDCA1 CIT CENPE BUB1B KIF11 MAD2L1 BRRN1 CEP55 SPAG5 CCND1 CCNA2 CDK6 CCND3 CCNB2 | 42 | 157 | $7.04 \times 10^{-18}$ |

| GO term | Gene symbol | Regulated genes | Genes on array | GOstat p-value |
|---|---|---|---|---|
| | NEDD9 RACGAP1 CDC20 KIF23 PTTG1 CCNE2 NEK2 ANLN PRC1 CDCA8 HCAP-G | | | |
| cell cycle | CDKN3 ESPL1 DDIT3 BUB1 E2F7 AURKB RAD50 PBK E2F8 PDGFA FGF1 MCM5 CDC6 RGC32 MCM6 CHEK1 DIRAS3 HRASLS3 KIF11 MKI67 CKAP2 CEP55 MCM2 BARD1 CDK6 CCND3 YWHAH RACGAP1 CDC20 BRIP1 TPX2 PTTG1 NEK2 ANLN KIF15 KIF2C DLG7 UHRF1 HK2 ZWINT CDCA5 PLK1 CCNB1 AURKA TCF19 CDC2 HDAC9 NUSAP1 SGOL2 MSH2 UBE2C WEE1 VEGF CIT CENPE BUB1B MAD2L1 BRRN1 SPAG5 SPIN3 PLK4 VEGFC CCNA2 CCNB2 NEDD9 TTK CCNE2 KIF23 KNTC2 MCM7 PRC1 SESN2 CDCA8 HCAP-G | 75 | 462 | $1.13 \times 10^{-14}$ |
| cytoskeleton organization and biogenesis | DIAPH1 KIF20A ESPL1 KIF21A TUBA1 ZWINT MPHOSPH1 AURKA ADRA2A MICAL1 ARPC5 NUSAP1 LASP1 UBE2C KIF14 CNN1 CENPE PALLD BUB1B KIF11 FSCN1 SPAG5 DBN1 EPB41L2 LOC146909 KIF4A YWHAH CDC42EP5 RACGAP1 NEDD9 TTK KNS2 KIF23 CXCL12 KNTC2 PRC1 EPB41L3 SGCD KIF15 KIF2C ARHGDIB | 41 | 201 | $1.45 \times 10^{-11}$ |
| microtubule-based process | BUB1B KIF20A ESPL1 KIF21A KIF11 TUBA1 ZWINT MPHOSPH1 SPAG5 AURKA LOC146909 KIF4A TTK NUSAP1 KNS2 UBE2C KIF23 KNTC2 KIF14 PRC1 CENPE KIF15 KIF2C | 23 | 83 | $7.67 \times 10^{-10}$ |
| regulation of progression through cell cycle | CDKN3 ESPL1 HK2 DDIT3 BUB1 E2F7 PLK1 CCNB1 CDC2 E2F8 TCF19 HDAC9 NUSAP1 PDGFA MSH2 FGF1 MCM5 CDC6 UBE2C WEE1 RGC32 VEGF CHEK1 DIRAS3 BUB1B HRASLS3 MAD2L1 MKI67 CCND1 PLK4 BARD1 VEGFC CCNA2 YWHAH CCND3 CDK6 NEDD9 CCNB2 TTK CDC20 BRIP1 CCNE2 NEK2 SESN2 DLG7 | 45 | 302 | 0.00000089 |
| regulation of cell cycle | CDKN3 ESPL1 HK2 DDIT3 BUB1 E2F7 PLK1 CCNB1 CDC2 E2F8 TCF19 HDAC9 NUSAP1 PDGFA MSH2 FGF1 MCM5 CDC6 UBE2C WEE1 RGC32 VEGF CHEK1 DIRAS3 BUB1B HRASLS3 MAD2L1 MKI67 CCND1 PLK4 BARD1 VEGFC CCNA2 YWHAH CCND3 CDK6 NEDD9 CCNB2 TTK CDC20 BRIP1 CCNE2 NEK2 SESN2 DLG7 | 45 | 304 | 0.00000103 |
| development | EMP1 EBF IGFBP1 CASC5 FOXC2 BDNF NRCAM SLC3A2 SEMA6D CSRP2 EDNRB NTRK2 TAGLN FGF1 PPL TNFRSF12A LAMA4 CYR61 PPARGC1A IFRD1 CLEC3B COL11A1 EPHA2 PALMD CAP2 DBN1 PHGDH SOX9 TNFRSF11B MEOX2 IER3 WNT5B YWHAH LPIN1 RACGAP1 HLF WISP1 MYLIP CTGF CAP1 CHL1 DDIT4L ALDH3A2 GPM6B NRAS FZD4 CYP1B1 TAGLN2 ALPL SEMA3G GHR DLX1 PDLIM5 CACNB2 PRRX2 HDAC9 TGFBR3 DACT1 HMGA2 FHL3 VEGF CIT DSP MET COMP EFNB2 FBLIM1 THBS1 ANGPTL2 CEBPG SEMA5A SPIN3 VEGFC VLDLR BHLHB3 ARNT2 NEDD9 CDC42EP5 KLF6 MBNL1 ANGPTL4 SGCD SMTN KITLG ARHGDIB | 85 | 786 | 0.0000117 |
| cell motility | THBS1 TPM1 TSPAN2 MMP12 CD97 VASP NRCAM ADRA2A VEGFC YARS HMMR CALD1 ARPC5 FPR1 TNFRSF12A SAA2 LAMA4 HSPB1 VEGF MYLIP CTGF ARHGDIB FN1 | 23 | 118 | 0.0000117 |
| localization of cell | THBS1 TPM1 TSPAN2 MMP12 CD97 VASP NRCAM ADRA2A VEGFC YARS HMMR CALD1 ARPC5 FPR1 TNFRSF12A SAA2 LAMA4 HSPB1 VEGF MYLIP CTGF ARHGDIB FN1 | 23 | 118 | 0.0000117 |
| locomotion | THBS1 TPM1 TSPAN2 MMP12 CD97 VASP NRCAM ADRA2A VEGFC YARS HMMR CALD1 ARPC5 FPR1 TNFRSF12A SAA2 LAMA4 HSPB1 VEGF MYLIP CTGF ARHGDIB FN1 | 23 | 118 | 0.0000117 |
| spindle organization and biogenesis | BUB1B TTK KIF11 ZWINT UBE2C KIF23 SPAG5 KNTC2 AURKA PRC1 | 10 | 17 | 0.0000906 |
| DNA replication | RFC3 NFIB RRM2 REV3L MCM2 GINS2 RRM1 TOP2A MCM4 GINS1 FEN1 MSH2 MCM5 CDC6 POLE2 MCM7 MCM6 TK1 RNASEH2A CTGF | 20 | 108 | 0.000231 |
| microtubule-based movement | KIF4A KIF20A LOC146909 KIF21A KIF11 TUBA1 MPHOSPH1 KNS2 KIF23 KIF14 CENPE KIF15 KIF2C | 13 | 40 | 0.000412 |
| chromosome segregation | ESPL1 NUSAP1 SGOL2 BRRN1 PTTG1 CDCA5 KNTC2 CENPE HCAP-G DLG7 | 10 | 24 | 0.000814 |
| organelle organization and biogenesis | DIAPH1 KIF20A ESPL1 KIF21A TUBA1 ZWINT MPHOSPH1 CDCA5 AURKA ADRA2A RAD50 CBX5 ARL4C MICAL1 HDAC9 ARPC5 KRR1 NUSAP1 LASP1 UBE2C HMGA2 PPARGC1A KIF14 CNN1 CLCN3 CENPE EXOSC9 PALLD TIMM8B BUB1B KIF11 BRRN1 HNRPD CEBPG SPAG5 FSCN1 DBN1 EPB41L2 YWHAH KIF4A LOC146909 TTK NEDD9 RACGAP1 CDC42EP5 KNS2 KIF23 PTTG1 CXCL12 KNTC2 EPB41L3 PRC1 SGCD KIF15 KIF2C HCAP-G ARHGDIB | 57 | 522 | 0.000957 |
| mitotic sister chromatid segregation | SPL1 NUSAP1 BRRN1 CDCA5 KNTC2 CENPE HCAP-G DLG7 | 8 | 14 | 0.000957 |
| sister chromatid segregation | ESPL1 NUSAP1 BRRN1 CDCA5 KNTC2 CENPE HCAP-G DLG7 | 8 | 15 | 0.00133 |
| cytoskeleton-dependent intracellular transport | KIF4A KIF20A LOC146909 KIF21A KIF11 TUBA1 MPHOSPH1 KNS2 KIF23 KIF14 CENPE KIF15 KIF2C | 13 | 47 | 0.00134 |
| microtubule cytoskeleton organization and biogenesis | BUB1B ESPL1 TTK NUSAP1 KIF11 ZWINT UBE2C KIF23 SPAG5 KNTC2 AURKA PRC1 | 12 | 40 | 0.00134 |
| second-messenger-mediated signaling | BUB1B FEN1 FPR1 ZWINT UBE2C SPAG5 KNTC2 AURKA ADRA2A CAP2 AGTR1 ADCY7 EDNRB TOP2A CAP1 | 15 | 64 | 0.0016 |
| cell communication | CLOCK IGFBP1 KIT CMKOR1 GKAP1 ITGA3 ARHGAP28 SCG5 AGTR1 INPP4B OPN1SW ARL4C EDNRB PXK ITGA5 RAB20 NTRK2 PLEKHG2 DDAH1 PDGFA FGF1 ANKRD1 PPARGC1A BAG1 PLCB4 ILK DIRAS3 CLIC1 EPHA2 ARHGAP22 RASD1 IL4R CAP2 DBN1 FAM13A1 ADCY7 TNFRSF11B PRKAR2B RAC2 SLC8A1 YWHAH WNT5B TAS2R38 GDF15 RACGAP1 PPP4R1 | 116 | 1321 | 0.00183 |

| GO term | Gene symbol | Regulated genes | Genes on array | GOstat p-value |
|---|---|---|---|---|
| | HMOX1 CXCL12 GNAL WISP1 PBEF1 RHOC CAP1 DLG7 GNB4 CHL1 ZWINT PLP2 FZD4 SNF1LK2 ADRA2A AURKA SAV1 MICAL1 SLC20A1 TOP2A MKNK2 RGS4 FEN1 PTGFR TGFBR3 KCNK3 DACT1 IL18R1 LIFR UBE2C VEGF CIT GEM MET EFNB2 ZYX ABAT FN1 BUB1B CD97 PCSK1 RAPH1 PDE7B SEMA5A SPAG5 VLDLR VEGFC TXNRD1 PDE3B CXCL13 RAGE ARNT2 TNFRSF21 NEDD9 ECT2 ARHGEF2 RAB3B FPR1 DEPDC1 ARHGAP18 ANGPTL4 LEP KNTC2 KCNMB1 DAPK3 TGFB1I1 PTGER2 RASL11B ARHGDIB KITLG | | | |
| regulation of mitosis | YWHAH BUB1B ESPL1 TTK NUSAP1 MAD2L1 BUB1 UBE2C NEK2 CCNA2 DLG7 | 11 | 36 | 0.00223 |
| organismal physiological process | DIAPH1 PLAT DHRS3 CYP1B1 OPN1SW ALPL AGTR1 EDNRB PXK HDAC9 PTGFR ELF4 CDO1 KCNK3 IL18R1 SAA2 PPARGC1A GEM CNN1 SERPINE1 EXOSC9 ABAT TIMM8B COL11A1 FN1 THBS1 TPM1 GBP1 CD97 CEBPG PDE7B IGSF4 RP2 BARD1 IL4R MGLL DBN1 MEOX2 SLC8A1 CD24 CXCL13 CALD1 PDCD1LG2 SPG3A YWHAH TAS2R38 AKR1C2 KIAA1199 COL4A3BP KLF6 FPR1 ZNF354A AQP3 CXCL12 KCNMB1 WDR1 AQP7 SMTN CTSC ULBP2 ARHGDIB | 61 | 593 | 0.00248 |
| phosphoinositide-mediated signaling | BUB1B FEN1 ZWINT UBE2C SPAG5 KNTC2 AURKA AGTR1 EDNRB TOP2A | 10 | 32 | 0.00388 |
| organ development | DDIT4L CEBPG NRAS TAGLN2 VEGFC CYP1B1 SOX9 PHGDH ALPL CSRP2 GHR TNFRSF11B BHLHB3 PDLIM5 CACNB2 HDAC9 TAGLN KLF6 FGF1 MBNL1 TNFRSF12A ANGPTL4 FHL3 VEGF IFRD1 COMP SGCD SMTN CLEC3B KITLG COL11A1 | 32 | 244 | 0.0041 |
| cell adhesion | FBLIM1 THBS1 CHL1 TSPAN2 CD97 DDIT4L ITGA3 NLGN4X SEMA5A IGSF4 NRCAM HAPLN1 ITGA5 NEDD9 CXCL12 SAA2 TNFRSF12A CTNNAL1 LAMA4 CYR61 WISP1 COL8A1 BOC COMP CTGF ZYX ILK ARHGDIB KITLG COL11A1 FN1 | 31 | 250 | 0.0067 |
| establishment of organelle localization | ESPL1 NUSAP1 CENPE CDCA5 DLG7 | 5 | 7 | 0.0106 |
| signal transduction | CLOCK IGFBP1 KIT CMKOR1 GKAP1 ITGA3 ARHGAP28 SCG5 AGTR1 INPP4B OPN1SW ARL4C EDNRB PXK ITGA5 RAB20 NTRK2 PLEKHG2 DDAH1 PDGFA FGF1 ANKRD1 PPARGC1A BAG1 PLCB4 ILK DIRAS3 CLIC1 EPHA2 ARHGAP22 RASD1 IL4R CAP2 FAM13A1 ADCY7 TNFRSF11B PRKAR2B RAC2 YWHAH WNT5B TAS2R38 GDF15 RACGAP1 PPP4R1 HMOX1 CXCL12 GNAL WISP1 PBEF1 RHOC CAP1 GNB4 CHL1 ZWINT PLP2 FZD4 SNF1LK2 AURKA ADRA2A SAV1 MICAL1 TOP2A SLC20A1 MKNK2 RGS4 FEN1 PTGFR TGFBR3 DACT1 IL18R1 LIFR UBE2C VEGF CIT GEM MET ZYX FN1 BUB1B CD97 RAPH1 PDE7B SPAG5 VEGFC VLDLR TXNRD1 PDE3B RAGE ARNT2 TNFRSF21 NEDD9 ECT2 ARHGEF2 RAB3B FPR1 DEPDC1 ARHGAP18 LEP KNTC2 DAPK3 TGFB1I1 PTGER2 RASL11B KITLG ARHGDIB | 105 | 1228 | 0.0106 |
| cell cycle checkpoint | BUB1B TTK MAD2L1 BUB1 BRIP1 CDC6 CCNE2 CHEK1 CCNA2 | 9 | 31 | 0.0106 |
| cell differentiation | CHL1 CASC5 CEBPG SEMA5A GPM6B NRCAM SEMA6D VEGFC CSRP2 DBN1 BHLHB3 YWHAH ARNT2 HDAC9 NTRK2 LPIN1 KLF6 FGF1 PPL MBNL1 TNFRSF12A ANGPTL4 PPARGC1A VEGF CIT DSP IFRD1 EFNB2 | 28 | 229 | 0.0154 |
| organelle localization | ESPL1 NUSAP1 CENPE CDCA5 DLG7 | 5 | 8 | 0.0154 |
| response to stimulus | DNAJB4 CLOCK REV3L DDIT3 DHRS3 RAD50 OPN1SW EDNRB CDO1 ANKRD1 SAA2 PPARGC1A CYR61 HSPB1 CHEK1 ATF4 CIRBP SERPINE1 NEIL3 TIMM8B COL11A1 GBP1 IL4R BARD1 DCLRE1B TAS2R38 BRIP1 ZNF354A PTTG1 CXCL12 CTGF USP1 ULBP2 UHRF1 DIAPH1 PLAT HSPB2 PLP2 CYP1B1 TOP2A HDAC9 FEN1 MSH2 ELF4 IL18R1 VEGF GEM EXOSC9 ABAT FN1 THBS1 CD97 CEBPG IGSF4 RP2 VLDLR MGLL CCNA2 CD24 ME1 CXCL13 PDCD1LG2 SPG3A ARNT2 COL4A3BP KIAA1199 KLF6 FPR1 ANGPTL4 POLE2 WDR1 CTSC ADIPOQ ARHGDIB | 74 | 816 | 0.0185 |
| G-protein signaling, coupled to cAMP nucleotide second messenger | ADRA2A CAP2 ADCY7 FPR1 EDNRB CAP1 | 6 | 14 | 0.0185 |
| cAMP-mediated signaling | ADRA2A CAP2 ADCY7 FPR1 EDNRB CAP1 | 6 | 15 | 0.024 |
| cell proliferation | CDKN3 EMP1 TSPAN2 BUB1 PLK1 ADRA2A CSRP2 TCF19 PDGFA FGF1 STIL ELF4 CDC6 CYR61 VEGF CHEK1 MET BUB1B MKI67 FSCN1 VEGFC BHLHB3 CDK6 TTK RACGAP1 INSIG1 TPX2 PBEF1 KIF15 KIF2C DLG7 KITLG | 32 | 283 | 0.0248 |
| cell-cell signaling | CD97 PCSK1 PDE7B SEMA5A DBN1 SCG5 PXK CXCL13 YWHAH GDF15 PDGFA FGF1 KCNK3 CXCL12 WISP1 LEP KCNMB1 EFNB2 ZYX PBEF1 ABAT DLG7 | 22 | 171 | 0.027 |
| regulation of lyase activity | ADRA2A CAP2 ADCY7 EDNRB CAP1 | 5 | 10 | 0.027 |
| regulation of cyclase activity | ADRA2A CAP2 ADCY7 EDNRB CAP1 | 5 | 10 | 0.027 |
| regulation of adenylate cyclase activity | ADRA2A CAP2 ADCY7 EDNRB CAP1 | 5 | 10 | 0.027 |
| DNA-dependent DNA replication | RFC3 REV3L MSH2 MCM5 MCM2 CDC6 MCM6 MCM7 TOP2A MCM4 | 10 | 51 | 0.0519 |
| G-protein coupled receptor protein signaling pathway | CD97 CMKOR1 FZD4 RASD1 CAP2 ADRA2A AGTR1 OPN1SW SCG5 ADCY7 EDNRB RGS4 TAS2R38 FPR1 PTGFR CXCL12 GNAL PTGER2 CAP1 | 19 | 148 | 0.0612 |
| regulation of catalytic | CDKN3 TRIB3 HIP1 CAP2 ADRA2A ADCY7 EDNRB CCNA2 RGS4 | 19 | 148 | 0.0612 |

| GO term | Gene symbol | Regulated genes | Genes on array | GOstat p-value |
|---|---|---|---|---|
| activity | YWHAH CYCS FPR1 CDC6 CCNE2 ANGPTL4 RGC32 CHEK1 CAP1 DIRAS3 | | | |
| nervous system development | THBS1 CHL1 ALDH3A2 BDNF SEMA5A GPM6B NRCAM VLDLR SEMA6D PHGDH DBN1 EDNRB YWHAH ARNT2 RACGAP1 NTRK2 MBNL1 VEGF MYLIP CIT EFNB2 | 21 | 171 | 0.0641 |
| actin cytoskeleton organization and biogenesis | ARPC5 DIAPH1 NEDD9 RACGAP1 CDC42EP5 CXCL12 FSCN1 ADRA2A DBN1 CNN1 EPB41L3 EPB41L2 ARHGDIB | 13 | 87 | 0.0716 |
| system development | THBS1 CHL1 ALDH3A2 BDNF SEMA5A GPM6B NRCAM VLDLR SEMA6D PHGDH DBN1 EDNRB YWHAH ARNT2 RACGAP1 NTRK2 MBNL1 VEGF MYLIP CIT EFNB2 | 21 | 173 | 0.0716 |
| mitotic checkpoint | BUB1B TTK MAD2L1 BUB1 CCNA2 | 5 | 14 | 0.0716 |
| G-protein signaling, coupled to cyclic nucleotide second messenger | ADRA2A CAP2 ADCY7 FPR1 EDNRB CAP1 | 6 | 21 | 0.0716 |
| biological_process | GOL2 STIL ELF4 UBE2C LIFR VEGF FBLIM1 UACA TPM1 CD97 RAPH1 SEMA5A IGSF4 FSCN1 CCND1 FOXM1 PDCD1LG2 SPG3A CCNB2 COL4A3BP RAB3B MBNL1 AQP3 POLE2 ATP1B1 WDR1 MCM7 ARRDC3 DAPK3 RPL31 PRC1 TGFB1I1 KITLG IGFBP1 GKAP1 CASC5 DDIT3 CMKOR1 PRDM16 BDNF PSAT1 AGTR1 CBX5 PPM2C EXOSC6 DDAH1 PDGFA GPT2 MCM5 ANKRD1 SAA2 RGC32 LAMA4 CHEK1 MELK NEIL3 MXRA5 COL11A1 ZNF436 KIF11 GBP1 CKAP2 CEP55 C1ORF24 PALMD NR1D2 TNFRSF11B MEOX2 FBXL5 LOC146909 WNT5B RACGAP1 PITPNC1 TAS2R38 LPIN1 CDC20 ZNF354A NP CXCL12 EPB41L3 ULBP2 UHRF1 DHCR7 DIAPH1 PCK2 HK2 POR RRM2 DDIT4L HIP1 ZWINT CLCN4 MPHOSPH1 FZD4 SNF1LK2 ADRA2A SLC7A11 TOP2A SLC20A1 DLX1 RGS4 MICAL2 FEN1 IL18R1 LIPE GEM COMP EFNB2 CSAD ABAT NANOS1 THBS1 UAP1 CEBPG RP2 PLK4 BHLHB3 CCNA2 LARP6 TXNRD1 ME1 TNFRSF21 TSC22D3 TTK THNSL1 CDC42EP5 ARHGEF2 PHLDA1 CCNE2 ACOT7 KNTC2 KDELR3 SESN2 RASL11B NEXN CDKN3 PGD TSPAN2 BUB1 E2F7 DHRS3 SLC3A2 SEMA6D SCG5 PBK RAD50 LOC92270 ARL4C PXK KRR1 PLEKHG2 GYG2 PRRG4 LASP1 FGF1 CDC6 TNFRSF12A CYR61 PC BAG1 GCNT1 CHI3L1 ATF4 IFRD1 WDHD1 CLEC3B TIMM8B CLIC1 PDK4 ARHGAP22 MCM2 HSD17B6 RASD1 DBN1 FAM13A1 DCLRE1B LOC91461 TRIP13 MCM4 CCND3 AKR1C2 PPP4R1 INSIG1 HLF ARSJ PTTG1 WISP1 COL8A1 NEK2 CTGF APOBEC3B USP1 PBEF1 KIF15 FLJ20920 GNB4 MMP12 CDCA5 CH25H NUPL1 NRAS GINS2 CYP1B1 AURKA ALPL CDC2 UBE2T EGR1 SAV1 PDLIM5 CACNB2 PRRX2 HDAC9 NUSAP1 TEF MSH2 PTGFR DACT1 HMGA2 WEE1 CDCA1 KIF14 CLCN3 GPAM EXOSC9 FN1 BUB1B MAD2L1 RNF144 BRRN1 PDE7B HAPLN1 RRM1 MOCS1 PDE3B ARNT2 ECT2 KLF6 FPR1 KIF23 DEPDC1 B3GALT2 SGCD SMTN AQP7 CDCA8 CTSC HCAP-G HSD3B7 ADIPOQ ARHGDIB | 415 | 6383 | 0.0725 |
| vitamin metabolism | PGD BBOX1 PSAT1 ALDH1B1 PBEF1 DHRS3 ME1 | 7 | 29 | 0.0725 |
| muscle development | HDAC9 TAGLN MBNL1 FHL3 TAGLN2 CSRP2 IFRD1 SGCD SMTN CACNB2 | 10 | 56 | 0.0764 |
| protein amino acid phosphorylation | BUB1B TRIB3 EPHA2 PDK4 KIT BUB1 PLK1 AURKB AURKA PLK4 SNF1LK2 PBK CDC2 PRKAR2B LOC91461 MKNK2 RAGE CDK6 TTK COL4A3BP NTRK2 WEE1 NEK2 DAPK3 CHEK1 CIT MELK LIPE MET MXRA5 ILK | 31 | 296 | 0.0811 |
| cytokinesis | ESPL1 NUSAP1 RACGAP1 ANLN PRC1 | 5 | 15 | 0.0811 |
| cell surface receptor linked signal transduction | KIT CMKOR1 PLP2 ITGA3 FZD4 SNF1LK2 ADRA2A SCG5 OPN1SW AGTR1 EDNRB MKNK2 ITGA5 RGS4 NTRK2 PDGFA PTGFR TGFBR3 DACT1 LIFR VEGF BAG1 GEM ILK FN1 CD97 RASD1 CAP2 ADCY7 WNT5B GDF15 TAS2R38 NEDD9 FPR1 CXCL12 GNAL WISP1 CAP1 PTGER2 | 40 | 411 | 0.0812 |
| water-soluble vitamin metabolism | PGD BBOX1 PSAT1 ALDH1B1 PBEF1 ME1 | 6 | 23 | 0.0875 |
| DNA replication initiation | MCM6 MCM7 MCM5 MCM2 MCM4 | 5 | 16 | 0.0902 |
| cyclic-nucleotide-mediated signaling | ADRA2A CAP2 ADCY7 FPR1 EDNRB CAP1 | 6 | 24 | 0.0977 |
| morphogenesis | FBLIM1 EMP1 IGFBP1 DDIT4L CEBPG NRAS NRCAM SLC3A2 VEGFC CAP2 PALMD CSRP2 BHLHB3 PDLIM5 IER3 YWHAH NEDD9 CDC42EP5 FGF1 MBNL1 TNFRSF12A ANGPTL4 CYR61 WISP1 VEGF CTGF COMP EFNB2 CAP1 KITLG | 30 | 291 | 0.0987 |
| regulation of cyclin-dependent protein kinase activity | CDKN3 CHEK1 CDC6 CCNE2 CCNA2 DIRAS3 RGC32 | 7 | 33 | 0.0987 |
| actin filament-based process | ARPC5 DIAPH1 NEDD9 RACGAP1 CDC42EP5 CXCL12 FSCN1 ADRA2A DBN1 CNN1 EPB41L3 EPB41L2 ARHGDIB | 13 | 93 | 0.0987 |
| hormone metabolism | YWHAH SCG5 DHRS3 HSD3B7 HSD17B6 | 5 | 17 | 0.0987 |
| microtubule motor activity | KIF4A KIF20A LOC146909 KIF21A KIF11 MPHOSPH1 KNS2 KIF23 KIF14 CENPE KIF15 KIF2C | 12 | 32 | 0.00155 |
| actin binding | DIAPH1 TPM1 TPM4 HIP1 VASP FSCN1 DBN1 PXK PDLIM5 EPB41L2 CALD1 YWHAH TAGLN LASP1 WDR1 ANLN CNN1 EPB41L3 CAP1 TPM2 SMTN | 21 | 119 | 0.00155 |
| purine nucleotide binding | KIF21A TUBA1 KIT BUB1 AURKB RAD50 PBK SCG5 ARL4C FIGNL1 RAB20 NTRK2 ACACB MCM5 CDC6 PC MCM6 CHEK1 TK1 MELK MXRA5 ILK DIRAS3 ATAD2 PDK4 EPHA2 KIF11 MKI67 GBP1 MCM2 RASD1 PRKAR2B RAC2 LOC91461 TRIP13 MCM4 ACTG2 | 86 | 933 | 0.021 |

| GO term | Gene symbol | Regulated genes | Genes on array | GOstat p-value |
|---|---|---|---|---|
| | LOC146909 CDK6 FAM83D TPX2 BRIP1 GNAL NEK2 KIF15 RHOC KIF2C KIF20A PCK2 DOCK11 TRIB3 HK2 MPHOSPH1 PLK1 DCK AURKA SNF1LK2 CDC2 YARS TOP2A MKNK2 MSH2 WEE1 EHD1 KIF14 CIT GEM MET CENPE BUB1B RP2 PLK4 RRM1 TXNRD1 SPG3A ME1 KIF4A RAGE TTK THNSL1 RAB3B FRY KIF23 MCM7 DAPK3 RASL11B | | | |
| cytoskeletal protein binding | DIAPH1 TPM1 TPM4 HIP1 VASP FSCN1 NRCAM DBN1 PXK PDLIM5 EPB41L2 CALD1 YWHAH RACGAP1 TAGLN LASP1 MYLIP WDR1 ANLN EPB41L3 CNN1 TPM2 SMTN CAP1 PALLD | 25 | 182 | 0.021 |
| motor activity | KIF4A KIF20A LOC146909 KIF21A KIF11 MPHOSPH1 KNS2 KIF23 KIF14 CENPE KIF15 KIF2C | 12 | 57 | 0.0516 |
| nucleotide binding | RFC3 KIF21A REV3L TUBA1 KIT BUB1 DHRS3 AURKB SCG5 PBK RAD50 ARL4C FIGNL1 RAB20 NTRK2 MCM5 ACACB CDC6 RP11-301I17.1 PC PPARGC1A MCM6 CHEK1 TK1 MELK CIRBP MXRA5 ILK DIRAS3 KIF11 ATAD2 PDK4 EPHA2 GBP1 MKI67 HNRPD MCM2 RASD1 PRKAR2B RAC2 LOC91461 TRIP13 MCM4 ACTG2 LOC146909 CDK6 FAM83D TPX2 BRIP1 GNAL NEK2 KIF15 RHOC KIF2C KIF20A PCK2 DOCK11 TRIB3 HK2 POR MPHOSPH1 PLK1 DCK LOC81691 SNF1LK2 AURKA CDC2 YARS TOP2A MKNK2 MSH2 WEE1 EHD1 KIF14 CIT GEM MET CENPE BUB1B RP2 PLK4 RRM1 LARP6 TXNRD1 SPG3A ME1 RAGE KIF4A TTK THNSL1 RAB3B FRY KIF23 MCM7 DAPK3 RASL11B | 96 | 113 | 0.0516 |
| ATP binding | KIF21A KIT BUB1 AURKB RAD50 PBK FIGNL1 NTRK2 ACACB MCM5 CDC6 PC MCM6 CHEK1 MELK TK1 MXRA5 ILK ATAD2 PDK4 EPHA2 KIF11 MKI67 MCM2 LOC91461 MCM4 TRIP13 CDK6 LOC146909 ACTG2 FAM83D TPX2 BRIP1 NEK2 KIF15 KIF2C KIF20A TRIB3 HK2 MPHOSPH1 PLK1 DCK AURKA CDC2 YARS TOP2A MKNK2 MSH2 WEE1 KIF14 EHD1 CIT MET CENPE BUB1B RP2 PLK4 RRM1 RAGE KIF4A TTK THNSL1 FRY KIF23 MCM7 DAPK3 | 67 | 720 | 0.0526 |
| adenyl nucleotide binding | KIF21A KIT BUB1 AURKB RAD50 PBK FIGNL1 NTRK2 ACACB MCM5 CDC6 PC MCM6 CHEK1 MELK TK1 MXRA5 ILK ATAD2 PDK4 EPHA2 KIF11 MKI67 MCM2 LOC91461 PRKAR2B MCM4 TRIP13 CDK6 LOC146909 ACTG2 FAM83D TPX2 BRIP1 NEK2 KIF15 KIF2C KIF20A TRIB3 HK2 MPHOSPH1 PLK1 DCK AURKA SNF1LK2 CDC2 YARS TOP2A MKNK2 MSH2 WEE1 KIF14 EHD1 CIT MET CENPE BUB1B RP2 PLK4 RRM1 TXNRD1 ME1 RAGE KIF4A THNSL1 TTK FRY KIF23 MCM7 DAPK3 | 70 | 763 | 0.0526 |
| signal transducer activity | CLOCK KIT CMKOR1 ITGA3 BDNF SEMA6D OPN1SW AGTR1 EDNRB GREM2 ITGA5 NTRK2 PDGFA FGF1 LASP1 TNFRSF12A SAA2 LAMA4 PPARGC1A BAG1 PLCB4 NR1H3 MXRA5 EPHA2 IL4R NR1D2 TNFRSF11B WNT5B YWHAH GDF15 TAS2R38 HMOX1 CXCL12 GNAL PBEF1 RHOC ULBP2 GNB4 DIAPH1 LOXL4 FZD4 ADRA2A GHR SEMA3G YARS PDLIM5 SLC20A1 RGS4 TGFBR3 PTGFR LIFR IL18R1 VEGF MET EFNB2 THBS1 EVI2A CD97 ANGPTL2 SEMA5A IGSF4 VLDLR VEGFC CXCL13 PDCD1LG2 TNFRSF21 ARNT2 ECT2 FPR1 LEP KDELR3 TGFB1I1 PTGER2 KITLG ADIPOQ | 75 | 834 | 0.0527 |

GOstat analysis results for genes showing differential regulation 24 h after initiation of osteogenic transdifferentiation are depicted under the same prerequisites as described for tab. 18. Altogether, 1,196 target probe sets were found and analysed to the reference of all 24,108 reliably measured probe sets 24 h after initiation of transdifferentiation.

## 7.4 Abbreviations

| | |
|---|---|
| °C | degree Celsius |
| µg | microgram(s) |
| µm | micrometre(s) |
| µM | micromolar = micromol per litre |
| 1D | one dimensional |
| ALP | alkaline phosphatase |
| APS | ammonium persulfate |
| bp | base pair |
| cDNA | complementary deoxyribonucleic acid |
| CHAPS | (3-[(3-Cholamidopropyl)-dimethylammonio]-propane-sulfonate) |
| $CO_2$ | carbon dioxide |
| cRNA | complementary ribonucleic acid |
| d | day(s) |
| ddNTPs | dideoxynucleotide triphosphates |
| DMEM | Dulbecco's modified eagle's medium |
| DMSO | dimethylsulfoxide |
| DNA | deoxyribonucleic acid |
| dNTPs | deoxynucleotide triphosphates |
| DTT | dithiothreitol |
| E | extinction unit |
| EDTA | ethylendiamintetraacetic acid |
| FBS | foetal bovine serum |
| FGF1 | fibroblast growth factor 1 |
| fig. | figure |
| h | hour(s) |
| HCl | hydrochloric acid |
| HPLC | high performance liquid chromatography |
| IBMX | 3-isobutyl-1-methylxanthine |
| IGF1 | insulin-like growth factor 1 |
| l | litre |
| mA | milliampere |
| min | minute(s) |
| ml | microlitre(s) |
| mM | millimolar = millimol per litre |
| M-MLV | moloney murine leukemia virus |
| mRNA | messenger RNA |
| MSC | mesenchymal stem cell |
| nM | nanomolar = nanomol per litre |
| PBS | phosphate buffered saline |
| rhCYR61 | recombinant human cysteine-rich angiogenic inducer 61 |
| rhFGF acidic | recombinant human fibroblast growth factor, acidic |
| rhIGF-I | recombinant human insulin like growth factor I |
| rhOPG/TNFRSF11B | recombinant human osteoprotegerin/tumor necrosis factor receptor superfamily, member 11b |
| rmsFRP2 | mouse recombinant secreted frizzled-related protein 2 |
| RNA | ribonucleic acid |
| rpm | rounds per minute |
| RT | reverse transcriptase |
| RT-PCR | reverse transcriptase polymerase chain reaction |
| SDS | sodium dodecyl sulfate |
| SDS-PAGE | sodium dodecyl sulfate polyacrylamide gel electrophoresis |

| | |
|---|---|
| SFRP2 | secreted frizzled-related protein 2 |
| tab. | table |
| *Taq* | *Thermus aquaticus* |
| TEMED | N,N,N',N'-tetramethyl ethylenediamine |
| TNFRSF11B | tumor necrosis factor receptor superfamily, member 11b (osteoprotegerin) |
| Tris base | tris(hydroxymethyl)aminomethane |
| U | unit(s) |
| UV | ultraviolet |
| v/v | volume per volume |
| w/v | weight per volume |
| x | times, -fold |

## 7.5  Curriculum Vitae

### *Personal information*

| | |
|---|---|
| Surname and first names: | **Schilling, Maria <u>Tatjana</u>** |
| Date of birth: | 5 February 1979 |
| Place of birth: | San Miguel de Tucuman, Argentina |
| Address: | St.-Nepomuk-Str. 6, D-97218 Gerbrunn, Germany |
| Status: | unmarried |
| Nationality: | German |

### *Education and training*

| | |
|---|---|
| 1985 - 1989 | Elementary school, Baunach |
| 1989 - 1998 | Grammar school "Gymnasium der Englischen Fräulein", Bamberg |
| June 1998 | General qualification for university entrance ("Abitur") |
| 1998 - 2003 | Studies of biology at the Julius Maximilians University Würzburg, Main subjects: biotechnology, cellular and developmental biology, and microbiology Diploma thesis at the Chair of Biotechnology: "Cryoprotection of Cells" |
| December 2003 | Diploma certificate as biologist |
| 2004 - 2007 | PhD thesis at the Julius Maximilians University Würzburg, Orthopedic Clinic, Orthopedic Center for Musculoskeletal Research, Molecular Orthopedics and Cell Biology, supervised by PD Dr. Norbert Schütze and Prof. Dr. Franz Jakob |

### *Scholarships and awards*

| | |
|---|---|
| March 2007 | "Von Recklinghausen" award of the "Deutsche Gesellschaft für Endokrinologie" (German Society of Endocrinology) for the manuscript **"**Plasticity in Adipogenesis and Osteogenesis of Human Mesenchymal Stem Cells" (see 7.6) |
| March 2006 | Scholarship of the "Deutsche Akademie der osteologischen und rheumatologischen Wissenschaften" (German Academy of Osteologic and Rheumatologic Sciences) to attend the Young Investigator Osteology Symposium 2006 (YIOSS'2006) within the Osteology 2006 conference in Köln, Germany |
| September 2005 | Conference scholarship of the "Deutsche Akademie der osteologischen und rheumatologischen Wissenschaften" to attend the 5th Baltic Bone and Cartilage Conference 2005 in Naantali, Finland |

October 2004        Poster award: best poster of the session at the 90th annual conference of
                    the "Deutsche Gesellschaft für Orthopädie und Orthopädische Chirurgie"
                    (German Society for Orthopaedics and Orthopaedic Surgery) 2004 in
                    Berlin, Germany; title: "Plasticity between Adipogenic and Osteogenic
                    Differentiation in Human Mesenchymal Stem Cells of the Bone Marrow"

## 7.6  Publications

### *Publications in peer reviewed journals*

**Schilling T**, Küffner R, Klein-Hitpass L, Zimmer R, Jakob F, Schütze N. 2007. Microarray Analysis of Transdifferentiated Mesenchymal Stem Cells, J Cell Biochem, manuscript accepted (original research paper)

**Schilling T**, Nöth U, Klein-Hitpass L, Jakob F, Schütze N. 2007. Plasticity in Adipogenesis and Osteogenesis of Human Mesenchymal Stem Cells. Mol Cell Endocrinol, in press (original research paper)

Ebert R, Schütze N, **Schilling T**, Seefried L, Weber M, Nöth U, Eulert J, Jakob F. 2007. Influence of Hormones on Osteogenic Differentiation Processes of Mesenchymal Stem Cells, Expert Rev Endocrinol Metab 2(1):59-78 (review)

Schütze N, Wagemanns R, **Schilling T**, Jakob F. 2006. CCN1. UCSD-Nature Molecule Pages, doi: 10.1038/mp.a003362.01 (online publication)

### *Published abstracts of national and international symposia*

**Schilling T**, Küffner R, Nöth U, Zimmer R, Jakob F, Schütze N. 2006. Microarray Analyses of Plasticity between the Osteogenic and Adipogenic Differentiation Pathway of Human Mesenchymal Stem Cells, *ASBMR 28th Annual Meeting* in Philadelphia, Pennsylvania, USA, J Bone Miner Res 21(Suppl1)

**Schilling T**, Küffner R, Nöth U, Zimmer R, Jakob F, Schütze N. Towards Molecular Understanding of Plasticity of Human Mesenchymal Stem Cells by Microarray Analyses. 2006. *2$^{nd}$ International Conference "Strategies in Tissue Engineering"* in Würzburg, Germany, Cytotherapy 8(Suppl2)

**Schilling T**, Küffner R, Nöth U, Zimmer R, Jakob F, Schütze N. 2006. Genarray-Analyse transdifferenzierter humaner Mesenchymaler Stammzellen, *Osteologie 2006* in Köln, Osteologie 15(Suppl1)

Meyer U, **Schilling T**, Küffner R, Nöth U, Zimmer R, Jakob F, Schütze N. 2006. Regulation hypothetischer Genprodukte währed der Transdifferenzierung humaner Mesenchymaler Stammzellen, *Osteologie 2006* in Köln, Osteologie 15(Suppl1)

**Schilling T**, Nöth U, Jakob F, Schütze N. 2005. Gene Regulation in Adipogenic Transdifferentiation of Committed Osteoblasts, *ASBMR 27$^{th}$ Annual Meeting* in Nashville, Tennessee, USA, J Bone Miner Res 20(Suppl1)

**Schilling T**, Nöth U, Jakob F, Schütze N. 2005. Gene Array Analysis of Adipogenic Transdifferentiation of Committed Osteoblasts, *2$^{nd}$ Joint Meeting of the European Calcified Tissue Society and the International Bone and Mineral Society*, Geneva, Switzerland, Bone 36(Suppl 2)

**Schilling T**, Nöth U, Schneidereit J, Jakob F, Schütze N. 2004. Plasticity in Adipogenic and Osteogenic Differentiation Pathways using Human Bone Marrow derived Mesenchymal Stem Cells, *ASBMR 26$^{th}$ Annual Meeting* in Seattle, Washington, USA, J Bone Miner Res 19(Suppl1)

Schütze N, **Schilling T**, Nöth U, Schneidereit J, Eulert J, Jakob F. 2004. Plasticity in Adipogenic and Osteogenic Differentiation Pathways Originating from Human BM-Derived Mesenchymal Stem Cells by Microarray Analyses. *1$^{st}$ International Conference "Strategies in Tissue Engineering"* in Würzburg, Germany, Cytotherapy 6(3)

Schütze N, **Schilling T**, Nöth U, Schneidereit J, Jakob F. 2004. Plastizität zwischen adipogener und osteogener Differenzierung humaner mesenchymaler Stammzellen des Knochenmarks. 90. Jahrestagung der Deutschen Gesellschaft für Orthopädie und Orthopädische Chirurgie 2004 in Berlin, Z Orthop 142(Suppl1)

## 7.7 Acknowledgement